

Advances in Pulmonary Drug Delivery via High Frequency Acoustic Nebulization



A thesis submitted for the degree of
Doctor of Philosophy

by

Anushi Rajapaksa

Department of Mechanical and Aerospace Engineering
Monash University
Australia

March 2013

Notice 1

Under the Copyright Act 1968, this thesis must be used only under the normal conditions of scholarly fair dealing. In particular no results or conclusions should be extracted from it, nor should it be copied or closely paraphrased in whole or in part without the written consent of the author. Proper written acknowledgement should be made for any assistance obtained from this thesis.

Dedication

To my dear parents and beloved husband...

Declaration

I declare that, to the best of my knowledge, the research described herein is original except where the work of others is indicated and acknowledged, and that the thesis has not, in whole or in part, been submitted for any other degree at this or any other university.

Under the Copyright Act 1968, this thesis must be used only under the normal conditions of scholarly fair dealing. In particular no results or conclusions should be extracted from it, nor should it be copied or closely paraphrased in whole or in part without the written consent of the author. Proper written acknowledgement should be made for any assistance obtained from this thesis.

I certify that I have made all reasonable efforts to secure copyright permissions for third-party content included in this thesis and have not knowingly added copyright content to my work without the owner's permission.

Anushi Rajapaksa

Melbourne

March 2013

Acknowledgments

I owe my deepest gratitude to both my PhD advisors, Professors James Friend and Leslie Yeo for supporting me during these past four years. James and Leslie are extremely passionate about their research and inspire people around them with their love for their work. I hope that I can be as enthusiastic and energetic and someday command an audience as well as they can. Both James and Leslie have given me the freedom to pursue various projects. I am very grateful to them for their support, scientific advice and knowledge and many insightful discussions and suggestions, without which this work would not have been possible. Their enthusiasm and knowledge in the area made this an interesting and challenging project.

A special thank you also goes to the inspiring Monash researchers I have met through various projects, including David Piedrafita, Ross Coppel, Els Meeusen, Robert Bischof, Michelle Tate, Tri-Hung Nguyen and Michelle McIntosh. Their insightful advice on the project greatly enhanced my interdisciplinary technical skills, allowing me to become the well-rounded scientist I am today.

I am deeply indebted to my laboratory mates, particularly Aisha Qi, Jenny Ho, Ricky Tjeung, Charles Ma, Kartika Setyabudi, Rimi Chakrabarti, Hamish McWilliams and Gary Nguyen for their support for my research, and their friendship and encouragement during my studies.

It was a pleasure to share doctoral studies and life with wonderful people like Philip Sheath, David Collins, Derrek Lobo and Nyomi Uduman, my office-mates, who have become very close friends.

I thank the rest of the Micro-Nano Physics group at the Melbourne Centre for Nanofabrication including Peggy Chan, Christina Cortez-Jugo, Jeremy Blamey, Nick Glass and Michael Dentry for providing support and for expert criticism of my research.

I am also forever grateful for all the animals that were sacrificed in the name of science, to form the major findings of my research. Laboratory animals help shape science as we know it, and I hope that the scientific discoveries made as a result, will save lives plagued by disease.

I also would like to thank the staff of the department of Mechanical and Chemical Engineering for their support during my studies at Monash University. My sincere appreciation goes to the office and administration staff, including my caretaker supervisor, Chris Davies, and postgraduate research coordinator, Helen Frost, for ensuring the countless forms and paperwork were correctly completed and filed. The assistance provided by Dr. Alex McKnight in proof reading the thesis is greatly appreciated.

I especially thank my mother, father, brother and sister. My hard-working parents have sacrificed their lives for their children and provided unconditional love and care. To my parents, I owe everything I have achieved in my life. I know I always have my family to count on when times are tough.

I offer special thanks to my new family, including my husband, mother-in-law and sister-in-law, for all have been tremendously supportive and caring. I could have not have prayed for better in-laws, and I am extremely grateful for having you in my life.

This note is incomplete without acknowledging the assistance from two family friends, who I consider my brothers, Sisira Kulatunga and Buddhika Agalakumbura. Thank you

for offering a helping hand during the last few months leading to thesis submission.

I have been incredibly blessed by the recent birth of my son, Tarush, who has brought enormous joy to my life. It is true that "Life is what happens" when you are completing your PhD. Life does not stand still, nor wait until you are finished. Tarush, you are the biggest achievement in my life, and I look forward to cherishing all the moments we will share in life.

Lastly, and most importantly, my greatest gratitude extends to my best friend, soul-mate and husband, Sanjeeva. Without him I would be a very different person today, and it would have been certainly much harder to finish the PhD. He has been non-judgmental of me and instrumental in instilling confidence. He had faith in me and my intellect even when I lost faith in myself. These past several years have not been easy, both academically and personally. I am forever indebted to him for helping me through the difficult times, and for all the emotional support, comraderie, and caring he provided. I truly thank Sanjeeva for supporting me, even when I was irritable and depressed. I feel that what we have both learned a lot about life and strengthened our commitment to each other and our determination to live life to the fullest.

Publications

Journal Articles

Qi, A., Chan, P., Ho, J., **Rajapaksa A.E.**, Friend, J. and Yeo, L. (2011) Novel Template-Free Microfluidic Synthesis and Encapsulation Technique for Layer-by-Layer Polymer Nanocapsule Fabrication , ACS Nano, 5, 9583-9591.

Rajapaksa, A. E., Ho, J., Qi, A., Friend J. R. and Yeo L.Y., Pulmonary Delivery of Unprotected pDNA via Surface Acoustic Wave Nebulization provides effective Influenza Vaccination, submission under review.

Rajapaksa, A. E., Qi A., Tan M. K., Coppel R., Yeo L. Y. and Friend J. R., Amplitude Modulation Scheme as a Route Towards the Miniaturisation of Low Power Surface Acoustic Wave Microfluidic Drug Delivery Platforms, submission under review.

Conference Papers

Rajapaksa, A. E., Qi, A., Chan, P., Yeo, L.Y. and Friend, J. (2011) Optimised Surface Acoustic Wave Atomisation via Amplitude Modulation [Conference Presentation] Smart Nano-Micro Materials and Devices - SPIE 2011. Melbourne, Australia - December 2011

Rajapaksa, A. E., Ho, J., Qi, A., Yeo, L.Y., Friend, J., McIntosh, M.P., Piedrafita, D., Meeusen, E. and Morton, A.V. (2011) Pulmonary Gene Delivery Platform via Ultrafast

Microfluidics [Conference Presentation] Advances in Microfluidics and Nanofluidics and Asian-Pacific International Symposium on Lab on Chip, AMN - APLOC 2011. Biopolis, Singapore - January 2011

Rajapaksa, A. E., Ho, J., Qi, A., Yeo, L.Y. and Friend, J.(2011) Ultrafast DNA Vaccines Delivery driven by Surface Acoustic Wave Devices [Conference Presentation] Australian Colloid and Interface Symposium (ACIS 2010)- January 2011

Rajapaksa, A. E., Ho, J., Qi, A., Yeo, L.Y. and Friend J.(2010) A Portable Pulmonary Delivery System for Nano-engineered DNA Vaccines driven by Surface Acoustic Wave Devices [Conference Presentation] The Engineering and Physical Sciences in Medicine and the Australian Biomedical Engineering Conference (epsm abec 2010) - December 2010

Rajapaksa, A. E., Ho, J., Qi, A., Yeo, L.Y. and Friend, J.(2010) A Delivery System for Nano-Engineered Genetic Immuno-Therapeutics driven by Portable Surface Acoustic Wave Devices [Conference Presentation] IgV (Immunology Group of Victoria) 18th Annual Meeting - September 2010

Rajapaksa, A. E., Ho, J., Qi, A., Yeo, L.Y. and Friend, J.(2010) A Portable Delivery System for Nano-Engineered Cargo-Carrying Genetic Immuno-Therapeutics driven by Surface Acoustic Wave Devices [Conference Presentation] Chemeca 2010. Adelaide, Australia- September 2010

Chan, P., Qi, A., **Rajapaksa, A. E.,** Friend, J. and Yeo, L.Y. (2011) Microfluidic Synthesis of Multi-layer Nanoparticles for Drug and Gene Delivery [Conference Paper] Chemeca 2011. Sydney, Australia - September 2011

Rajapaksa, A. E., Friend, J. R., Ho, J. and Forde, G. M. (2009) Nano-Vehicles for Defeating Infectious Diseases: Surface Acoustic Wave Atomisation for the Production of Immuno-nanoparticles for Gene Therapeutics [Poster]. Melbourne: Monash University

Research Students Poster Exhibition - August 2009.

Ho, J., **Rajapaksa, A. E.**, Qi, A., Friend, J. R. and Yeo, L.Y. (2010) Miniature Pulmonary DNA Vaccination Platform using Microfluidic Atomization [Conference Poster]. Dubai: 2nd International Conference on Drug Discovery and Therapy - February 2010.

Patent

Rajapaksa, A.E., Ho, J., Qi, A., Yeo, L.Y., Friend, J.R., McIntosh, M.P. and Morton A.V. (2010) Microfluidic Apparatus for the Atomisation of a Liquid [Patent currently at National Phase] (PCT/AU2010/000548)

Media Releases

Delivering Medicines, ABC Catalyst (Special Edition: Little Wonders Medical Nanotechnology), Television Broadcast date: 25 August 2011 (Australian Broadcasting Corporation).

Abstract

There has been significant interest in the potential of pulmonary-delivered genetic vaccination in treating pulmonary diseases to mitigate vaccine safety issues and to obviate the requirement for needles and skilled, expensive personnel to handle them. Plasmid DNA (pDNA) offers a rapid production route to vaccines without significant side effects nor an extensive cold chain, which is especially important in being prepared for a pandemic caused by a highly infectious agent such as influenza. However, delivering therapeutics such as pDNA to the lung is challenging. Conventional methods including jet and ultrasonic nebulizers for the pulmonary DNA delivery of gene therapeutics are currently ineffective, as they largely fail to maintain the viability of large biomolecules such as pDNA due to the large shear stresses induced during the nebulization process.

This thesis proposes a novel platform for the production of monodispersed aerosol-laden pDNA within a defined size range ($0.5\text{-}5\ \mu\text{m}$) suitable for efficient pulmonary delivery to the lower respiratory airways for optimal dose efficacy, based on SAW (Surface Acoustic Wave) nebulization. SAWs are 10 nm order amplitude sound waves that originate as a result of the application of an alternating voltage onto an interdigital transducer patterned on a piezoelectric substrate. The megahertz ($>10\ \text{MHz}$) order SAW vibration frequencies facilitate fluid and particle manipulation at a much finer scale, allowing extremely efficient transfer of acoustic radiation from the substrate into a drop comprising the drug solution. The acoustic energy is concentrated within a thin region in the drop adjacent to

the substrate, which causes the drop interface to rapidly destabilize and breakup to form micron-dimension aerosol droplets containing the therapeutic molecule. The shear gradient generated within such a short period is not sufficient to degrade biomolecules such as pDNA, since the oscillation period of the SAW vibration at these frequencies is far shorter than the typical macromolecular relaxation time-scale in liquids.

Extensive experimental studies were carried out to investigate the effect of SAW waves on pDNA. First, during *in vitro* studies, a solution containing a pDNA vector encoding a potential malaria vaccine candidate, merozoite surface protein 4/5, was nebulized using both 20 and 30 MHz SAW devices and the condensed mist was collected carefully. High levels of gene expression was observed in Western blots from *in vitro* experiments conducted using immortalized African green monkey kidney cells that were transfected with the post-nebulized pDNA. Next, *in vivo* studies were carried out using a pDNA encoding a yellow fluorescent protein (YFP) which was collected following 30 MHz SAW nebulization. Successful gene expression was observed in mouse lung epithelial cells, when SAW-nebulized pDNA was delivered to a male Swiss mouse via intratracheal instillation. Subsequently, *in vivo* immunization trials were carried out using pDNA vector encoding an influenza A virus surface antigen, human hemagglutinin ((H1N1) strain) that was nebulized using a 30 MHz SAW device. Powerful pharmacodynamic responses were detected following the pDNA vaccination in sera of female Sprague-Dawley rats (n=8 per group) delivered via intratracheal instillation and female Merino-cross ewe lambs (n=4) delivered via nebulized mist inhalation. Moreover, these immunization trials demonstrated antibody responses with high functional activity as shown by the successful inhibition of viral agglutination of chicken red blood cells. These observations validate the use of SAW nebulization as a viable delivery platform for aerosol gene therapy.

To enable miniaturization, the hand-held nebulizer system required the optimization of the usage of available power systems in the simplest manner. Amplitude modulation (AM) was investigated as a simple yet effective means for optimizing the power requirement for

the SAW nebulizer. The effect of AM on shear-sensitive biomolecules was shown to be minimal. By employing AM less than 10 kHz, more efficient atomization was achieved and energy savings of around 40% were obtained. In addition, AM had little effect on the mean aerosol diameter, which is particularly important when therapies are targeted to the deep lung regions. Thus, AM holds great promise for use in SAW nebulizers for non-invasive inhalation therapy.

SAW technology offers an in-home and clinical nebulizer which can be used to administer biologically-based medications to the lungs, with a broad ability to control droplet size through formulation to target specific regions of the lung most affected by disease. This research clearly demonstrates the potential of SAW technology as a needle-free, portable pulmonary delivery platform for gene therapy and DNA vaccination.

Contents

1	Introduction	1
1.1	Pulmonary Drug Therapy and Vaccination	1
1.2	Challenges in Pulmonary Drug Therapy and Genetic Vaccination	2
1.3	Towards Modern Aerosol Delivery Systems for the Efficient Delivery of Difficult Therapeutics: Surface Acoustic Wave (SAW) Nebulization	4
1.4	Thesis Objectives and Scope	7
1.4.1	Aerosol Gene Therapy via Ultra Fast Microfluidics Driven by SAW Nebulization	7
1.4.2	Effective Miniaturization Strategy for the SAW Nebulizer Using an Amplitude Modulation Scheme	9
1.4.3	Thesis Contributions	9
1.5	Thesis Outline	11
2	Towards Non-Invasive Genetic Vaccination	12
2.1	Introduction	12
2.2	Towards a Better Vaccination Strategy: DNA Vaccination	14
2.3	Towards the Patient-Friendly Administration of Vaccinations	16
2.4	Platforms for Non-Invasive Genetic Vaccination	18
2.4.1	Transdermal DNA Vaccination	18
2.4.2	Oral Genetic Vaccination	20

2.4.3	Ocular DNA Vaccination	22
2.4.4	Nasal DNA Vaccination	23
2.5	Pulmonary DNA Vaccination: State-of-the-Art	24
2.5.1	Pulmonary DNA Delivery	24
2.5.2	Inhalers for Pulmonary DNA Delivery	26
2.5.3	Nebulizers for Pulmonary DNA Delivery	30
2.5.4	Other Aerosolization Devices for Pulmonary DNA Delivery	33
2.6	Surface Acoustic Wave Nebulization for Safe Pulmonary Delivery of Un-protected DNA Vaccines	34
2.6.1	Surface Acoustic Waves	34
2.6.2	SAW Microfluidics	35
2.6.3	Surface Acoustic Wave Atomization	36
2.6.4	Surface Acoustic Wave Device for Atomization	36
2.6.5	Mechanism of Generation of Droplets via SAWs	37
2.6.6	Surface Acoustic Wave Atomization for the Delivery of Biomolecules	38
2.7	Conclusions	39

3 Effect of High Frequency Acoustic Wave Nebulization on pDNA in order to achieve Pulmonary DNA Vaccination 41

3.1	Introduction	41
3.2	Experiments and Materials	45
3.2.1	Surface Acoustic Wave Nebulizer	45
3.2.2	Preparation, Culture and Purification of plasmid DNA	45
3.2.3	Plasmid Nebulization using SAW	46
3.2.4	Agarose Gel Electrophoresis	46
3.2.5	AFM Imaging of plasmid DNA	47
3.2.6	<i>In vitro</i> Cellular Transfection	47
3.2.7	SDS-PAGE and Immunoblotting Analysis	48

3.2.8	Aerosol Characterization	48
3.2.9	Statistical Analysis	49
3.3	Results and Discussion	50
3.3.1	Aerosol Size Distribution	50
3.3.2	Physical Stability of pDNA Molecules Irradiated by SAW	52
3.3.3	Bioactivity of plasmids During <i>In vitro</i> Transfection.	55
3.4	Conclusions	56
4	Effective Pulmonary DNA Vaccination via High Frequency Acoustic Wave Nebulization	59
4.1	Introduction	59
4.2	Experiments and Materials	61
4.2.1	Surface Acoustic Wave Nebulizer	61
4.2.2	Preparation, Culture and Purification of plasmid DNA	62
4.2.3	Animal Trials	62
4.2.4	Detection of Gene Expression <i>In vivo</i> following Intratracheal Delivery into Swiss Mice	63
4.2.5	Pulmonary Vaccinations using Pre-SAW nebulized plasmid DNA via Intratracheal Delivery	64
4.2.6	Pulmonary DNA Vaccination of Sheep using SAW via Inhalation	64
4.2.7	Evaluation of Antibody Responses to Enzyme-Linked Immunosorbent Assay	66
4.2.8	Evaluation of Hemagglutination Inhibition Activity	66
4.2.9	Statistical Analysis	67
4.3	Results and Discussion	67
4.3.1	<i>In vivo</i> Detection of Gene Expression in Mice Lungs.	67
4.3.2	Antibody Responses following DNA Vaccination following Intratracheal Delivery of SAW Nebulized VR1020-HA.	69

4.3.3	Hemagglutination Inhibition (HAI) Activity of Antibodies Raised Against Vaccinations with SAW Nebulized DNA in Rats.	70
4.3.4	Aerosol Vaccination of Sheep and the Hemagglutination Inhibition (HAI) Activity of Antibodies Raised.	71
4.4	Conclusions	73
5	Optimization of High Frequency Acoustic Wave Nebulization for Improved Drug Delivery using Amplitude Modulation	77
5.1	Introduction	77
5.2	Experiments and Materials	81
5.2.1	Surface Acoustic Wave Nebulizer	81
5.2.2	Effect of Amplitude Modulation on the Aerosol Size	82
5.2.3	Atomization Rate with Amplitude Modulated Surface Acoustic Waves	82
5.2.4	Effect on Plasmid DNA Delivery During the Use of Amplitude Modulation	83
5.2.5	Effect of Amplitude Modulation on the Protein Nebulization	85
5.2.6	Statistical Analysis	86
5.3	Results and Discussion	86
5.3.1	Aerosol Production Rate	86
5.3.2	Aerosol Size	88
5.3.3	Post-Atomization Biomolecular Integrity and Viability	90
5.4	Conclusions	92
6	Conclusions and Future Directions	95
6.1	Thesis Summary	95
6.2	Conclusions	103
6.3	Future Directions	103

A Patent: Microfluidic Apparatus for the Atomization of a Liquid	106
B Template-free Synthesis and Encapsulation Technique for Layer-by-Layer Polymer Nanocarrier Fabrication	116
C Pulmonary Gene Delivery Platform for DNA Vaccines via Ultrarfast Microfluidics	126
D Microfluidic Synthesis of Multi-Layer Nanoparticles for Drug and Gene Delivery	132
E A Portable Delivery System for Nano-Engineered Cargo Carrying Genetic Immuno-Therapeutics Driven by Surface Acoustic Wave Devices	143
F Optimised Surface Acoustic Wave Atomisation via Amplitude Modulation	152
G A Business Case for Respire[®]: A Novel Nebulizer for Pulmonary Drug Delivery	160

List of Figures

2.1	Images showing vaccination devices used for (A) classical ID immunization; and strategies for transdermal immunization such as (B) Soluvia TM (BD) pre-filled microinjection system; (C) Applicator for an improved solid microneedle array ; (D) solid microneedles of the Macroflux [®] using ; (E) array of silicon microneedles ; (F) coated microneedles ; (G) coated and hollow microneedle arrays (3M); (H) silicon hollow microneedle ; (I) hollow microneedle array, MicronJet [®] (NanoPass); (J) dissolvable microneedle array from BioSerenTach; (K and L) blunt-tipped microneedle array, OnVax [®] (BD) and its electron microscopy image used for genetic immunization by Mikszta <i>et al.</i> in 2002 (1); (M) smart vaccine patch from Intercell; (N) PassPort TM patch (Altea) used for a a clinical trail involving recombinant influenza protein vaccination ; (O) powder jet system used for clinical studies involving DNA vaccines for HIV, influenza, hepatitis B and malaria. Images are re-printed with permission from Bal <i>et al.</i> (2010). Copyright 2010, Journal of Controlled Release.	21
2.2	A schematic showing the configuration of a pMDI.	28
2.3	A schematic showing a jet nebulizer.	31
2.4	A schematic showing an ultrasonic mesh nebulizer.	32

2.5 A schematic of the generation and propagation of SAW on a lithium niobate piezoelectric substrate from the application of a sinusoidal electrical signal. The SAW itself is a retrograde traveling wave, and a point on the surface travels in a retrograde fashion in comparison to the propagation direction of the SAW across the substrate. The energy of the SAW is confined to within a few wavelengths of the substrate surface. This acoustic energy leaks into and drives strong acoustic waves in the fluid drop that in turn lead to acoustic streaming, recirculation, and the formation of capillary waves on the drop's surface. With sufficient input energy, these waves become large enough to cause droplets to be ejected from some of the crests in an intermittent fashion. (b) Image of the SAW device showing the aluminium-chromium IDT electrodes patterned on the piezoelectric substrate. The enlargement shows the IDTs, and specifically the relationship between the width and gap between the fingers and the SAW wavelength λ . (c) Image of the 30 MHz SAW device patterned with a pair of aluminium-chromium single-phase unidirectional transducers (SPUDTs). The curved geometry of the electrodes allows the SAW to be focused for more efficient operation. 40

3.1 Measured using laser diffraction (Spraytec, Malvern, UK), the size distribution of droplets nebulized using SAW at 30 MHz and 3 W of applied power from an aqueous suspension of 100 $\mu\text{g}/\text{m}\ell$ of pDNA is generally reduced as the concentration of glycerol is increased to 20%. 52

3.2 Structural analysis of pVR1020-MSP4/5 before and after SAW nebulization at 30 MHz by AFM imaging in air. (a) pre-nebulized (control), and (b) post-nebulized supercoiled structures of 5.6 kbp DNA. (c) Ethidium bromide agarose gel electrophoresis for the assessment of the naked pDNA structural integrity before and after SAW nebulization. Lane M: 1 kbp DNA ladder; lanes 1 and 4: control pDNA prepared at 85 $\mu\text{g}/\text{ml}$ and 50 $\mu\text{g}/\text{ml}$ concentrations, respectively; lanes 2 and 5: recovered 85 $\mu\text{g}/\text{ml}$ and 50 $\mu\text{g}/\text{ml}$ pDNA nebulized with 20MHz SAWs, respectively. Each lane was loaded with 200ng of pDNA and representative gels from three independent experiments are shown. Arrows indicate the position of open circular (OC) and supercoiled (SC) forms of pDNA along the vertical direction. Statistical analysis showing the proportion of (d) supercoiled, (e) open circular and (f) fragmented pDNA, for 20 and 30 MHz SAW nebulization. The amount of supercoiled, open circular and fragmented pDNA was assessed with results from the agarose gel electrophoresis and are the average of triplicate nebulization runs in which the error bars indicate the standard deviation of the data. 57

3.3 (a) Western blot detection of PyMSP4/5 expressed in COS-7 cells at 48 hrs post-transfection. Lane M: marker showing molecular mass standard (kDa) on the left; lanes 1-3: the cells transfected with pDNA recovered from 30, 50 and 85 $\mu\text{g}/\text{ml}$ pDNA nebulized using 30 MHz SAW; lanes 4-8: the cells transfected with pDNA recovered from 25, 35, 50, 65 and 85 $\mu\text{g}/\text{ml}$ pDNA nebulized using 20 MHz SAW. (b) Statistical analysis of the *in vitro* transfection efficiency of naked pDNA recovered after SAW nebulization. The results are the mean of triplicate nebulization runs, where the error bars indicate the standard deviation of the data. . . . 58

- 4.1 Schematic drawing of pulmonary DNA vaccination system to sheep via inhalation where room air was drawn through a bacterial/viral filter and a one-way valve placed in the inspiratory limb of where pDNA was introduced by nebulization with the 30 MHz SAW device in a chamber that was placed in line with a mechanical ventilator to be drawn by the sheep. Each sheep received three immunizations, once per three week period, with a pDNA aerosol containing sterile pVR1020 encoding HA in 5% dextrose at a concentration of 85 $\mu\text{g}/\text{ml}$ for 20–30 minutes through an endotracheal tube inserted through the nostril with proximal end connected to the respiratory wall. The expired gas was passed through a second filter-valve combination before exhausted through the ventilator. 65
- 4.2 Confocal microscopy of mouse lung parenchyma cryosections after (a, b, c) dosage with post-nebulized pVR1020–YFP in 0.9% NaCl aqueous solution, compared to an (d,e,f) untreated case (scale bars: 100 μm). The lung structure (a,d) and (b,e) cell nuclei are indicated with a counterstain of hematoxylin and eosin, and with DAPI, respectively. Lung cells expressing YFP from instilled pVR1020–YFP appear green in (c) the treated lung sample; note absence of green in the (f) untreated sample. The control lung samples were imaged at a higher resolution to confirm the absence of YFP response. 69
- 4.3 YFP expression in a cluster of epithelial cells around the terminal airways. (a) Lung cell nuclei stained with 4',6-diamidino-2-phenylindole dilactate (DAPI dilactate) appear blue while cells expressing YFP appear green (scale bar = 5 μm); (b) another view of a part of the YFP-expressing cell region shows the YFP distribution in the cells with appropriate filtering to show only the nuclei (left panel) and YFP (right panel) (scale bar = 5 μm). 74

4.4	Western blot of the supernatant obtained from homogenized mice lungs harvested (left lane) 24 hrs post-transfection with pVR1020–YFP plasmid that was SAW nebulized at 30 MHz and instilled, compared to (right lane) the supernatant from untreated mice lungs. The resulted YFP protein appears clearly at 27 kDa.	75
4.5	Examination of mouse lung cross-sections stained with Perl’s Prussian blue and counterstained with neutral red shows no hemosiderin deposits, indicating the absence of microhemorrhages in the tissue of (a) lungs instilled with pVR1020-YFP plasmid solution post-SAW nebulization and (b) untreated lungs. (scale bars indicate = 100 μm).	75
4.6	Systemic and mucous antibody responses detected in the sera of female Sprague-Dawley rats ($n = 8$ per group) following pVR1020-HA pDNA vaccination encoding an influenza A virus surface antigen, human hemagglutinin via lung instillation. No significant (NS) differences between the pre- and post-SAW nebulized vaccine instillation were found ($p = 0.163$ for IgG and $p = 0.486$ for IgA, respectively), and a significant difference between these and the naïve rats was found ($p < 0.001$).	76
5.1	(a) Initial prototype of the battery-powered circuit to be used to drive the SAW microfluidic aerosol delivery platform (scale bar = 1 cm). (b) Typical signal generator and amplifier used in laboratory settings to provide sufficient power for the SAW atomization (scale bar = 3 cm).	80

5.2 (a) Image of a 30 MHz SPUDT SAW device. The fluid is delivered to the SAW substrate through a paper strip embedded in a capillary tube which is connected to a reservoir. In order to record the aerosol production rate, the capillary tube was marked along its length at 0.5 cm intervals. (b) Enlarged view of the SPUDT. The width and gap of the interleaved finger electrodes determine the SAW wavelength λ_{SAW} , 132 μm for a 30 MHz device. (c) The left panel is a schematic illustration of the SAW atomization mechanism. The SAW (not shown to scale) propagates along the substrate and leaks energy into the liquid film to drive the destabilization of its free surface (2). The right panel illustrates the set-up used to condense and collect the aerosolized DNA or antibodies within a conical Falcon tube for further *in vitro* characterization of their post-atomization viability. 83

5.3 Representation of pVR1020 with vector encoding the hemagglutinin (HA) gene sequence. Gene encoding HA is inserted in plasmid VR1020 that contains secretion signal of tissue plasminogen activator (TPA), human cytomegalovirus (CMV) early promoter, CMV intron A, bovine growth hormone (BGH) terminator and kanamycin resistance gene. 84

5.4 (a) Gel electrophoresis of post-atomised plasmid DNA showing the effect of the amplitude modulation at various frequencies on the structural integrity of the pDNA. Lane M: 1 kbp DNA ladder; Lane 1: Atomization at 1.5 W without amplitude modulation; Lanes 2–9: Atomization at 1.5 W with amplitude modulation at 500 Hz, 1 kHz, 5 kHz, 10 kHz, 20 kHz and 40 kHz, respectively. Each lane was loaded with 250 ng pDNA and representative gels from three independent experiments are shown. Arrows indicate the position of the open circular (OC) and supercoiled (SC) forms of the pDNA. (b) Percentage retention of post-atomised supercoiled (shaded) and open circular (unshaded) pDNA compared to the unatomized sample. The results shown are the mean of triplicate atomization runs with the error bar showing the standard error of the mean. . . . 93

5.5 Post-atomized YFP antibody samples spotted onto a dot blot showing the preservation of the bioactivity of protein molecules in samples with and without amplitude modulation. Lane 1: No atomization; Lane 2: Atomization at 1.5 W in the absence of amplitude modulation; Lanes 3–8: Atomization at 1.5 W with amplitude modulation at frequencies of 500 Hz, 1 kHz, 5 kHz, 10 kHz, 20 kHz and 40 kHz, respectively. 94

6.1 A pDNA-laden meniscus forms at the end of the cellulose fiber wick upon the activation of (a) the SAW nebulizer and pDNA nebulization occurs inside the vial. Atomic force microscopy (b,c) and ethidium bromide agarose gel electrophoresis (d) of pVR1020–PyMSP4/5 (b) before and (c) after nebulization. Lane M: 1 kbp DNA ladder; control lanes 1 and 4, recovered pDNA post-30 MHz lanes 2 and 5, and post-20 MHz SAW nebulization lanes 3 and 6 are each at 85 and 50 $\mu\text{g}/\text{ml}$ concentrations, respectively. The proportion of (d) supercoiled (SC), open circular (OC) and (e) fragmented pDNA quantifies the damage ($n = 3$). The error bars indicate the standard error of the mean. 99

List of Tables

3.1	Distribution of data collected from experiments in study.	49
3.2	The de Brouckere mean aerosol droplet diameter (D_{43}) using a 30 MHz SAW nebulizer at 3 W of applied power ($n = 4$).	52
4.1	Distribution of data collected from experiments in study.	68
4.2	Hemagglutination inhibition (HAI) activity for each rat; $n = 8$ for the control, naïve rats and for the vaccinated mice. HAI is strongly ($\gg 40$) induced in the sera by lung immunization with a post-nebulized pDNA sample encoding an influenza antigen at similar levels to a non-nebulized pDNA sample.	72
4.3	Hemagglutination inhibition (HAI) activity for each sheep ($n = 4$). HAI is strongly (> 40) induced in the sera by lung immunization via inhalation with a pDNA sample encoding an influenza antigen at significantly higher levels to pre-immunization.	72
5.1	Effect of amplitude modulation at various frequencies on the atomization rate	87

5.2 Effect of amplitude modulation at various frequencies on the aerosol volume mean diameter D_{v50} . For each experiment, the fluid was atomized for 20 seconds with 50 data points sampled every second. This was repeated four times for every parameter set, i.e., $n = 4000$ data points for each set of parameter values 88

List of Acronyms

APC	Antigen Presenting Cell
COPD	Chronic Obstructive Pulmonary Disease
CTL	Cytotoxic T lymphocyte
DPI	Dry Powder Inhalers
EHDA	ElectroHydroDynamic Atomization
ELISA	Enzyme-Linked Immunosorbent Assay
FDA	Food and Drug Administration
GAVI	Global Alliance on Vaccines and Immunization
HA	Haemagglutinin
IDT	Interdigital Transducer
LN	Lithium Niobate (LiNbO ₃)
SAW	Surface Acoustic Wave
SPUDT	Single-Phase Uni-Directional Transducer
PATH	Program for Appropriate Technology in Health
pDNA	plasmid DNA
pMDI	Pressurized Metered Dose Inhaler
WHO	World Health Organization

List of Symbols

γ	Surface Tension
μ	Viscosity
ρ	Density
f	Excitation/Driving Frequency
f_c	Capillary Frequency
R	Characteristic Drop Dimension
λ	Capillary Wavelength
H/L	Liquid Film Height/Liquid Film Length
U	Wave Velocity
D_v	Aerosol Diameter in Volume Distribution

Chapter 1

Introduction

1.1 Pulmonary Drug Therapy and Vaccination

Inhalation therapy is the most efficient method for the treatment and prevention of lung disease because of its accessibility and the large surface area available for drug therapy; further, pulmonary delivery constitutes a pain-free non-invasive route that circumvents the challenges and risks associated with parenteral routes (3). Pulmonary delivery is extremely pertinent and effective for the management of diseases such as chronic obstructive pulmonary disease (COPD) and Asthma, especially when therapeutics are to be provided via inhalational or injectable routes. More recently, aerosol delivery has expanded the role of aerosol therapy into the fields of systemic drug delivery, gene therapy, and vaccination (4). The attractiveness of pulmonary delivery of vaccines for the treatment of respiratory diseases stems from the fact that topical drug deposition to the lung provides a fast therapeutic effect and reduces systemic side effects.

The rising incidence of respiratory disorders, and the growing prevalence of influenza, asthma and chronic obstructive pulmonary disease (COPD) as chronic lifestyle-induced disorders mean that innovations in pulmonary drug delivery technologies, and improved patient outcomes, will stimulate global pulmonary drug delivery technologies market,

which is predicted to reach US\$37.7 billion by 2015 (5). Innovations in pharmaceutical formulations, the significant potential of protein-and peptide-based therapeutics, the emergence of sophisticated inhaler devices, consumer desire for alternatives to injections and the growing obscurity between a drug and its delivery are other factors, which currently guide growth patterns in the industry. The respiratory disease market is becoming increasingly saturated for most drug classes, such as inhaled steroids and bronchodilators. Since this trend will continue in the near future, choice of device-rather than choice of drug-is set to become one of the driving forces behind pulmonary disease management. The development of novel devices with improved features is therefore becoming increasingly important for companies in order to differentiate their product offerings (6).

The primary aim of this thesis is to address the current challenges associated with the pulmonary devices used for drug therapy in the area of DNA vaccination through the application of a novel non-invasive pulmonary vaccination method based on surface acoustic wave nebulization. This chapter begins with Section 1.2 which introduces the current challenges faced during effective pulmonary drug therapy and explains the need for a novel platform, followed by Section 1.3 which provides an overview of the surface acoustic wave technology proposed. Then, Section 1.4 identifies open issues in existing mitigation strategies in the field of aerosol drug therapy, and outlines the objectives and contributions of the research presented in this thesis. Section 1.5 provides an outline of the thesis structure.

1.2 Challenges in Pulmonary Drug Therapy and Genetic Vaccination

The most commonly used pulmonary delivery devices include metered-dose inhalers (MDIs), dry powder inhalers (DPIs), jet or ultrasonic nebulizers and electrohydrodynamic

(EHD) devices. Inhalers generally require either hand-inhalation coordination or passive breath-driven aerosolisation, rendering them ineffective for many patients suffering from severe forms of COPD, who are unable to self-medicate (7). In addition, macromolecules such as pDNA are not soluble in propellants and have to be formulated as solid dispersed systems, resulting in instability of the formulations for practical use (8). A significant limitation in the use of nebulizers for pulmonary gene delivery (including other nucleic acid vaccines such as pDNA, siRNA and mRNA) to date arises due to the denaturing of non-complexed DNA as a consequence of the large hydrodynamic shear stresses or shock waves that arise during the jet or ultrasonic nebulization process (9). Although active aerosolisation methods such as nebulizers are more appropriate for this specific patient group, these nebulizers lack efficiency, usability and the flexibility to accommodate patient breathing and lung variability, thus failing to cater for the “one-size-fits-all” strategy. Moreover, the delivery of sufficient drug into the diseased lung remains challenging because it requires a pulmonary delivery device which is able to generate drug particles in a narrow range of 1–5 μm to achieve optimal lung deposition (1–2 μm = Deep lung, 3–5 μm = upper lung) (10). Current inhalers are simply unable to deliver the appropriate dosage, with published data showing over 50% of users with asthma cannot obtain the proper dose into their lungs due to improper use of the device (11). The incidence of misdosage in the treatment of COPD is far higher because of the broad variety of lung capacities and physiology among people with this disease. Furthermore, the formulation of particles of a drug suitable for pMDI, DPI, and BAI delivery can significantly add to its development cost (>20%)-for drugs that can be formulated into dry particles; a substantial proportion of candidate drugs cannot survive spray or freeze drying (6). Choosing a suitable device to administer a drug is therefore as crucial to effective treatment as the selection of the drug itself.

To achieve effective immunization, multiple dosing regimes may be required, although the delivery challenges remain the same. Highly immunogenic genes such as for influenza,

may only require a single dose, but in most cases, more than one immunization is required to provide a response strong enough to be protective (12). Thus, the vaccine delivery platform must accommodate the relevant DNA vaccination dosage strategies.

An ideal device could therefore lead to improved disease control. However, none of the devices on the market have all the characteristics of an ideal device, meaning that physicians need to compromise to achieve beneficial outcomes in selecting a match between a device, a drug and a patient population in order to overcome the drawbacks of the delivery technology.

1.3 Towards Modern Aerosol Delivery Systems for the Efficient Delivery of Difficult Therapeutics: Surface Acoustic Wave (SAW) Nebulization

The primary focus of this thesis is to adopt a technology ubiquitous in another field but entirely new to drug delivery to eliminate the drawbacks discussed earlier. Surface acoustic wave (SAW) technology has been used in mobile phones for years, multiplexing/demultiplexing voice and data in collision-free communication between many users' phones and the communications towers placed about a region to provide service to these phones. It has also been a key means to provide a controlled frequency and a timer, in the form of the most common type of device, anachronistically called a crystal. For decades, fluids-especially isopropyl alcohol-have been used to identify the vibration of these materials and confirm their operation (13). Surprisingly, the idea to manipulate fluids and nebulize them into a mist awaited someone who realized the potential applications for such technology.

Recently, a miniaturized nebulizer using SAW technology was developed as a pulmonary drug delivery platform, termed Respire[®] (14). The Respire[®] technology is a 'first in

class' nebulizer based on SAW technology (15) for the delivery of nebulized fluids containing biologically-based medications to the lungs. The technology offers dose control through delivery timing upon inhalation and a broad ability to control droplet size through formulation to target specific regions of the lung most affected by disease. Using SAW nebulization and through the development of refined formulation technology, we can solve the formulation and aerosol problems for drug delivery to the lung and create a discreet, handheld nebulizer that will accommodate unique drug classes and patient variability in inhalation profiles and dosage needs.

The unique advantages are attributable to the ultrasonic nebulization based on SAW atomization. Surface acoustic waves are MHz to GHz-order, transverse-axial polarized elliptical electroacoustic waves with displacement amplitudes of only a few nanometers. They are generated on and traverse the surface along the x-axis of 127.86° y-rotated single-crystal lithium niobate (LiNbO_3), a piezoelectric material which is low-cost as a consequence of its ubiquitous usage in telecommunications for the past three decades. Unlike typical ultrasound, a bulk phenomenon, the SAW is confined close to the substrate surface, its amplitude decaying rapidly over a depth of four to five wavelengths (for example, this corresponds to several hundred microns in a 20 MHz SAW device) into the substrate material, making mounting the device straightforward in contrast to standard ultrasonic atomizers. Further, compared to these same ultrasonic atomizers that consume power on the order of 10 W, SAW atomizers only consume between 0.5–3 W, since most of the acoustic energy is isolated to a small region near the surface and efficiently transmitted into the fluid.

Moreover, the 10–100 MHz order frequency employed in SAW devices, being significantly higher than the 10 kHz–1 MHz frequency range of typical ultrasonic devices, induces vibrations with a period much shorter than the molecular relaxation time-scale associated with large molecules in liquids, and thus the risk of denaturing molecules or lysing cells is greatly reduced. Further, as the frequency is increased, the power required

to induce cavitation increases far beyond what is needed for atomization, eliminating the effect of cavitation-induced lysis or shear in SAW atomizers.

The Respire[®] system generates monodisperse drug aerosols of controlled size, from 1 to 20 microns in diameter, in a range definable by the characteristics of the atomizing fluid and atomizer design; over many runs of the device, the range of the droplet mist diameter falls within 100% of the target diameter. Most desktop nebulizers produce broadly polydisperse mists, from a few microns to hundreds of microns in diameter and not in the 1–6 μm range which is optimal for regional lung deposition. This wastes the drug in the process. Only the latest mesh nebulizers avoid this problem by driving fluid through the orifices of a mesh. However, a mesh is easily clogged and difficult to clean, and any alterations to a drug's formulation will not alter droplet size.

The Respire[®] technology is simple, it does not require multiple steps and specific skills to operate it. The technology is efficient enough to operate using battery power, and can deliver even large doses of drug in a few inhalations due to reduced waste, in notable contrast to the large nebulizers that are a fixture of doctors' offices. The design of the proposed device utilizes IC MEMS wafer-based manufacturing suitable for mass production and therefore inexpensive, making it practical for clinical translation.

In an *in vitro* proof-of-concept study using a short-acting β_2 -agonist, the Respire[®] technology generated a mean aerosol diameter of $2.84 \pm 0.14 \mu\text{m}$ (14). This lies within the optimum size range, confirmed by a twin-stage impinger lung model, demonstrating that approximately 70 to 80% of the drug supplied to the atomizer is deposited within the lung as opposed to the typical 30%–40% lung dose obtained through current nebulization technologies.

Thus the Respire[®] technology presents a paradigm shift in drug delivery to the lungs by offering an in-home and clinical nebulizer which can be used to administer biologically based medications to the lungs. The technology offers a broad ability to control droplet

size through formulation to target specific regions of the lung most affected by disease.

1.4 Thesis Objectives and Scope

1.4.1 Aerosol Gene Therapy via Ultra Fast Microfluidics Driven by SAW Nebulization

There has been significant interest to date in the potential of pulmonary-delivered gene therapy in treating pulmonary diseases caused by single gene mutation such as cystic fibrosis and α 1-antitrypsin deficiency (16). This is because of the benefits associated with pulmonary delivery previously mentioned in Section 1.1, which circumvents the logistic difficulties and risks associated with parenteral routes (e.g., infection, provision of clean needles and systemic side effects) (3). Pulmonary vaccination is useful against a range of infecting pathogens since it induces immunity at mucosal sites through which these agents enter the body (17).

Conventional methods including jet and ultrasonic nebulizers for the pulmonary DNA delivery of gene therapeutics are currently ineffective, as they largely fail to maintain the viability of large biomolecules such as DNA due to the large shear stresses induced during the nebulization process (9).

The first objective of this research is the development of a novel platform for the production of monodispersed aerosol-laden plasmid DNA (pDNA) within a defined size range suitable for efficient pulmonary delivery to the lower respiratory airways for optimal dose efficacy, based on surface acoustic wave (SAW) nebulization.

Unlike other nebulization systems, the Respire[®] system is actuated by a SAW mechanism where a traveling nanometre-amplitude acoustic wave propagates atomisation of a

sessile drop of drug solution to form aerosol droplets. Due to the localization of the electroacoustic energy to within four to five wavelengths (a wavelength is typically 200 μm) in depth from the surface, SAWs are a highly efficient method for transferring energy into a fluid, requiring far less energy than ultrasound, where the acoustic energy is transferred through the bulk of the medium instead of being localized on the surface. When atomised, the size of the droplets generated may be changed by about an order of magnitude in a few microseconds in a controlled manner by switching from standing-wave to traveling-wave SAW on the substrate. Hence, a SAW approach has significant advantages over the current generation of ultrasonic medical nebulizers, which represent the current state-of-the-art. Due to the large surface acceleration associated with the propagation of the SAW, typically 10 million g's, a fluid drop placed on the substrate will rapidly destabilize beyond a threshold power, around 1W, and be atomised to form a monodisperse mist of aerosol droplets within the 1-6 μm optimal range for regional lung deposition.

The potential of the technology as a portable pulmonary delivery platform for gene therapy and DNA vaccination is demonstrated in Chapters 3 and 4. Most importantly, extensive studies had been carried out to demonstrate the preservation of the viability of pDNA after being subjected to the SAW nebulization process. To investigate the gene expression of SAW-nebulized pDNA, *in vitro* experiments were conducted using immortalized African green monkey kidney cells. The cells were transfected with a condensed solution containing a SAW nebulized pDNA vector encoding a potential malaria vaccine candidate, merozoite surface protein 4/5, to assess the transfection efficiency.

In the second phase of this research program, based on the understanding of the effect of SAW nebulization on pDNA, *in vivo* studies of SAW-nebulized pDNA were carried out. First, *in vivo* gene expression studies were carried out using male Swiss mice when pDNA was delivered via intratracheal instillation. Next, *in vivo* immunization trials were carried out using a SAW nebulized pDNA vector encoding an influenza A virus surface antigen, human hemagglutinin ((H1N1) strain). Here, vaccine efficacy studies were carried out

using two animal models. First, pDNA vaccination was delivered via intratracheal instillation in female Sprague-Dawley rats. Then, SAW nebulized mist inhalation was carried out in female Merino-cross ewe lambs. In both those animal trials, pharmacodynamic and antibody responses were investigated following the pDNA vaccinations.

1.4.2 Effective Miniaturization Strategy for the SAW Nebulizer Using an Amplitude Modulation Scheme

As the last objective of the research program, the developed SAW nebulization platform for the delivery of pDNA vaccines was optimized. In particular, the use of miniature, portable chip-based microfluidic nebulization platforms in the current inhalation therapy market could potentially be accelerated by the optimization of the usage of available power systems in the simplest possible manner. In Chapter 5, amplitude modulation (AM) is presented as a simple yet effective means of optimizing the power requirement for a microfluidic nebulizer driven by surface acoustic waves. The effect of the AM at modulation frequencies of 500 Hz, 1 kHz, 5 kHz, 10 kHz, 20 kHz and 40 kHz sinusoidal signals on shear-sensitive biomolecules such as plasmid DNA and antibody molecules is presented in this chapter. Potential energy savings were sought, with those AM frequencies investigated for more efficient atomization. The effect of the AM scheme on the mean aerosol diameter was tested, which is particularly important when therapies are to be targeted for the deep lung regions.

1.4.3 Thesis Contributions

The research outlined in this thesis is novel, since the application of a SAW nebulization system for the safe aerosol delivery of a largely shear-sensitive bio-molecule such as a plasmid DNA vaccine has not been exploited to date. The ultimate goal was to achieve

aerosol vaccination by eliminating the need for needle injections and the associated problems. This achievement represents a breakthrough in the current state-of-the-art as it has not been achieved to date with the current nebulization systems, due to the significant levels of induced fragmentation, causing such biomolecules to lose their biological function. All of the work involved was initiated and carried out individually by the author with training provided by experts at Monash University in the respective areas. Tremendous efforts were taken to extend the project from a bench study to testing of the nebulizer in a large animal model (sheep). All of the work involved in the sheep experiment was completed as part of the PhD, including planning the experiments, preparation of the drug, testing and composition of the nebulization system with the accompanying circuitry, experimentation and the subsequent assays performed to test the effectiveness. This result is the first known successful vaccination via inhalation using an unprotected pDNA vaccine in a large animal model; hence it is the first in the field to provide a new means of needle-free DNA immunization in areas or at times when there is a shortage or lack of medical infrastructure and skilled personnel.

In the second aim of the research project, amplitude modulation was applied to SAW atomization, which requires the highest energy input levels of all known SAW microfluidic processes. The application of an amplitude modulation scheme for the delivery of biomolecules using SAW atomization has never been studied to date. Here, the results showed that power savings of around 40% could be achieved through the initiation and subsequent application of the testing of this scheme for use in the delivery of shear-sensitive biomolecules. This discovery has enabled an exciting miniaturization strategy (invention disclosure submitted) to enable the SAW nebulizer to be used as a portable system. In addition, the results of the study can also be extrapolated to reduce the power requirements. This will enable the miniaturization and integration of the power supply with the existing chip-based SAW microfluidic platform to drive a whole range of microscale and nanoscale fluid actuation and bioparticle manipulation processes on a truly

integrated chip-scale device.

In summary, all of the above contributions are significant, and involve not only a great deal of novelty but also initiation and innovation.

1.5 Thesis Outline

The structure of the thesis is as follows: a critical review of non-invasive gene delivery approaches reported in the research literature is presented in Chapter 2. In Chapters 3 and 4, the research outcomes that resulted in the exploitation of SAW nebulization for the delivery of unprotected plasmid DNA (pDNA) vaccines are presented. Firstly, in Chapter 3, the effect of SAW nebulization on pDNA is investigated. This understanding was then used to achieve successful DNA vaccination *in vivo*, as demonstrated in Chapter 4. These chapters also detail the experimental methods used in the investigation and are followed by the results and discussion. Thirdly, the developed SAW nebulizer was optimized via the application of the amplitude modulation scheme, leading to the improved performance for the delivery of biomolecules such as proteins and pDNA. These results are included in Chapter 5, together with validated results for the justification of such use. Conclusions of the research project and suggestions for future research directions are provided in Chapter 6.

Chapter 2

Towards Non-Invasive Genetic Vaccination

2.1 Introduction

Vaccination is one of the greatest successes of medical science, and saves more than 8 million lives annually (18). A successful vaccine stimulates pathogen-specific immune responses by inducing strong B cell and T cell responses against microbes by exposure to antigens of the microbe in question to protect against subsequent challenge. Smallpox is the only human disease that has been intentionally eradicated from the earth due to a worldwide vaccination program. Polio and many other diseases such as diphtheria, measles, tetanus have been controlled by vaccination (19).

Vaccination is regarded as the key intervention for emerging diseases such as influenza, a major public health concern with a huge annual toll of morbidity, mortality, and economic loss. Currently, the preventive bottleneck is primarily due to the lack of facilities to create and deliver suitable vaccines. An increasing body of evidence demonstrates that successful vaccination is not only dependent on the nature of the vaccine's immunogenic properties, but also on the delivery technologies used for vaccine administration (20). Therefore, the search for an effective vaccine formulation and delivery system is of

paramount importance.

Several features of DNA vaccines make them more attractive than conventional vaccines; thus, DNA vaccines have gained global interest for a variety of applications, whereby the disease treatment occurs at a molecular level through the induction of gene based products *in vivo*. DNA vaccine plasmids can be constructed using simple recombinant DNA techniques, where number of immunological components can be encoded against different antigens of the same pathogen or different pathogens. The generic production and verification techniques employed during pDNA vaccine manufacture processes simplifies vaccine development. Moreover, pDNA vaccines are thermally stable and does not need a series of refrigerators required to maintain the viability which dramatically reduces vaccine storage costs.

Ideally, pDNA vaccination would address the many shortcomings of injection (21), but alternative routes—pulmonary, for example (22)—have proven disappointing. The safe generation of pDNA aerosols appropriately sized for deep-lung delivery is of great interest when tackling diseases with the potential to create a pandemic such as influenza (23), especially in developing areas of the world that lack sufficient medical infrastructure. Moreover, since vaccination via the respiratory route mimics the natural route of infection for many pathogens, the induction of a protective immune response at the pulmonary mucosal site would be ideal (24).

In this chapter, first in Section 2.2, a brief introduction to the exciting field of gene therapy and DNA vaccination will be provided. Then, Section 2.3 explains the need to create patient-friendly vaccination strategies that are non-invasive for the safe delivery of genomic material. This is followed by Section 2.4, where a comprehensive survey of current strategies for non-invasive gene delivery is presented. The current state of patient-friendly vaccination technologies available for DNA vaccination, such as needle-free injection, sublingual/buccal delivery, ocular delivery, transdermal delivery and intranasal delivery,

will then be discussed for their merits and shortcomings. Next, in Section 2.5, DNA vaccination to the inhalation/pulmonary route will be discussed in greater detail. Next, Section 2.4 contains a brief review of the aerosolization devices used for gene delivery and DNA vaccination. The drawbacks associated with current technologies will be presented here, justifying the need for a novel aerosolization platform that addresses those issues.

The rest of the chapter is organized as follows. Section 2.6 describes the development of the safe pulmonary delivery of unprotected DNA vaccines using a novel technology employing SAW atomization. This section also provides background information on the SAW mechanism for the generation of biological aerosols. In the last section, some conclusions are included.

2.2 Towards a Better Vaccination Strategy: DNA Vaccination

Various strategies have been exploited to develop vaccines targeted at the immune system for infectious diseases caused by agents such as viruses, bacteria or protozoan parasites. Some of the most effective vaccines against human and animal infectious diseases are composed of attenuated whole organisms that have been inactivated so that they no longer infectious, whilst retaining their antigenicity. Immunization is primarily achieved through the stimulation of the production of neutralizing antibodies against microbial antigens that protect the individual in subsequent challenges. Many of these have been empirically designed without a thorough understanding of the protection mechanisms, which has led to dreadful side effects in the past, seen in pertussis (whooping cough), Sabin polio and measles, among others (25; 26). The complex nature of these traditional vaccines allows poor batch-to-batch reproducibility, leading to issues related to quality control (26).

The recent development of the fields of microbial pathogenesis and proteomics has enabled the production of much safer alternatives to vaccines. These include sub-unit vaccines comprising microbial proteins and polysaccharides that work similarly to traditional vaccines, and conjugate antigens coupled to proteins that activate T helper cells with higher affinity. In spite of the safety advantages offered by these vaccines, they have very short half lives *in vivo* and are highly immunogenic owing to multiple dosage requirements and consequently high production costs (25). Due to the recent realization of the unique advantages of adjuvants or stabilizing compounds over other types of vaccines, including the ability to stimulate cell-mediated immunity, which has constituted a long-term challenge in the field, there has been a sudden increase in demand for such compounds. The new approach of inducing cellular-mediated immunity includes the incorporation of microbial antigens into viral vectors, which then infect host cells to produce antigens inside the cells. Currently, research is underway to achieve adequate attenuation of the virulence associated with those vaccines after noticing adverse reactions during human testing (27).

The explosive development of our knowledge in the field of genomics has enabled us to manipulate disease-causing genes for the treatment and elimination of the cause of disease. This area of research is referred to as “gene therapy”, and is a ‘non-viral’ approach, where the defective biological function is restored at the molecular level within cells during disease treatment. Unlike other vaccines comprised of protein and ribonucleic acid (RNA), deoxyribonucleic acid (DNA) has the potential to lead a new generation of reverse-engineered biopharmaceuticals in terms of production simplicity and high thermal stability (28). Genetic vaccination using plasmid DNA (pDNA) involves the recombination of the gene sequence, encoding a therapeutic antigen into the closed circular piece of pDNA and effective delivery to the target cells in the patient. Successful uptake of DNA by the target cells via endocytosis is necessary for subsequent entry into the nucleus (after escaping the degradative pathways) for the *in vivo* expression of the therapeutic

antigen (29). Most importantly, with this exciting approach, all types of desired immunity, including adaptive immunity (antibodies, helper T cells, cytolytic T-lymphocytes), and even innate immune responses can be induced (30).

2.3 Towards the Patient-Friendly Administration of Vaccinations

Despite the successful use of effective vaccination over many years to eradicate disease states, a large proportion of lives continue to be lost for a number of reasons, including the lack of vaccines against many diseases, coupled with poor immunogenicity, inefficiency, and unsafe vaccination practices. The widespread introduction of new vaccines hinges upon addressing key challenges associated with the significant cost of vaccination (31), which can be largely reduced by embarking on a vaccine delivery system that does not rely on the cold chain. Moreover, the inaccessibility of vaccines due to the high costs involved in acquiring the vaccines, transportation difficulties, and the lack of "point-of-care" nature of the methods used to deliver the vaccines contribute to this burden. Moreover, injecting vaccines can be a complex process requiring trained personnel for administration, and used syringes and needles create a major waste disposal problem. Administration of drugs via unsafe injections is a major concern in developing countries, where 30-50% of immunizations can be delivered via unsterile injections (32). Therefore, in addition to effective yet cheap-to-produce vaccines such as pDNA vaccines, there is a growing need for a non-invasive delivery platform for such vaccines that can be applied universally.

The quest for the elimination of the use of needles and syringes has been prioritized by the Global Alliance on Vaccines and Immunization (GAVI), the Program for Appropriate Technology in Health (PATH) and the World Health Organization (WHO) (33). Moreover,

the search for non-invasive delivery of drugs is primarily advanced by the biopharmaceutical and specialty vaccine delivery industries investing in ways to address the shortcomings of the traditional injectable routes of administration (34). This is primarily to create new product opportunities and innovative treatment strategies that improve patient compliance and which can be easily implemented during mass immunization programmes. For injectable vaccines, patient compliance issues, such as injection-site reactions and patient preferences (needle phobia), suboptimal absorption and distribution of the administered drug to the intended target site, can potentially preclude the pharmaceutical market entry.

To create patient-friendly options that circumvent such problems, successful strategies for non-invasive vaccine drug delivery include needle-free injection, sublingual/buccal delivery, ocular delivery, transdermal delivery, intranasal delivery and inhalation/pulmonary delivery. The preferred immunisation route is pre-determined by the type of formulation to be used (e.g., suspensions, emulsions, powders, tablets) and the targeted patient group (e.g. children). For example, young children represent the largest cohort of vaccine consumers, and impose restrictions on strategies employed for vaccine delivery where poor patient compliance contributes to incomplete vaccination campaigns (35). Since infants and toddlers are less able to swallow tablets and capsules and nasal delivery has been shown to be related to increased wheezing (observed in clinical trial with FluMist) (36), alternative non-invasive vaccination methods such as pulmonary delivery would be ideal. Hence the rationale for using a vaccine delivery technology (e.g. microneedles, nasal sprayers and pulmonary inhalers) is aimed at improving the performance of the vaccine for the intended patient group.

2.4 Platforms for Non-Invasive Genetic Vaccination

In the successful development of effective genetic vaccines that are safe for human and veterinary applications, a diverse range of potential and proven technologies for non-invasive mechanical DNA administration have attracted significant interest (37). A comprehensive review of non-invasive vaccine drug delivery strategies, such as oral delivery, ocular delivery, transdermal delivery, intranasal delivery and inhalation/pulmonary delivery, is discussed in detail in the following sections.

2.4.1 Transdermal DNA Vaccination

Recent progress in the development of user-friendly injection systems to address the drawbacks associated with traditional needle injection systems has stimulated the ongoing clinical development of technologies for cutaneous vaccination (See Fig. 2.1). As the skin is the most accessible organ of the body, with unique immunological properties (high density of antigen presenting cells), it offers safe immune stimulation by allowing sustained and controlled delivery.

Successful DNA vaccination through the skin was initially demonstrated by the topical skin application of naked plasmid DNA formulations (38; 39; 40). Due to attention this approach received in the field of genetic vaccines, later research studies were undertaken to understand the kinetics underlying penetration by naked pDNA, and Kang *et al.* demonstrated the success of DNA delivery across skin tissue (41). However, the dose of plasmid DNA used by Kang *et al.* was 300 g/mouse, which is about 3- to 10-fold the amount used in other studies (39; 42), raising issues related to scalability for future use in humans.

The cellular barriers of the uppermost layer of the skin, the stratum corneum, pose a major challenge to successful transdermal DNA vaccination requiring access either via physical or electrical means, preferably in a minimally invasive manner (43). To allow

the efficient delivery of DNA cargo, physical modes to enhance skin permeability via the use of photoacoustic waves (44), low frequency sonophoresis (45), and microneedles (46; 47) have been used. Much of the research on physical DNA vaccination to the skin has been pursued in the use of either drug-encapsulating or drug-coated microfabricated needles, usually in the form of a transdermal patch (48). The first use of microneedles to DNA vaccinate mice was demonstrated by Mikszta *et al.* in 2002, where they used pDNA-encoding hepatitis B surface antigen to induce both antibody titers and antigen-specific cytotoxic T cells (1). However, in this study, the amount of DNA vaccine that was delivered by BD Biosciences's OnVax[®] device was very low, hindering the use of the device in clinical studies. More recently, coated microneedles have been successfully used for DNA vaccination against hepatitis C, and results have shown effectively primed cytotoxic T lymphocytes in mice (49). However, coating biomolecules such as DNA onto microneedles can be a complex process and there have been reports of the reduction of immunogenicity during the coating process, leading to the need for the use of stabilizers during drying (50). In addition, skin irritability is often an issue with physical modes of cutaneous gene delivery, and therefore, other approaches involving the use of electric and acoustic fields via methods such as iontophoresis (51), electroporation (52) and ultrasonic processes (53) has been pursued. A number of research studies have demonstrated the feasibility of using electroporation in the delivery of DNA vaccination to the skin (54; 55; 56; 57; 58) and a combination of microneedles with electroporation was used for the successful pre-clinical demonstration of a smallpox DNA vaccine trial involving EasyVax[®] (59). However, methods involving electroporation and ultrasound requires careful placement of the source of radiation such that the energy is concentrated at the required region, which makes the process and the devices used quite complex. In some cases, excessive radiation can cause discomfort to the user and even result in jeopardizing the integrity of the sensitive biomolecules.

Needle-free injection systems, such as jet immunization, have been used for pre-clinical

and clinical evaluation of DNA vaccination systems using a PMEDTM device for numerous diseases such as HIV (60), influenza (61; 62), hepatitis B (63), malaria (64; 65) and for HIV (66), and using a Biojector[®] device for diseases such as rotavirus (67) and dengue (68). Similar to microneedle application, jet immunisation disrupts the cell barrier by employing a high impact force to deliver the biomolecules to the skin. In some cases, this causes unfavorable side-effects, such as mild burning at the application site, which usually lasts for a few hours (61; 62).

In summary, despite the potential advantages of DNA vaccination via the skin, the full benefits of this approach have not been fully realized, partly due to the lack of delivery devices that accurately and reproducibly administer vaccines to the skin. A review by Foldvari *et al.* in 2006 reported that there were no gene delivery systems proven as optimal for cutaneous gene therapy (69) and the field therefore remains somewhat less established. However, the future appears quite promising as transdermal DNA vaccination technologies proceed through clinical trials and become available for more widespread clinical and commercial use.

2.4.2 Oral Genetic Vaccination

DNA vaccination via the oral route presents one of the greatest therapeutic opportunities from a user's perspective because of its attractive factors, such as ease of administration. The oral route offers access to a large mucosal surface that is enriched with immune inductive cells (gut-associated lymphoid tissues) for successful induction of both mucosal and systemic immunity (70; 71). However, oral vaccine delivery has been one of the greatest challenges facing the drug delivery industry due to the hostile environment presented by the gastro-intestinal tract, with the presence of degradative enzymes coupled with the low pH, leading to denaturation of the DNA, hindering efficient delivery to the targeted intestinal epithelium. For successful oral DNA vaccination, a number of

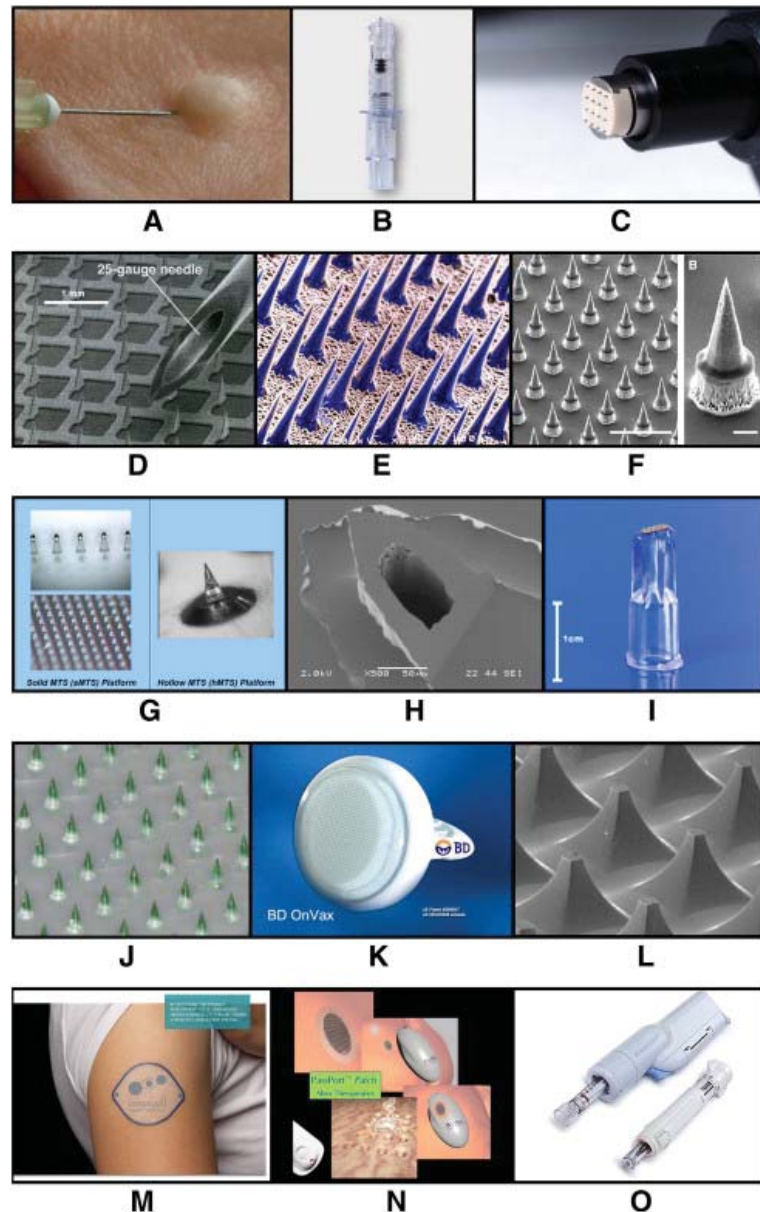


Figure 2.1: Images showing vaccination devices used for (A) classical ID immunization; and strategies for transdermal immunization such as (B) SoluviaTM (BD) pre-filled microinjection system; (C) Applicator for an improved solid microneedle array ; (D) solid microneedles of the Macroflux[®] using ; (E) array of silicon microneedles ; (F) coated microneedles ; (G) coated and hollow microneedle arrays (3M); (H) silicon hollow microneedle ; (I) hollow microneedle array, MicronJet[®] (NanoPass); (J) dissolvable microneedle array from BioSerenTach; (K and L) blunt-tipped microneedle array, OnVax[®] (BD) and its electron microscopy image used for genetic immunization by Mikszta *et al.* in 2002 (1); (M) smart vaccine patch from Intercell; (N) PassPortTM patch (Altea) used for a clinical trail involving recombinant influenza protein vaccination ; (O) powder jet system used for clinical studies involving DNA vaccines for HIV, influenza, hepatitis B and malaria. Images are re-printed with permission from Bal *et al.* (2010). Copyright 2010, Journal of Controlled Release.

research studies have focussed on the use of live bacterial vectors derived from attenuated bacterial pathogens such as Salmonella and Shigella, for the induction of systemic and mucosal antibody responses (72; 73; 74; 75; 76). To overcome barriers associated with cellular uptake, formulated DNA with a polymer delivery system has been explored extensively (77). Biodegradable polymer carriers such as poly(dl-lactide-co-glycolide) (PLGA) (78; 79; 80; 81) and chitosan (82), have been used to encapsulate the plasmid DNA vaccines to induce a protective immune response. Despite these efforts, oral DNA vaccination has been largely ignored compared to other non-invasive modes of vaccination, and no single oral vaccine has successfully completed phase I clinical trials to date (83).

2.4.3 Ocular DNA Vaccination

Gene delivery to the cornea represents an exciting therapeutic opportunity for the treatment of corneal and anterior segment diseases due to the benefits it offers, including ease of administration to an immune-privileged site (84; 85). The potential of ocular gene therapy has been realized in a large number of animal models (86; 87) and to date in six human clinical trials in retinal gene therapy, which have reported no safety concerns (88; 89; 90). However, DNA vaccination to the eye has gained little attention over the years with a limited number of studies reporting successful protective immune responses in animal models (91; 92). More recently, a research study reported ocular mucosal administration using a DNA vaccine encapsulated in an iron oxide nanoparticle and showed strong specific immune responses and protection against mucosal challenge with the herpes simplex virus in mice (93). Thus the full potential of this relatively new field of genetic immunization to the eye is yet to be realized.

2.4.4 Nasal DNA Vaccination

Since the respiratory tract is a common site of entry for numerous pathogens, DNA vaccination to the nasal epithelium may open the way to better vaccine efficacy. This method of vaccination has the potential to prevent pathogens from colonizing the mucosal surfaces, due to the presence of immune-rich tissue just beneath the nasal epithelial linings (nose-associated lymphoid tissues) (94; 95). In addition to the easily accessible tissue offering a simpler vaccination process with a lower antigen dose requirement over the oral route (96), the cost effectiveness offered is especially useful during mass vaccination campaigns.

Number of studies have demonstrated successful gene delivery to the nasal epithelium (97; 98; 99; 100; 101; 102; 103). In brief, the administration by nasal instillation of PEI-PEG (polyethylenimine-polyethylene glycol) to DNA complexes in mice resulted in significant levels of transgene expression in the lungs (97). Research has shown efficacious liposome-mediated gene transfer via nasal administration for the treatment of insulin-dependent diabetes mellitus (98). Moreover, successful liposome-assisted plasmid DNA vaccination was achieved in mice for a lethal influenza infection model (99) and for hepatitis B (100; 101). DNA-protein complexes (102) and more recently, immunostimulatory complexes (103) have been used for the induction of immune responses in mice.

For the successful development and application of DNA vaccination via the nasal route, the choice of the delivery device used for intranasal administration of vaccines is critical. Devices such as micropipettes and mechanical metered-dose spray pumps, that are typically used for intranasal delivery of vaccines, suffer from problems such as local irritation and nose-bleeds coupled with the unpleasant taste of concentrated drugs reaching the mouth (104). Moreover, accurate and repeated delivery of the formulated vaccine in a uniform manner to the nasal mucosa is often a challenge with these devices. Devices

such as OptiMist have been developed by BD Biosciences (105) to address most of these challenges with protein vaccines, and bidirectional nasal delivery has been demonstrated as a promising technology in a human clinical trial (106).

Given the success of technologies in the market (as seen with Flumist) for protein vaccination to the nasal epithelium, the potential of nasal vaccination is evident. However, DNA vaccination by the same route for human use has a number of obstacles to be overcome, including successful demonstration of efficacious, safe and easy to administer formulations, in conjunction with a device capable of repeated and targeted delivery.

2.5 Pulmonary DNA Vaccination: State-of-the-Art

2.5.1 Pulmonary DNA Delivery

The lung presents an attractive site for non-invasive delivery of gene therapy and DNA vaccination agents for a host of pulmonary and related conditions, because it is easily accessible, and has a large surface area for transfection that is highly vascularized. More importantly, pulmonary vaccination is associated with reduced systemic toxicity when compared to other vaccination methods as it avoids potentially deleterious interactions with the cellular barriers and serum proteins that are inevitably encountered via more invasive delivery approaches (107). Moreover, the lung is continuously exposed to the surrounding environment, including airborne pathogens such as the influenza virus, which represent a major global health burden. Vaccination to the lung ensures mucosal immunity for such infections; an important first line of defence that most systemically administered vaccines fail to generate adequately.

Effective pulmonary delivery would circumvent important barriers that have been observed in other routes of delivery especially in animals (for example, genomic integration

or autoimmunity) (4; 108). More importantly, adverse events that were observed with intranasal delivery of vaccines such as Bell's Palsy that were seen with FluMist in the early stages, can be clearly addressed by pulmonary delivery (109).

Pulmonary DNA delivery can be achieved in one of three ways: nebulization of DNA usually in a liquid suspension; aerosolization of a dry powder formulation containing DNA with a carrier molecule; or alternatively via pressurized expulsion with the help of a propellant dispersant. The most commonly used pulmonary delivery devices include metered-dose inhalers (MDIs), dry powder inhalers (DPIs), jet or ultrasonic nebulizers and electrohydrodynamic (EHD) devices.

The development of a safe and effective aerosol gene delivery platform that would be comparable to intravenous delivery has been a considerable challenge to the health care industry. Problems regarding efficiency, toxicity, convenience and the ability to repeatedly treat patients with chronic conditions need to be solved. In particular, the production of aerosol droplet sizes appropriate for optimal delivery to the peripheral lung to maximize the dose of DNA delivered to lung surfaces has been an issue. Most importantly, in order to comply with stringent regulatory requirements on product quality, it is necessary to demonstrate the retention of the supercoiled structure of the plasmid during the aerosolization process (22; 9).

The delivery of naked plasmid constructs in the size range of 5-20 kilo-base pairs (kbp) has been particularly challenging due to the shearing effects of the aerosolization process. To date, numerous studies have been undertaken in order to determine the feasibility of various pulmonary delivery devices for delivering non-complexed pDNA to the lungs (23; 22; 9). Overall, the results have been largely disappointing, with the supercoiled tertiary structures of pDNA with sizes larger than 5 kilo-base pairs (kbp) being sheared into open circular and fragmented DNA by the hydrodynamic shear and shock waves introduced during the aerosolization process. Gene transfer agents such as cationic lipids (110; 111)

and cationic polymers (112)(113) are used to form complexes with pDNA, which aim to protect pDNA from shear forces and increase its stability during aerosolization. This has led to successful gene expression after aerosol delivery to the lungs of mice (114; 110), rabbits (115) and sheep (116). However, not all lipoplexes and polyplexes retain biological efficacy after aerosolization (117; 118) and to date only formulations based on genzyme lipid 67 have successfully progressed to phase I clinical trials (119; 120).

The following sections will attempt to provide a brief review of the aerosolization devices used for gene delivery and DNA vaccination and outline the associated drawbacks, justifying the need for a novel aerosolization platform that addresses those issues.

2.5.2 Inhalers for Pulmonary DNA Delivery

Portable inhalers can be subdivided further into two broad categories, namely, metered-dose inhalers (MDIs) and dry powder inhalers (DPIs).

Metered-Dose Inhalers for Pulmonary Gene Delivery

MDIs were first introduced in the United States in the mid-1950s. Since then, the technology has continued to advance, improving drug delivery efficiency and patient convenience. Following the 1987 Montreal Protocol, chlorofluorocarbon (CFC)-based MDIs are being phased out, to be replaced by hydrofluoroalkane (HFA)-based MDIs. The first HFA-based MDI was introduced in the United States in 1995. Currently, pressurized metered-dose inhalers (pMDIs, or, more commonly, MDIs) are the most commonly used inhalers on the respiratory market, despite their low efficacy. In general, pMDIs consist of a container for the drug in the form of a suspension or solution, a metering valve attached to the container, and an actuator that connects the metering valve to an orifice (121), as shown in Fig. 2.2. A pMDI utilizes “hydrodynamic flow focusing” where external pressure is used to expel drug solutions from a nozzle.

Despite the popular use of pMDIs, they suffer from several technological complications during attempts at macromolecule aerosolization (such as pDNA) coupled with significant patient misuse (122; 123). The effective operation of a pMDI is reliant on the patient's coordination skills during inhalation, as patients are required to press the actuator, which then releases the drug solution with a single metered dose such that it passes through the orifice/nozzle sufficiently quickly to break up into aerosols, causing the pMDI devices to be low in efficiency. Moreover, the low lung deposition of pMDIs, with reported values in the range as low as 10–20% (124), is also attributable to the dependency on the fast evaporation of the aerosol to obtain the required 1–5 μm optimal size distribution from the large droplets initially produced by the device. Unfortunately, macromolecules such as pDNA are not soluble in pMDI propellants and have to be re-formulated as dispersed systems, which sometimes leads to instability issues associated with agglomeration (125). For this reason, biodegradable polymers such as chitosan have been investigated as a potential carrier for therapeutic pDNA during administration to the lungs, to improve compatibility in a pMDI delivery system (126). More recently, surfactant-coated pDNA nanoparticles have been used for pulmonary gene delivery via a pMDI and have shown successful gene expression with no significant toxicity in human lung epithelial cells when exposed to aerosolised pDNA particles (127). In this study, the cationic liposomal transfection agent dioleoyl-trimethylammonium propane (DOTAP) was shown to be essential in conferring the *in vitro* gene expression observed (127). However, further *in vivo* studies need to be conducted in order to validate such use of transfection agents for gene delivery and DNA vaccination via a pMDI before human use.

Dry Powder Inhalers for Gene Delivery to the Lung

DPIs were only introduced in the 1970s, and their use has been limited due to the overwhelming dominance of MDIs. Triggered by the 1987 Montreal Protocol, the use of DPIs has been increasing in the United States. Currently, DPIs (compressor-based) are

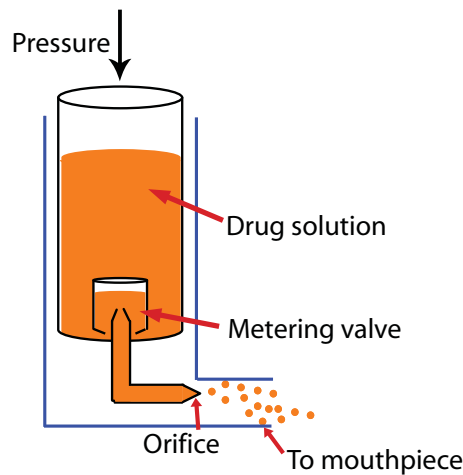


Figure 2.2: A schematic showing the configuration of a pMDI.

the highest-selling group of devices on the lung delivery market based on revenue, while pMDIs are sold in the highest volumes. This is simply because DPIs are available as simple, cheap, highly compact and disposable devices in a single-use format, making them especially useful during mass vaccination campaigns.

Although dry powder formulations for DPIs have considerable potential for gene therapy to the lung, several issues hinder their practical use. First, in order to obtain an effective lung dose from a DPI, it requires sufficient inhalation force from a patient's inspiration to draw the dry powder out of the inhaler and subsequently break them into smaller sizes to enable their transport into the lung for therapy. Therefore, if the inhalation is not sufficiently strong, or if there is a lack of hand-mouth coordination, insufficient dose delivery and incomplete powder break-up may result, leading to the unsatisfactory performance of the delivery.

Moreover, the formulation of chemically-unstable macromolecules such as pDNA as a dry powder formulation suitable for delivery via a DPI is also a complex and challenging process. Enhancement of the dispersibility of pDNA powders for improved aerosolization properties, sometimes requires the use of absorption enhancers such as dimethyl-beta-cyclodextrin (DMC) (128) and amino acids such as arginine and phenylalanine (129).

In addition, processes such as spray–freeze drying (130) and dispersing in supercritical carbon dioxide (131; 132) have been demonstrated as effective strategies to produce inhalable dry pDNA powders protected with chitosan for pulmonary gene therapy. In those studies, successful gene expression has been observed following pulmonary administration to mice (130; 131; 132). However, more toxicological studies are necessary before the clinical application of dry pDNA powders via a DPI could be approved.

Other Inhalers for Gene Delivery to the Lung

Breath-actuated inhalers (BAIs) overcome many of the compliance disadvantages associated with DPIs and pMDIs (i.e. coordination with inhalation), but they represent only a small share of the respiratory market, due to their relatively high price per standard unit of drug delivered and their limited availability. For this reason, there are no reports of their application for gene delivery purposes.

Summary

In summary, inhalers generally require either hand-inhalation coordination or passive breath-driven aerosolisation, rendering them ineffective for many patients suffering from severe forms of chronic obstructive pulmonary disease (COPD), who are unable to self-medicate and who are in most urgent need of treatment (133). Macromolecules such as pDNA are not soluble in propellants and have to be formulated as solid dispersed systems, resulting in instability of the formulations for practical use (8). As a result, extensive work has been undertaken on alternative methods of pulmonary DNA delivery.

2.5.3 Nebulizers for Pulmonary DNA Delivery

Nebulization remains the delivery method of choice for animal and clinical studies for achieving non-invasive gene therapy to the lung, as it can generate respirable liquid aerosols for a wider dose range accompanied by dose sparing. Nebulizers are generally used in hospital settings with the help of an external energy source and to administer liquid formulations in the doctor's office that can often not be administered via MDIs. The therapeutic is usually administered over a longer period of time, often to patients with poorer capacity to inhale drugs or with acute incidences of a particular lung disease, who are unable to use hand-held inhalers. The types of nebulizers commonly used for respiratory drug delivery are pneumatic or jet nebulizers and ultrasonic nebulizers.

Jet Nebulizers for Pulmonary Gene Therapy

First introduced in the middle of the nineteenth century, air-jet nebulizers represent the most commonly used class of nebulizers. The operation of a jet nebulizer entails the delivery of a pressurized gas to a liquid-gas interface to disrupt the surface tension forces, which subsequently breaks up the liquid into micron-sized aerosols (See in Fig. 2.3). A baffle or solid surface is subsequently used to collect large droplets by inertial impaction, while the remaining smaller droplets are entrained into the gas stream for patient delivery (134).

Past attempts to deliver non-complexed or naked pDNA via jet nebulization processes have been largely disappointing and caused the poor transfection observed. Unfortunately, the supercoiled tertiary structures of pDNA with sizes larger than 5 kilo-base pairs (kbp) were sheared into open circular and fragmented DNA by the hydrodynamic shear and shock waves created during the nebulization process when Pari LC[®] star and DeVilbiss[®] jet nebulizers are employed (135; 136). For this reason, cationic lipid systems (137; 117; 138; 139), polymeric carriers such as polyethyleneimine (PEI) (112; 140; 141) and

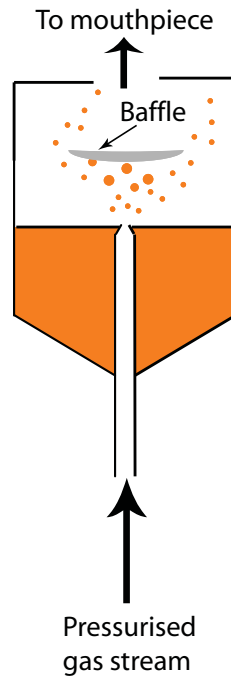


Figure 2.3: A schematic showing a jet nebulizer.

polycationic peptides such as protamine (142) and more recently biodegradable polymer nanoparticles composed of chitosan (143) have been exploited with the aim of protecting the pDNA from the shearing forces during the nebulization process.

Ultrasonic Nebulizers for Pulmonary Gene Therapy

Ultrasonic nebulizers have the potential for improved patient outcomes and greater lung deposition compared with inhalers and jet nebulizers because there is little requirement for patient coordination and little drug residual volume. They have quiet operation and provide high dosage delivery and fast drug delivery. An ultrasonic nebulizer utilizes a vibrating ceramic piezoelectric element connected to an alternating current at a frequency between tens of kiloHertz to a few megaHertz. The acoustic vibration generated by the piezoelectric element is then transmitted into a reservoir containing the drug solution, causing the formation of capillary waves. When sufficient destabilization is induced in the liquid meniscus at the reservoir orifice, the fluid breaks up into micro/submicron sized

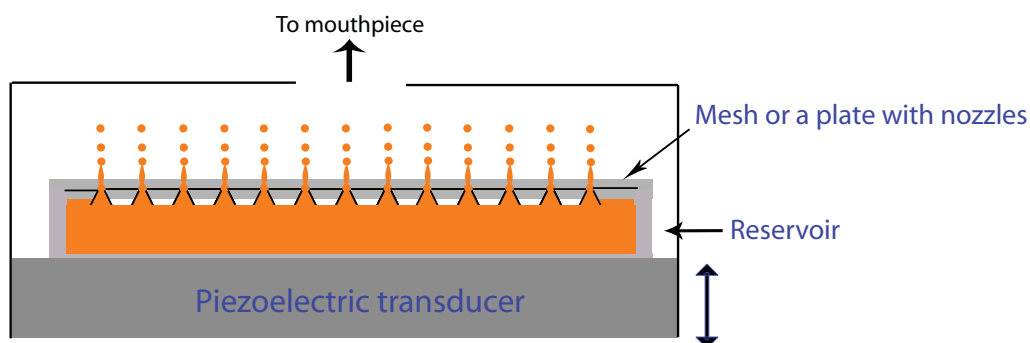


Figure 2.4: A schematic showing an ultrasonic mesh nebulizer.

aerosols (See Fig. 2.4).

The use of ultrasonic nebulizers to administer biomolecular agents such as pDNA has many important limitations, leading to their limited acceptance. They are expensive, more prone to electrical and mechanical breakdown and cumbersome, due to the larger AC power source required for their operation. For these reasons, they have not been widely researched for gene delivery applications compared to pMDIs, DPIs or air-jet nebulizers.

Only a limited number of studies have been performed on the use of ultrasonic nebulization of DNA for pulmonary delivery (22; 144). Most of these investigations have focused on protecting DNA from cavitation and mechanical shear forces by complexing the DNA with cationic agents such as cationic lipids, resulting in successful transfection in lungs of mice (145; 146) and also modified PEI (135), resulting in successful *in vitro* transfection of alveolar and bronchial cells (147).

Summary

Although active aerosolization methods such as nebulizers are more appropriate for geriatric and pediatric populations, these nebulizers in general lack efficiency, usability and

the flexibility to accommodate patient breathing and lung variability. Further, nebulizers typically are always-on instruments, producing inhalable mists with a broad size range which is wasted as the patient exhales. For these reasons, nebulizers are more expensive per dose. Moreover, the dependence on an external compressed air supply, or a large battery-driven compressor, makes the nebulizers cumbersome, noisy and less portable.

The research studies that have reported successful gene transfection following aerosol delivery via jet and ultrasonic nebulization platforms for complexed pDNA through the use of cationic agents (145; 146; 135; 147) may encounter problems during subsequent clinical studies. For instance, synthetic polymers like PEI are highly cytotoxic (148) and will encounter problems with approval for human use. Moreover, liposomes are not as effective for gene delivery to human airway cells *in vivo* when compared with transfection of airway cells *in vitro* (149).

Given the current limitations associated with nebulizers, there remains an urgent need to exploit other aerosolization strategies for gene delivery and DNA vaccination applications.

2.5.4 Other Aerosolization Devices for Pulmonary DNA Delivery

New devices such as mesh nebulizers (150), electrohydrodynamic (EHD) devices (151) and miniaturized nebulization catheter devices (152) claim to offer greater aerosolization efficiencies, and preserve the integrity of pDNA in the aerosols. However, these devices require more clinical studies before successful commercialization can take place for human usage.

2.6 Surface Acoustic Wave Nebulization for Safe Pulmonary Delivery of Unprotected DNA Vaccines

In order to improve genetic vaccination to the lung, the need for an efficient yet safe delivery platform for the aerosol delivery of DNA vaccines is evident. For this purpose, the use of naked DNA vaccines has advantages over other delivery methods, as it circumvents the potential host responses elicited by viral vectors and avoids the toxicity of cationic liposomal vectors. Moreover, the application of naked DNA is cost-effective, simple and less labour-intensive than other approaches, and may allow repeated treatments. However, it is of paramount importance that upon delivery of naked pDNA, its delicate structural properties are preserved. We therefore propose the use of surface acoustic wave devices as an appropriate platform to achieve this milestone.

2.6.1 Surface Acoustic Waves

Surface acoustic waves (SAWs) have been used for the manipulation of fluids since the 1880s when Lord Rayleigh investigated the propagation of SAWs in isotropic solids (153). In 1965, the first SAW device was invented by White and Voltmer, who used interdigital transducers (IDTs) to directly couple periodic radio frequency waves into a piezoelectric substrate to generate SAWs (154). IDTs consist of a series of interleaved electrodes made from metal that are deposited on a piezoelectric substrate by means of standard photolithography. Since the discovery of IDTs, SAW devices have become very popular in telecommunication applications and in commercial electronic devices such as delay lines and band-pass filters, among others (155).

SAWs have an amplitude of the order of nanometers that propagates over thousands of wavelengths of distance (which corresponds to several centimetres) along the surface of a low-loss piezoelectric material like lithium niobate (LiNbO_3 or LN) (2). Of the different

SAWs that exist, the most commonly used is the Rayleigh wave for atomization (2). The work involved in the present thesis involves the use of SAW technology for the production of sub-micron aerosols. It is therefore essential to review some seminal work conducted on this technique.

2.6.2 SAW Microfluidics

A comprehensive review of SAW microfluidic devices can be found in the literature (156; 157) and many SAW devices have been proposed for applications ranging from fluid manipulation, such as droplet transport (158; 159), microchannel pumping (160; 161; 162), mixing (163; 164) and jetting (165), and particle sorting and concentration (166; 164; 167) to chip-scale chemical and biochemical synthesis (168; 169), biosensing (170), and microfluidic chip interfacing with mass spectrometry (171; 172). In addition, it is also possible to exploit SAW to drive these microfluidic manipulations on disposable superstrates (173; 174).

It has been shown previously that SAWs can be used to produce particles of a defined size range through the manipulation of the factors that predict the droplet diameter (2). The feasibility of this technique has been demonstrated by Friend et al, where biodegradable polymer particles comprising poly- ϵ -caprolactone (PCL) were produced. These PCL aggregates were between 150 and 200nm in size and each aggregate was composed of nanoparticles of 5 - 10nm in diameter (175). In this research, a nucleate templating process was employed for rapid spatially-inhomogeneous solvent evaporation following SAW assisted nebulization of the polymer solution. Subsequently this work was extended to carry out layer-by-layer assembly of multiple layer polymeric carries encapsulating pDNA assisted via ultra-fast SAW atomization. Successive atomization - suspension layering steps were repeated to produce as many as eight layers for controlled therapeutic release and plasmid's viability was demonstrated through successful *in vitro* transfection

of the human mesenchymal progenitor and COS-7 cells. Further details can be found in Appendix B.

2.6.3 Surface Acoustic Wave Atomization

SAW atomization for the production of aerosolized droplets is derived from ultrasonic atomization and involves the use of higher driving frequencies ($>10\text{MHz}$) than conventional ultrasonic atomization ($<1\text{ MHz}$). The technique was not used until the 1990s, when a group of researchers lead by Kurosawa first proposed the use of the SAW atomizer (176; 177). In comparison to ultrasonic atomization, SAW atomization is more efficient at transferring the energy into fluid to produce droplets, since SAW energy is localized on the substrate before it is coupled upon direct contact with fluid. For this reason, the power consumption for the atomization process is far lower than most conventional methods of atomization.

Atomization is a result of the SAW wave described in Section 2.6.1, which travels in the x direction for a 127.86° Y -rotated, X cut lithium niobate (LN) device and is an elliptical electro-acoustic wave, as shown in Fig. 2.5(a) (153). The SAW wave leaks into the fluid, causing particles in the fluid to move in both the transverse direction to the substrate surface and in the longitudinal direction along the propagation direction of the wave. This causes the entire free surface of the drop to destabilize and cause atomization. Fundamental investigations have been carried out to unveil the underlying physical mechanism by which SAW atomization produces droplets (2). This phenomenon will be described in more detail in Section 2.6.5.

2.6.4 Surface Acoustic Wave Device for Atomization

For the research reported in the present thesis, the classic IDT patterned 20 MHz device and a more efficient form of IDT, the SPUDT (Single-phase uni-directional transducer)

patterned, elliptical focusing, 30 MHz device were used for atomization (See Fig. 2.5(c)) (14). In the conventional IDT-patterned SAW devices, the SAW wave travels in both the forward and reverse directions, resulting in loss of energy. To overcome this problem, the SPUDT design incorporates an internal reflector within each pair of IDTs to force the SAW wave to travel only in the forward direction. Moreover, in the 30MHz device the SPUDT is patterned as an elliptical focusing type of IDT to achieve high efficiencies in focussing the SAW energy into the fluid being atomized using concentric circular electrodes.

2.6.5 Mechanism of Generation of Droplets via SAWs

When an alternating sinusoid electrical signal (20 or 30 MHz) is supplied to the substrate through the IDTs or SPUDTs, mechanical oscillations occur on the substrate via the inverse piezoelectric effect, producing the SAW in the form of a Rayleigh wave that subsequently propagates along the surface of the substrate. As the SAW encounters a liquid drop placed on top of the substrate, as illustrated in Fig. 2.5(a), the mismatch in the propagation speeds between that in the substrate and that in the liquid cause about a third of the SAW energy to diffract into the drop at an angle known as the Rayleigh angle, which is defined by $\theta_R = \sin^{-1}(c_w/c_s) \sim 22^\circ$, where c_s (=3965 m/s) and c_w (=1485 m/s) represent the propagation speed of SAW on LiNbO₃ substrate and the speed of sound in water, respectively. The diffracted acoustic energy gives rise to a longitudinal compression wave that, in turn, induces a time-average fluid recirculation within the drop, known as acoustic streaming (156; 178). The time-dependent compression of the liquid, reflected throughout the closed drop, also leads to the destabilization of the free surface of the liquid drop, giving rise to strong capillary wave undulations. When driven at an input power that is sufficiently high, the capillary wave destabilization finally exceeds the restoring surface tension that holds the drop intact, resulting in the break-up of the free surface to form aerosol droplets (2; 14), as illustrated in Fig. 2.5(a).

The droplet size can be estimated using the following relationship approximated for the capillary wavelength denoted by λ ,

$$D \approx \lambda \sim \gamma H^2 / \mu f L^2, \quad (2.6.1)$$

where γ and μ are the surface tension and dynamic viscosity, f is the resonance frequency of the capillary wave, and H and L are the characteristic height and length scales of the source drop, respectively (2; 179). Thus the size of the droplet can be manipulated by changing the parameters that govern the relationship above. This approach will be used for the applications that follow in the Chapters 3, 4 and 5 of this thesis, which report on the experimental program.

2.6.6 Surface Acoustic Wave Atomization for the Delivery of Biomolecules

To overcome the difficulties associated with the various nebulization platforms conventionally used for pulmonary gene delivery, SAW atomization is proposed. The SAW-driven atomization system is a simple-to-use, novel, portable and efficient device that can be tailored to a variety of therapies in aerosol delivery. In an *in vitro* proof-of-concept study using a short-acting β_2 -agonist, SAW technology successfully generated a respirable fraction greater than 70%, which far exceeds the typical 30 - 40% lung dose obtained using current nebulization technologies (14). It is clear that SAWs are a highly efficient method for transferring energy into fluid, and require far less power than conventional ultrasound (14). Moreover, the risk of denaturing molecules is greatly reduced since the period to induce vibrations in SAW devices by employing 10 - 100 MHz order frequencies is much shorter than the molecular relaxation time-scale of macromolecules

in liquids. Cavitation is absent during SAW atomization due to its operation at high frequency (few MHz) and this eliminates the effect of cavitation-induced lysis or shear for shear-sensitive molecules such as naked pDNA (14).

2.7 Conclusions

It is evident that the SAW-driven approach has significant advantages over the current generation of ultrasonic medical nebulizers that represent the current state-of-the-art (2). The research presented in this thesis aims to demonstrate the feasibility of SAW atomization as an aerosol delivery platform for pulmonary genetic therapeutics, especially for shear-sensitive naked pDNA encoding an influenza vaccine candidate.

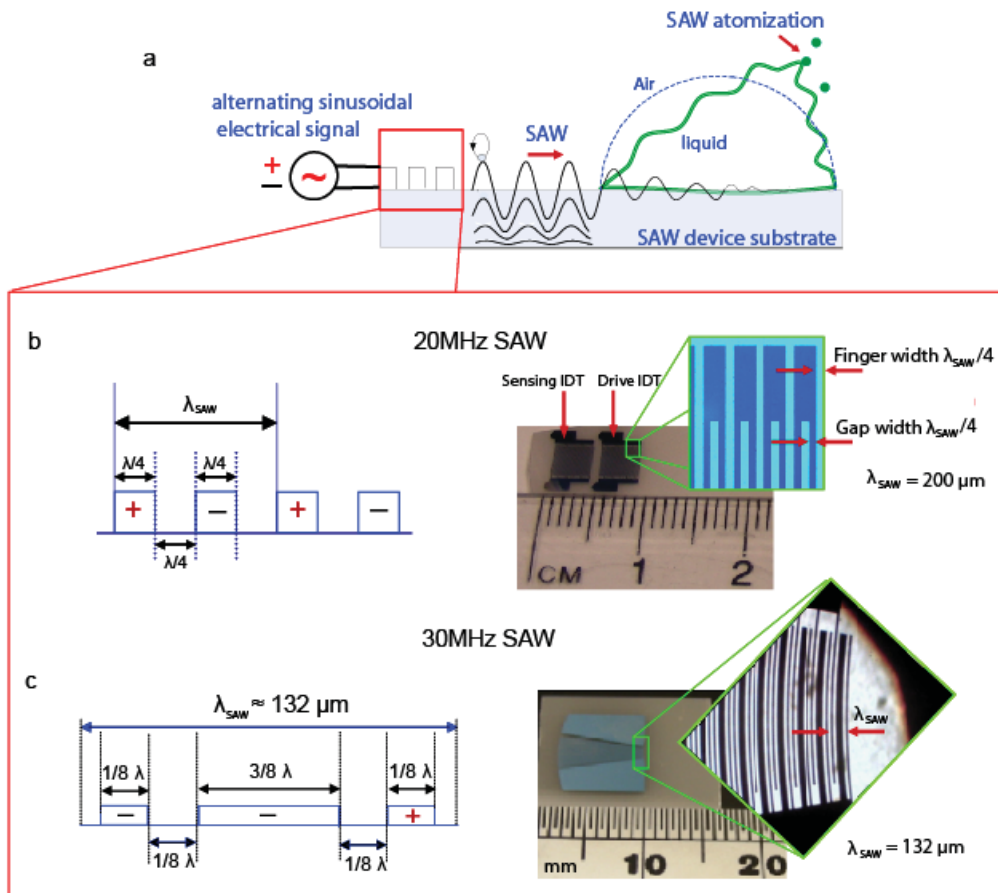


Figure 2.5: A schematic of the generation and propagation of SAW on a lithium niobate piezoelectric substrate from the application of a sinusoidal electrical signal. The SAW itself is a retrograde traveling wave, and a point on the surface travels in a retrograde fashion in comparison to the propagation direction of the SAW across the substrate. The energy of the SAW is confined to within a few wavelengths of the substrate surface. This acoustic energy leaks into and drives strong acoustic waves in the fluid drop that in turn lead to acoustic streaming, recirculation, and the formation of capillary waves on the drop's surface. With sufficient input energy, these waves become large enough to cause droplets to be ejected from some of the crests in an intermittent fashion. (b) Image of the SAW device showing the aluminium-chromium IDT electrodes patterned on the piezoelectric substrate. The enlargement shows the IDTs, and specifically the relationship between the width and gap between the fingers and the SAW wavelength λ . (c) Image of the 30 MHz SAW device patterned with a pair of aluminium-chromium single-phase unidirectional transducers (SPUDTs). The curved geometry of the electrodes allows the SAW to be focused for more efficient operation.

Chapter 3

Effect of High Frequency Acoustic Wave Nebulization on pDNA in order to achieve Pulmonary DNA Vaccination

3.1 Introduction

The lung is an attractive site for the delivery of gene therapy and DNA vaccination agents because it is accessible, has a large surface area for transfection and is highly cellular and vascularised. Further, pulmonary delivery constitutes a pain-free non-invasive route that circumvents the logistical difficulties and risks associated with parenteral routes (e.g., infection, provision of clean needles and systemic side effects) (3). Indeed, there has been significant interest to date in the potential of pulmonary-delivered gene therapy in treating pulmonary diseases caused by single gene mutation such as cystic fibrosis and 1-antitrypsin deficiency (16). Pulmonary vaccination is theoretically useful against a range of infecting pathogens, since it induces immunity at mucosal sites through which these agents enter the body (3).

Effective delivery requires that the DNA successfully enters the target cell via endocytosis, thus avoiding degradation by lysosomal or cytoplasmic nucleases (180; 181). Subsequently it must be transcribed within the nucleus to produce the desired gene product (182). Whilst viral vectors have certain advantages, they also have significant disadvantages, as they invoke specific and non-specific inflammatory and immune responses in the host. These disadvantages militate against repeated administration, a usual requirement for gene therapy and vaccination (183). On the other hand, non-viral vectors, such as plasmid DNA (pDNA), which contain the desired gene sequences that encode a therapeutic protein in a closed circular piece of DNA, have the benefit of low immunogenicity and are easily produced at low cost.

Delivering therapeutics such as pDNA to the lung presents a number of technical challenges. As previously outlined, the most commonly used pulmonary delivery devices include pressurized metered-dose inhalers, dry powder inhalers, and jet or ultrasonic nebulizers. Inhalers generally require either hand-inhalation coordination, rendering them ineffective for many patients who are unable to self-medicate, or breath-actuated aerosolization, which is difficult for patients suffering from severe forms of chronic obstructive pulmonary disease (184; 185). In addition, macromolecules such as pDNA are typically unstable in propellants and solid dispersed formulations, and thus have a short shelf-life, increasing the overall cost (3). There are also safety issues with regard to these formulations for chronic use (186; 187). Although active aerosolization methods such as nebulizers are more appropriate for these specific patient groups and are currently the mechanism of choice for pulmonary gene delivery (in fact, nebulizers are the only delivery method considered in the UK Cystic Fibrosis Gene Therapy Consortium (3; 188)), current nebulizers lack efficiency, portability and the flexibility to accommodate patient breathing and lung variability (179).

A further significant limitation in the use of nebulizers for pulmonary gene delivery arises

from the denaturation of non-complexed DNA as a consequence of the large hydrodynamic shear stresses or shock waves that arise during the jet or ultrasonic nebulization process (179; 9). In particular, supercoiled tertiary structures of pDNA with sizes larger than 5 kbp are severely sheared resulting in open circular and fragmented DNA (135; 22; 144). The loss in the DNA transfection ability that results can be considerable and efficiencies as low as 10% have been encountered (142). The Center for Biologics Evaluation and Research of the US Food and Drug Administration (CBER/FDA) recommends that a minimum fraction of 80% of the pDNA should retain its supercoiled (sc) structure if gene-based products are to be used in humans (189). In addition to retaining transfectability, it is also vital that the nebulization platform generates a mono-dispersed distribution of aerosol droplets in the appropriate size range for optimal delivery to the targeted lung region (9).

The emergence of new devices such as mesh nebulizers (150), electrohydrodynamic (EHD) devices (151), and miniaturized nebulization catheter devices (152) claim to offer greater aerosolization efficiency, while preserving the integrity of pDNA in the aerosols. However, these devices require further clinical studies to prove these claims before they can be generally used. Gene transfer agents such as cationic lipids (111) and cationic polymers (113) are used to form complexes with pDNA that protect the pDNA from shear forces and increase its stability during aerosolization. This has led to successful gene expression after aerosol delivery to the lungs of mice (114), rabbits (115) and sheep (116). However, not all lipoplexes and polyplexes retain biological efficacy after aerosolization (117; 118) and some synthetic polymers have been demonstrated to induce cytotoxicity both *in vitro* (190) and *in vivo* (191).

The present thesis investigates the use of a generic SAW nebulization platform as a simple-to-use, novel, portable and efficient device that can be tailored for a variety of pulmonary drug therapies (14). The SAW approach is a highly efficient method for transferring energy into fluid, requiring far less power to achieve a given fluid response than

conventional bulk piezoelectric ultrasonic radiators (2).

Moreover, the risk of denaturing molecules is greatly reduced by employing 10-100 MHz order frequencies since the oscillation period of the SAW vibration at these frequencies is far shorter than the typical macromolecular relaxation time-scale in liquids (192; 193). Cavitation is also absent when the frequency is increased beyond a few MHz, thus eliminating the possibility of cavitation-induced lysis or shear on cells and shear-sensitive molecules such as naked pDNA. Li *et al.* demonstrated that little damage is imposed on mesenchymal stem cells when subjected to SAW irradiation, thus preserving their viability, proliferation and differentiation (194). Further, when used for nebulization, the size of droplets generated by SAW can be rapidly tailored by switching from standing-wave to travelling-wave SAW on the substrate. Hence, the SAW nebulization approach has significant theoretical advantages over the current generation of ultrasonic medical nebulizers (2).

The aim of this chapter is to demonstrate the feasibility of SAW nebulization as an aerosol delivery platform for DNA into the lung, especially with shear-sensitive naked (non-complexed) pDNA encoding genes for treating infectious diseases such as malaria, a major lethal disease and health problem in Africa (195; 196). Here, homologues of the candidate vaccine molecules, *Plasmodium falciparum* merozoite surface proteins 4 and 5 were utilized, which are glycosylphosphatidylinositol (GPI)-anchored integral membrane proteins with similar structural features. In a rodent malaria model, a pDNA molecule encoding the *P. yoelli* merozoite surface protein 4/5 (PyMSP4/5), is highly effective at protecting mice against lethal challenge (197) and is the homologue of the human malaria proteins. After examining the structural integrity of pDNA recovered after SAW nebulization, the physical stability of the pDNA was subsequently confirmed through characterization of the *in vitro* transfection efficiencies. Thereafter, the likelihood of high lung deposition efficiency by SAW pulmonary therapeutic delivery was demonstrated by showing aerodynamic size distributions which are close to those known to be optimal for

effective droplet delivery to the lower respiratory tract.

3.2 Experiments and Materials

3.2.1 Surface Acoustic Wave Nebulizer

The SAW nebulizer was custom-designed and fabricated at the Melbourne Centre for Nanofabrication in Clayton, Australia. A pair of 20 MHz aluminium-chromium IDTs was fabricated using sputter deposition (Hummer Triple-Target Magnetron Sputter System, Anatech, USA), standard UV photolithography and wet etching onto a 127.86° Y-rotated, X-propagating single-crystal LiNbO₃ substrate, as shown in Fig. 2.5(b) in Chapter 2. Fig. 2.5(c) shows a 30 MHz SAW device patterned with a pair of aluminium-chromium single-phase uni-directional transducers (SPUDTs). Unlike the typical IDTs in Fig. 2.5(b), the SAW generated from SPUDTs propagates in a single direction. Less energy is therefore lost and the risk of interfering reflection is also reduced. A focused design is also employed to concentrate the SAW at a focal point where nebulization is performed in order to achieve optimal efficiency.

3.2.2 Preparation, Culture and Purification of plasmid DNA

The mouse malaria *P. yoelli* merozoite surface protein 4/5 (PyMSP4/5) was cloned into the mammalian expression vector pVR1020 for use throughout the *in vitro* work (197). A colony of *E. coli* DH5 α harbouring plasmid pVR1020-PyMSP4/5 (~5.6 kbp) was picked from a streaked selective plate and inoculated in 10 ml of LB medium containing 100.0 μ g/ml of kanamycin. The starter culture was incubated at 37°C and agitated at 200 rpm for 8 hrs before being transferred to five separate 200 ml LB media, and further cultured for 12 hrs. The cell cultures were stored at -70°C for subsequent use. The plasmids were purified from cells using an endotoxin-free plasmid purification kit (QIAGEN Mega,

Australia) according to the manufacturer's instructions.

3.2.3 Plasmid Nebulization using SAW

Various concentrations of pVR1020–PyMSP4/5 pDNA solutions ranging from 5–85 $\mu\text{g}/\text{ml}$ in deionized water were nebulized using both 20 and 30 MHz SAW devices and carefully collected in microcentrifuge tubes for further analysis. The concentration of pDNA in the collected samples was determined by a UV spectrophotometer (NanoDrop 1000, Thermo Scientific, USA) at a wavelength of 260 nm. The purity of pDNA samples was assessed by the samples' absorbance at 260 and 280 nm; if the ratio is lower than 1.8, it signifies the presence of protein, phenol and other contaminants.

3.2.4 Agarose Gel Electrophoresis

Both control and nebulized pDNA samples were analyzed for potential alterations in the plasmid structure with 0.8% agarose gel electrophoresis using a 1 kbp DNA ladder and ethidium bromide (EtBr) staining. The gel was made up of 0.8 g agarose at 50 \times dilution of TAE buffer (242.0 g Tris base, 57.1 ml CH_3COOH , 9.3 g of EDTA). The gel was stained with 3 $\mu\text{g}/\text{ml}$ ETBr and the electrophoresis was carried out under 60 V for 90 mins. The resulting gel was analyzed and imaged in a Molecular Imager Gel Doc XR system (Bio-Rad, Australia). The intensity of the bands for each structure corresponds to the number of DNA molecules. The percentage of supercoiled (sc) and open circular (oc) to degraded linear pDNA was quantified via densitometry software (Quantity One, Bio-Rad, Australia) by comparing pre- and post-nebulized samples. However, it was found that the binding of ethidium bromide to different plasmid structures is dependent on the DNA topology, thus the measured fluorescence values of the supercoiled structure are multiplied by the correction factor 1.36 to obtain the adjusted values (198).

3.2.5 AFM Imaging of plasmid DNA

A freshly cleaved 10 mm diameter mica disc was coated with 10 $\mu\ell$ of 10 mM Ni(NO₃)₂ to render the mica surface cationic for adsorption of anionic pDNA. Ten microliters of pDNA solution (6–25 $\mu\text{g}/\text{m}\ell$) was pipetted onto the mica surface. Two to five minutes were allowed to elapse to enable the pDNA to absorb onto the surface, after which the mica disc was rinsed with ultra-pure water and dried under a gentle stream of N₂ gas prior to AFM imaging. The surface morphology of pDNA was imaged with an Ntegra Scanning Probe Laboratory (NT-MDT, Zelenograd, Russia) operating in intermittent contact (or tapping) mode in air using MikroMasch NSC15 probes. Images of 512 \times 512 pixels with a scan size of 3 \times 3, 1 \times 1, 0.5 \times 0.5 μm^2 were acquired at scan rates of 1–2 Hz. AFM images were processed to correct plane tilt, arcing and line fluctuations. For the presented images, a further 3 \times 3 Gaussian noise filtering and 3D rendering was also applied using WsXM freeware (version 5, build 1.1, Nanotec Electronica S.L., Spain).

3.2.6 *In vitro* Cellular Transfection

In vitro cellular transfection studies were performed using COS-7 cells grown in a complete RPMI 1640 medium containing 10% foetal calf serum, 2 mM of L-glutamine, 100 U/ml of penicillin and 100 $\mu\text{g}/\text{m}\ell$ of streptomycin. Freshly grown 2 \times 10⁵ cells were seeded into each of the six-well format tissue culture plates, and incubated in 5% CO₂ at 37°C for 24 hrs until 70-80% confluent. The cells were washed and combined with 1 ml of serum-free RPMI 1640 medium. Transfection of 1.0 μg plasmid VR1020-PyMSP4/5 per well for pre- and post-nebulized samples was facilitated by lipofectamine 2000 according to the manufacturer's instructions. After 5 hrs incubation, 1 ml of RPMI 1640 medium containing 20% foetal calf serum, 4 mM of L-glutamine, 200 U/ml of penicillin and 200 $\mu\text{g}/\text{m}\ell$ of streptomycin was added. After incubation for 48 hrs, the cells were washed with phosphate-buffered saline (PBS) pH 7.4, and both the cells and

culture medium were collected and stored at -20°C .

3.2.7 SDS-PAGE and Immunoblotting Analysis

Post-transfection, the COS-7 cells were subjected to SDS-PAGE under reducing conditions (199). Proteins from cells were fractionated and then electrophoretically transferred to PolyScreen PVDF transfer membrane for immunoblotting, as previously described (200). The membranes were incubated in TBS/T (0.05 M Tris-HCl pH 7.4, 0.15 M NaCl, 0.05% Tween 20) containing 5% non-fat milk powder overnight at 4°C . Subsequently, the membranes were probed with rabbit anti-PyMSP4/5 antisera for 1 hr at room temperature, and washed three times in TBS/T for 10 mins each time. Primary antibody reactivity to immunoblotted proteins was detected with anti-rabbit immunoglobulin conjugated to horse radish peroxidase (HRP) (Silenus Laboratories). The HRP was visualized by Renaissance Western Blot Chemiluminescence Reagent (NEN Life Science Products, PerkinElmer, Massachusetts, USA). The intensities of the fluorescence associated with the immunoblotted proteins were quantified as the total pixels within a defined boundary drawn on the image using Image J (Version 1.41, National Institutes of Health, USA). The intensities or the amount of PyMSP 4/5 expressed were converted to nanograms of protein using a standard curve prepared with an *E. coli* expressed protein standard.

3.2.8 Aerosol Characterization

De Brouckere (volume moment, D_{43}) mean diameter is the average particle size relevant to the dose's delivery efficiency when the particles are droplets of unit density. The size distributions of the pDNA-laden aerosol droplets in this study were measured using laser diffraction (Spraytec, Malvern Instruments, UK) including the desired 1–5 μm range for pulmonary delivery. In order to characterize the pDNA aerosol size distribution, D_{43} was recorded during the measurements.

Table 3.1: Distribution of data collected from experiments in study.

Study	Freq. (MHz)	Shapiro-Wilk normality test statistic	Normally distributed?
Agarose gel electrophoresis of DNA			
Supercoiled	20	0.119	No
	30	0.110	No
Open circular	20	0.251	No
	30	0.620	No
Fragmented	20	0.021	Yes
	30	0.038	Yes
Western blot of PyMSP4/5			
	0	0.862	No
	20	0.692	No
	30	0.098	No

3.2.9 Statistical Analysis

All statistical analysis was performed using SPSS (Version 19, IBM Corporation, Armonk, USA). One-way ANOVA with a Tukey's post-hoc test was used for data that survived Shapiro-Wilk's (SW) normality test with significance $p > 0.05$, suggesting the data is normally distributed and therefore ANOVA was suitable. In instances where the SW test was significant ($p < 0.05$), the non-parametric Kruskal-Wallis (KW) test was used instead to test for the overall significance between independent groups. Where differences were observed, the Mann-Whitney (MW) tests were performed between two independent samples to identify the differences. For statistical testing involving two related samples that were not normally distributed, the Wilcoxon Signed Rank Test was used. All data are expressed as the mean \pm standard deviation. The results were considered significant if $p < 0.05$. Most agarose gel electrophoresis and Western blot results were not normally distributed, as verified in Table 3.1.

3.3 Results and Discussion

3.3.1 Aerosol Size Distribution

The impaction of aerosol in the upper airways is governed by Stokes law and droplets with aerodynamic diameter below $5\mu\text{m}$ are desired for efficient deep-lung deposition (10; 201; 202). As a consequence, it is crucial to generate aerosols with an optimal aerodynamic droplet size to deliver the required dose to the lower respiratory tract, such that dose efficacy is maximized and wastage due to deposition in the oropharyngeal region is avoided. During SAW atomization, the diameter of the droplets ejected from the liquid-free surface is governed by the capillary wavelength λ . This in turn, can be predicted from a balance between the forces that dominate the capillary wave destabilization process, namely, the capillary and viscous forces that dominate at the surface, such that the droplet diameter is given by,

$$D \approx \lambda \sim \gamma H^2 / \mu f L^2, \quad (3.3.1)$$

where γ and μ are the surface tension and dynamic viscosity, f is the resonance frequency of the capillary wave, and H and L are the characteristic height and length scales of the source drop, respectively (2; 179). It has been previously shown that λ and hence the capillary resonant frequency of the drop is quite independent of the excitation frequency applied to the device via an alternating current (179). From the above scaling relationship, the possibility of tuning the dimension of pDNA-laden aerosols simply by varying the surface tension and viscosity of the liquid sample becomes apparent.

We note that the generation of aqueous pDNA aerosol droplets of sizes smaller than the $5\mu\text{m}$ diameter required for optimal deposition in the deep-lung region is particularly difficult due to the high surface tension of water. In this study, a formulation of pDNA containing glycerol was chosen to lower the surface tension and to increase the viscosity

of the liquid drop to be nebulized. Given its low toxicity, it is approved by the FDA and has been widely used in many pharmaceutical and medical formulations; toxicological evaluations on aerosolized glycerol have shown no adverse effect on rats (203). In our study, glycerol concentrations of 10%, 20% and 40% (w/w) were used, for which narrow monodisperse aerosol distributions with droplet sizes under $5\ \mu\text{m}$ were reliably obtained. Fig. 3.1 shows the cumulative aerosol size distributions for pDNA with a concentration of $100\ \mu\text{g}/\text{m}\ell$ with different glycerol weight ratios, which allow the drop viscosity and hence the dimensions of the aerosol droplets to be manipulated.

As shown in Table 3.2, increasing the concentration of glycerol reduces the average aerosol diameter for a fixed pDNA concentration, in qualitative agreement with the scaling argument in Eq. 3.3.1. This confirms the possibility of establishing some control over the desired aerosol dimension through the physical properties of the liquid. However, there appears to be some variability in the data when the pDNA concentration is altered. The effect is not significant, primarily since the variation in the drop viscosity is far more sensitive to the glycerol concentration (over 1 Pa.s from 0 to 40% (w/w) of glycerol) compared to the pDNA concentration (only several mPa.s) (204). In any case, the possibility of finely tuning the aerosol droplet dimension to the desired size ($<5\ \mu\text{m}$) for optimum dose administration is demonstrated, thus providing reasonable confidence that the nebulized pDNA should be targeted to the alveolar region for maximum dose efficacy. These results are certainly encouraging compared to the size distributions obtained for naked pDNA aerosols generated using a catheter-based nebulization device where size ranges obtained were around $33 \pm 2\ \mu\text{m}$, which is well beyond the optimal range for lung delivery (152).

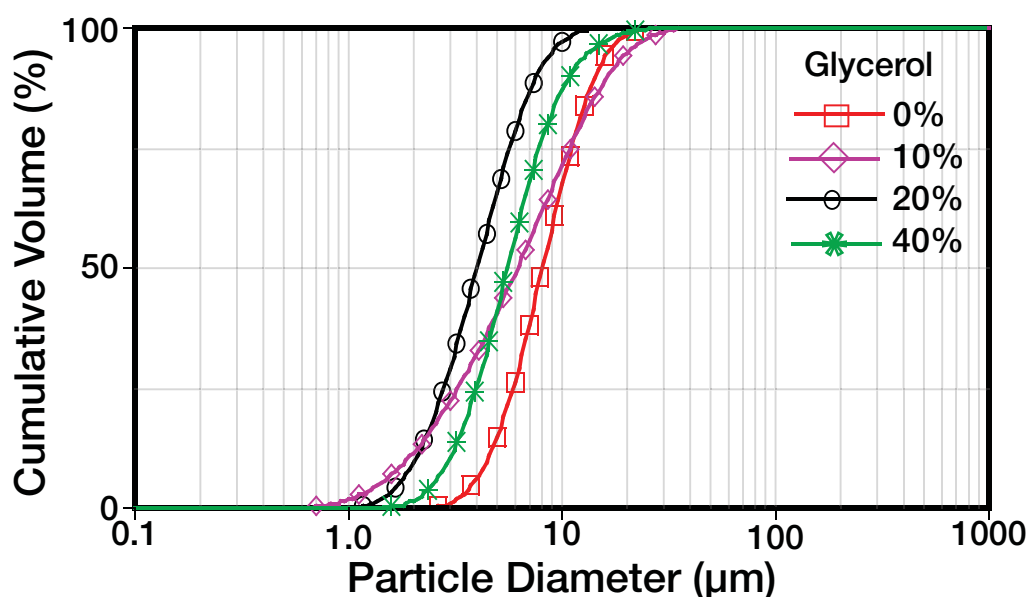


Figure 3.1: Measured using laser diffraction (Spraytec, Malvern, UK), the size distribution of droplets nebulized using SAW at 30 MHz and 3 W of applied power from an aqueous suspension of 100 $\mu\text{g}/\text{mL}$ of pDNA is generally reduced as the concentration of glycerol is increased to 20%.

Table 3.2: The de Brouckere mean aerosol droplet diameter (D_{43}) using a 30 MHz SAW nebulizer at 3 W of applied power ($n = 4$).

pDNA concentration ($\mu\text{g}/\text{mL}$)	%w/w glycerol	D_{43} (μm)
100	0	8.25 ± 0.34
	10	7.61 ± 0.94
	20	4.12 ± 0.13
50	20	5.49 ± 0.10
10	20	4.08 ± 0.02

3.3.2 Physical Stability of pDNA Molecules Irradiated by SAW

pDNA molecules in post-nebulized droplets must retain the supercoiled and covalently closed circular form of plasmid DNA for efficacy, and to comply with the FDA's regulatory requirements relating to the purity and potency of plasmid products (189; 205). The supercoiled structure of pDNA is maintained by the covalent bonds in its phosphodiester backbone and by hydrogen bonding between bases. The torsional energy stored in the native compact supercoiled plasmid will be released upon bond scission of either strand of the molecule, relaxing into an open circular form. Further cleavage of

strands at the same location on the opposite strand of the DNA helix will result in a linear polynucleotide. This full-length linear molecule will be fragmented further with additional bond breaks (206). AFM imaging of the pVR1020-MSP4/5 in Fig. 3.2(a-b) indicates the tightly twisted supercoiled geometry before SAW nebulization. Different concentrations of pVR1020-MSP4/5 were then nebulized using prototype 20 and 30MHz SAW devices and subsequently collected for analysis to determine their post-nebulization structure using AFM (Fig. 3.2(b)) and agarose gel electrophoresis (Fig. 3.2 (d-e)).

Interestingly, agarose gel electrophoresis revealed that the unprotected, naked pDNA was preserved during the SAW nebulization process. The change in supercoiled, open circular and fragmented pDNA structures prior to and after nebulization is shown in Fig. 3.2(c). In most cases, more than 90% of the initial supercoiled pDNA is still present after being nebulized (Fig. 3.2(d)). The degradation that was seen can be attributed principally to the damaged pDNA feedstock, since a small proportion of the pDNA prior to SAW nebulization was found to be fragmented during the early stages of plasmid purification and preparation, particularly at a pDNA concentration of $5 \mu\text{g}/\text{m}\ell$, which has around 50% and 20% of supercoiled and fragmented pDNA, respectively. The key parameter affecting the shear sensitivity of pDNA molecules appears to be its hydrodynamic diameter. Linear double-stranded DNA molecules have been found to be very susceptible to flow-induced stress in previous studies (207; 208; 209) and minor differences in their characteristic dimension appear to have large effects on their response to hydrodynamic stress (210).

Similarly, isoforms of pDNA present in the initial preparation (purification process) such as open circular and linear forms are more sensitive to hydrodynamic forces that arise during SAW nebulization due to their unfolded state. The increase the length and hydrodynamic diameter of plasmids (open circular and linear) due to their tertiary structure lowers the shear threshold, and relaxed forms are acted on by larger forces and subsequently become fragmented (208). Experimental and theoretical studies indicate that

stretching hydrodynamic forces greater than 300 pN will cause irreversible strand separation and formation of nicks even before reaching a force sufficient to break covalent bonds (1600-5000 pN) (9). The particle displacement velocity of a surface ultrasonically driven by piezoelectric materials near the limit of the electromechanical material is typically 1 ms^{-1} , regardless of the excitation frequency. As a consequence, the surface acceleration at the frequencies used in SAW is extremely high (10^7 – 10^8 ms^{-2}), despite the amplitude of the acoustic wave being less than 10 nm. Such huge accelerations are responsible for the destabilization of the capillary waves that lead to atomization, as discussed in Section 2.6.5 (2). Thus relaxed forms of the pDNA located close to the free surface of the drop are more likely to be susceptible to shear-induced damage, because large shear stress gradients are primarily responsible for the break-up of the interface to form aerosol droplets that eject from the free surface.

We also observed that degradation of pDNA was found to be somewhat dependent on the pDNA concentration during nebulization. Whereas both the 50 and 85 $\mu\text{g/ml}$ samples showed similar levels of post-nebulized intact pDNA (>75% of supercoiled pDNA), the 85 $\mu\text{g/ml}$ sample was found to be subject to a larger extent of degradation (20% degradation) as compared with the 50 $\mu\text{g/ml}$ sample (<9%). The same outcome was found for samples possessing lower integrity, whereas only around 13% of pDNA degradation was observed for the 5 $\mu\text{g/ml}$ sample (Fig. 3.2(f)). These observations are consistent with past studies (210; 136) that showed similar damage dependence on the pDNA concentration (beyond the range of 20 $\mu\text{g/ml}$) due to the interaction of shear with the drop-free surface. It has been suggested that the concentration of intact pDNA after atomization c_k is dependent upon the initial DNA concentration c_i , the degradation rate constant k , and the residence time in the system, governed by the relationship, $c_k = c_i - kt$ (206; 208).

In comparison, conventional ultrasonic transducers operate at 20-80 kHz, in a range where cavitation is easily generated, inducing extreme fluid-shear during formation, and growth

and the subsequent collapse of bubbles, in turn damaging the supercoiled pDNA, as discussed in Section 4.1. Indeed, pDNA molecules within the solution act as nucleation sites for cavitation (144). In contrast, the nebulization platform proposed here retains the benefits of using intense acoustic fields for driving fluid motion, namely, the large actuation effects and the associated flow nonlinearities, while preventing the cavitation damage seen with conventional ultrasonic methods. The megahertz (>10 MHz) order SAW vibration frequencies facilitate fluid and particle manipulation at much finer scales, and at far lower powers because of an energy-efficient mechanism wherein the acoustic energy is concentrated within a thin region of the drop adjacent to the substrate (178). These inherent properties associated with SAW nebulization avoid damage to pDNA, since the shear gradient generated within such a short period of time is not sufficient to degrade the pDNA (192; 193). Consequently, the percentage of post-nebulized fragmented pDNA is far lower in SAW nebulization in comparison to that in conventional ultrasonic nebulization (>35%) and vibrating mesh nebulization (>40%) for a similar-sized plasmid (of the order of 5 kbp) (22).

3.3.3 Bioactivity of plasmids During *In vitro* Transfection.

The *in vitro* transfection efficiency of SAW atomized pVR1020-MSP4/5 was subsequently investigated in immortalized African green monkey kidney cells (COS-7). The gene expression results from these studies are in agreement with the agarose gel electrophoresis observations: higher post-nebulized open circular and fragmented pDNA ratios are directly correlated to lower gene expression. Fig. 3.3 shows that transfection efficiencies as high as 75% and 84% were observed for the *in vitro* MSP4/5 gene expression of recovered pDNA after both 20 and 30 MHz SAW nebulization, compared to the corresponding unnebulized (control) pDNA after 48 hrs. The levels of *in vitro* transfection efficiency offer further evidence that the pDNA molecules are not damaged during the SAW nebulization process, supporting the contention that this is an efficient platform for the aerosol delivery

of shear-sensitive biomolecules.

3.4 Conclusions

This chapter has reported the initial investigations of the feasibility of SAW nebulization for the generation of aerosols containing shear-sensitive bio-therapeutics such as pDNA. Integrity of the large biomolecule was preserved with almost negligible denaturation of the supercoiled content. The plasmid-laden aerosols have droplet sizes below $5 \mu\text{m}$ for optimal deep lung deposition and remain biologically active, as evidenced by the successful induction of gene expression in mammalian cells. This work has laid the foundation for the application of SAW nebulization for potential non-invasive gene therapy using plasmid DNA molecules.

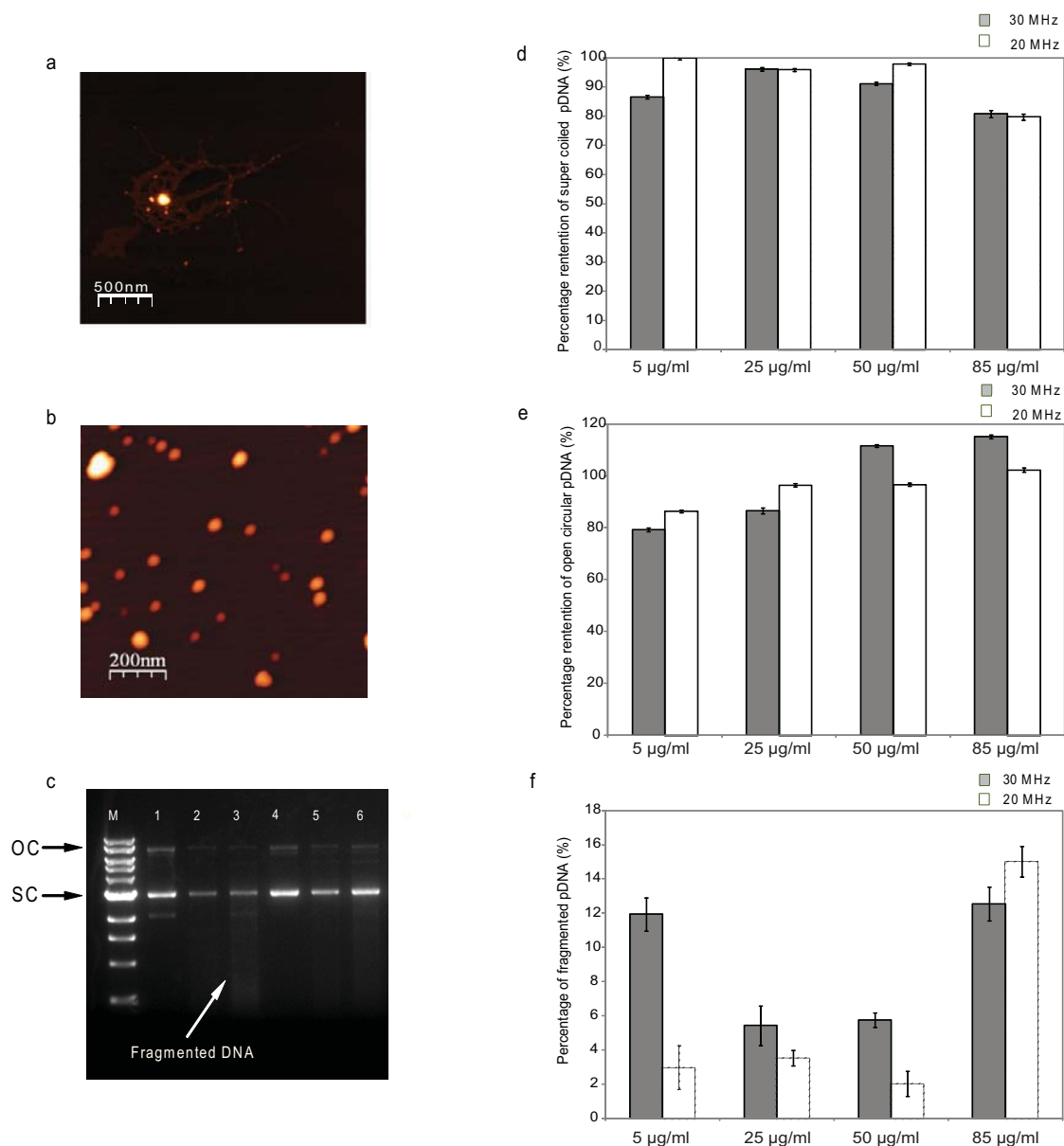


Figure 3.2: Structural analysis of pVR1020-MSP4/5 before and after SAW nebulization at 30 MHz by AFM imaging in air. (a) pre-nebulized (control), and (b) post-nebulized supercoiled structures of 5.6 kbp DNA. (c) Ethidium bromide agarose gel electrophoresis for the assessment of the naked pDNA structural integrity before and after SAW nebulization. Lane M: 1 kbp DNA ladder; lanes 1 and 4: control pDNA prepared at 85 $\mu\text{g/ml}$ and 50 $\mu\text{g/ml}$ concentrations, respectively; lanes 2 and 5: recovered 85 $\mu\text{g/ml}$ and 50 $\mu\text{g/ml}$ pDNA nebulized with 20MHz SAWs, respectively. Each lane was loaded with 200ng of pDNA and representative gels from three independent experiments are shown. Arrows indicate the position of open circular (OC) and supercoiled (SC) forms of pDNA along the vertical direction. Statistical analysis showing the proportion of (d) supercoiled, (e) open circular and (f) fragmented pDNA, for 20 and 30 MHz SAW nebulization. The amount of supercoiled, open circular and fragmented pDNA was assessed with results from the agarose gel electrophoresis and are the average of triplicate nebulization runs in which the error bars indicate the standard deviation of the data.

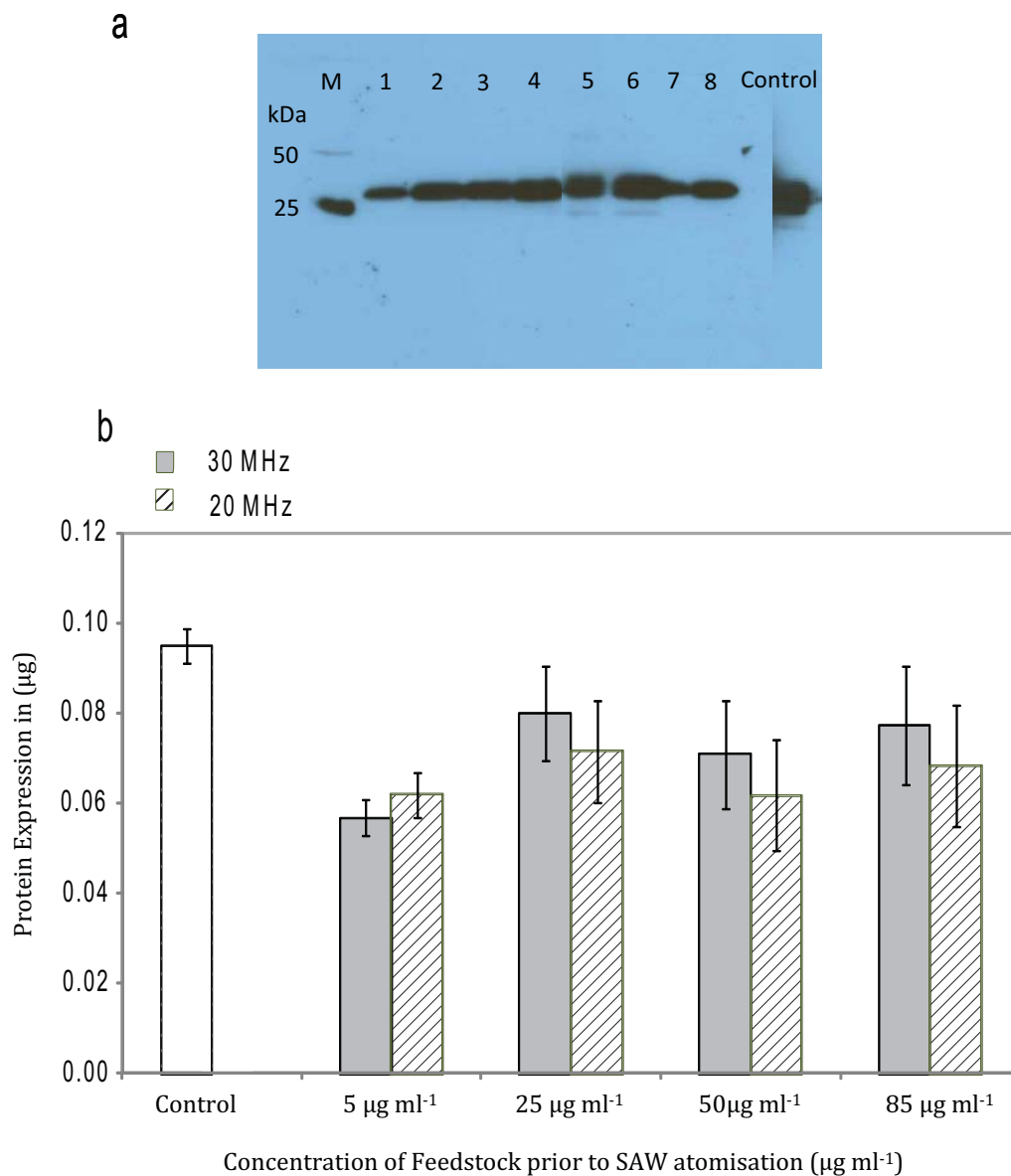


Figure 3.3: (a) Western blot detection of PyMSP4/5 expressed in COS-7 cells at 48 hrs post-transfection. Lane M: marker showing molecular mass standard (kDa) on the left; lanes 1-3: the cells transfected with pDNA recovered from 30, 50 and 85 $\mu\text{g/ml}$ pDNA nebulized using 30 MHz SAW; lanes 4-8: the cells transfected with pDNA recovered from 25, 35, 50, 65 and 85 $\mu\text{g/ml}$ pDNA nebulized using 20 MHz SAW. (b) Statistical analysis of the *in vitro* transfection efficiency of naked pDNA recovered after SAW nebulization. The results are the mean of triplicate nebulization runs, where the error bars indicate the standard deviation of the data.

Chapter 4

Effective Pulmonary DNA Vaccination via High Frequency Acoustic Wave Nebulization

4.1 Introduction

With a novel, highly infectious agent such as a pandemic flu strain, vaccine production constraints may have a very serious impact on the final outcome. In Australia, for example, the first doses of vaccine for use against the recent H1N1 swine flu epidemic took 4.5 months to prepare and seasonal flu production in the USA typically takes in the order of 6–8 months (211; 212). Current global production of trivalent seasonal influenza vaccine is 700 million doses annually. Without a major boost in production capacity or the development of highly effective dose-sparing adjuvants, it could take two or more years to immunize the world's population, even presuming a well-functioning administration capacity that might be severely compromised by infection among health professionals. The production time of vaccines such as the flu vaccine can be considerably shortened by substituting a protein-based sub-unit vaccine with a DNA vaccine. There are well-documented issues with immunogenicity and efficacy (182) that, if overcome, would lead

to a crucial shortening of vaccine development time to as little as two weeks from construction to first dose production (213). Early deployment of even a partially effective vaccine leads to a major lowering of transmission and mortality and a reduction in attack rate of over 75% (214).

Parenteral vaccination, although undoubtedly effective in preventing disease, requires needles and skilled, expensive personnel to handle them, cannot be deployed in developing areas of the world that lack medical infrastructure, nor can it be developed quickly enough to address acute needs due to the protracted effort required in cell or bacterial culture vaccine production. Replacement of the parenteral route with alternative modes of administration would mitigate vaccine safety issues and the requirement of skilled personnel. Plasmid DNA (pDNA) offers a rapid production route to vaccines without significant side-effects nor an extensive cold chain (215).

pDNA can be introduced into the lung by aerosol inhalation. Following deposition in the airways, the plasmid is available for uptake by bronchial epithelium, alveolar epithelium and interstitial cells (216). Delivery efficiency and integrity of the gene vectors prior to and during pulmonary delivery are critical parameters that must be maximized for this approach to be successful. In addition, it is important that the size of aerosol droplets are below a certain value ($<5\mu\text{m}$) for the droplets to reach the lower respiratory airway (alveoli), where the absorption and transfection efficiency of the gene vectors is likely to be greatest (8).

The previous chapter demonstrated that the SAW nebulization approach safeguards the structural integrity of shear-sensitive non-complexed pDNA encoding genes for treating infectious diseases whilst retaining transfectability. Moreover, the nebulization platform generated a mono-dispersed distribution of pDNA-laden aerosol droplets in the appropriate size range for optimal delivery to the targeted lung region. The true significance of these findings can be realized following investigations of transfectability *in vivo*, which

is the purpose of this chapter. Here, the application of SAW nebulization as an aerosol delivery platform for DNA vaccination into the lung using is demonstrated using three animal models. Studies were also conducted to test the capacity of nebulized DNA to induce immune responses in these animals. Since mice and rats are unable to inhale mist from a nebulizer, preliminary experiments in these animals involved the recovery of nebulized material followed by intratracheal instillation of the condensate. However, to assess the effectiveness of the SAW nebulization platform in providing effective DNA vaccination via inhalation against influenza, a sheep lung model was chosen. Sheep have long been used as relevant models for human lung development, structure, physiology and disease. Sheep are also ideal animal models for drug delivery studies as compared to small rodent models, the size and structure of the lung is similar to that of humans, including the extensive branching of the upper airways, which has been shown to contribute significantly to regional drug deposition in the lung. In addition, repetitive sample measurements can be made in sheep using the same techniques and instruments used in the clinical environment.

4.2 Experiments and Materials

4.2.1 Surface Acoustic Wave Nebulizer

A 30 MHz SAW device patterned with a pair of aluminium-chromium single-phase unidirectional transducers (SPUDTs), custom-designed and fabricated at the Melbourne Centre for Nanofabrication in Clayton, Australia, as shown in Fig. 2.5 was used for the experimental work reported in this chapter.

4.2.2 Preparation, Culture and Purification of plasmid DNA

The pVR1020 plasmid encoding yellow fluorescent protein (YFP) was used for the *in vivo* studies to aid visualization of the gene expression. For the immunization trial, a plasmid DNA was prepared from an influenza A virus surface antigen, a classic protective protein, human hemagglutinin (A/Solomon Islands/3/2006 (egg passage) (H1N1) strain), was cloned into the mammalian expression vector pVR1020 (Vical Inc., USA). The entire coding sequence of HA was amplified by PCR using primers forward and reverse that incorporated a BamHI site at the 5 prime end and a EcoRI site at the 3 prime end, forward: 5 prime-CGCGGATCCATGAAAGTAAACTACTGGTCCTGTTATG-prime; reverse: 5 prime-CCGGAATTCTTGTGGTAATCCCATTAATGGCATTGTTGT-3 prime.

The PCR product was digested with BamHI / EcoRI and ligated into the vector, pVR1020, resulting in plasmid pVR1020-HA. Purification of pVR1020-YFP (~5.7 kbp) or pVR1020-HA (~6 kbp) was carried out as previously described in Section 3.2.2.

4.2.3 Animal Trials

For gene expression detection studies, male Swiss mice (8–10 weeks old) were used, weighing 37–40 g, and for the genetic immunization trial via intratracheal instillation, female Sprague-Dawley rats (8–10 weeks old), weighing 241–270 g, were purchased from the Animal Resources Centre (Canning Vale, Australia). Both mice and rats were housed under specific pathogen-free conditions and had access to food and water *ad libitum* at the Monash Institute of Pharmaceutical Sciences animal facility (Parkville, Australia). For the DNA vaccination of sheep via inhalation, female Merino-cross ewe lambs (5-6 months of age) used in these studies were housed in pens and fed *ad libitum* (Department of Physiology animal facility, Clayton, Australia) and judged free of significant pulmonary disease on the basis of clinical examination. All experimental animal procedures were approved by the Animal Experimentation Ethics Committee of Monash University,

following guidelines set by the National Health and Medical Research Council (NHMRC) of Australia.

4.2.4 Detection of Gene Expression *In vivo* following Intratracheal Delivery into Swiss Mice

For *in vivo* transfection, the mice were anesthetized by an intraperitoneal injection of 100 mg/kg body weight of ketamine (Parnell Laboratories, Australia) and 10 mg/kg body weight of xylazine (Tony Laboratories, Australia). A solution of sterile pVR1020 encoding YFP in 0.9% NaCl at a concentration of 1.5 mg/ml was nebulized using a 30 MHz SAW nebulizer and the condensed aerosol containing the nebulized plasmid was carefully collected as described earlier. For intratracheal instillation, the mice were suspended at 45 degrees by the upper teeth on a rodent dosing board and the trachea was visualized using a fiber optic stylet connected to an endotracheal tube (Biolite small animal intubation system, Kent Scientific Corp, USA). The trachea was intubated and post-nebulized plasmid in saline (50 $\mu\ell$) was delivered followed by 200 $\mu\ell$ of air. The mice were sacrificed 24 hrs later, and their lungs were harvested and subsequently frozen in Jung tissue-freezing medium (Leica Microsystems, Germany) and used for analysis. Cryosections (10 μm) were cut in a rotary paraffin microtome (microTec Laborgeräte GmbH, Germany), fixated with 1% paraformaldehyde and mounted with mowiol (4–88 Reagent from Calbiochem, Australia) solution to which 4',6-diamidino-2-phenylindole dilactate (DAPI, dilactate) was added, and subsequently examined under a confocal laser scanning microscope (A1, Nikon Instruments Inc., Japan) for YFP gene expression. Lung and airway morphology was examined on adjacent sections with hematoxylin and eosin. As additional confirmation of the detection of YFP in the mice lungs, the lung samples were homogenized using lysis buffer containing 50 mM Tris (pH 7.5), 100 mM NaCl and 1% Triton X-100.

The homogenate was then centrifuged and the supernatant was used for Western blot detection of the YFP protein. SDS-PAGE and immunoblotting analysis procedures were carried out as previously described, except that the membranes were probed with rabbit anti-YFP antisera.

4.2.5 Pulmonary Vaccinations using Pre-SAW nebulized plasmid DNA via Intratracheal Delivery

For pulmonary vaccinations, a solution of sterile pVR1020 encoding HA in 5% dextrose at a concentration of 300 $\mu\text{g}/\text{ml}$ was nebulized using a 30 MHz device and the condensed aerosol containing the nebulized plasmid was carefully collected as described earlier. The immunizations were carried out using the intratracheal instillation technique also described earlier. The tracheae of the rats were intubated and 300 μg of post-nebulized plasmid in 5% dextrose ($n = 8$, post-nebulized group), 300 μg of pre-nebulized plasmid in 5% dextrose ($n = 8$, pre-nebulized group), and 5% dextrose ($n = 8$, naïve group) in a total volume of 100 μl was delivered, followed by 200 μl of air. Subsequent immunizations were carried out 2 weeks (secondary) and 3 weeks (tertiary) after the primary immunization. Serum was collected prior to the commencement of the study and 5 weeks after the first immunization. Blood (1 ml) was collected from the tail vein using a 23-gauge needle, then left to coagulate for the collection of sera and subsequently stored at -20°C until further analyzed.

4.2.6 Pulmonary DNA Vaccination of Sheep using SAW via Inhalation

Sheep ($n = 4$) were immunized via inhalation through an endotracheal tube inserted through the nostril with sterile pVR1020 encoding HA in 5% dextrose at a concentration of 85 $\mu\text{g}/\text{ml}$, nebulized using a 30 MHz SAW device in a chamber placed in line with

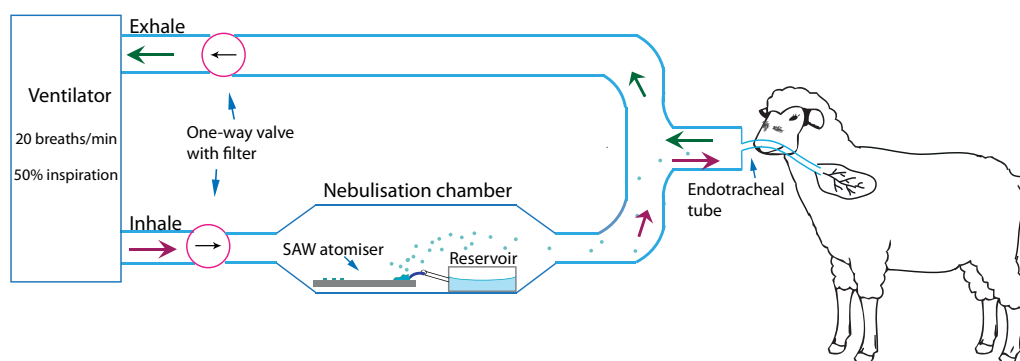


Figure 4.1: Schematic drawing of pulmonary DNA vaccination system to sheep via inhalation where room air was drawn through a bacterial/viral filter and a one-way valve placed in the inspiratory limb of where pDNA was introduced by nebulization with the 30 MHz SAW device in a chamber that was placed in line with a mechanical ventilator to be drawn by the sheep. Each sheep received three immunizations, once per three week period, with a pDNA aerosol containing sterile pVIR1020 encoding HA in 5% dextrose at a concentration of $85 \mu\text{g}/\text{ml}$ for 20–30 minutes through an endotracheal tube inserted through the nostril with proximal end connected to the respiratory wall. The expired gas was passed through a second filter-valve combination before exhausted through the ventilator.

the inspiratory limb of the mechanical ventilator (ventilator Model 55-0723; Harvard Apparatus, MA) set at 20 breaths/min at 50% inspiration for 20-30 minutes (as per Fig. 4.1). Two bacterial/viral filters (Hudson RCI, USA) and two low flow resistance, Hudson one-way valves (Hudson RCI, USA) were placed at each end of the inspiratory and expiratory limbs in line with the rest of the connecting tubing. In order to calculate the delivered mass of pDNA to the ovine lung, all tubing including the filters and valves, was carefully washed with deionized water to recoup any pDNA present, and subsequently quantified via an UV spectrophotometer described earlier. Subsequent immunizations were carried out 3 weeks (secondary) and 6 weeks (tertiary) after the primary immunization. Serum from peripheral blood samples that were collected prior to the commencement of the study and 1 week after the last immunization was stored frozen prior to determination of hemagglutination inhibition activity.

4.2.7 Evaluation of Antibody Responses to Enzyme-Linked Immunosorbent Assay

For the detection of anti-influenza (HA) antibodies in the serum samples, enzyme-linked immunosorbent assays (ELISAs) were performed in 96-well MaxiSorp plates (Nunc, Denmark). The plates were coated with 100 μL per well with 0.05 μg HA protein (Immune Technology Corp., USA) in carbonate coating buffer (0.015 M Na_2CO_3 , 0.035 M NaHCO_3 , 0.003 M NaN_3 , pH 9.6) and incubated at 4°C overnight. The coated plates were then washed three times with ELISA wash buffer (PBS-T; PBS with 0.05% v/v Tween 20 (Sigma Aldrich, Australia)). Two hundred microliters of blocking agent (2% w/v skim milk powder in PBS-T) was added to each well and incubated at 37°C for 60 mins. Plates were washed three times as before and 100 μL of 1 in 2 serial dilutions of undiluted serum in duplicates were added. Plates were incubated at 37°C for 90 mins and washed three times. Fifty microliters of a 1:10,000 dilution of anti-sheep IgG horseradish peroxidase (HRP) conjugated immunoglobulin (DAKO, Denmark) or 1:5,000 dilution of anti-sheep IgA horseradish peroxidase (HRP) conjugated immunoglobulin (AbCam, Australia) was then added to each well. Following incubation at 37°C for 60 mins and three washes, the plates were developed by the addition of 100 μL of 3,3',5,5'-tetramethylbenzidine (TMB) (Sigma Aldrich, Australia) substrate solution as previously described (217). Color development was stopped after 15 mins (in the case of IgG readings) and 20 mins (in the case of IgA readings) with 50 μL of 2 M H_2SO_4 . Absorbance was determined using a universal microplate reader (ELx80, Bio-tek Instruments Inc., USA) where the optical density was read at 450 nm and endpoint titers were calculated.

4.2.8 Evaluation of Hemagglutination Inhibition Activity

The serum samples were tested for inhibition activity against the A/Solomon Islands/3/2006 virus in round-bottom 96-well microtiter plates at room temperature using 1% v/v chicken

erythrocytes. Virus-induced hemagglutination titers were determined as the dilution of the samples that inhibited agglutination of chicken erythrocytes following 30 mins of incubation when 4 hemagglutinating units (HAU) of virus was added.

4.2.9 Statistical Analysis

Statistical analysis was performed using SPSS (Version 19, IBM Corporation, Armonk, USA). One-way ANOVA with a Tukey's post-hoc test was used for data that survived Shapiro-Wilk's (SW) normality test with significance $p > 0.05$, suggesting the data is normally distributed and therefore ANOVA was suitable. In instances where the SW test was significant ($p < 0.05$), the non-parametric Kruskal-Wallis (KW) test was used instead to test for the overall significance between independent groups. Where differences were observed, the Mann-Whitney (MW) tests were performed between two independent samples to identify the differences. For statistical testing involving two related samples that were not normally distributed, the Wilcoxon Signed Rank Test was used. All data are expressed as the mean \pm standard deviation. The results were considered significant if $p < 0.05$. Most immunization results were not normally distributed, as verified in Table 4.1.

4.3 Results and Discussion

4.3.1 *In vivo* Detection of Gene Expression in Mice Lungs.

Fig. 4.2 shows modest amounts of YFP expression were observed *in vivo* in mice following intratracheal instillation with condensed VR1020-YFP plasmid, which was previously nebulized using a 30MHz SAW device. Importantly, the amount of YFP expression was considerably larger compared to the YFP expression in an untreated mouse lung. The transfection efficiency was expected to be moderate, since it is widely known that naked

Table 4.1: Distribution of data collected from experiments in study.

Antibody responses to enzyme-linked immunosorbent assay from rat immunization		
Study	Shapiro-Wilk normality test statistic	Normally distributed?
IgG Responses		
Naïve	1.000	No
Post-vaccinated with non-nebulized pDNA	0.634	No
Post-vaccinated with SAW-nebulized pDNA	0.029	Yes
IgA Responses		
Naïve	1.000	No
Post-vaccinated with non-nebulized pDNA	0.299	No
Post-vaccinated with SAW-nebulized pDNA	0.319	No
Hemagglutination inhibition activity		
Rat Immunization		
Naïve	1.000	No
Post-vaccinated with non-nebulized pDNA	0.000	Yes
Post-vaccinated with SAW-nebulized pDNA	0.000	Yes
Sheep Immunization		
Pre-vaccination	1.000	No
Post-vaccination	0.024	Yes

plasmid is susceptible to rapid degradation *in vivo* (218). The YFP-positive cells that were detected in the mouse lung were mostly located within a region close to the epithelium of the conducting airways, where they displayed discrete aggregates of YFP protein (Fig. 4.3), consistent with other studies of GFP (Green Fluorescent Protein) gene expression following plasmid delivery to mouse lungs (113; 219). The Western blot result (Fig. 4.4) further confirmed these findings, showing YFP protein present in the lung samples that were transfected with the condensed VR1020-YFP plasmid previously nebulized using a 30MHz SAW device, compared to that of an untreated mouse lung where the respective band was not present. The absence of hemosiderin deposits that would otherwise result from microhemorrhages in the lung tissue was confirmed using sections that were stained with Perl's Prussian blue and counterstained with neutral red (Fig.4.5). These observations further support the *in vitro* gene expression results, and further validate the use of SAW nebulization as a viable delivery platform for aerosol gene therapy.

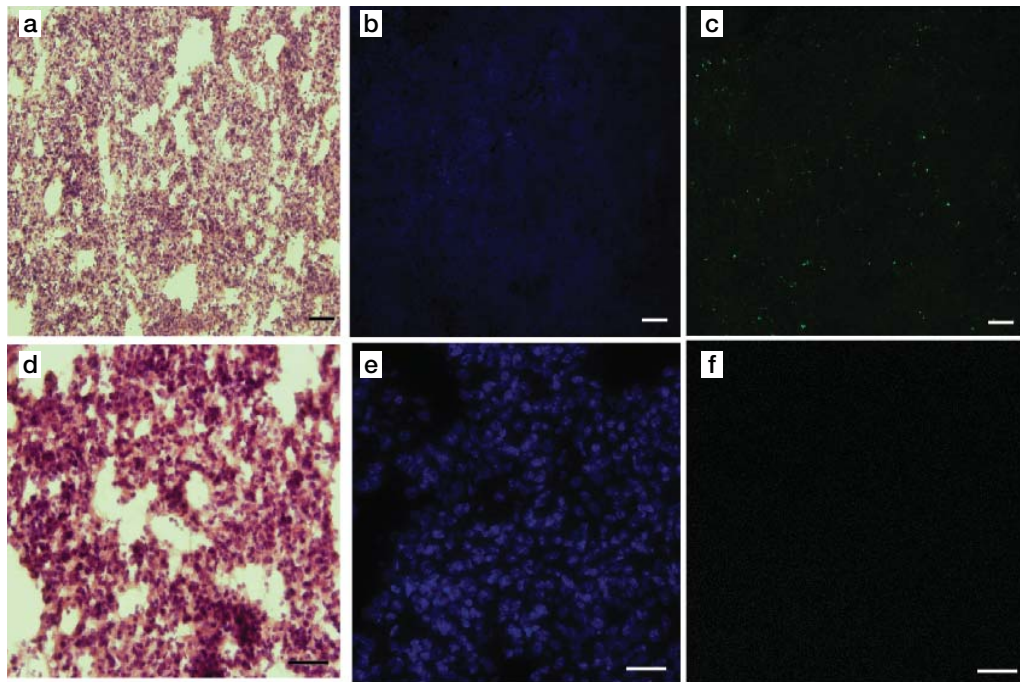


Figure 4.2: Confocal microscopy of mouse lung parenchyma cryosections after (a, b, c) dosage with post-nebulized pVR1020–YFP in 0.9% NaCl aqueous solution, compared to an (d,e,f) untreated case (scale bars: 100 μ m). The lung structure (a,d) and (b,e) cell nuclei are indicated with a counterstain of hematoxylin and eosin, and with DAPI, respectively. Lung cells expressing YFP from instilled pVR1020–YFP appear green in (c) the treated lung sample; note absence of green in the (f) untreated sample. The control lung samples were imaged at a higher resolution to confirm the absence of YFP response.

4.3.2 Antibody Responses following DNA Vaccination following Intratracheal Delivery of SAW Nebulized VR1020-HA.

Sera collected before the commencement of the study and five weeks after the first immunization were used to evaluate systemic antibody responses to the protein antigen encoded by the pDNA. Significant increases in both immunoglobulin (Ig) G and A antibody titer levels against the influenza antigen, human hemagglutinin, were observed in both groups of female Sprague-Dawley rats that received plasmid DNA vaccinations via intratracheal instillation compared to the naïve rat group (See Figure 4.6, $p < 0.001$ for both; KW following significant LTEV). The anti-influenza antibody titers are comparable to earlier studies in which plasmid encoding influenza A HA protein and protected with PEI was

delivered via intranasal DNA injection in BALB/c mice (220). This result is encouraging, given the fact that naked plasmid DNA was used for the current study, a form highly susceptible to DNAase degradation *in vivo*.

Importantly, no significant differences in both IgG and IgA levels were observed between the groups that received the nebulised and non-nebulised form of the plasmid DNA vaccine (Figure 4.6, $p = 0.163$ for IgG comparison and $p = 0.486$ for IgA comparison; KW following significant LTEV). The result suggests that the bioactivity of the DNA vaccine is preserved during the nebulisation process, an important consideration if DNA vaccination is to be performed by SAW technology. Because of the properties of a rat lung anatomy including airway size and surface anatomy, it is not possible for the rat to directly respire nebulized droplets. It is also not possible to accurately determine the lung dose to a rat due to prolonged skin exposure and uptake of pDNA droplets via the skin during the nebulization process. Thus, it is possible that the aerosol form of a DNA vaccine may be different to the recovered, intratracheal formulation used in this study. Additional experiments in large animals such as sheep will be necessary for the study of the immunogenicity of directly inhaled SAW-nebulized particles.

4.3.3 Hemagglutination Inhibition (HAI) Activity of Antibodies Raised Against Vaccinations with SAW Nebulized DNA in Rats.

Importantly, the antibody responses showed functional activity, as demonstrated by the inhibition of viral agglutination of chicken red blood cells (See Table 4.2 for the hemagglutination inhibition activity). Protection against flu can be predicted from HAI titers, such that serum IgG with HAI activity ($\gg 40$) is considered to be protective by the World Health Organisation (WHO). Both groups that received the plasmid DNA vaccine achieved this level of activity. There were significant differences in HAI titers between

two groups of rats that were immunized three times via intratracheal instillation to the lungs with a 300g plasmid DNA vaccine encoding hemagglutinin in 5% dextrose (pre and post-nebulised), compared to those of the control group ($p < 0.001$ for both; KW following significant LTEV). The serum antibody HAI activity achieved compares well to other studies, where 10g of DNA vaccine encoding a similar HA protein derived from a swine flu strain (H1N1) 2009 formulated with the cationic polymer PEI was administered intranasally to BALB/c mice twice at 4-week intervals (HAI titer averaging 1800) (220). The results of the current research also compare well to a protein vaccination study, in which HA protein was injected into sheep (221) subcutaneously or delivered to the lung with adjuvant ISCOMATRIX, HAI titers of around 95 (15 g of flu HA protein) and 122 (0.04 g of flu HA protein) respectively was obtained after the tertiary dose.

Most importantly, there were no significant differences between the groups that received plasmid DNA vaccine in the pre-nebulised form and the post-nebulised form (Table 4.2: $p = 0.602$; KW following significant LTEV), demonstrating the preservation of the immunogenicity of the anti-influenza DNA vaccine that was subjected to the SAW nebulisation process. This again validates the use of the nebuliser for genetic vaccination via the pulmonary route.

4.3.4 Aerosol Vaccination of Sheep and the Hemagglutination Inhibition (HAI) Activity of Antibodies Raised.

The nebulized mist was found to induce a powerful pharmacodynamic response when inhaled into the lungs of sheep under mechanical respiration, with similar levels of antibody response to those observed in rats. Tabulated in Table 4.3, HAI titers averaging 192 ($n = 4$) were detected in the sera of these large animals after immunization three times at three-week intervals using a 30 MHz SAW device placed between the nasally-intubated

Table 4.2: Hemagglutination inhibition (HAI) activity for each rat; $n = 8$ for the control, naïve rats and for the vaccinated mice. HAI is strongly ($\gg 40$) induced in the sera by lung immunization with a post-nebulized pDNA sample encoding an influenza antigen at similar levels to a non-nebulized pDNA sample.

Animal	Naïve		Pre-nebulized		Post-nebulized	
	Pre-Vaccination	Post-Vaccination	Pre-Vaccination	Post-Vaccination	Pre-Vaccination	Post-Vaccination
1	< 5	< 5	< 5	800	< 5	800
2	< 5	< 5	< 5	1600	< 5	800
3	< 5	< 5	< 5	1600	< 5	800
4	< 5	< 5	< 5	1600	< 5	1600
5	< 5	< 5	< 5	1600	< 5	1600
6	< 5	< 5	< 5	1600	< 5	1600
7	< 5	< 5	< 5	1600	< 5	1600
8	< 5	< 5	< 5	1600	< 5	1600

Table 4.3: Hemagglutination inhibition (HAI) activity for each sheep ($n = 4$). HAI is strongly (> 40) induced in the sera by lung immunization via inhalation with a pDNA sample encoding an influenza antigen at significantly higher levels to pre-immunization.

Animal	Pre-Vaccination	Post-Vaccination
1	< 1	256
2	< 1	128
3	< 1	256
4	< 1	128

sheep and a mechanical ventilator. The sheep received $156 \pm 44 \mu\text{g}$ (mean of $n = 8$ independent experiments, with error showing standard deviation) pDNA vaccine encoding HA in 5% dextrose, via inhalation through an endotracheal tube inserted through the nostril. Given the difficulty of inducing functional antibody responses using DNA vaccination in large animals (222), we report here the first instance of successful vaccination via inhalation using an unprotected pDNA vaccine in sheep, a model relevant to human lung development, structure, physiology, and disease (223).

4.4 Conclusions

This work further confirms the feasibility of SAW nebulization technology as an efficient pulmonary delivery platform for plasmid DNA molecules, proteins and other biomolecules (224), as evidenced by the successful induction of IgG and IgA antibody levels with hemagglutination inhibition activity in immunized animals. These findings suggest the SAW nebulizer may serve to effectively deliver rapidly-produceable pDNA vaccines. This represents a significant outcome in the context of pandemic episodes in the developing world without either a sufficient health workforce or access to safe injection methods.

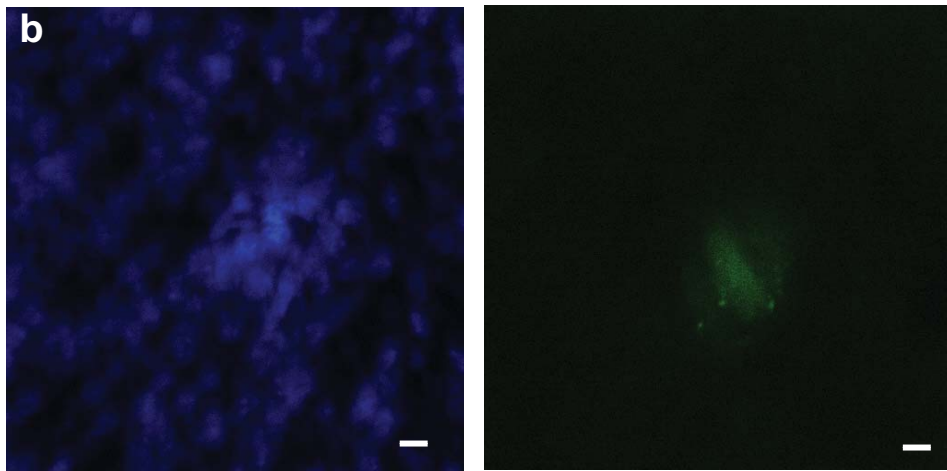
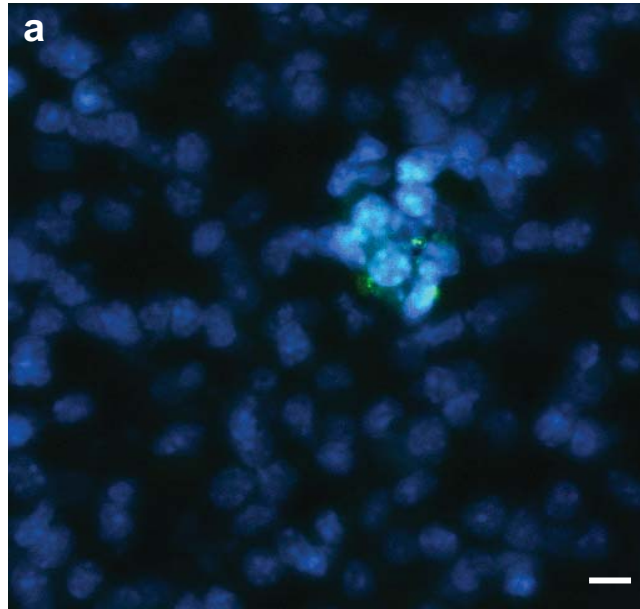


Figure 4.3: YFP expression in a cluster of epithelial cells around the terminal airways. (a) Lung cell nuclei stained with 4',6-diamidino-2-phenylindole dilactate (DAPI dilactate) appear blue while cells expressing YFP appear green (scale bar = 5 μm); (b) another view of a part of the YFP-expressing cell region shows the YFP distribution in the cells with appropriate filtering to show only the nuclei (left panel) and YFP (right panel) (scale bar = 5 μm).

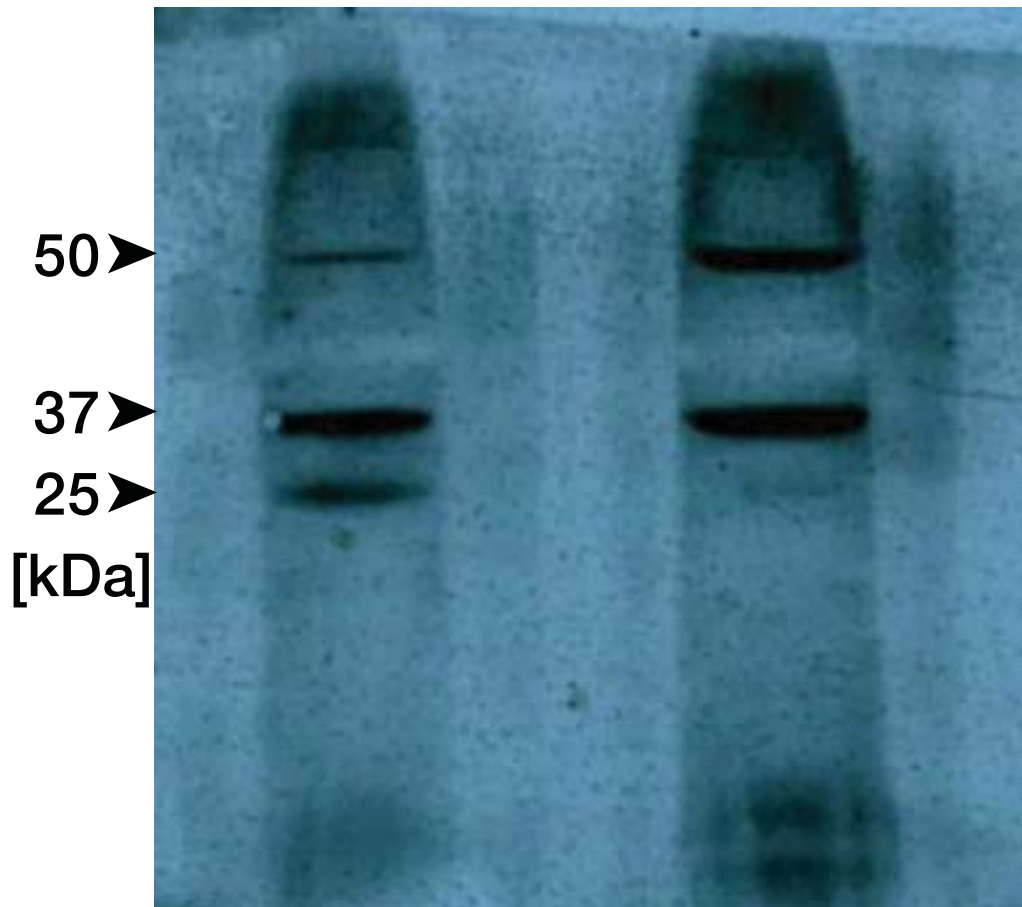


Figure 4.4: Western blot of the supernatant obtained from homogenized mice lungs harvested (left lane) 24 hrs post-transfection with pVIR1020–YFP plasmid that was SAW nebulized at 30 MHz and instilled, compared to (right lane) the supernatant from untreated mice lungs. The resulted YFP protein appears clearly at 27 kDa.

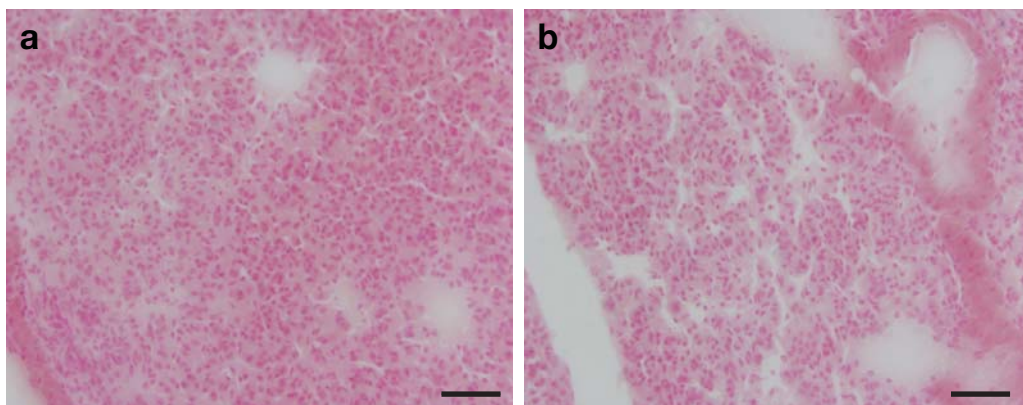


Figure 4.5: Examination of mouse lung cross-sections stained with Perl's Prussian blue and counterstained with neutral red shows no hemosiderin deposits, indicating the absence of microhemorrhages in the tissue of (a) lungs instilled with pVIR1020-YFP plasmid solution post-SAW nebulization and (b) untreated lungs. (scale bars indicate = 100 μm).

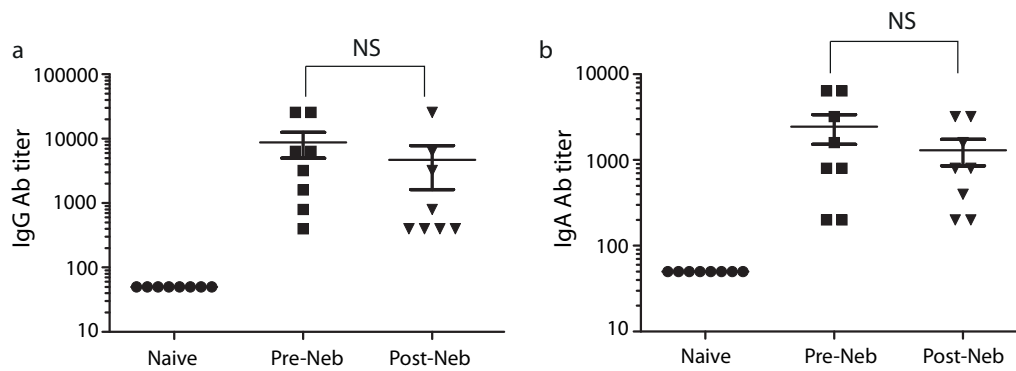


Figure 4.6: Systemic and mucous antibody responses detected in the sera of female Sprague-Dawley rats ($n = 8$ per group) following pVR1020-HA pDNA vaccination encoding an influenza A virus surface antigen, human hemagglutinin via lung instillation. No significant (NS) differences between the pre- and post-SAW nebulized vaccine instillation were found ($p = 0.163$ for IgG and $p = 0.486$ for IgA, respectively), and a significant difference between these and the naïve rats was found ($p < 0.001$).

Chapter 5

Optimization of High Frequency Acoustic Wave Nebulization for Improved Drug Delivery using Amplitude Modulation

Practical, commercially viable microfluidic devices depend upon the miniaturization and integration of all components onto a chip-based platform, including pumps, circuitry, power—all that is required for a given device to function. In this chapter, amplitude modulation is presented as a simple, effective means for reducing the power necessary in SAW microfluidics that has been shown to be useful for pulmonary DNA vaccination in the previous chapter.

5.1 Introduction

While pulmonary drug delivery has for several decades constituted a highly effective and widely administered form of therapy, particularly for the treatment of asthma and chronic obstructive pulmonary disease, widely available pressurized metered-dose inhalers and

dry powder inhalers are nearly identical to the original push-and-breathe concept introduced in the 1950s (179). This is despite many advances in inhaler and nebulizer technology, including particularly the development of adaptive delivery technology that synchronizes delivery of the aerosol to the patient's breathing pattern in order to optimize delivery and reduce the amount of drug wasted during exhalation (225). Such state-of-the-art technologies often involve a combination of built-in sensors, electronic control schemes and active aerosol generation mechanisms. Although recent achievements in adapting integrated-circuit fabrication techniques to microfluidics promise to address issues of cost and integration, the requirement of a large and complex power supply and ancillary equipment to drive such devices leaves them impractical for their intended application: personal, daily use by a patient.

This is also an impediment to broader implementation of inhalation therapy. Vaccination, gene therapy and the treatment of other diseases such as cystic fibrosis and lung cancer all represent potential therapeutic applications of a personal nebulizer, given the suitability of pulmonary drug administration for efficient, reproducible, non-invasive, safe and low-cost systemic delivery of certain peptides, proteins and pDNA (226; 8). Effective disease treatment and vaccination options in disadvantaged areas of the world are almost absent; the pulmonary route represents one of the few ways to deliver medications without increasing the risk of infection and cross-contamination of disease due to needle sharing and unsanitary conditions. An inexpensive pulmonary delivery system would represent a potential solution to this problem.

Although the original concept of the SAW microfluidic aerosol delivery platform (14; 224) was intended to be driven by a palm-sized battery-powered circuit (Fig. 5.1), the limited power output available from the circuit imposed a constraint on the aerosol production rate. Increasing the power available to the device requires the use of larger driver circuits (Fig. 5.1(b)) that prohibit a complete, miniaturized package for portable use. Here, we investigate a method to reduce the power requirements of the SAW atomization technique.

A low-power SAW atomization design has been previously proposed by compressing the width of the SAW propagation through the use of a metallic horn and waveguide pattern placed in front of the interdigital transducer electrodes (IDTs) used to generate the SAW (227). While reducing the power required for atomization by a third, the atomization rate still did not exceed $50 \mu\ell/\text{min}$. Another simple yet effective means of improving power efficiency in SAW devices is through pulse width modulation (1 kHz) of the input signal (into a 9.8 MHz device) (228), where an optimal atomization rate of little over $600 \mu\ell/\text{min}$ was achieved, but extremely high voltages are necessary, as high as $180 \text{ V}_{\text{p-p}}$, and the aerosol size distribution is known to be more polydisperse.

We propose an amplitude modulation scheme for further reducing the power requirements to allow battery-powered operation from a similar driver circuit, but which also increases the aerosol delivery rate. Amplitude modulation is already widely used in radio communication where the sinusoidal radio-frequency signal is modulated by an audio-frequency signal before transmission (229). The power of the transmitted signal is concentrated at the carrier frequency, thus comprising a useful means for power optimization. The use of modulated surface acoustic waves to drive larger oscillations and quicker motion of the drops with low power droplets was recently reported by Baudoin *et al.* (230). However, the application of amplitude modulation to SAW atomization, which requires the highest energy input levels of all known SAW microfluidic processes, for the delivery of biomolecules has never been studied to date and will be the focus of this chapter.

In the application of amplitude modulation to SAW atomization, it is important to appreciate that the aerosols are formed due to the destabilization and break-up of the parent drop's free surface that is governed by a capillary-viscous mechanism. A dominant force balance between the capillary and viscous stresses suggests that the capillary-viscous resonant frequency scales according to the relationship below, (2)

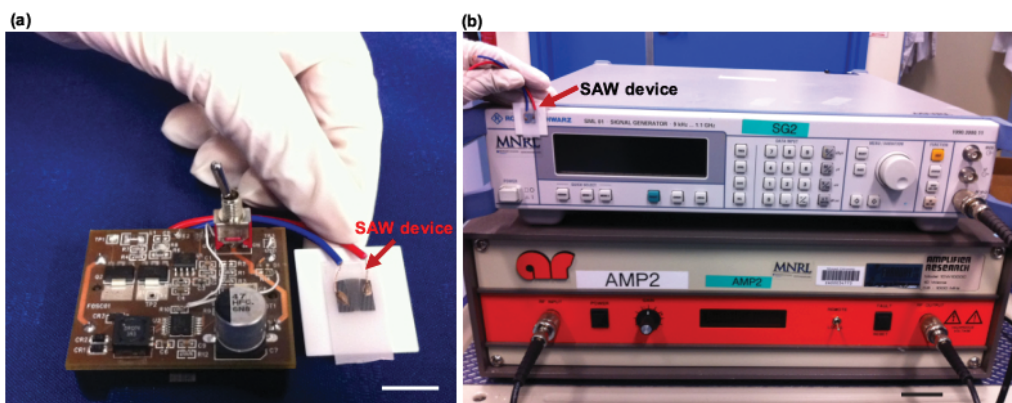


Figure 5.1: (a) Initial prototype of the battery-powered circuit to be used to drive the SAW microfluidic aerosol delivery platform (scale bar = 1 cm). (b) Typical signal generator and amplifier used in laboratory settings to provide sufficient power for the SAW atomization (scale bar = 3 cm).

$$f \sim \frac{\gamma}{\mu R}, \quad (5.1.1)$$

implying that a parent drop with a characteristic dimension $R \sim 10^{-3}$ m comprising typical fluids with surface tension $\gamma \sim 10^{-2}$ kg/s² and viscosity $\mu \sim 10^{-2}$ – 10^{-3} kg/(ms⁻¹) typically vibrates under resonance at 1–10 kHz-order frequencies. Such intuitive consideration of the underlying fundamental physical mechanism governing the atomization process is useful, as it suggests a means to provide acoustic energy directly at the capillary wave resonance to efficiently drive drop vibration instead of relying on a nonlinear parametric coupling mechanism to downshift the 10–100 MHz order SAW excitation to kHz-order capillary wave generation, a phenomenon observed directly in our studies (231). Consequently, it is possible to simultaneously exploit the combined advantages of both high (MHz-order) and low (kHz-order) frequency operation to potentially achieve more efficient atomization.

One of the common concerns of relatively low frequency (audible to ultrasonic) excitation is the damage to large molecules in the fluid to be atomized (22). This is caused by large shear stresses exerted on the molecule either, directly by the hydrodynamics

or indirectly through cavitation. A significant portion of our study reported below was therefore devoted to the investigation of the continued viability of large biomolecules post-atomization. Since the intention is to use this technology for pulmonary gene and vaccine delivery, DNA and antibodies are used during the atomization process as exemplars of typical biomolecules that might be used with the system, although in past work there has been some evidence of the survival of proteins, polymers and even cells through the SAW atomization process (224; 232; 175). However, it is also necessary to verify that the aerosol drop size distribution still lies within the optimum respirable size range (1–10 μm) necessary for oropharyngeal and deep lung delivery (10; 202; 201).

While we demonstrate the use of amplitude modulation here for reducing the power requirements in SAW nebulization devices, the same scheme can be applied to the entire range of SAW microfluidics for miniaturization towards true lab-on-a-chip functionality. Therefore, the findings of this chapter can be applied to a myriad of SAW devices proposed for applications ranging from fluid manipulation (e.g. particle sorting, microchannel pumping, droplet transport) to chip-scale chemical and biochemical synthesis.

5.2 Experiments and Materials

5.2.1 Surface Acoustic Wave Nebulizer

The 30 MHz SAW device employed in this experiment consisted of a low-loss piezoelectric material, 127.86° *Y*-rotated, *X*-propagating single-crystal lithium niobate (LiNbO_3), upon which were fabricated a pair of single-phase unidirectional transducers (SPUDTs) via standard UV photolithography processes in 5 nm Cr under 250 nm Al. The width and gap of the interlaced finger patterns of the SPUDT determines the SAW wavelength λ_{SAW} ; in this study, $\lambda_{\text{SAW}} = 132 \mu\text{m}$ corresponds to a SAW frequency of 30 MHz (carrier frequency). The curved SPUDTs focus the acoustic energy to which fluid is delivered

from a reservoir via a pre-wetted paper wick embedded at the tip of a capillary tube (224) that allows continuous flow of fluid without the need of a syringe pump. Images of the device are shown in Fig. 5.2. As a sinusoidal electrical input at the SAW frequency (convolved with amplitude modulation where appropriate) is applied to the SPUDT, SAWs are generated that propagate along the LiNbO_3 substrate across to the leading edge of the paper wick, where they continuously draw liquid out from the paper onto the substrate to form a thin film (224). Since acoustic energy also leaks into the liquid film, the free surface of the film destabilizes and beyond a critical input power, breaks up to form aerosol droplets (Fig. 5.2(c)). There is no observable flow onto the device in the absence of SAW (for example, which might be present due to evaporation). Therefore, the flow rate through the capillary tube, measured using the graduated scale marked on the tube, is a good estimate of the aerosol production rate, given that the film dimensions can be assumed to be fairly constant during atomization.

5.2.2 Effect of Amplitude Modulation on the Aerosol Size

The aerosol size distributions of the deionized water droplets generated via SAW nebulization were measured using laser diffraction (Spraytec, Malvern Instruments, Malvern, UK) for measurement. Here, we measured a single aerosol size parameter D_{v50} , representing the mean diameter across the 50th percentile within the volume size distribution.

5.2.3 Atomization Rate with Amplitude Modulated Surface Acoustic Waves

The paper wick and capillary tube (without the reservoir) were filled with deionized water as a model fluid. As the water was atomized, the time was recorded when the meniscus retracted past consecutive graduation marks on the capillary tube shown in Fig. 5.2(a). Experiments were repeated three times at each sinusoidal amplitude modulation frequency:

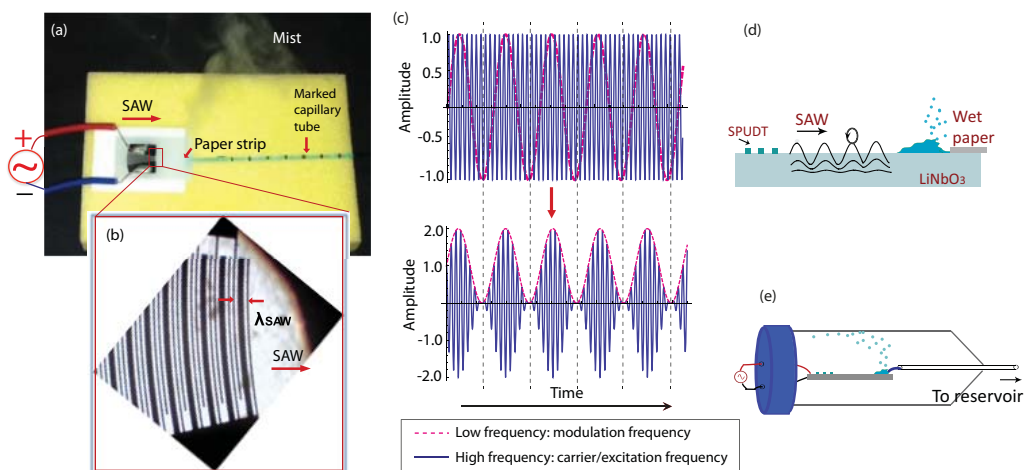


Figure 5.2: (a) Image of a 30 MHz SPUDT SAW device. The fluid is delivered to the SAW substrate through a paper strip embedded in a capillary tube which is connected to a reservoir. In order to record the aerosol production rate, the capillary tube was marked along its length at 0.5 cm intervals. (b) Enlarged view of the SPUDT. The width and gap of the interleaved finger electrodes determine the SAW wavelength λ_{SAW} , 132 μm for a 30 MHz device. (c) The left panel is a schematic illustration of the SAW atomization mechanism. The SAW (not shown to scale) propagates along the substrate and leaks energy into the liquid film to drive the destabilization of its free surface (2). The right panel illustrates the set-up used to condense and collect the aerosolized DNA or antibodies within a conical Falcon tube for further *in vitro* characterization of their post-atomization viability.

500 Hz, 1 kHz, 5 kHz, 10 kHz, 20 kHz and 40 kHz. Since the amplitude modulation results in more efficient atomization through lower energy consumption, the power input was kept at low levels (1.5 and 2 W). Control experiments were carried out in the absence of amplitude modulation where power levels of 1.5, 2, 3 and 4 W were used.

5.2.4 Effect on Plasmid DNA Delivery During the Use of Amplitude Modulation

Preparation and purification of plasmid DNA

Plasmid DNA (pDNA) was prepared from an influenza A virus surface antigen, human hemagglutinin (A/Solomon Islands/3/2006 (egg passage) (H1N1) strain), once cloned

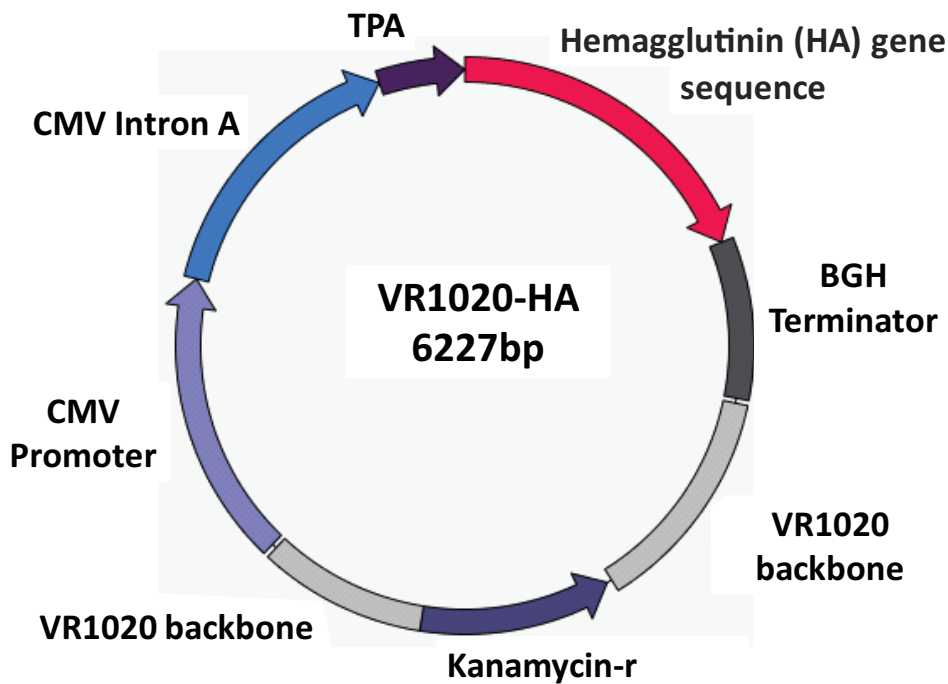


Figure 5.3: Representation of pVR1020 with vector encoding the hemagglutinin (HA) gene sequence. Gene encoding HA is inserted in plasmid VR1020 that contains secretion signal of tissue plasminogen activator (TPA), human cytomegalovirus (CMV) early promoter, CMV intron A, bovine growth hormone (BGH) terminator and kanamycin resistance gene.

into the mammalian expression vector VR1020 (Vical Inc., San Diego, CA) (Fig. 5.3). The entire coding sequence of HA was amplified by PCR using primers forward and reverse that incorporated a BamHI site at the 5° end and a EcoRI site at the 3° end. Forward: 5°-CGCGGATCCATGAAAGTAAACTACTGGTCCTGTTATG-3°; reverse: 5°-CCGGAATTCTTGTGGTAATCCCATTAATGGCATTGTTGT-3°. The PCR product was digested with BamHI / EcoRI and ligated into the 3°C plasmid VR1020, resulting in plasmid VR1020–HA. A colony of *E. coli* DH5 α transformed with the plasmid VR1020–HA (~6 kbp) was picked from a streaked selective plate and inoculated in 10 ml of LB medium containing 100.0 g/ml of kanamycin. The starter culture was incubated at 37°C and agitated at 200 rpm for 8 hrs before being transferred to five separate 200 ml LB media, and further cultured for 12 hrs. The cell cultures were stored at –70°C for subsequent use. The plasmids were purified from cells using an endotoxin-free plasmid purification

kit (Plasmid Mega Kit, QIAGEN Pty. Ltd., Doncaster, VIC, Australia) according to the manufacturer's instructions.

SAW Nebulization of plasmid DNA

Atomization was confined in a 50 ml conical Falcon tube (BD Bioscience, Franklin Lakes, NJ), as depicted in Fig. 5.2(d). Plasmid DNA aerosols were collected after condensation on the Falcon tube wall. Both control and atomized pDNA samples were analysed for potential alterations in the plasmid structure with 1% agarose gel electrophoresis using GelRedTM staining, and a 1 kbp DNA ladder was employed as a size marker. The gel was made up of 5 g agarose at 1x dilution of TAE buffer (242.0 g Tris base, 57.1 ml CH₃COOH, 9.3 g of EDTA). The electrophoresis was carried out under 120 V_{DC} for 60 mins. The resulting gel was analysed and imaged in an automated gel imaging system (Molecular Imager[®] Gel Doc XR, Bio-Rad Laboratories Inc., Hercules, CA). The intensity of the bands for each structure corresponds to the number of DNA molecules. The percentage of supercoiled (sc) and open circular (oc) to fragmented DNA was quantified via densitometry software (Quantity One[®], Bio-Rad Laboratories Inc., Hercules, CA) by comparing pre- and post-atomized samples.

5.2.5 Effect of Amplitude Modulation on the Protein Nebulization

Atomization of rabbit anti-YFP antiserum solution (diluted at 1:20) obtained from collaborators at the Coppel Laboratory (Department of Microbiology, Monash University) was carried out in the same manner as that for the pDNA. The antibody was then detected using dot blot analysis when 5 μ l of YFP protein solution was dotted onto a transfer membrane (PolyScreen[®] PVDF, PerkinElmer Inc., Waltham, MA) for immunoblotting. The membranes were incubated overnight at 4°C in TBS-T buffer (0.05 M Tris-HCl pH 7.4,

0.15 M NaCl, 0.05% Tween 20) containing 5% non-fat milk powder. The membranes were then probed with atomized anti-YFP antiserum solutions for 1 hr at room temperature, and washed three times in TBS-T for 10 mins each time. Primary antibody reactivity to immunoblotted proteins was detected with anti-rabbit immunoglobulin conjugated to horse radish peroxidase (HRP; Silenus Laboratories Pty. Ltd., Hawthorn, VIC, Australia) and visualized by Renaissance[®] Western Blot Chemiluminescence Reagent (NEN Life Science, PerkinElmer Inc., Waltham, MA).

5.2.6 Statistical Analysis

Statistical analysis was performed using SPSS (Version 19, IBM Corporation, Armonk, NY USA). One-way ANOVA with a Tukey's post hoc test was used for data that survived Levene's test of equality of error variances; in other words, when the null hypothesis of equal variances between the data sets is judged to be valid with significance $p \geq 0.05$, suggesting the data is normally distributed and therefore ANOVA was suitable. In instances where the Levene's test of equality of error variances was significant ($p < 0.05$), the non-parametric Kruskal-Wallis test was used instead to test for significance. All data are expressed as the mean \pm standard deviation. The results were considered significant if $p < 0.05$.

5.3 Results and Discussion

5.3.1 Aerosol Production Rate

Table 5.1 shows the atomization rate at each power level, with and without the application of amplitude modulation. The rate at which aerosols are produced at 1.5 and 2 W is roughly quadrupled and trebled, respectively, when amplitude modulation is employed.

Table 5.1: Effect of amplitude modulation at various frequencies on the atomization rate

Input power (W)	No ampl. mod. Rate ($\mu\ell/\text{min}$)	Amplitude modulation	
		Freq. (kHz)	Rate ($\mu\ell/\text{min}$)
1.5	23.4 ± 2.1	0.5	103.7 ± 14.2
		1	85.1 ± 16.3
		5	80.5 ± 9.4
		10	43.2 ± 4.3
		20	56.6 ± 6.3
		40	50.4 ± 5.9
2	50.8 ± 2.2	0.5	126.8 ± 22.8
		1	103.8 ± 13.5
		5	100.3 ± 11.5
		10	111.4 ± 13.3
		20	77.0 ± 8.0
		40	74.9 ± 6.4
3	134.9 ± 15.2		
4	211.9 ± 71.1		

To express this in a different way, the power required to achieve satisfactory aerosol delivery for a portable handheld nebulization device, typically $100 \mu\ell/\text{min}$ or more, is halved with the use of the amplitude modulation scheme. From Table 5.1, we note that the atomization rate is slightly reduced as the amplitude modulation frequency is increased, particularly beyond 10 kHz; as the modulation frequency grows beyond the capillary-viscous resonant frequency of around 1–10 kHz order (as estimated from Eq. (5.1.1)), the resonant interaction is possibly weakened, causing the atomization rate to drop.

When comparing the optimal aerosol production rate to the results obtained with past SAW atomizers employing pulse width modulation (1 kHz) of the input signal for a SAW device at 9.8 MHz (228), voltages of around 120-140 V_{p-p} were required to achieve production rates of $200 \mu\ell/\text{min}$. For the SAW devices in the current study without amplitude modulation, voltages of around 50 V_{p-p} are required to achieve similar aerosol production rates. Employing amplitude modulation substantially reduces the required voltage to as little as 35 V_{p-p} .

Table 5.2: Effect of amplitude modulation at various frequencies on the aerosol volume mean diameter D_{v50} . For each experiment, the fluid was atomized for 20 seconds with 50 data points sampled every second. This was repeated four times for every parameter set, i.e., $n = 4000$ data points for each set of parameter values

Input power (W)	No amplitude mod. D_{v50} (μm)	Amplitude modulation	
		Freq. (kHz)	D_{v50} (μm)
1.5	7.29 ± 0.90	0.5	9.75 ± 1.89
		1	8.55 ± 0.72
		5	7.94 ± 0.08
		10	8.63 ± 0.89
		20	8.32 ± 0.15
		40	7.76 ± 0.21
2	8.53 ± 1.06	0.5	9.69 ± 1.38
		1	11.25 ± 0.61
		5	9.15 ± 0.53
		10	9.01 ± 1.36
		20	8.13 ± 0.10
		40	7.80 ± 0.34
3	10.51 ± 1.09		
4	10.18 ± 0.70		

5.3.2 Aerosol Size

Table 5.2 is a compilation of measured aerosol sizes showing the effect of amplitude modulation and the effect of the amplitude modulation frequency.

In our previous work (14), the aerosol diameter D was estimated from the wavelength λ associated with the interfacial instability, which, from a balance between the dominant axial capillary stress and the viscous stress, reads (2)

$$D \sim \frac{\gamma H^2}{\mu f_c L^2}, \quad (5.3.1)$$

where H and L are characteristic height and length scales of the liquid drop or film, suggesting that the geometry of the parent liquid plays a role in the aerosol size. According to the theory expounded above for a sessile drop, higher input powers would deform the liquid into a conical drop with a H/L ratio close to 1, therefore leading to the production

of larger aerosol diameters upon atomization. Although the meniscus is trapped by the paper wick in the arrangement used in this study, the net thickness of that meniscus can still be altered by the applied power in the same manner. During continuous operation without amplitude modulation at 3 and 4 W of input power, the meniscus forms a conical shape akin to that seen for sessile drop atomization, resulting in a larger H/L ratio and hence larger aerosol size; at lower power levels the fluid spreads into a thin film with small H/L ratio and hence generates a smaller aerosol size (2; 14). This is consistent with the result in Table. 5.2, where a significant (Tukey's post hoc test) increase in aerosol size from the low 1.5 W input to higher power levels of 3 W ($p = 0.016$) and 4 W ($p = 0.028$) is seen.

Importantly, other than the increase in the aerosol size with the application of amplitude modulation, in the specific case of 1 kHz at 2 W ($p = 0.03$), there was no significant change in the atomization due to amplitude modulation at both 2 W (Tukey's post hoc test) and 1.5 W (Kruskal-Wallis Test). The paper wick effectively prevented changes in the depth of the meniscus and the associated aspect ratio H/L , and therefore the aerosol droplet diameter remained unaffected. Nevertheless, since the capillary wave resonant frequency is independent of either the excitation frequency (an argument that is strongly supported by past work (2; 233)) or the carrier frequency, we therefore do not expect the carrier frequency at which the amplitude modulation signal is driven to give rise to appreciable differences in the aerosol size, as is observed here (the reverse logic is also true: the fact that we do not see any effect of the carrier frequency lends further support to the idea that the excitation and capillary wave resonance frequencies are independent). In any case, the absence of any significant change in the aerosol size with amplitude modulation of the SAW signal is encouraging from a practical perspective, given the necessity for the aerosol diameters to lie in the 1–10 μm range for optimal deposition in the oropharyngeal and lower respiratory tract region for successful drug delivery to the lung.

5.3.3 Post-Atomization Biomolecular Integrity and Viability

The integrity of cells and proteins under 10–100 MHz order SAW irradiation has been previously investigated at intensity levels up to where atomization occurs (224; 232; 194). In these studies, little damage due to shear lysis of these biomolecules has been found. This was primarily attributed to the short time-scales associated with the periodic reversal associated with the electromechanical field of the 10–100 MHz order oscillating signal, at least several orders of magnitude smaller than the characteristic hydrodynamic time scale (2). Consequently, there is typically insufficient time to cause hydrodynamic shear unfolding of biomolecular structures. These previous investigations did not account for lower kHz-order frequency effects associated with the amplitude modulation, which are a concern since acoustic sonoporation of cells and molecular scission via hydrodynamic shear and cavitation are often carried out using ultrasonication at frequencies between 20 and 50 kHz (135; 144; 9). We therefore carried out a brief study employing two model molecules to span the spectrum of potential applications for the SAW inhalation therapy platform across gene and vaccine delivery, namely plasmid DNA (pVR1020-HA) and an antibody (rabbit anti-YFP antisera).

We note that pDNA fragmentation largely occurs under typical strain rates of 10^{-5} – 10^{-6} s^{-1} , corresponding to oscillations in the 100 kHz to 1 MHz range. Although these are fortuitously between the 10–100 MHz order SAW carrier and the 1–10 kHz order modulation frequencies, the true range of strain rates that lead to pDNA damage is unclear. In fact, 80% of the retained supercoiled pDNA is intact after atomization, even in the absence of amplitude modulation (Fig. 5.4). Turning on amplitude modulation at 500 Hz, the retained supercoiled pDNA fraction remains roughly similar, gradually decreasing to around 50% as the modulation frequency is increased to 10 kHz, only to sharply drop to 30% as the carrier frequency is increased further to 40 kHz. This transition is closer to our estimate of the 100 kHz order frequencies at which the shear rates are sufficient to

induce uncoiling and damage of the pDNA, and is consistent with the 20–50 kHz frequencies of ultrasonication for sonoporation and scission. A reasonable rationale in selecting amplitude modulation frequencies during atomization is therefore to choose lower frequencies, at 1 kHz for example, to minimize pDNA denaturation. It is also interesting to note that, while there is less effect of the amplitude modulation frequency on the open circular conformation of the pDNA, the increase (>100%) in the number of such structures in the absence of amplitude modulation is beyond that in the feedstock prior to atomization. This suggests that some of the supercoiled pDNA relaxed into an open circular form rather than being fragmented, an encouraging result given that biological function is usually retained even with open circular structures.

Similarly, antibodies constitute both sensitive and fragile proteins and hence their post-atomised bioactivity must be verified if they are to be delivered via the SAW atomiser to demonstrate it as a viable platform for pulmonary administration of protein- and peptide-based vaccines. Due to the small quantities of antibody present in the post-atomised samples, it was not possible to obtain quantitative measurements of the post-atomised antibody bioactivity; nevertheless, the qualitative results from the dot blot test in which YFP was spotted using post-atomised rabbit anti-YFP antisera (Fig. 5.5) confirm that there is no observed degradation of the active sites of the protein molecule during amplitude modulation at all carrier frequencies investigated. These results therefore confirm that the application of amplitude modulation at kHz-order frequencies to the SAW causes no significant damage to active sites on protein molecules, which therefore retain their bioactivity.

5.4 Conclusions

In this chapter, we have demonstrated the feasibility of applying amplitude modulation to halve the required power while maintaining the aerosol production rate of SAW atomization. This is an important consideration that addresses current issues hindering the miniaturization and integration of the power supply into a practical and commercially realisable portable handheld nebulizer platform for the pulmonary administration of a wide variety of therapeutic targets. We verified that the introduction of amplitude modulation in the system does not significantly alter the aerosol droplet diameter from the respirable size range for optimal dose administration to the oropharyngeal and lower respiratory tract. Judiciously limiting the amplitude modulation carrier frequency to 1 kHz simultaneously optimises the atomization rate, while limiting the loss of bioactivity through pDNA fragmentation as well as protein denaturation, both of which represent important therapeutic targets for gene and vaccine delivery. These results therefore lend support for the attractiveness and feasibility of the SAW atomization platform as a true miniaturized and integrated handheld platform for portable inhalation therapy from a practical and commercial standpoint. Potential applications are as diverse as asthma and chronic obstructive pulmonary diseases to exciting future possibilities in non-invasive gene and vaccine administration to treat a variety of diseases.

In addition, the results of the study can also be extrapolated to reduce the power requirements and hence permit the miniaturization and integration of the power supply with the existing chip-based SAW microfluidic platform to drive a wide range of microscale and nanoscale fluid actuation and bioparticle manipulation processes on a truly integrated chip-scale device.

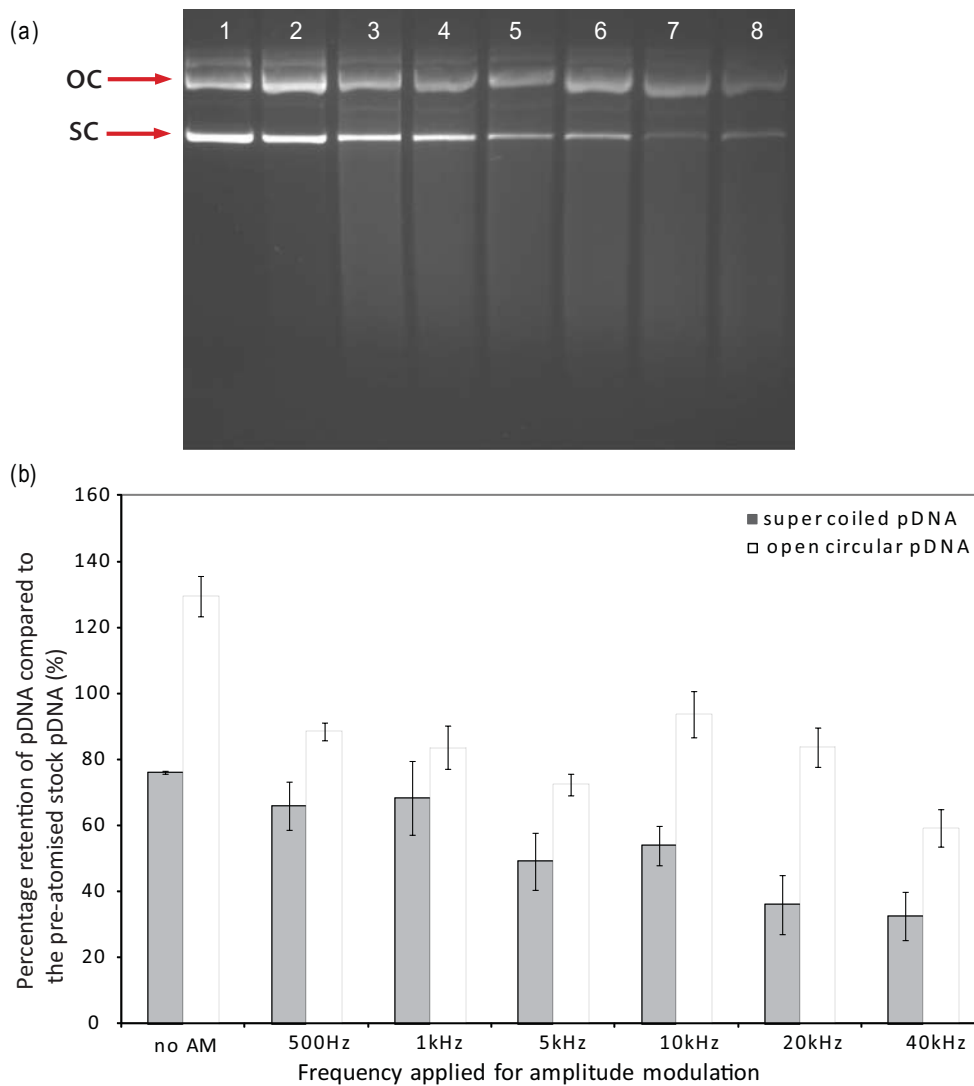


Figure 5.4: (a) Gel electrophoresis of post-atomised plasmid DNA showing the effect of the amplitude modulation at various frequencies on the structural integrity of the pDNA. Lane M: 1 kbp DNA ladder; Lane 1: Atomization at 1.5 W without amplitude modulation; Lanes 2–9: Atomization at 1.5 W with amplitude modulation at 500 Hz, 1 kHz, 5 kHz, 10 kHz, 20 kHz and 40 kHz, respectively. Each lane was loaded with 250 ng pDNA and representative gels from three independent experiments are shown. Arrows indicate the position of the open circular (OC) and supercoiled (SC) forms of the pDNA. (b) Percentage retention of post-atomised supercoiled (shaded) and open circular (unshaded) pDNA compared to the unatomized sample. The results shown are the mean of triplicate atomization runs with the error bar showing the standard error of the mean.

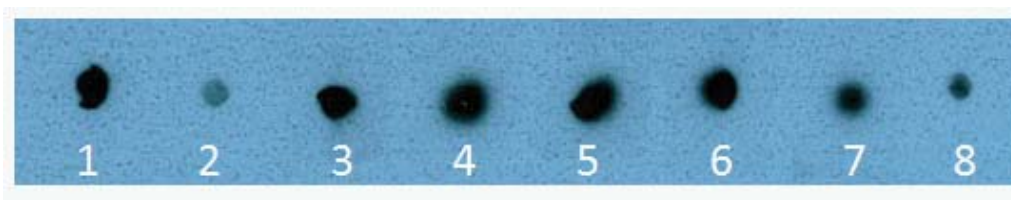


Figure 5.5: Post-atomized YFP antibody samples spotted onto a dot blot showing the preservation of the bioactivity of protein molecules in samples with and without amplitude modulation. Lane 1: No atomization; Lane 2: Atomization at 1.5 W in the absence of amplitude modulation; Lanes 3–8: Atomization at 1.5 W with amplitude modulation at frequencies of 500 Hz, 1 kHz, 5 kHz, 10 kHz, 20 kHz and 40 kHz, respectively.

Chapter 6

Conclusions and Future Directions

This chapter concludes the thesis by giving a summary and major findings of the research performed. Future directions related to this work are then outlined.

6.1 Thesis Summary

The research work undertaken in this thesis has developed the first known successful inhalation vaccination using an unprotected plasmid DNA vaccine in a large animal model, providing a new route to needle-free immunization. Ideally, pDNA vaccination would address the many shortcomings of injection (21), but alternate routes including pulmonary, for example (22) have proven disappointing. Safely generating pDNA aerosols sized for deep-lung delivery, the novel, low-power (<1 W), surface acoustic wave, handheld nebulizer described in this thesis delivers unprotected pDNA encoding an influenza A surface antigen, producing systemic and mucosal antibody responses in female Sprague-Dawley rats via post-nebulized, condensed fluid instillation and in female Merino-cross ewe lambs via aerosol inhalation.

The research presented in this thesis has sought to re-engineer the process of vaccine development and administration via a new technique of pulmonary delivery. Because

of its pain-free and non-invasive access via inhalation and large surface area, the lung is an attractive target for both gene therapy and DNA vaccination: potential systemic side effects and adverse interactions with plasma proteins encountered after intravenous administration are minimized (3).

A plethora of pulmonary delivery devices are available for pulmonary DNA delivery, including pressurised metered-dose inhalers; dry powder inhalers; electrohydrodynamic devices; and jet, ultrasonic, mesh, or catheter nebulizers. However, effective pulmonary administration of DNA has not previously been possible. Aerosols containing pDNA can reach and adhere to the bronchial and alveolar epithelia and interstitial cells only if the aerosol droplets are between 1 and 5 μm , enabling entry and expression of the genes carried by the pDNA (8). Nebulizers are the delivery method of choice for macromolecules because of their instability in propellants and solid formulations (8). Delivery of non-complexed pDNA is impractical in current nebulizers, not only due to their inability to control the droplet size to 1–5 μm , but also due to the hydrodynamic shear stresses sufficient to shear pDNA molecules possessing masses larger than 5 kbp into open circular and fragmented configurations during nebulization (9; 144). This justifies complexation of the DNA (142) in an attempt to protect it, for example, with cationic polymers (113) that has led to modestly successful gene expression after aerosol delivery in sheep (116). However, not all polyplexes (nor lipoplexes) retain biological efficacy after aerosolization (118), and some commonly used synthetic polymers like polyethyleimine (PEI) are highly cytotoxic (148). Effective delivery by the pulmonary route requires the aerosolized DNA to be internalized into the target cell via endocytosis, avoiding degradation either during delivery or via exposure to lysosomal or cytoplasmic nucleases, and subsequently transcribed and translated within the nucleus to produce the desired gene product (182).

These problems have been overcome with our proposed SAW (Surface Acoustic Wave) nebulizer. The transfection efficiency of such post-nebulized DNA has been shown to be as low as one-tenth, an already modest value. As detailed in Section 3.2.1, Rayleigh

surface acoustic wave (SAW) nebulization has recently been found to effectively form aerosols of a short acting β_2 -agonist with a respirable fraction of over 70%, much more than the typical 30–40% lung dose available via current nebulizers. Rayleigh SAWs, transverse-axial polarized electroacoustic waves generated by a sinusoidal electric field between the interlaced fingers of an interdigital transducer (IDT) electrode, are formed and propagate at nanometer amplitudes at MHz to GHz-order frequencies along piezoelectric lithium niobate (LiNbO_3). The SAW is localized to the substrate surface, and consequently, a substantial majority of the energy input into the system is near the surface and transferred into fluid resting upon it. This is the reason why SAW is, overall, far more efficient than conventional bulk piezoelectric ultrasonic radiators and suitable for handheld devices (2).

During SAW nebulization, the droplets ejected are sized by the wavelength, λ , of the capillary waves generated on the surface of the source drop, which are in turn predicted by the balance between the capillary and viscous forces that dominate at the surface, such that the droplet diameter $D \approx \lambda \sim \gamma H^2 / \mu f L^2$, where γ and μ are the surface tension and dynamic viscosity, f is the resonance frequency of the capillary wave, and H and L are the characteristic height and length scales of the source drop, respectively (2). The nebulized droplet size is independent of the excitation frequency, but its strong dependence on the fluid characteristics provides a route to effectively tune droplet size (14). Using glycerol to safely (203) counter the very high surface tension of water, the SAW nebulizer delivers droplets with a mean diameter less than 5 μm . Such a mist is effective for deep lung deposition, a significant improvement on a catheter-based nebulization device delivering droplets at $33 \pm 2 \mu\text{m}$ (151). The concentration of the pDNA has a minor effect on the droplet diameter that can be addressed by changing the glycerol concentration.

This method of administration preserves the DNA's integrity. More than 90% of the initial supercoiled pDNA was still present after SAW nebulization, an essential requirement for vaccine administration and efficacy, as the compact supercoiled configuration of DNA

is the most immunogenic form and, according to FDA requirements, must be present at >80% in a licensable vaccine (234; 213). Scission of one of the two strands of the pDNA releases torsional energy stored in the supercoiled plasmid, causing it to relax into an open circular form, and scission of both strands results in a linear polynucleotide; further cleavage results in DNA fragments (206). Atomic force microscopy (AFM) and ethidium bromide agarose gel electrophoresis of the pVR1020–PyMSP4/5 before and after SAW nebulization indicate the tightly twisted supercoiled geometry is effectively maintained, as summarized in Fig. 6.1. The frequency of the SAW nebulizer has little effect on the results, and, likewise, pDNA concentrations in the source drop prior to nebulization from 5 to 85 $\mu\text{g}/\text{m}\ell$ have a minimal effect on the percentage of supercoiled pDNA left after nebulization.

A small proportion of the pDNA prior to SAW nebulization was found to be fragmented, most likely during plasmid purification and preparation. This was especially evident at a pDNA concentration of 5 $\mu\text{g}/\text{m}\ell$, with around 50% and 20% of supercoiled and fragmented pDNA, respectively. Linear, double-stranded DNA is very susceptible to flow-induced stresses, and minor differences in their characteristic dimensions — that arise from scission, for example — have large effects on their response to hydrodynamic stresses (210). Stretching hydrodynamic forces of only 0.3 nN, well below the 1.6–5.0 nN required to break the covalent bonds within, are known to cause irreversible strand separation and formation of nicks, degrading the pDNA (9). Although cavitation is absent in SAW nebulization (2), accelerations in the fluid of 10^7 – 10^8 m/s^2 are typical due to the MHz-order frequencies used in the system. If the relaxed forms of the pDNA are adjacent to the fluid interface, it is possible that the gradient in the acceleration, and consequently the shear stress across such pDNA molecules, is sufficient to cause further damage. However, the relaxation time scale of the fluid shear, ~ 10 ns, is two orders of magnitude smaller than that required to shear large molecules, suggesting the risk of denaturing molecules like DNA (193) is negligible. Compared to standard ultrasonic nebulization

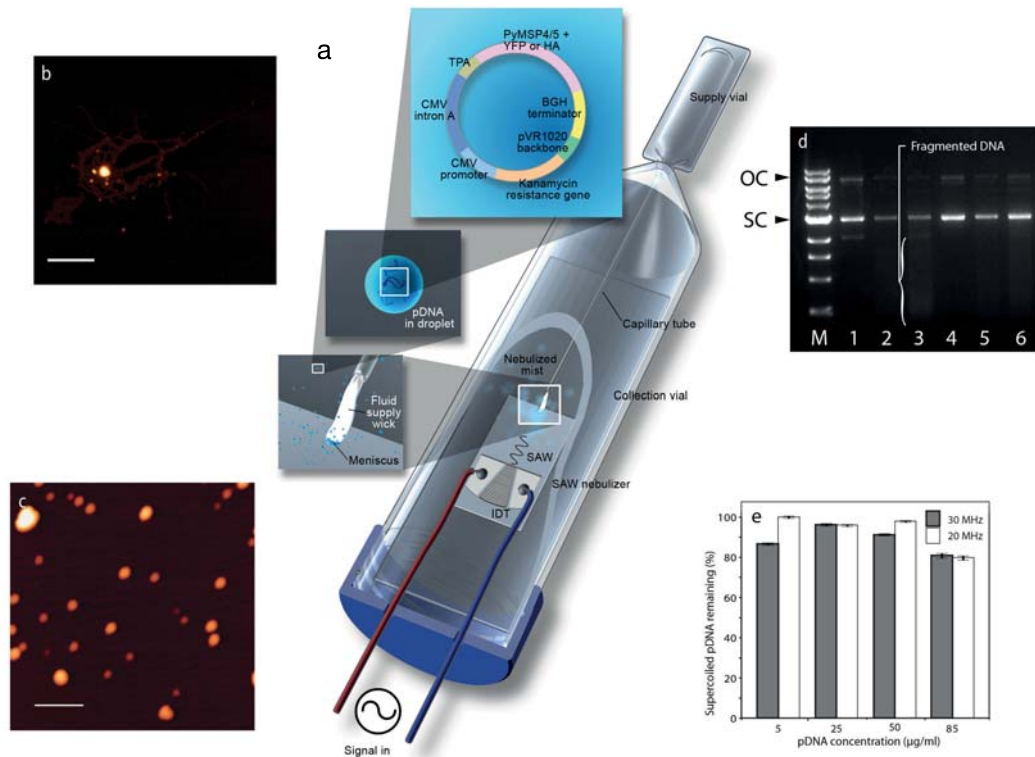


Figure 6.1: A pDNA-laden meniscus forms at the end of the cellulose fiber wick upon the activation of (a) the SAW nebulizer and pDNA nebulization occurs inside the vial. Atomic force microscopy (b,c) and ethidium bromide agarose gel electrophoresis (d) of pVR1020–PyMSP4/5 (b) before and (c) after nebulization. Lane M: 1 kbp DNA ladder; control lanes 1 and 4, recovered pDNA post-30 MHz lanes 2 and 5, and post-20 MHz SAW nebulization lanes 3 and 6 are each at 85 and 50 $\mu\text{g/ml}$ concentrations, respectively. The proportion of (d) supercoiled (SC), open circular (OC) and (e) fragmented pDNA quantifies the damage ($n = 3$). The error bars indicate the standard error of the mean.

at 20–80 kHz, where cavitation is prevalent and large molecules like pDNA in solution actually serve as cavitation bubble nucleation sites (144) causing wholesale destruction of such molecules, the damage caused by SAW nebulization is minor: for 5 kbp plasmids, the percentage of fragmented pDNA after nebulization is far lower with SAW (< 20%) than with conventional (> 35%) or vibrating mesh nebulizers (> 40%) (22). Hence, the SAW nebulization approach has several key advantages over the current generation of ultrasonic medical nebulizers for the delivery of large molecules (2).

The work outlined in this thesis set out to test the capacity of nebulized DNA to induce immune responses in animals. Since mice and rats are unable to inhale mist from a nebulizer, preliminary experiments in these animals involved the recovery of nebulized material followed by intratracheal instillation of the condensate. When post-nebulized pVR1020–YFP plasmid was introduced into the lungs of mice, the modest expression of yellow fluorescent protein (YFP) indicated some transfection that was entirely absent in the lungs of untreated mice (refer to Section 4.3.1). The expression of YFP as discrete aggregates close to the epithelium of the conducting airways is consistent with gene expression patterns in mouse lungs in other studies (151) and was expected to be modest, as it is well known that naked plasmids rapidly degrade *in vivo* (218). Moreover, Western blots of the treated and untreated lung tissue confirmed the presence of the YFP only in treated samples, and there was no evidence of microhemorrhages in the lung due to the absence of hemosiderin deposits.

More importantly, SAW nebulization has no apparent effect on the vaccine's activity. Significant ($p < 0.001$) increases in both immunoglobulin IgG and IgA antibody titer levels against the hemagglutinin (HA) of influenza A virus (A/Solomon Islands/3/2006, H1N1) was observed in the sera of female Sprague-Dawley rats collected five weeks after the start of a series of pDNA intertracheal instillation vaccinations in comparison to naïve rats. The anti-HA antibody titers are comparable to vaccination results using a similar pDNA influenza vaccine yet protected with toxic PEI (113). This result suggests that

naked pDNA can be delivered to the lung with effective transfection, despite its rapid degradation. No significant differences in IgG ($p = 0.195$) or IgA ($p = 0.505$) levels were observed between groups of Sprague-Dawley rats vaccinated via instillation with nebulized and non-nebulized forms of the pDNA vaccine.

Hemagglutination inhibition (HAI) titers of sera from rats, five weeks following vaccination with pDNA encoding the HA, indicated that a substantial humoral response was elicited. Serum HAI titers significantly greater than 40 (per World Health Organization standards) ($p < 0.001$) were observed in rats immunized with the instilled pDNA vaccine, regardless of whether it was nebulized with the SAW device beforehand or not ($p = 0.721$), with an HAI titer of < 5 for all ($n = 8$) pre-vaccinated rats, 1500 ($n = 8$) for rats vaccinated with non-nebulized vaccine, and 1300 ($n = 8$) for rats vaccinated with nebulized vaccine. These results are very favorable in comparison to past reports of vaccination using $10 \mu\text{g}$ pDNA encoding swine H1N1 but with PEI administered intranasally to BALB/c mice resulting in an HAI titer of ~ 1800 (220), the administration of HA protein to sheep via subcutaneous injection and via the lung with the adjuvant ISCOMATRIX resulting in HAI titers of ~ 95 – 122 depending on HA dosages (221).

The nebulized mist was found to induce a powerful pharmacodynamic response when inhaled into the lungs of sheep under mechanical respiration, with similar levels of antibody response to that observed in rats. As seen from Table 4.3 in Chapter 4, the observed HAI titers averaging 192 ($n = 4$) were detected in sera of these large animals after immunization three times at three-week intervals using a 30 MHz SAW device placed between the nasally-intubated sheep and a mechanical ventilator. The sheep received $156 \pm 44 \mu\text{g}$ (mean of $n = 8$ independent experiments, with error showing standard deviation) pDNA vaccine encoding HA in 5% dextrose, via inhalation through an endotracheal tube inserted through the nostril. Given the difficulty of inducing functional antibody responses using DNA vaccination in large animals (222), we have reported here the first instance of successful vaccination via inhalation using an unprotected pDNA vaccine in sheep, a

model relevant to human lung development, structure, physiology, and disease (223). This work therefore holds great promise for gene therapy using a non-invasive aerosol-based approach.

As outlined in Chapter 5, the practical implementation and commercial realization of microfluidic devices such as the SAW nebulizer depend on the miniaturization and integration of all components onto a chip-based platform. This includes ancillary equipment such as pumps, as well as power supplies and electronic circuitry. In this thesis, amplitude modulation is presented as a simple yet effective means for reducing the power requirement in surface acoustic wave microfluidic platforms whose true microfluidic functionality has already been demonstrated through the development of on-chip pumps, separators and droplet manipulators.

The thesis specifically demonstrates the use of the amplitude modulation scheme for the reduction of the power requirements for SAW atomization, which by far requires the highest energy input levels of all SAW microfluidic processes. It demonstrates that amplitude modulation of 10–100 MHz order SAW at 1–10 kHz order frequencies can approximately halve the power required, while maintaining monodisperse aerosol droplet sizes in the 1–10 micron range and aerosol production rates commensurate with the prerequisites of practical nebulization devices for inhalation therapy. In addition, the thesis verifies that the superposition of the kHz order carrier signal does not cause appreciable damage to shear-sensitive biomolecules, in contrast to sonoporation and cell lysis processes which are carried out at similar frequencies. In particular, this thesis has demonstrated that, with amplitude modulation at approximately 1 kHz, it is possible to maximize the aerosol production rate with 40% less power while minimizing denaturing of plasmid DNA or antibodies, both of which represent exciting future therapeutic targets for pulmonary gene and vaccine delivery.

The net result of this work allows the SAW microfluidic aerosol delivery platform to be

driven by a palm-sized, battery-powered circuit that may be integrated with the chip-scale SAW atomization device to constitute a low-cost, portable, handheld nebulization platform for pulmonary drug administration with many advantages over conventional inhalation and nebulization systems.

6.2 Conclusions

In conclusion, the research presented in this thesis suggests that the SAW nebulizer may serve to effectively deliver rapidly-produceable pDNA vaccines, by a by a palm-sized, portable device. This is a significant outcome in the context of pandemic episodes and the developing world which lacks a sufficient health workforce or access to safe injection methods. It is also a technology that has the potential for global usage in terms of manufacturing ease, broad population administration and safety.

6.3 Future Directions

This thesis has developed and conducted a comprehensive validation of a portable nebulization platform for pDNA vaccination using surface acoustic wave nebulization on a large animal model, a necessary step towards obtaining regulatory approval for commercialization of the technology.

This work has laid the foundation for applications in non-invasive gene therapy and it opens up several avenues for future work in the development of the SAW nebulizer as a platform for mass vaccination programs for both veterinary and human use.

Firstly, the SAW nebulizer can be employed for the delivery of veterinary DNA vaccines. For example, acute and highly contagious respiratory infectious disease of chickens continues to be a major health problem in the poultry industry worldwide. Chickens of all ages may be infected, causing mortality and severe economic losses due to poor weight

gain and reduction in egg quality and quantity. Aerosol vaccination of large cohorts of chickens presents a safe and rapid-response method that can reduce flock mortality considerably in the case of a pandemic outbreak. The SAW nebulizer presented in this thesis would be an ideal technology for such use. However, there needs to be further work before such use, involving further modifications to the prototype design, followed by more rigorous validation experiments.

Whilst we have demonstrated the ability of SAW atomization for the delivery of aerosolized shear-sensitive biomolecules such as plasmid DNA, little is known about the mechanism by which this occurs and how the concentration of the pDNA feedstock affects this process. The knowledge of the extent of damage to such particles due to acoustic radiation is crucial in understanding the survival of the particles. Considerable work remains to be carried out before a detailed understanding of this complex process can be achieved.

The findings of the current research using pDNA can be theoretically extrapolated to other nucleic acids such as mRNA. RNA based vaccines and therapeutics, which include therapeutic ribozymes, aptamers, and small interfering RNAs (siRNAs) are being considered as a potential paradigm shift in vaccinology (235). Despite the unprecedented versatility, RNA is inherently unstable (236). This area of research presents an exciting opportunity for investigations in the use of SAW nebulization for the delivery of RNA based vaccines via the pulmonary route.

Further work could be carried out to validate the *in vivo* assays performed in the current research as part of the sheep trials, where conclusive evidence can be demonstrated by further challenge experiments in either small animals namely ferrets or with a sheep model. Although ferrets are currently considered the best model for the demonstration of flu challenge experiments, by using a sheep model, which is more representative of human physiology, all the circulating flu strains (A and B) could be investigated. Moreover, the evaluation of the quality of vaccination via investigation of T and/or B cell memory would

be critical in the evaluation of the technology further, especially since the pulmonary route will allow better feasibility to access these cells of the immune system more readily than other routes of immunization.

The research presented in thesis shows conclusive evidence of the advantages of employing amplitude modulation to obtain power savings, a primary concern for portable lab-on-a-chip, which demands low power consumption. However, there needs to be further work to understand how biomolecules behave under the influence of such modulated surface acoustic waves such that their integrity is preserved. This work would also expand the currently limited knowledge of the physical mechanisms underlying fluid manipulation via the use of acoustic waves.

It is the expected that the application of the SAW nebulizer approach to aerosol gene therapy will make a great impact on the non-invasive vaccination field and lead to the eventual success and widespread adoption of the technology proposed in this thesis in mass vaccination programs for disadvantaged communities and third world countries.

Appendix A

Patent: Microfluidic Apparatus for the Atomization of a Liquid

Rajapaksa, A.E., Ho, J., Qi, A., Yeo, L.Y., Friend, McIntosh, M.P. and Morton A.V.

Patent Number PCT/AU2010/000548

filing date of 11 May 2009

MICROFLUIDIC APPARATUS FOR THE ATOMISATION OF A LIQUID

TECHNICAL FIELD

The present invention is directed to a microfluidic apparatus for the atomisation of a liquid. While the invention is described with respect to its use as a pulmonary delivery apparatus, it is to be appreciated that the invention is not restricted to this application, and that other applications are also envisaged.

BACKGROUND TO THE INVENTION

Inhalation therapy has become the treatment of choice for asthma and chronic obstructive pulmonary disease (COPD). Unlike oral dosing, inhalation therapy allows a high concentration of a drug to be administered and targeted directly to local inflammation sites within the lung, thereby enabling lower total dosages, reduction in systemic side effects, and potentially hastening the onset of action of the drug. Metered Dose Inhalers (MDIs) and Dry Powder Inhalers (DPIs) are commonly used for bronchodilator administration for asthma and COPD therapy; the patient inhales a pre-metered dose in a single forced inspiratory manoeuvre. There is a lively debate among researchers, however, in deciding whether MDIs or DPIs are the most effective or if continuous nebulization to a patient undergoing repeated tidal breathing for a period up to several minutes is required. Though the debate continues, critical factors in making such decisions are generally based on clinical judgements, taking into consideration such factors as dose level, drug efficacy and safety profile, patient age group, disease severity, ease of administration, and cost.

Nebulizers are capable of delivering more drug than current MDIs and DPIs because they operate over a longer period. Moreover, nebulizers do not require coordination skills from the patient, unlike MDIs, and do not require patient actuation via inhalation, unlike DPIs. Nebulizers are commonly used in acute cases of COPD or severe asthma attacks where the patient is unable to self-medicate. For this same reason, nebulizers may be more appropriate for paediatric and geriatric patient populations.

Historically, nebulizers have been large, cumbersome, less portable and more expensive than MDIs or DPIs. Furthermore, conventional nebulizers generally have low dose efficiencies; although more drug may be delivered into an aerosol, much of the aerosolized drug is subsequently wasted because:

1. aerosols are generated continuously, wasting drug as the patient exhales against the nebulizer's output,

2. the aerosols have polydisperse size distributions, with a significant fraction of droplets too large for deep lung deposition, and since

5 3. nebulizers typically have a large internal residual volume.

For inhalation therapy to be most effective, the droplet's aerodynamic behaviour (governed by Stokes' law) is of fundamental importance. For deep lung deposition, an aerodynamic diameter less than 5 μm or preferably 3 μm is considered appropriate, such that the aerosol can avoid inertial impaction in the oropharyngeal region. For deposition higher up in the airways, a larger aerodynamic diameter may be preferred. As a result, the aerosol droplet size is crucial to the efficacy of inhalation therapy, and therefore an ideal device capable of efficiently delivering high doses of a drug would permit precise control of the droplet size distribution and preferably offer large atomisation rates to deliver the desired dosage in as short a time period as possible to minimize patient distress and inconvenience.

Nebulization technology has rapidly progressed in recent years, with new methods that utilize ultrasound and electrohydrodynamic atomisation, allowing greater control over the atomisation process to provide aerosols with reduced spreads of polydispersity and with droplet size tuning capability. Furthermore, these methods may be miniaturized, offering an attractive alternative to the large and cumbersome nebulizers that are currently available commercially. Unfortunately, these methods have inherent limitations. For example, electrohydrodynamic atomisation is restricted to high voltage operation - typically several kilovolts - raising safety and reliability issues in consumer use. Various types of ultrasonic atomisation have been devised over the years, and the most common systems use a bath of liquid from which a piezoelectric disc generates an aerosol plume. These ultrasonic nebulizers are also relatively large in size, have limitations on output and size control, and often precipitate the solubilized drug onto the atomisation reservoir walls due to solvent evaporation, wasting the drug and requiring regular cleaning by the user. More recent designs using meshes for nebulization offer better portability, dosage rates, and aerosol monodispersity. The mesh has chemically or laser-cut microscopic holes, forming

thousands of orifices that generate droplets under irradiation by ultrasound although these meshes are prone to clogging, which significantly reduces throughput. In the context of these past and current technologies, a small, portable, reliable, and relatively cost-effective device remains out of reach, especially one that can effectively generate non-agglomerating droplet size distributions which are suitably monodisperse and less than 5–10 μm in diameter.

SUMMARY OF THE INVENTION

With this in mind, the present invention provides an apparatus for the atomisation of a liquid including:

- 10 a piezoelectric substrate having at least one working surface;
- at least one electrode supported on the piezoelectric substrate;
- a signal generating means for applying an ultrasonic signal to said electrode for generating a surface acoustic wave (SAW) in the working surface of the piezoelectric substrate;
- 15 a liquid delivery arrangement including a wick in contact with the working surface for delivering liquid thereof,
- wherein liquid delivered to the working surface by the wick is atomised by SAW irradiation.

The electrode may be in the form of an interdigital electrode. More preferably, the electrode configuration may be an elliptical, electrode width controlled single phase unidirectional transducer (EWC-SPUDT).

The electrode is preferably configured as EWC-SPUDT as this configuration gives the largest surface acoustic wave intensity into the liquid sitting on the substrate compared to straight standard and SPUDT-style interdigital transducer electrodes, circular EWC-SPUDTs, and other configurations known currently. For a given input power, the elliptical EWC-SPUDT therefore offers the best atomisation performance of these various configurations, and the width and ellipticity of the EWC-SPUDT so chosen is preferably tailored to the size of the liquid drop sitting upon the substrate. The relationship between the size of the droplet and the exit aperture (width) of the EWC-SPUDT depends on the liquid properties, but the ratio of drop diameter to exit aperture is preferably between 0.5 and 2.

Preferably more than one EWC-SPUDT may be used. For example, two may be used on very anisotropic piezoelectric materials like lithium niobate (class [3m]), while more can be used on less anisotropic materials like ZnO, AlN, or PZT.

5 The frequency of atomisation is preferably between 10MHz and 250MHz depending on the liquid to be atomized, and this defines the electrode finger width and the gaps between them in the EWC-SPUDT.

The wick of the liquid delivery arrangement may be provided by at least one paper strip or string, with the liquid being delivered through capillary action.
10 Other types of porous material providing a similar capillary action are also envisaged, for example cloth fabric, or other hydrophilic materials.

The liquid delivery arrangement may preferably also include a liquid reservoir container for containing the liquid to be delivered to the apparatus. The wick may extend from the surface of the piezoelectric substrate all the way to the
15 interior of the liquid reservoir. Alternatively, a capillary tube may extend from the liquid reservoir, the wick receiving the liquid via this capillary tube. The liquid reservoir itself may be provided by a replaceable vial.

The capillary tube may preferably be of various shapes (bent to accommodate device design, for example), and placed with wick in a variety of
20 orientations to contact the substrate and form the droplet. The capillary tube may however be omitted, with only the wick between the liquid reservoir and substrate.

A driver circuit preferably controls the apparatus based on the measurement of the user's breathing and safety interlocks on the apparatus as commanded through the user interface.

25 The use of surface acoustic wave (SAW) atomisation has a number of advantages over ultrasonic nebulization. Surface acoustic waves are MHz to GHz-order, transverse-axial polarized elliptical electroacoustic waves with displacement amplitudes of just a few nanometers. Here, they are generated on and traverse the surface of the piezoelectric substrate. Unlike typical ultrasound,
30 which is a bulk phenomenon, the SAW is confined close to the substrate surface, its amplitude decaying rapidly over a depth of four to five wavelengths (several hundred microns) into the substrate material. Compared to conventional ultrasonic atomizers that consume power on the order of 10 W, the apparatus

according to the present invention may only consume between 0.5–3 W since most of the energy is contained within a localized region close to the surface of the substrate and hence can be transmitted into the liquid much more efficiently than ultrasound. Moreover, the apparatus and power supply may be small showing the potential of the apparatus for portable applications. Moreover the 5 10-500 MHz order frequency employed in the apparatus is significantly higher than the 20 kHz-3 MHz frequency range of typical ultrasonic devices, induce vibrations with a period much shorter than the molecular relaxation time scale associated with large molecules in liquids, and thus the risk of denaturing 10 molecules or lysing cells is greatly reduced. Further, as the frequency is increased, the power required to induce cavitation increases far beyond what is needed for atomisation, eliminating the effect of cavitation-induced lysis or shear in the apparatus.

In preliminary experiments conducted by the inventors on the atomization 15 characteristics of a salbutamol ethanol/octanal solution, a mean aerosol diameter of $2.84 \pm 0.14 \mu\text{m}$ was achieved using SAW atomization. Salbutamol is a drug used in the treatment for asthma, and the aerosol diameters achieved are well within the optimal range for deep lung deposition.

Though the amplitude of a SAW is only a few nanometers, the acceleration 20 of the surface is incredibly high ($10^7 \text{ m}^2/\text{s}$) because of the high operating frequency. Therefore, when a SAW is transmitted into a liquid drop placed upon the substrate, it is able to not only form capillary waves across the free surface of the droplet but also drives it to break up into a mist of droplets with an average, controlled diameter of 1–10 μm . Micro and nanoparticles may be formed via 25 controlled evaporation of these droplets, but irrespective of the desired product the challenge is in maintaining a relatively stationary free liquid surface on the SAW apparatus as an atomisation source.

The liquid delivery arrangement according to the present invention resolves these issues. Using a wick to siphon liquid from a liquid reservoir to the 30 working surface of the apparatus provides it with continuous flow without pumping. The wick therefore permits atomisation without affecting the performance of the apparatus and offers a constraint sufficient to retain a stable meniscus outside the peripheral edge of the wick on the surface as noted in

recent experiments by the inventors using such a paper wick. In these experiments, it was found that the meniscus is constantly replenished by liquid passing from the paper wick by liquid passing from the paper and provides a surface for the formation and destabilization of a capillary wave to eject the aerosol. The aerosol is ejected at an angle dependent upon the shape of the meniscus, itself dependent upon the power used to generate the SAW. The fluid absorption rate of the paper defines the upper limit in flow rate for the apparatus.

BRIEF DESCRIPTION OF THE DRAWINGS

It will be convenient to further describe the invention with respect to the accompanying drawings which illustrates a preferred embodiment of the apparatus according to the present invention. Other embodiments of the invention are possible, and consequently, the particularity of the accompanying drawings is not to be understood as superseding the generality of the preceding description of the invention.

In the drawings:

Figure 1 is a schematic view of an apparatus for the atomization of a liquid according to the present invention; and

Figure 2 is a schematic plan view of an interdigital electrode for the apparatus of Figure 1.

As shown in Figure 1, the apparatus 1 according to the present invention includes a transducer element 3 having a piezoelectric substrate 5 providing a working surface 7 for the apparatus.

Supported on the working surface 7 is an interdigital electrode 9 it has been found that the preferred electrode configuration is an elliptical electrode with controlled signal phase unidirectional transducer (EWC-SPUDT). It has been found that such an electrode provides the largest SAW intensity to the liquid delivered to the working surface 7. The interdigital electrode 9 is better shown in Figure 2 which shows the electrode having a series of interlaced elliptically curved electrode fingers 10. The width and gap of these fingers may preferably be set to be a quarter of the SAW wavelength.

A liquid delivery arrangement 11 is provided for delivering liquid to the working surface 7. This arrangement includes a liquid reservoir 13 which may be in the form of a replaceable vial. A capillary tube 15 extends from the liquid

reservoir 11 for supplying liquid to a wick 17 having one end thereof in contact with the working surface, the opposing end thereof being located within the capillary tube 15. The liquid delivery arrangement therefore enables a liquid meniscus 19 to be formed on the working surface 7 for atomisation.

5 The wick 17 can be in the form of a strip or string of paper, with one end of the wick being in contact with the working surface 7. As liquid is supplied to the working surface 7 through the wick 17, the meniscus 19 is formed between the end of the wick 17 and the working surface 7. This meniscus 19 is continuously replenished by liquid passing from the wick 17 and provides a surface for the
10 formation and destabilisation of a capillary wave to eject the atomised droplets therefrom.

 A driver circuit 21 applies an ultrasonic signal to the interdigital electrode 9, typically between 10 to 250MHz, thereby resulting in a SAW 23 being generated in the working surface 7. The interaction of the SAW 23 with the liquid
15 meniscus 19 results in an atomised mist of droplets.

 The driver circuit 21 is controlled based on measurements of the user's breathing by a detection sensor 25, and by safety interlocks in a safety circuit 27 control through a user interface 29.

 Modifications and variations as would be deemed obvious to the person
20 skilled in the art are included within the ambit of the present invention as claimed in the appended claims.

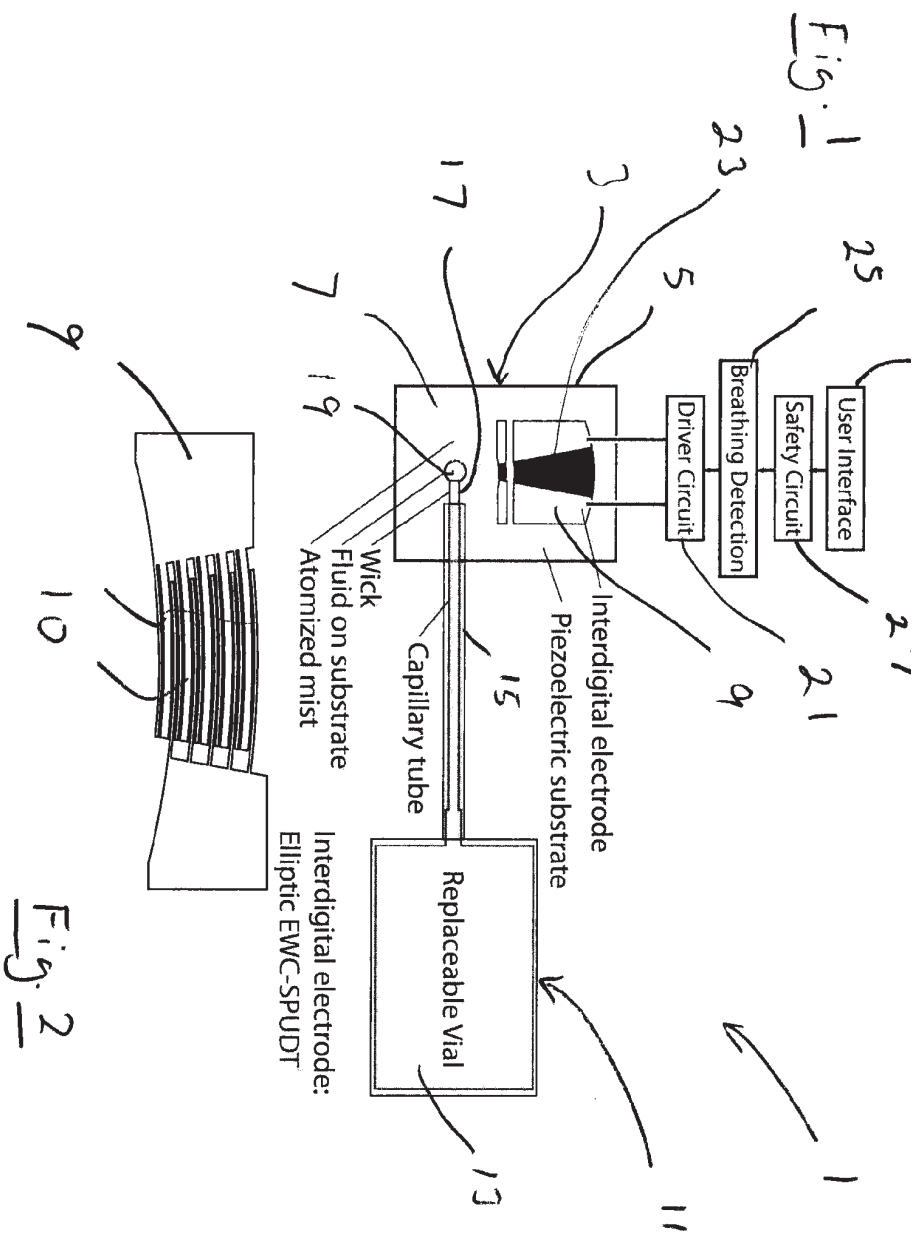
CLAIMS:

1. An apparatus for the atomisation of a liquid including:
a piezoelectric substrate having at least one working surface, at least one electrode supported on the piezoelectric substrate, a signal generating means for
5 applying an ultrasonic signal to said electrode for generating a surface acoustic wave (SAW) in the working surface of the piezoelectric substrate;
a liquid delivery arrangement including a wick in contact with the working surface for delivering liquid thereof,
wherein liquid delivered to the working surface is atomised by SAW
10 irradiation.
2. An apparatus according to claim 1, wherein the electrode is an elliptical electrode width controlled single phase unidirectional transducer (EWC-SPUDT).
- 15 3. An apparatus according to claim 1 or 2, wherein the wick of the liquid delivery arrangement is provided by at least one paper strip or string.
4. An apparatus according to claim 3, wherein the liquid delivery arrangement further includes a liquid reservoir for containing the liquid to be delivered to the apparatus.
- 20 5. An apparatus according to claim 4, further including a capillary tube extending from the liquid reservoir, the wick receiving the liquid via this capillary tube.

MONASH UNIVERSITY

WATERMARK PATENT & TRADE MARK ATTORNEYS

P31836AUP1



Appendix B

Template-free Synthesis and Encapsulation Technique for Layer-by-Layer Polymer Nanocarrier Fabrication

Aisha Qi, Peggy Chan, Jenny Ho, **Anushi Rajapaksa**, James R. Friend and Leslie Y.

Yeo

ACS Nano

12, 9583-9591 (2012)

Copyright © 2012 American Chemical Society

DOI: 10.1021/nm202833n

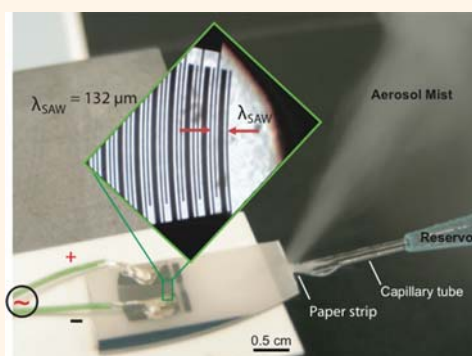
Template-free Synthesis and Encapsulation Technique for Layer-by-Layer Polymer Nanocarrier Fabrication

Aisha Qi, Peggy Chan, Jenny Ho, Anushi Rajapaksa, James Friend, and Leslie Yeo*

Micro/Nanophysics Research Laboratory, RMIT University, Melbourne, VIC 3001, Australia

Nanocarriers comprising multiple polyelectrolyte assemblies whose properties (e.g., dimension, composition, stability, and functionality) can be specifically tuned allow precise control over not only the biocompatibility of each layer to a specific targeted *in vivo* region but also the selective release of the drug within each region.¹ This is extremely attractive for a broad range of applications across drug delivery, regenerative medicine, medical imaging, biomolecular sensing, catalysis, and even cosmetics,² in addition to their utility as microscale reactors for chemical synthesis within confined environments.³ To date, the prevalent method for synthesizing multilayer carriers is the so-called layer-by-layer (LbL) approach. First demonstrated for the assembly of multiple polymer layers on rigid planar substrates,⁴ the LbL technique has been extended to engineer hollow multilayered carriers by the stepwise alternate deposition of oppositely charged polyelectrolytes onto a colloidal particle template, which is then sacrificially removed.⁵ Drug loading into these multilayered carriers however poses some challenges. Molecular diffusion through pH-controlled pores in the carrier,⁶ while simple, is plagued by low loading efficiency and poor reproducibility,⁷ and is limited to drug molecules that are sufficiently small to permeate through.² Enhancing the loading efficiency through the use of smaller molecular agents with high affinity for the drug is limited to the possibility of finding an appropriate sequestration agent that does not invoke an undesirable inflammatory response.^{2,8} While it is possible to directly deposit the polymer layers onto a drug crystal template⁹ or a porous colloidal template containing the drug,¹⁰ this relies on the formation of drug crystals or additional steps to sacrificially remove the porous core. Moreover, LbL methods are

ABSTRACT



The encapsulation of therapeutic molecules within multiple layers of biocompatible and biodegradable polymeric excipients allows exquisite design of their release profile, to the extent the drug can be selectively delivered to a specific target location *in vivo*. Here, we develop a novel technique for the assembly of multilayer polyelectrolyte nanocarriers based on surface acoustic wave atomization as a rapid and efficient alternative to conventional layer-by-layer assembly, which requires the use of a sacrificial colloidal template over which consecutive polyelectrolyte layers are deposited. Polymer nanocarriers are synthesized by atomizing a polymer solution and suspending them within a complementary polymer solution of opposite charge subsequent to their solidification in-flight as the solvent evaporates; reatomizing this suspension produces nanocarriers with a layer of the second polymer deposited over the initial polymer core. Successive atomization—suspension layering steps can then be repeated to produce as many additional layers as desired. Specifically, we synthesize nanocarriers comprising two and three, and up to eight, alternating layers of chitosan (or polyethyleneimine) and carboxymethyl cellulose within which plasmid DNA is encapsulated and show *in vitro* DNA release profiles over several days. Evidence that the plasmid's viability is preserved and hence the potential of the technique for gene delivery is illustrated through efficient *in vitro* transfection of the encapsulated plasmid in human mesenchymal progenitor and COS-7 cells.

KEYWORDS:

laboratory-based batch processes with limited scalability.

Reminiscent of a related technique employed for polyelectrolyte carrier patterning,¹¹ microfluidics has enabled a route for large-scale, continuous production of multilayer carriers with a diversity of customizable physicochemical properties.^{12,13} Liquid

* Address correspondence to

Received for review July 26, 2011
and accepted November 7, 2011.

Published online November 07, 2011
10.1021/nn202833n

© 2011 American Chemical Society

crystal droplets are made to flow within an immiscible continuous medium containing a dissolved polymer and surfactant. After polymer/surfactant coadsorption at the droplet interface, the continuous phase is replaced by a rinse solution followed by a polymer solution to form a layer; repeating the process then leads to an additional polymer layer.¹² The encapsulation of starch granules in alginate and chitosan bilayer carriers has also been demonstrated using hydrodynamic flow focusing in a microchannel. While alginate carriers are gelled using cross-linking agents and transferred from an oil continuum into a coflowing aqueous continuum by tailoring the wettability of a microchannel section, deposition of the subsequent chitosan layer however necessitated an external batch centrifugation process.¹³ Moreover, not only are the channel's surface properties crucial in maintaining the desired flow, fabrication inaccuracies and the presence of contaminants also contribute to nonuniformity in carrier morphology. The most severe limitation of microfluidic LbL synthesis, however, is the lower bound on the carrier size (10–100 μm) imposed by the microchannel dimension—too large for most targeted drug delivery applications where carrier dimensions typically on the order of 100 nm are necessary.^{14,15} In targeted cancer therapy, for example, the upper limit on drug particle size to extravasate tumor microvasculature is 400–600 nm, extravasation being most effective when the particles are below 200 nm.^{16,17}

We report here a fast and simple aerosolization-based technique for multilayer nanocarrier synthesis and encapsulation that retains the advantages of conventional LbL assembly but negates the necessity for a colloidal template or affinity enhancers while circumventing limitations associated with microfluidic platforms. As with the conventional LbL method, the stepwise formation of these carriers allows the possibility for the introduction of multiple functionalities such that a variety of other species such as drugs, their adjuvants, proteins and DNA could potentially be encapsulated. Moreover, the 100 nm order dimensions of the synthesized carriers are ideal for drug delivery applications. The underlying approach employed is surface acoustic wave (SAW) atomization (Figure 1a),¹⁸ a powerful method for the generation of monodisperse, micrometer-scale aerosol droplets¹⁹—a platform that has already been exploited, for example, for protein extraction and characterization for paper-based diagnostics,²⁰ mass spectrometry interfacing with microfluidic devices,^{21,22} and, most relevantly, portable pulmonary delivery of asthmatic steroids.²³

The basis of the present technique is the possibility of using the SAW to atomize solutions of polymeric excipients or proteins such that the subsequent evaporation of the solvent in-flight after the aerosol droplets are generated leaves behind 10–100 nm

dimension polymer or protein nanoparticles.^{24,25} Homogeneous protein encapsulation is also possible by dispersing the protein within the polymer solution to be atomized.²⁶ The tedious and cumbersome procedures associated with traditional benchtop protocols for encapsulation involving polymer solvent extraction from a double emulsion by evaporation, phase separation (coacervation or precipitation) and spray drying can therefore be avoided. Moreover, lysis of shear-sensitive drug molecules is avoided, in contrast to contemporary atomization techniques using electric fields (electrospraying), bulk piezoelectric elements or Langevin transducers. This is because the time scale associated with the high frequency (>10 MHz) of the SAW is much shorter²⁷ than the characteristic time scale for cavitation nucleation¹⁹ and molecular relaxation.²⁸ This simple SAW nanoparticle synthesis and encapsulation technique can therefore be extended to synthesize multilayer polyelectrolyte carriers by successively atomizing a polyelectrolyte solution into its oppositely charged complementary pair. To illustrate the flexibility of this technique and its practical therapeutic applicability, plasmid DNA (pDNA) is encapsulated within the nanocarriers with little added complexity and subsequently used to demonstrate good *in vitro* transfection. Altogether, the system constitutes a scalable, miniature, and inexpensive platform for precise and rapid multilayer nanocarrier synthesis.

RESULT AND DISCUSSION

The strategy for the synthesis of the multilayer polyelectrolyte nanocarriers and the encapsulation of therapeutic molecules within them is described in detail in the Methods section. Briefly, the SAW, generated when an oscillating electrical signal is applied to the electrodes shown in Figure 1b, initially atomizes the fluid containing a polymer solution delivered to the substrate (Figure 1c). As the atomized droplets travel through the heated spiral tube assembly, the solvent evaporates leaving behind solidified polymer nanocarriers which are then collected in a solution comprising a complementary polymer of opposite charge. Reatomizing this dispersion then leads to the deposition of the second complementary polymer layer over the initial polymer core. Additional polymer layers of alternating charge can subsequently be deposited by repeating the atomization–evaporation–resuspension process without requiring washing steps between coatings. This is shown with model polymers chitosan (Chi), carboxymethyl cellulose (CMC), and linear polyethyleneimine (PEI); we note that the polymer layering is relatively insensitive to processing conditions. At an atomization rate of 0.2 mL/min, the number density of nanocarriers synthesized, allowing for losses, is around $10^3/\mu\text{L}$. Evidence of the consecutive layering of these polymers is provided through zeta-potential measurements and

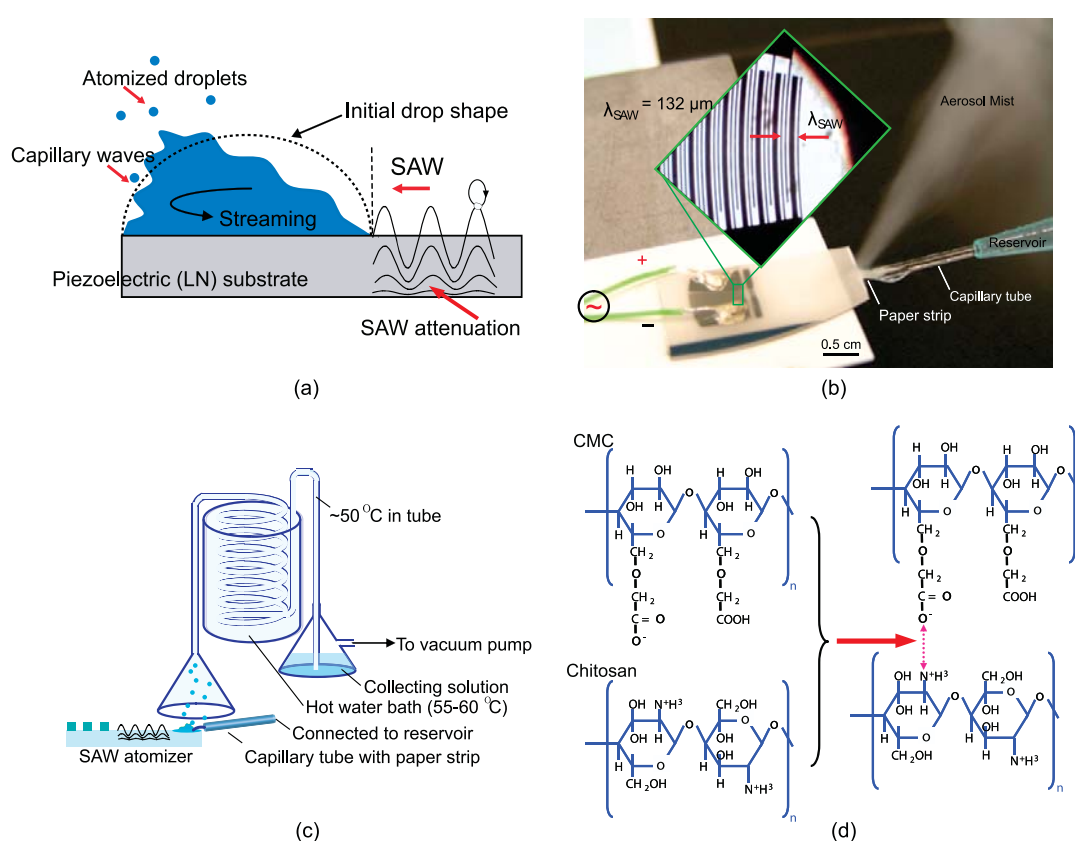


Figure 1. (a) Depiction of the atomization process: SAW leakage into a millimeter-dimension sessile drop placed on the piezoelectric substrate rapidly destabilizes and breaks up the interface to produce micrometer-sized aerosol droplets.¹⁹ Note that the SAWs have amplitudes of around 1–10 nm and hence are not drawn to scale. (b) Image of the experimental setup showing the SAW device on which finger pairs of the single-phase unidirectional transducer (SPUDT) electrode are patterned (enlarged in the inset). The working fluid is delivered from a reservoir to the SAW substrate through the capillary wicking action of a small paper strip placed at the tip of a shortened capillary tube. (c) Schematic illustration of the experimental setup used to synthesize a nanocarrier comprising a single polymer. The polymer, dissolved in an appropriate solvent and held in a reservoir is fed *via* the capillary tube and paper wick to the SAW device to be atomized. The solvent in the aerosol droplets then evaporate in-flight within the conical funnel and spiral tube, aided through heating of the tube by immersing the entire assembly in a hot water bath. The solidified polymer nanocarriers that remain are then channeled into a collecting solution that consists of the complementary polymer that is to form the next layer, dissolved in an appropriate solvent. This suspension is then fed to the SAW device and reatomized using the same setup to obtain the next polymer layer. Further layers can simply be obtained by repeating the entire process for as many times as the number of layers desired. (d) Ionic complexation between chitosan and carboxymethyl cellulose (CMC).

compositional analysis of the nanocarriers using Fourier transform infrared spectroscopy. Together with microscopy and fluorescence imaging, these constitute a culmination of the main techniques used in recent studies,^{29–32} among others; we refrain from carrying out characterization using a quartz crystal microbalance since this can only verify layer deposition of thin films on *planar substrates* rather than on *nanoparticles*. Encapsulation of pDNA, for example, within the polymer layer(s) may be accomplished by dispersing them within the initial polymer solution that is atomized to form the carrier's core.

Size distribution. Figure 2a shows particle size distributions obtained using dynamic light scattering (DLS) for the various nanocarriers. Their 100 nm order dimension, one order of magnitude smaller than that obtained using microfluidic LbL technology^{12,13} and within the desirable range for targeted delivery,

particularly for cancer therapy,^{16,17} is confirmed by the atomic force microscopy (AFM) images shown in the inset of Figure 2a. This is representative of images obtained over many samples; the AFM-measured diameter is slightly smaller than the DLS-determined hydrodynamic diameter due to the swelling of polymeric particles in the presence of solvents common in DLS measurements.³³ The images also reveal that the nanocarriers assume a slightly oval shape, possibly due to the rigid and extended conformation of CMC. Quite counterintuitively, however, we observe the mean nanocarrier diameter in Figure 2a to *decrease* with the addition of a successive polyelectrolyte layer or the encapsulation of pDNA: 322.5 nm (standard deviation 64.3 nm) for sample A (Chi nanocarriers suspended in CMC solution), 198.2 nm (standard deviation 56.8 nm) for sample B (Chi/CMC bilayer nanocarriers), and 162.7 nm (standard deviation 89.4 nm) for sample

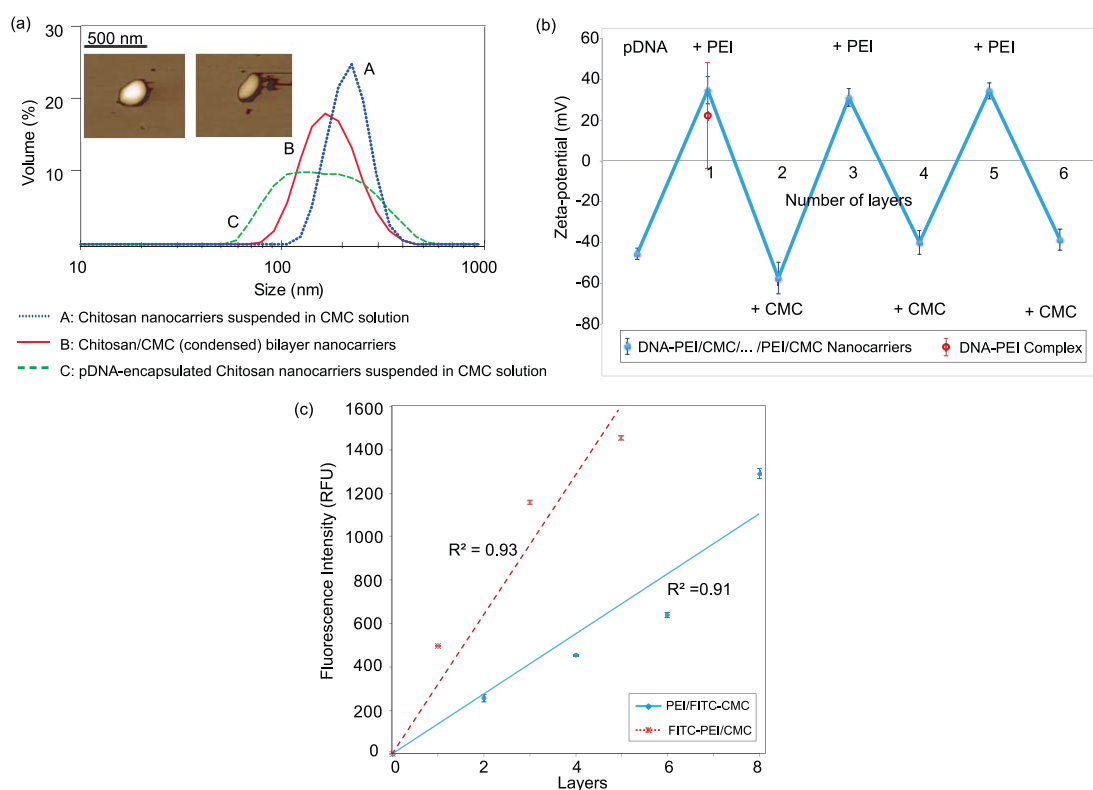


Figure 2. (a) Nanocarrier size distribution from dynamic light scattering experiments for Chi nanocarriers suspended in CMC solution (sample A), Chi/CMC bilayer nanocarriers (sample B) generated by atomizing sample A, and, pDNA-encapsulated Chi nanocarriers suspended in CMC solution (sample C). The inset shows representative AFM images of Chi/CMC bilayer nanocarriers. The diameter across the oval-shaped nanocarrier is typically between 150–300 nm, falling within the size distribution obtained by DLS. (b) Zeta-potential measurements of the outer layer of PEI/CMC nanocarriers encapsulated with pDNA, obtained after every successive layering step; also shown is the large variation in the zeta-potential measurements for the direct complexation of pDNA and PEI. We note that for each sample, the zeta-potential alternated between positive and negative, thus verifying that alternating complementary layers of PEI and CMC were successfully deposited in turn. (c) Intensity measurements (in relative fluorescence units, RFUs) of the fluorescence emitted by successive layers of the nanocarriers wherein one of the two complementary polyelectrolytes has been labeled with fluorescein isothiocyanate (FITC) (dashed line, nanocarriers comprising alternate layers of FITC labeled PEI and label-free CMC; solid line, nanocarriers comprising alternate layers of FITC labeled CMC and label-free PEI). The measurements were taken after each layering step and the lines indicate linear regression of the data using a least squares fit, showing the departure from linearity.

C (pDNA-encapsulated Chi nanocarriers suspended in CMC solution). The size decrease upon deposition of the CMC layer over the Chi core could be due to the strong electrostatic attraction of the adsorbed polyelectrolyte layer to the oppositely charged polyelectrolyte core, resulting in the condensation of both polymers. The observed size decrease when pDNA is encapsulated within Chi can be attributed to DNA condensation into compact structures as a result of polycation adsorption,³⁴ possibly due to ionic complexation.³⁵

While fairly broad, the size distribution is typically acceptable in a number of applications; more importantly, the nanocarriers have not been filtered after synthesis, which also has the associated downside of potential loss of material. This is in contrast to the typical approach used for other processes where filtering is a key step in obtaining the desired results at the cost of yield efficiency. In any case, the nanocarrier size and size distribution as well as the thickness of the

layers can be controlled through the atomizing fluid's physical properties (e.g., viscosity and surface tension); these are known to strongly influence the destabilization wavelength, the aerosol size, and hence the nanocarrier dimension.¹⁹ Surfactants to alter the surface tension or glycerine to modify the viscosity, for example, have been used to control nanoparticle size as well as its size distribution,^{24,25} together with the judicious choice of the SAW operating frequency among the fundamental and harmonic resonances of the electrode and its various designs, it is thus possible to control the nanocarrier size and morphology. Nevertheless, a detailed study on the control of the nanocarrier size and distribution as well as its layer morphology is beyond the scope of this proof-of-concept study, constituting a topic for thorough investigation to be reported subsequently.

Spectroscopy. Figure 3 reveals the Fourier transform infrared (FT-IR) spectra for the pure CMC (curve A), pure Chi (curve B), Chi/CMC/Chi trilayer (curve C), and Chi/CMC bilayer (curve D) nanocarriers, respectively. Two

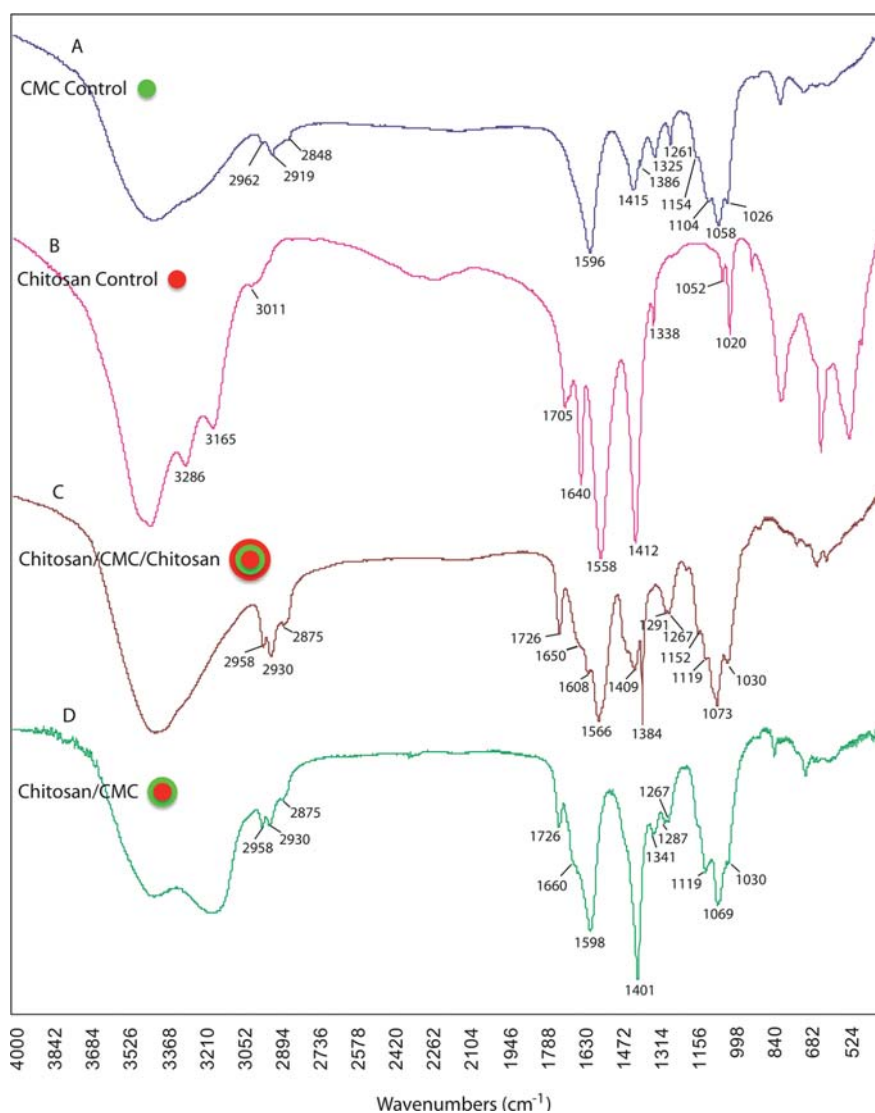


Figure 3. FT-IR spectra for the pure CMC (curve A), pure Chi (curve B), Chi/CMC/Chi trilayer (curve C), and Chi/CMC bilayer (curve D) nanocarriers, respectively. The different characteristic spectra of both trilayer and bilayer (curves C and D, respectively) nanocarriers from pure CMC and Chi (curves A and B, respectively) indicate that ionic complexation between the $-\text{NH}_2$ groups in Chi and $-\text{COOH}$ groups in CMC has taken place.

characteristic bands at 1596 and 1415 cm^{-1} can be seen for pure CMC (curve A), and can be attributed to the asymmetric and symmetric stretching of the carboxylate group, respectively. Characteristic bands at 1154 , 1058 , and 1026 cm^{-1} , on the other hand, correspond to the polysaccharide skeletons of the CMC molecule.³⁶ For the Chi spectrum (curve B), characteristic bands at 1640 and 1558 cm^{-1} are associated with the amide I and amide II peaks, respectively, whereas the bands at 1052 and 1020 cm^{-1} are characteristic of the polysaccharide skeleton of the Chi molecule.³⁷ Clearly, curves C and D show characteristic spectra different from that of pure CMC and Chi. The amide I band at 1640 cm^{-1} in the bilayer and trilayer nanocarriers has shifted to 1660 and 1650 cm^{-1} , respectively, reflecting the interactions between the $-\text{COOH}$ groups in the CMC molecule and the $-\text{NH}_2$ groups in the Chi molecule.

The shift in the characteristic bands corresponding to the polysaccharide skeletons for the multilayer nanocarriers in curves C and D also suggest that ionic complexation between Chi and CMC has taken place.

Zeta-Potential. Additional verification of the existence of successive polyelectrolyte layering within the nanocarriers can be obtained through zeta-potential measurements as the layers are formed. As shown in Figure 2b, the sign of the zeta-potential reverses as each alternating layer of PEI and CMC is deposited over the initial pDNA, which has a strong negative charge. The alternate reversal in the zeta-potential observed here is consistent with that observed in conventional LbL synthesis,³⁸ and confirms the consecutive deposition of successive layers on the nanocarrier comprising polyelectrolytes of opposite charge. We also note a considerable reduction in the variation in the zeta-potential

of the pDNA–PEI complex formed during the SAW atomization–evaporation process compared to that due to direct complexation, indicating that the atomization and evaporation leads to enhanced polyelectrolyte binding.

Fluorescence Intensity. Further evidence of the presence of multiple polyelectrolyte layers can be obtained by fluorescently labeling either PEI or CMC (while leaving the other complementary polymer pair unlabeled). Figure 2c shows the fluorescence intensity of the nanocarriers as additional layers of PEI and CMC are alternately deposited. We observe the fluorescence intensity to gradually increase, albeit nonlinearly, with the increase in nanocarrier mass upon the addition of each labeled polymer layer which binds *via* electrostatic interaction to the underlying polymer. Similar nonlinear increases in the fluorescence intensity with additional polymer layering have been reported elsewhere,^{39,40} and reflects a complexed (as opposed to a core–shell) structure of the nanocarriers synthesized in the present work owing to the interpenetration of the polyelectrolyte molecules which are embedded and intertwined across multiple layers in a manner similar to that proposed by Ladam *et al.*⁴¹ Other factors are also known to contribute to nonlinear growth of the fluorescence signal. The increase in surface area of the nanocarrier with the deposition of each additional layer, for example, allows greater polyelectrolyte and fluorophore coverage, leading to the departure in the linearity of the signal intensity especially when the thickness of the deposited layers are non-negligible compared to the nanocarrier dimension.³⁹ This is a plausible explanation for the trend observed for the labeled CMC (solid line). On the other hand, the size of the polyelectrolyte can also influence its coverage and hence the fluorescence signal.⁴⁰ A larger number of short polyelectrolytes, for example, are required to saturate the nanocarrier surface compared to the case of longer polyelectrolytes, and may explain the faster initial rate of increase for PEI (25 kDa) compared to that for CMC (90 kDa). The increase in fluorescence intensity for labeled PEI (dotted line) is however observed to taper off as the number of layers increases, possibly due to self-quenching of the fluorophores.⁴² The shorter PEI chains allow more efficient penetration into the voids that form due to heterogeneous deposition of prior layers,⁴¹ resulting in more compacted structures with higher coverage densities. The close packing between the fluorophore molecules as a consequence is known to lead to lower fluorescence yields due to fluorophore self-quenching.^{39,42}

In Vitro pDNA Release. Figure 4 shows the *in vitro* release profile of encapsulated pDNA from both Chi/CMC bilayer (sample A) and Chi/CMC/Chi trilayer (sample B) nanocarriers. Unbound/excess pDNA adhering to the outer shell of the nanocarriers appears to provide an initial burst in the release profile over about

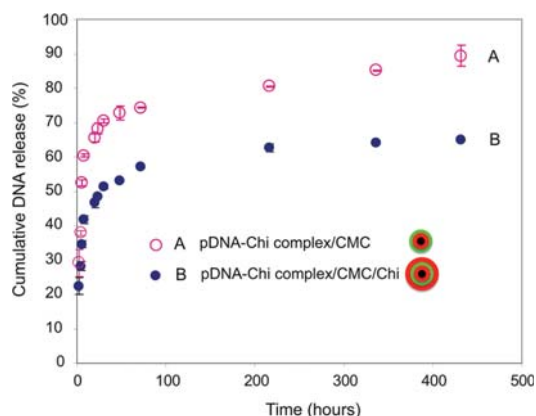


Figure 4. *In vitro* release profile for pDNA encapsulated in Chi/CMC bilayer (sample A) and Chi/CMC/Chi trilayer (sample B) nanocarriers over a period of 19 days.

5 h for both nanocarrier sets, followed by a slower continuous release of the pDNA encapsulated within the nanocarrier over several days. The additional Chi layer on sample B serves to dramatically slow the release of the encapsulated pDNA compared to sample A, releasing DNA over the course of 19 days. The quantized control of the release rate based on the number of polyelectrolyte layers deposited over the drug molecule is attractive from the standpoint of tailoring the drug carrier to the desired release dynamics. Slower release, for the delivery of plasmid encoding growth factors in regenerative medicine, for example, is achievable with more layers. Likewise, fast release—to initiate an immune response for DNA vaccination, for instance—is a matter of reducing the number of layers. The added control provided by the atomization process in manipulating the polymer materials, the N/P ratio between the DNA and polymer, and the polymer mass ratio, among other properties, should enable finely tailorable delivery solutions for a broad spectrum of drugs and serves as a means for studying the formation of specific nanocarriers to treat particular diseases in the future.

In Vitro Cell Transfection. Given the susceptibility of pDNA to shear- or cavitation-induced lysis, gene transfection experiments were carried out to assess whether the nanocarriers and encapsulated plasmid DNA retain their viability and functionality throughout the synthesis. A yellow fluorescent protein (YFP) reporter gene-encoded plasmid was encapsulated in a PEI/CMC bilayer nanocarrier and transfected into mammalian COS-7 and human mesenchymal progenitor cells (MPCs); COS-7 cells represent a target for cellular engineering applications (*e.g.*, protein overexpression, *etc.*), whereas MPCs represent a potent target for stem cell therapy applications. Qualitative evidence of successful gene survival and transfection by pDNA encapsulated within the PEI/CMC nanocarriers is illustrated through the fluorescence expressed by the YFP (depicted in green) in the cytoplasm of both COS-7 cells and MPCs observed in

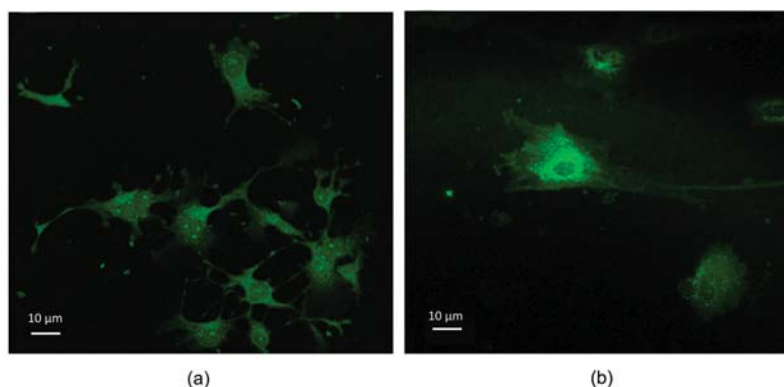


Figure 5. Confocal laser scanning microscopy images of (a) COS-7 cells and (b) MPCs transfected with pVR1020-YFP encapsulated within PEI/CMC bilayer nanocarriers. The cells exhibited granular fluorescent spots distributed throughout the cytoplasm 72 h post-transfection.

the confocal microscopy images taken 72 h post-transfection (Figure 5). The nanocarrier synthesis and plasmid encapsulation using the SAW does not appear to cause degradation of the pDNA—a result consistent with our previous studies reporting postatomization cell and molecular viability.^{25,26} On the basis of the evidence from the size distributions reported above, the surrounding polyelectrolyte layers of the nanocarriers appear to condense the DNA into a much more compact structure, thereby shielding them from shear, heat, and possibly other means of degradation.

CONCLUSIONS

A new technique to synthesize multilayer polyelectrolyte nanocarriers using surface acoustic wave atomization is demonstrated. Evidence of the consecutive layering of oppositely charged polyelectrolytes and pDNA is shown through FT-IR spectroscopy and zeta-potential measurements, in addition to AFM and fluorescence imaging. In contrast to conventional bench-top procedures, the method offers a low cost, rapid, and simple synthesis route, in addition to circumventing the limitations associated with conventional and microfluidic layer-by-layer formation techniques, namely, the necessity of sacrificial colloidal templates

in the former and the large *microcarrier* dimensions in the latter, as well as the difficulties of encapsulation typically encountered. Nanocarriers with up to eight alternating complementary polyelectrolyte layers were synthesized in this study, although additional layers can be deposited in principle simply by successively repeating the atomization–evaporation–resuspension layering process. The nanocarriers have dimensions of around 200 nm or less, which is attractive from the perspective of targeted drug delivery applications. Further, we demonstrate the possibility of encapsulating therapeutic molecules within the multilayered nanostructures using pDNA as a model drug. The additional polyelectrolyte layer is observed to slow down the release rate considerably, therefore offering the opportunity for tuning the release of the drug simply by altering the number of deposited layers. Finally, we verify *in vitro* gene transfection of pDNA-encapsulated nanocarriers into human mesenchymal progenitor and mammalian COS-7 cells. The gene expression in these cells not only indicates that the functionality of the pDNA is preserved during synthesis but also provides evidence of the transfection ability of the therapeutic agents encapsulated within the multilayer nanocarriers for a host of gene delivery applications.

METHODS

SAW Device. Together with standard UV photolithography and wet-etching, a single-phase unidirectional transducer (SPUDT) electrode was sputter-deposited (Hummer Triple Target Magnetron Sputter System, Anatech, Orange, MA, USA) onto a 127.68° γ -cut x -propagating single crystal lithium niobate (LN) substrate (Roditi Ltd., London, UK), as shown in Figure 1b. The width and gap of the SPUDT finger patterns specify the SAW frequency—in this case, the SPUDT is patterned to produce a SAW with 30 MHz resonant frequency corresponding to a wavelength of 132 μm . To generate the SAW, an oscillating electrical signal at the resonant frequency is supplied to the SPUDT using a signal generator (SML01, Rhode & Schwarz, Munich, Germany) and amplifier (model 10W1000C, Amplifier Research, Souderton, PA, USA). To facilitate delivery of

the working fluid to the SAW device for atomization, a short paper (Polyester-Cellulose, LymTech, Chicopee, USA) wick was placed at the tip of a shortened capillary tube connected to a reservoir (Figure 1b).

Nanocarrier Generation. The rest of the experimental setup is schematically illustrated in Figure 1c. The SAW device together with the capillary tube connected to the reservoir containing the polymer solution to be atomized is mounted securely under a conical funnel leading to a spiral tube assembly submerged in a water bath maintained at approximately 40–50 °C. The other end of the spiral tube is submerged in the oppositely charged complementary polymer solution placed within a glass flask. As a consequence of atomizing the initial polymer solution, the aerosols generated navigate through the heated spiral tube. During this process, the solvent in the aerosol droplets evaporate

and hence leave behind solidified polymer nanocarriers. These nanocarriers were then deposited in the collection solution containing a polymer of opposite charge—the polymer system that is to constitute the subsequent layer over the initial polymer core—dissolved in an appropriate solvent. Unbound polymer was removed by dialysis prior to further analysis. If an additional layer is desired, the nanocarrier suspension can be purified prior to their return to the SAW device for reatomization into an alternate polymer solution. This atomization—evaporation—resuspension process can be repeated as many times as the number of additional polymer layers desired.

Polymers. The model polymers employed comprised positively charged chitosan (Chi, MW \approx 120 kDa) or linear polyethyleneimine (PEI, MW \approx 25 kDa, Polysciences Inc., Warrington, PA, USA) and negatively charged carboxymethyl cellulose (CMC, MW \approx 90 kDa). Chi and CMC are commonly used polymers for *in vivo* drug delivery given their biocompatibility and low cytotoxic nature.⁴³ Chi can efficiently condense pDNA and also increase the permeability of macromolecules across the gastrointestinal tract.⁴⁴ Linear PEI is well-known as an efficient carrier for pDNA delivery. In our experiments, PEI in water or Chi in sodium acetate buffer was atomized into CMC in water, and subsequently reatomized into another Chi or PEI solution. Unless stated otherwise, all reagents and solvents of biological grade were obtained from Sigma-Aldrich Pty. Ltd. (Castle Hill, NSW, Australia) and used without further purification.

Multilayer Nanocarrier Characterization. To demonstrate the bonding between successive polyelectrolyte layers and hence provide evidence of the existence of each layer, we examined the properties of the nanocarriers at every step of the LbL technique prior to reatomization. Several characterization techniques were employed as described as follows:

Size Distribution. Immediately after each atomization—evaporation—resuspension process, the hydrodynamic diameter of the nanocarriers was measured using dynamic light scattering (DLS; Zetasizer Nano S, Malvern Instruments Ltd., UK). Atomic force microscopy (AFM; NT-MDT Ntegra, Zelenograd, Russia) was also used to observe the individual nanocarrier morphologies. In addition, visual inspection of their dimensions also provide additional verification to that obtained using DLS.

Spectroscopy. The compositional analysis of multilayer nanocarriers was carried out using Fourier transform infrared spectroscopy (FT-IR spectrometer, Spectrum 100 series, PerkinElmer, Waltham, MA, USA). Prior to the analysis, the synthesized nanocarriers were recovered through dialysis followed by lyophilization.

Zeta-Potential. We expect the zeta-potential of the nanocarrier to reverse with the successive deposition of each additional layer of alternately charged polyelectrolyte. The zeta-potential of the nanocarriers was measured after each layering step using an electrophoretic light scattering spectrophotometer (Zetasizer Nano S, Malvern Instruments, Malvern, UK).

Fluorescence Intensity. The sequential bonding of each successive polyelectrolyte layer onto the surface of the nanocarrier was detected by selectively labeling the polymers. Fluorescein isothiocyanate (FITC) labeled CMC was prepared by activating CMC using 0.318 mmol of N-hydroxysuccinimide and 0.318 mmol of N-(3-dimethylaminopropyl)-N-ethylcarbodiimide hydrochloride in 100 mL of deionized (DI) water followed by dropwise addition of 0.318 mmol fluoresceinamine dissolved in methanol. The reaction was performed at pH 4.7 and at room temperature for 24 h in the dark. FITC labeled PEI was prepared by adding 90.4 mg of fluorescein-5-isothiocyanate (Invitrogen Corp., Carlsbad, CA, USA) dissolved in 2 mL of dimethylsulfoxide dropwise to 1 g of PEI dissolved in water. The reaction was performed at room temperature for 24 h in the dark. The labeled polymers were purified by dialysis against running water (MWCO 3500 dialysis tubing, Spectrum Laboratories, Rancho Dominguez, CA, USA) for 3 days in the dark and freeze dried. Multilayer nanocarriers composed of FITC labeled PEI and label-free CMC, or, FITC labeled CMC and label-free PEI were prepared using the atomization procedures described above. Fluorescence measurements were carried out on a multimode spectrophotometer (SpectraMax M2, Molecular Devices, Sunnyvale, CA, USA) under excitation and emission wavelengths of 490 and 525 nm, respectively.

pDNA Encapsulation and *in Vitro* Release. Plasmid DNA pEGFP-N1 (4733bp, 1.8×10^6 g/mol, Clontech Laboratories Inc., Mountain View, CA, USA) was employed as a therapeutic gene model. The plasmid was first added to the Chi solution to form a pDNA–Chi complex and subsequently atomized into the CMC solution, which was then reatomized into the Chi solution to form the Chi/CMC bilayer nanocarrier within which the pDNA is trapped. To form the encapsulated Chi/CMC/Chi trilayer nanocarrier, an additional layering step was performed. The pDNA release study was carried out under near-physiological conditions. Briefly, the pDNA-encapsulated nanocarriers were dispersed in acetate buffer inside a dialysis bag, which was then immersed in agitated acetate buffer at 37 °C to simulate the pH of the endosomal (pH \sim 6) and lysosomal (pH \sim 5) microenvironments. Samples were collected at different time intervals for pDNA quantification using the Quant-iT PicoGreen dsDNA reagent (Invitrogen Corp., Carlsbad, CA, USA) assay according to the manufacturer's guidelines. The fluorescent intensity was measured using the multi-mode spectrophotometer under excitation and emission wavelengths of 490 nm and 525 nm, respectively. The cumulative fraction release was normalized with respect to the total amount of pDNA encapsulated in the nanocarriers.

***In Vitro* Cell Transfection.** African green monkey kidney COS-7 cells acquired from the American Type Culture Collection (ATCC, Rockville, MD, USA) were cultured in DMEM following the protocol supplied. Human mesenchymal progenitor cells (MPC) obtained from the Monash Institute of Medical Research (Clayton, VIC, Australia) were separately maintained in complete DMEM medium, supplemented with 10% fetal bovine serum (FBS), 100 μ M L-ascorbate-2-phosphate magnesium, 2 mM L-glutamine and 50 units/mL penicillin–streptomycin at 37 °C in a humidified 5% carbon dioxide incubator.

Cells were seeded at 80% confluence on a four-well Lab-Tek chambered coverglass (Nunc GmbH & Co. KG, Langensfeld, Germany) and grown overnight. Bilayer PEI/CMC nanocarriers encapsulating DNA vaccine-type plasmid pVR1020 encoding yellow fluorescent protein reporter (pVR1020-YFP) were prepared using the same procedures described above under aseptic conditions. The spent media was removed and replaced with DMEM containing 2% FBS. Nanocarriers containing 10 μ g of plasmid were added to the cells and allowed to incubate for 4 h, following which the medium was removed and replaced with growth medium. Each control well received 3.75 mg of PEI reagent complexed with 10 μ g DNA (N/P ratio = 5). After 72 h, cells were monitored for gene expression using confocal laser scanning microscopy (A1Rsi Multiphoton System, Nikon Pty. Ltd., Lidcombe, NSW, Australia) under excitation and emission wavelengths of 514 and 527 nm, respectively. The original grayscale images from the fluorescence channel were mapped to an arbitrary green color to represent the fluorescence of the YFP.

Acknowledgment. Funding for this work was provided through Australian Research Council Discovery (ARC) Project Grant DP2433214 and National Health and Medical Research Council (NHMRC) Development Grant 546238. L.Y.Y. is also grateful to the Australian Research Council for an Australian Research Fellowship under ARC Discovery Project Grant DP2433179. The authors acknowledge the help of Fatin Al-Deen (Chemical Engineering, Monash University) who provided assistance in obtaining preliminary fluorescence microscopy images and Adam Mechler (School of Molecular Sciences, La Trobe University) for his assistance with acquiring the AFM images. We also thank Graham Jenkin (Monash Institute of Medical Research) for kindly supplying us with the stem cells and Justin Cooper-White and Dmitry Ovchinnikov (University of Queensland) for helpful discussions regarding the work and early attempts with the *in vitro* transfection.

REFERENCES AND NOTES

1. LaVan, D. A.; McGuire, T.; Langer, R. Small-scale systems for *in vivo* drug delivery. *Nat. Biotechnol.* **2003**, *21*, 1184–1191.
2. Johnston, A. P.; Cortez, C.; Angelatos, A. S.; Caruso, F. Layer-by-layer engineered capsules and their applications. *Curr. Opin. Colloid Interface Sci.* **2006**, *11*, 203–209.

3. Shchukin, D. G.; Sukhorukov, G. B. Nanoparticle synthesis in engineered organic nanoscale reactors. *Adv. Mater.* **2004**, *16*, 671–682.
4. Decher, G. Fuzzy nanoassemblies: Toward layered polymeric multicomposites. *Science* **1997**, *277*, 1232–1237.
5. Caruso, F.; Caruso, R. A.; Möhwald, H. Nanoengineering of inorganic and hybrid hollow spheres by colloidal templating. *Science* **1998**, *282*, 1111–1113.
6. Sukhorukov, G. B.; Antipov, A. A.; Voigt, A.; Donath, E.; Möhwald, H. pH-controlled macromolecule encapsulation in and release from polyelectrolyte multilayer nanocapsules. *Macromol. Rapid Commun.* **2001**, *22*, 44–46.
7. Peyratout, C.; Dähne, L. Tailor-made polyelectrolyte microcapsules: From multilayers to smart containers. *Angew. Chem., Int. Ed.* **2004**, *43*, 3762–3783.
8. Khopade, A.; Caruso, F. Stepwise self-assembled poly(amidoamine) dendrimer and poly(styrenesulfonate) microcapsules as sustained delivery vehicles. *Biomacromolecules* **2002**, *3*, 1154–1162.
9. Caruso, F.; Trau, D.; Möhwald, H. Renneberg, Enzyme encapsulation in layer-by-layer engineered polymer multilayer capsules. *Langmuir* **2000**, *16*, 1485–1488.
10. Zhu, Y.; Shi, J.; Shen, W.; Dong, X.; Feng, J.; Ruan, M.; Li, Y. Stimuli-responsive controlled drug release from a hollow mesoporous silica sphere/polyelectrolyte multilayer core-shell structure. *Angew. Chem., Int. Ed.* **2005**, *44*, 5083–5087.
11. Shchukin, D. G.; Kommireddy, D. S.; Zhao, Y.; Cui, T.; Sukhorukov, G. B.; Lvov, Y. M. Polyelectrolyte micropatterning using a laminar-flow microfluidic device. *Adv. Mater.* **2004**, *16*, 389–393.
12. Priest, C.; Quinn, A.; Postma, A.; Zelikin, A. N.; Ralston, J.; Caruso, F. Microfluidic polymer multilayer adsorption on liquid crystal droplets for microcapsule synthesis. *Lab Chip* **2008**, *8*, 2182–2187.
13. Wong E. H. m. The development of a continuous encapsulation method in a microfluidic device. Ph.D. Thesis, The University of Queensland, Australia, 2009.
14. Kreuter, J. Nanoparticulate systems for brain delivery of drugs. *Adv. Drug Delivery Rev.* **2001**, *47*, 65–81.
15. Wissing, S. A.; Kayser, O.; Müller, R. H. Solid lipid nanoparticles for parenteral drug delivery. *Adv. Drug Delivery Rev.* **2004**, *56*, 1257–1272.
16. Yuan, F.; Dellian, M.; Fukumura, D.; Leunig, M.; Berk, D. A.; Torchilin, V. P.; Jain, R. K. Vascular permeability in a human tumor xenograft: Molecular size dependence and cutoff size. *Cancer Res.* **1995**, *55*, 3752–3756.
17. Gu, F. X.; Karnik, R.; Wang, A. Z.; Alexis, F.; Levy-Nissenbaum, E.; Hong, S.; Langer, R. S.; Farokhzad, O. C. Targeted nanoparticles for cancer therapy. *Nano Today* **2007**, *2*, 3, 14–21.
18. Friend, J.; Yeo, L. Y. Microscale acoustofluidics: microfluidics driven via acoustics and ultrasonics. *Rev. Mod. Phys.* **2011**, *83*, 647–704.
19. Qi, A.; Yeo, L. Y.; Friend, J. R. Interfacial destabilization and atomization driven by surface acoustic waves. *Phys. Fluids* **2008**, *20*, 074103.
20. Qi, A.; Yeo, L. Y.; Friend, J.; Ho, J. The extraction of liquid, protein molecules and yeast cells from paper through surface acoustic wave atomization. *Lab Chip* **2010**, *10*, 470–476.
21. Heron, S. R.; Wilson, R.; Shaffer, S. A.; Goodlett, D. R.; Cooper, J. M. Surface acoustic wave nebulization of peptides as a microfluidic interface for mass spectrometry. *Anal. Chem.* **2010**, *82*, 3985–3989.
22. Ho, J.; Tan, M. K.; Go, D.; Yeo, L. Y.; Friend, J.; Chang, H.-C. A paper-based microfluidic surface acoustic wave sample delivery and ionization source for rapid and sensitive ambient mass spectrometry. *Anal. Chem.* **2011**, *83*, 3260–3266.
23. Qi, A.; Friend, J. R.; Yeo, L. Y. Miniature inhalation therapy platform using surface acoustic wave microfluidic atomization. *Lab Chip* **2009**, *9*, 2184–2193.
24. Friend, J. R.; Yeo, L. Y.; Arifin, D. R.; Mechler, A. Evaporative self-assembly assisted synthesis of polymeric nanoparticles by surface acoustic wave atomization. *Nanotechnology* **2008**, *19*, 145301.
25. Alvarez, M.; Friend, J.; Yeo, L. Y. Rapid generation of protein aerosols and nanoparticles via surface acoustic wave atomization. *Nanotechnology* **2008**, *19*, 455103.
26. Alvarez, M.; Yeo, L. Y.; Friend, J. R.; Jamriska, M. Rapid production of protein-loaded biodegradable microparticles using surface acoustic waves. *Biomicrofluidics* **2009**, *3*, 014102.
27. Li, H.; Friend, J.; Yeo, L.; Dasvarma, A.; Traianedes, K. Effect of surface acoustic waves on the viability, proliferation and differentiation of primary osteoblast-like cells. *Biomicrofluidics* **2009**, *3*, 034102.
28. Oxtoby, D. W. Vibrational relaxation in liquids. *Annu. Rev. Phys. Chem.* **1981**, *32*, 77–101.
29. Leung, M. K. M.; Such, G. K.; Johnston, A. P. R.; Biswas, D. P.; Zhu, Z.; Yan, Y.; Lutz, J.-F.; Caruso, F. Assembly and degradation of low-fouling click-functionalized poly(ethylene glycol)-based multilayer films and capsules. *Small* **2011**, *7*, 1075–1085.
30. Chong, S.-F.; Lee, J. H.; Zelikin, A. N.; Caruso, F. Tuning the permeability of polymer hydrogel capsules: An investigation of cross-linking density, membrane thickness, and cross-linkers. *Langmuir* **2011**, *27*, 1724–1730.
31. Cortez, C.; Quinn, J. F.; Hao, X.; Gudipati, C. S.; Stenzel, M. H.; Davis, T. P.; Caruso, F. Multilayer buildup and biofouling characteristics of PSS-b-PEG containing films. *Langmuir* **2011**, *26*, 9720–9727.
32. Shutava, T. G.; Balkundi, S. S.; Vangala, P.; Steffan, J. J.; Bigelow, R. L.; Cardelli, J. A.; O'Neal, P.; Lvov, Y. M. Layer-by-layer-coated gelatin nanoparticles as a vehicle for delivery of natural polyphenols. *ACS Nano* **2009**, *3*, 1877–1885.
33. Minatti, E.; Viville, P.; Borsali, R.; Schappacher, M.; Deffieux, A.; Lazzaroni, R. Micellar morphological changes promoted by cyclization of PS-b-PI copolymer: DLS and AFM experiments. *Macromolecules* **2003**, *36*, 4125–4133.
34. Bloomfield, V. A. DNA condensation. *Curr. Opin. Struct. Biol.* **1996**, *6*, 334–341.
35. Danielsen, S.; Varum, K. M.; Stokke, B. T. Structural analysis of chitosan mediated DNA condensation by AFM: Influence of chitosan molecular parameters. *Biomacromolecules* **2004**, *5*, 928–936.
36. Biswal, D. R.; Singh, R. P. Characterisation of carboxymethyl cellulose and polyacrylamide graft copolymer. *Carbohydr. Polym.* **2004**, *57*, 379–387.
37. Rosca, C.; Popa, M. I.; Lisa, G.; Chitanu, G. C. Interaction of chitosan with natural or synthetic anionic polyelectrolytes. 1. The chitosan-carboxymethylcellulose complex. *Carbohydr. Polym.* **2005**, *62*, 35–41.
38. Katagiri, K.; Caruso, F. Monodisperse polyelectrolyte-supported asymmetric lipid-bilayer vesicles. *Adv. Mater.* **2005**, *17*, 738–743.
39. Johnston, A. P. R.; Zelikin, A. N.; Lee, L.; Caruso, F. Approaches to quantifying and visualizing polyelectrolyte multilayer film formation on particles. *Anal. Chem.* **2006**, *78*, 5913–5919.
40. Lee, L.; Johnston, A. P. R.; Caruso, F. Manipulating the salt and thermal stability of DNA multilayer films via oligonucleotide length. *Biomacromolecules* **2008**, *9*, 3070–3078.
41. Ladam, G.; Schaad, P.; Voegel, J. C.; Schaaf, P.; Decher, G.; Cuisinier, F. *In situ* determination of the structural properties of initially deposited polyelectrolyte multilayers. *Langmuir* **2000**, *16*, 1249–1255.
42. Imhof, A.; Megens, M.; Engelberts, J. J.; de Lang, D. T. N.; Sprik, R.; Vos, W. L. Spectroscopy of fluorescein (FITC) dyed colloidal silica spheres. *J. Phys. Chem. B* **1999**, *103*, 1408–1415.
43. Boonsongrit, Y.; Mitrevaj, A.; Mueller, B. W. Chitosan drug binding by ionic interaction. *Eur. J. Pharm. Biopharm.* **2006**, *62*, 267–274.
44. Bhavsar, M. D.; Amiji, M. M. Polymeric nano- and micro-particle technologies for oral gene delivery. *Expert Opin. Drug Delivery* **2007**, *4*, 197–213.

Appendix C

Pulmonary Gene Delivery Platform for DNA Vaccines via Ultarfast Microfluidics

Rajapaksa, A.E., Ho, J., Qi, A., Yeo, L.Y., Friend, J., McIntosh, M.P., Piedrafita, D.,
Meeusen, E. and Morton, A.V.

Advances in Microfluidics and Nanofluidics and Asian-Pacific International Symposium
on Lab on Chip, AMN - APLOC 2011

Biopolis, Singapore

Jan 2011

Pulmonary Gene Delivery Platform for DNA Vaccines via Ultrasonic Microfluidics

Anushi Rajapaksa^{1*}, Jenny Ho¹, Aisha Qi¹, Leslie Yeo¹, James Friend¹, Michelle P. McIntosh², David Piedrafita³, Els Meeusen³, David A. V. Morton²

¹Micro/Nanophysics Research Laboratory, Monash University, Australia

²Monash Institute of Pharmaceutical Sciences, Monash University, Australia

³Biotechnology Research Laboratories, Monash University, Australia

Abstract

Aerosol delivery of drugs represents the next generation of vaccine delivery where the drug is deposited into the lung, which provides a non-invasive route for the delivery of genetic therapeutics against emerging infections. The traditional methods attempted for the production of DNA aerosols include ultrasonic and jet nebulizers which fail to maintain the viability of large biomolecules such as DNA due to the high shear rates induced during the atomization process. A novel system is presented for the production of aerosols containing DNA in a defined size range using surface acoustic wave (SAW) devices. The SAW technology provides a portable platform to achieve this goal where aerosols in the size range of 0.5-5 μm suitable for pulmonary delivery can be obtained while causing little damage to the integrity of the DNA molecules. SAWs are essentially acoustic waves with 10 nm order amplitudes that originate as a result of the application of an alternating voltage onto an interdigital transducer patterned on a piezoelectric substrate. The leakage of acoustic radiation into a drop housing the DNA solution then results in its atomization to produce the micron dimension aerosols. A solution containing a plasmid DNA (pDNA) vector encoding a 45 kDa merozoite surface protein 4/5 (MSP4/5) which is a potential malaria vaccine candidate was nebulized using both 20 and 30 MHz SAW devices. High levels of

gene expression was observed in western blots from *in vitro* experiments conducted using COS-7 cells that were transfected with the condensed DNA, post-atomization. Modest levels of *in vivo* gene expression was observed when pDNA recovered after SAW atomization, was administered to the lung of mice via intratracheal instillation. The low power consumption of SAW nebulization (1-3 W) together with its potential for miniaturization aptly conveys the suitability of the SAW technology as a portable pulmonary gene delivery platform.

Introduction

The increase in the need for the effective delivery of potent vaccines against infectious diseases, require robust yet straightforward production of DNA-laden aerosols. Plasmid DNA-based approaches to gene therapy are often termed 'non-viral', involving recombination of gene sequence encoding a therapeutic protein into a closed circular piece of DNA and administered directly to patients to induce gene expression to produce a desired gene product, with the aim to treat the disease at the molecular level by restoring defective biological function [1, 2].

Aerosol delivery of drugs represents the next generation of vaccine delivery where the drug is deposited into the lung, which provides an ideal, non-invasive route. Optimization of delivery efficiency and durability of the gene vectors to comply with stringent requirements are the critical areas for this approach to be successful. In addition, the aerodynamic size ($< 5 \mu\text{m}$) of aerosols generated by an inhaler greatly influences the accessibility to the lower airway (alveolar) and subsequently the absorption and transfection efficiency of gene vectors [3].

To date, numerous studies have been undertaken in order to determine the feasibility of pulmonary delivery devices for delivering non-complexed pDNA to the lungs [3-5]. Unfortunately, the supercoiled tertiary structures of pDNA, extremely important for biological efficacy, were severely sheared into open circular and fragmented DNA by the hydrodynamic shear and shock waves during

the nebulization process in jet [6, 7] and ultrasonic [4, 8] nebulizers when the plasmid sizes were larger than 5 kilo-base pairs.

Surface Acoustic Wave (SAW) driven atomization system is a simple-to-use, novel, portable and efficient device that can be tailored to a variety of drug therapies in aerosol delivery [9]. Surface acoustic waves are megahertz (MHz) to gigahertz (GHz) order, transverse-axial polarized elliptical electroacoustic waves with displacement amplitudes of just a few nanometers. The waves that propagate along the low-loss piezoelectric substrates like lithium niobate (LiNbO_3) surface are generated by a sinusoidal electric field between the interlaced fingers of an interdigital transducer (IDT) electrode (Fig. 1). The SAW is localised to the substrate surface, and its amplitude decays rapidly within a few wavelengths (a wavelength is typically $200 \mu\text{m}$) into the substrate material. SAW is regarded as an highly efficient method for transferring energy into fluid, and requiring far less power than conventionally used ultrasound [10]. Moreover, the risk of denaturing molecules is greatly reduced since the period to induce vibrations in SAW devices is much shorter than the molecular relaxation time scale of macromolecules in liquids, by employing 10 – 100 MHz order frequency [11, 12]. Further, when used for atomization, the size of droplets generated by SAW can be changed by about an order of magnitude in a few microseconds in a controllable fashion by switching from standing-wave to travelling-wave SAW on the substrate. Hence, a SAW approach has significant advantages over the current generation of ultrasonic medical nebulizers [10].

The aim of this work is to demonstrate the feasibility of SAW atomization as an aerosol delivery platform for pulmonary genetic therapeutics, especially for shear-sensitive naked (non-complexed) pDNA encoding a desired gene.

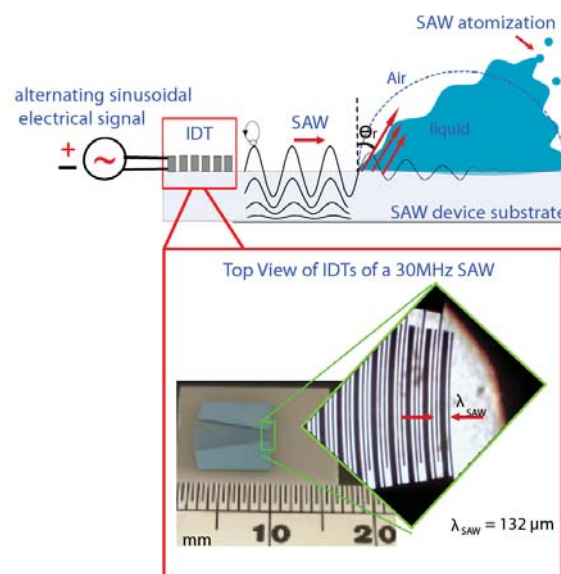


Figure 1: Schematic showing a SAW device together with the interaction of the SAW with a liquid drop upon the surface of the substrate upon application of an electrical signal. The acoustic energy leaks into the drop and deforms the drop at the Rayleigh angle θ_r . When the energy is sufficient, destabilized capillary waves break up into micron dimension aerosols causing atomization. The bottom panel shows an image of the aluminium-chromium IDT electrodes patterned on the piezoelectric (LiNbO_3) substrate with an enlargement of the IDTs showing the width between electrodes and capillary wavelength, λ_{SAW} .

Plasmid atomization using SAW

Different concentrations of pDNA solutions (vector encoding either a 45 kDa merozoite surface protein 4/5(MSP4/5) which is a potential malaria vaccine candidate or YFP yellow fluorescent protein) (Fig. 2) were atomized through the 20 MHz and 30 MHz SAW devices and collected carefully into microcentrifuge tubes for further analysis.

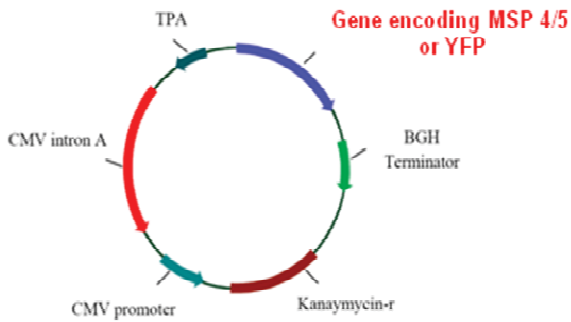


Figure 2: Schematic representation of the vector pVR1020 with vector encoding either MSP4/5 or YFP

Results and Discussion

The *in vitro* transfection efficiency of SAW atomized pVR1020-MSP4/5 was investigated in immortalized African green monkey kidney cells (COS-7) where plasmid DNA recovered after 30 MHz and 20 MHz SAW atomization showed high transfection efficiencies, compared to the corresponding un-atomized (control) pDNA at 48 h (Fig. 3) demonstrating that the pDNA molecules are intact after SAW atomization.

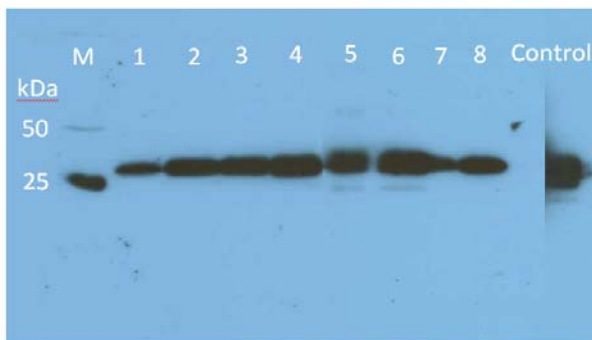


Figure 3: Western blot detections of PyMSP4/5 expressed in COS-7 cells at 48 h post-transfection. Lane M: marker shown molecular mass standards (kDa) on the left; lanes 1 – 3: the cells transfected with pDNA recovered from 35, 50 and 85 $\mu\text{g ml}^{-1}$ pDNA atomized with 30 MHz SAW; lanes 4 – 8: the cells transfected with pDNA recovered from 25, 35, 50, 65 and 85 $\mu\text{g ml}^{-1}$ pDNA atomized with 20 MHz SAW.

Moreover, modest levels of *in vivo* gene expression was observed when pDNA recovered

after 30 MHz SAW atomization, was administered to the lung of a 6 week old Swiss-strain male mice via intratracheal instillation. Mice were sacrificed 24 hours administration and lungs removed and lung sections (10 μm) were visualized for fluorescence of the YFP protein. The retention of the *in vivo* transfection efficiency (Fig. 4) offered additional evidence that the pDNA molecules were intact after SAW nebulization.

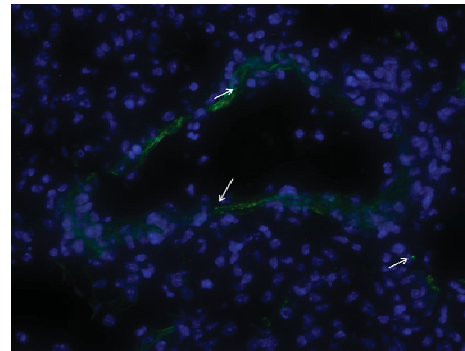


Figure 4: Fluorescence microscopic image showing *in vivo* positive expression of YFP protein (discrete green dots shown by arrows) in a mouse lung parenchyma where alveolar cell nuclei are stained with DAPI (4',6-diamidino-2-phenylindole, dilactate).

Once the preservation of the pDNA integrity was confirmed, it was then required that the pDNA aerosol size be optimised for aerosol lung delivery. The aerosol size distribution for pDNA aerosols generated via SAW atomization at several concentrations added with 20% w/w glycerol (carefully chosen to minimise the surface tension and to increase the surface tension of atomised pDNA) (Fig. 5) further confirmed our ability to finely tune the droplet size $< 5 \mu\text{m}$, optimal for deep lung deposition. The above result is encouraging compared to a previous nebulization catheter device which only managed to generate aerosols with sizes around $33 \pm 2 \mu\text{m}$ for naked pDNA [13].

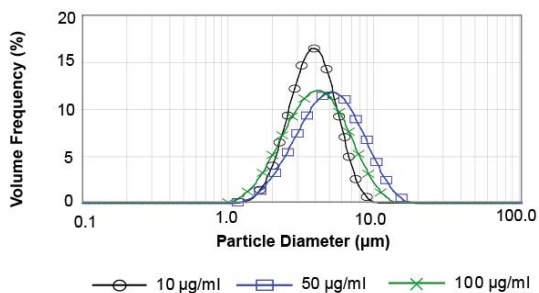


Figure 5: Volume-based droplet size distribution of pDNA aerosols obtained using laser diffraction at 10 (○), 50 (□) and 100 (×) μgml^{-1} indicates narrow mono-disperse distributions that are optimal for lung deposition.

Conclusions

The feasibility of SAW atomization at generating aerosols is demonstrated for a shear-sensitive biotherapeutics – plasmid DNA, and resulted in almost negligible denaturation of the supercoiled content as seen from both the *in vitro* and *in vivo* experiments. This work further strengthen the promising feasibility of miniaturized SAW technology as a pulmonary delivery platform for DNA molecules, proteins and other biomolecules [14]. Since SAW nebulization consumes low power levels (1-3 W) than that required with conventional ultrasonic nebulizers, thus confirming its potential for miniaturization in a portable palm sized device, powered by battery strongly conveys the suitability of the SAW technology as a portable pulmonary gene delivery platform.

Keywords: *DNA, gene therapy, pulmonary, aerosol, surface acoustic waves.*

References

- [1] M. A. Liu, "DNA vaccines: a review," *Journal Of Internal Medicine*, vol. 253, pp. 402-410, Apr 2003.
- [2] M. A. Liu, B. Wahren, and G. B. K. Hedestam, "DNA vaccines: Recent developments and future possibilities," *Human Gene Therapy*, vol. 17, pp. 1051-1061, Nov 2006.
- [3] E. Arulmuthu, D. Williams, and H. Versteeg, "The arrival of genetic engineering The Arrival of Genetic Engineering Strategies for Delivery of Nonviral Plasmid DNA-Based Gene Therapy," *Engineering in Medicine and Biology Magazine, IEEE*, vol. 28, pp. 40-54, 2009.
- [4] Y. K. Lentz, T. J. Anchordoquy, and C. S. Lengsfeld, "Rationale for the selection of an aerosol delivery system for gene delivery," *Journal of Aerosol Medicine-Deposition Clearance and Effects in the Lung*, vol. 19, pp. 372-384, Fal 2006.
- [5] E. R. Arulmuthu, D. J. Williams, H. Baldascini, H. K. Versteeg, and M. Hoare, "Studies on aerosol delivery of plasmid DNA using a mesh Nebulizer," *Biotechnology and Bioengineering*, vol. 98, pp. 939-955, Dec 2007.
- [6] E. Kleemann, L. A. Dailey, H. G. Abdelhady, T. Gessler, T. Schmehl, C. J. Roberts, M. C. Davies, W. Seeger, and T. Kissel, "Modified polyethylenimines as non-viral gene delivery systems for aerosol gene therapy: investigations of the complex structure and stability during air-jet and ultrasonic nebulization," *Journal of Controlled Release*, vol. 100, pp. 437-450, Dec 2004.
- [7] Y. K. Lentz, L. R. Worden, T. J. Anchordoquy, and C. S. Lengsfeld, "Effect of jet nebulization on DNA: identifying the dominant degradation mechanism and mitigation methods," *Journal of Aerosol Science*, vol. 36, pp. 973-990, Aug 2005.
- [8] Y. K. Lentz, T. J. Anchordoquy, and C. S. Lengsfeld, "DNA acts as a nucleation site for transient cavitation in the ultrasonic nebulizer," *Journal of Pharmaceutical Sciences*, vol. 95, pp. 607-619, Mar 2006.
- [9] A. S. Qi, J. R. Friend, L. Y. Yeo, D. A. V. Morton, M. P. McIntosh, and L. Spiccia, "Miniature inhalation therapy platform using surface acoustic wave microfluidic atomization," *Lab on a Chip*, vol. 9, pp. 2184-2193, 2009.
- [10] A. Qi, L. Y. Yeo, and J. R. Friend, "Interfacial destabilization and atomization driven by surface acoustic waves," *Physics of Fluids*, vol. 20, Jul 2008.
- [11] D. W. Oxtoby, "Vibrational relaxation in liquids," *Annual Review of Physical Chemistry*, vol. 32, pp. 77-101, 1981.
- [12] C. C. Hsieh, A. Balducci, and P. S. Doyle, "An experimental study of DNA rotational relaxation time in nanoslits," *Macromolecules*,

- vol. 40, pp. 5196-5205, Jul 2007.
- [13] M. Koping-Hoggard, M. M. Issa, T. Kohler, A. Tronde, K. M. Varum, and P. Artursson, "A miniaturized nebulization catheter for improved gene delivery to the mouse lung," *Journal of Gene Medicine*, vol. 7, pp. 1215-1222, Sep 2005.
- [14] A. Qi, L. Yeo, J. Friend, and J. Ho, "The extraction of liquid, protein molecules and yeast cells from paper through surface acoustic wave atomization," *Lab Chip*, vol. 10, pp. 470 - 476, 2010.

Brief Biography of author

Anushi Rajapaksa is a postgraduate student in the Department of Mechanical and Aerospace Engineering pursuing a PHD and is co-supervised by Prof. James Friend, Assoc. Prof. Leslie Yeo. She works at both the Micro/Nanophysics Research Laboratory (MNRL) and also at the Coppel Lab (Department of Microbiology) at Monash University, Australia. She completed her undergraduate studies in Electrical and Computer Systems Engineering from Monash University, Clayton in 2008, for which she was awarded first class honours and received acknowledgments from the Dean of Engineering of Monash University in 2006 & 2007 for outstanding academic achievements. Anushi was the recipient of the prestigious MGS (Monash Graduate Scholarship) and the MIPRS (Monash International Postgraduate Research Scholarship) to pursue her PHD studies and received student award for "Outstanding Research Contribution" at Monash Research Month in 2009.

Appendix D

Microfluidic Synthesis of Multi-Layer Nanoparticles for Drug and Gene Delivery

Chan, P.Y., Qi, A., **Rajapaksa, A.E.**, Friend, J. and Yeo, L.Y.

Chemeca 2011

Sydney, Australia

September 2011

MICROFLUIDIC SYNTHESIS OF MULTI-LAYER NANOPARTICLES FOR DRUG & GENE DELIVERY

Peggy P.Y. Chan¹, Aisha Qi¹, Anushi Rajapaksa¹, James Friend¹, Leslie Yeo¹

¹Micro/Nanophysics Research Laboratory, Monash University, Clayton VIC 3800, Australia

²Department of Chemical Engineering, Monash University, Clayton VIC 3800, Australia



ABSTRACT

Multiple layer nanoparticles offers a likelihood of success in drug delivery, as it provides a solution for a more controllable drug release, as with such structures, control over the capsule wall thickness, permeability, stability, and degradation characteristics can be achieved (Kumar, 2008). Using PDMS microfluidic devices to synthesize polymeric multilayer microparticles has become popular recently. The generation of complex emulsions, such as double and triple emulsions, is also achievable with such devices (Roney et al., 2005). However, limitations with these devices are: the microchannel surface property is crucial to maintain the desired flow within the microdevice; droplets which form within the microchannels require a cross-linking agent to be solidified into particles; the size of the droplets is limited to the size of microchannels, usually around 50-100 μm , which is too large to be used for drug delivery; and the amount of droplets or particles produced is limited as the droplets/particles are formed one by one. Therefore, in this study, we present a novel technique on fast multilayer polymeric nanoparticles synthesis via surface acoustic wave (SAW) atomization using a microfluidic device.

We are able to show (1) successful synthesis of multilayer polymeric structure, and (2) fast generation of monodispersed particles in nanosize. Compared to conventional methods, SAW atomization is fast and have less limitations in the usage of surfactant and templates. Compared to traditional ultrasonic atomization and electrospraying, SAW atomization driven at much higher frequency is more suitable for shear and heat sensitive drug delivery.

INTRODUCTION

The use of nanoparticles as drug or gene carrier offer several advantages such as better drug stability, feasibility to incorporate both hydrophilic and hydrophobic substances, and their enhanced permeability and retention effect for tumor therapy (Cho et al., 2008; Gelperina et al., 2005). The biodistribution of drug particles can be greatly improved by using particles with size range in submicron or nano-scale, and secondly, nanoparticles can also be modified or coated to target infected organs or tissues (Kumar, 2008; Roney et al., 2005; Fang et al., 2006; Li et al., 2001; Koziaraa et al., 2004). Multilayer polymeric encapsulation provides a solution for a more controllable in-vivo drug release; multi-functionality can be designed for such structure by using different polymer in different layer each carries a different functionality. In addition, the capsule

wall thickness, permeability, stability, and degradation characteristics in such structure can be controlled (Zelikin et al., 2008), and tailored for targeted delivery or successive releasing of drugs.

The conventional techniques used for nanoparticle formation and encapsulation all have difficulties in getting nanoparticles with narrow size distribution, unless it is synthesis with the aid of emulsion, surfactant and templates. These methods usually consist of several complicated steps, all of which require well optimized condition to allow for the formation of form homogeneous dispersed single layer particles (Wong, 2009), let alone synthesizing layer-by-layer capsules. For example, the coacervation/precipitation technique requires a careful selection of solvents, which can limits the range of materials that can be applied, especially for the case of synthesizing LbL particles. Spray drying, usually means ultrasonic atomization and electrospray. These methods seems to have less limitation in terms of the choice of solvents, also the usage of templates is not necessary; however, the harsh conditions involved in such technique can cause damage to drugs or biomolecules. For example, the high temperature use in spray drying can cause damage to heat-sensitive biomolecules. Ultrasonic atomization, driven at ~ 10 kHz order, imposes unavoidable shear forces that can damage many shear-sensitive molecules, for example, DNA. Electrospray, on the other hand, driven at \sim kV order voltage, still poses high risks of damaging molecules.

Using PDMS microfluidic devices to synthesize polymeric multilayer micro/nanoparticles has become popular recently. The generation of complex emulsions, such as double and triple emulsions, is also achievable with such devices (Wong, 2009; Priest et al., 2008). However, this technique share the same limitation as emulsion based method, in addition such technique is limited by: (1) the microchannel surface property is crucial to maintain the desired flow within the microdevice; (2) the need for a cross-linking agent to solidified the droplets that formed from the microchannels; (3) the size of the droplets is limited to the size of microchannels, usually around 50-100 μm ; and (4) the amount of droplets or particles produced is limited as the droplets/particles are formed one by one.

Previously, our group showed the synthesis of pure polymeric nanoparticles, protein nanoparticles, and protein loaded nanoparticles via surface acoustic wave (SAW) atomization (Friend et al., 2008; Alvarez et al., 2008; Alvarez et al., 2008). Surface acoustic waves (SAWs), with nanometer-order amplitude, can propagate over thousands of wavelengths, typically several centimeters, along the surface in a low loss piezoelectric material like 127.68° y-x cut lithium niobate (LiNbO_3 or LN). As its name indicated, the wave amplitude is rapidly attenuated with increasing depth into the LN substrate from the propagation surface. The x-propagating wave speed on the LN substrate c_s is 3965 m/s. When a SAW meets a liquid placed upon the substrate, it diffracts into it at the *Rayleigh* angle, defined by $\theta_R = \sin^{-1}(c_w/c_s) \sim 22^\circ$, where c_w , the sound speed in water, is 1485 m/s. The acoustic energy in the liquid causes the bulk recirculation, known as acoustic streaming, within the drop and a body force that causes the drop to translate in the direction of the SAW propagation. At high powers, though the displacement of the surface is only around 10 nm, when the driving frequency is in an order of 10 MHz, the accelerations of the surface is expected to be as high as in an order of 10^7 m/s^2 , which, when transmitted into a liquid drop, can induce very strong capillary waves on the drop free surface that are destabilized upon sufficient acoustic excitation. In this manner, a forcing mechanism for rapid and efficient atomization is

formed (Qi et al., 2008), as shown in Fig. 1.

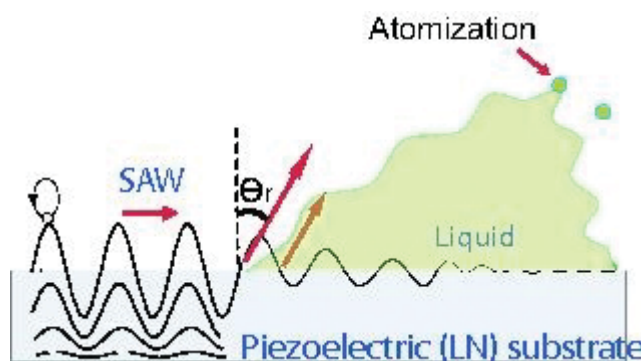


Fig. 1: A schematic atomization process (Qi et al., 2008; Qi et al., 2009) SAWs propagating into a drop at a Rayleigh angle, induce subsequent streaming within the drop and destabilize capillary wave on the free liquid surface. When the power is sufficient, capillary wave breaks up into aerosol, which is known as atomization.

Unlike other conventional ultrasonic atomization, SAW atomization works at much higher frequencies ($\gg 10\text{MHz}$), meaning that the time period of the molecule exposing to the shear force is much shorter than the molecular relaxation time scale in liquids (Oxtoby, 1981; Hsieh et al., 2001), the shear effect is therefore greatly minimized (Alvarez et al., 2009). In addition, SAW atomization, compared to electrospray, is driven at very low power ($\sim 1\text{-}3\text{ W}$), which can hardly cause damages to drugs and molecules (Qi et al., 2009; Qi et al., 2010). In this study, we demonstrate that SAW atomization technique can be extended to synthesis multilayer polymeric nanoparticles in a layer-by-layer manner. Herein, we synthesis DNA containing multilayer nanoparticles to demonstrate the flexibility and therapeutic applicability of the SAW atomization approach.

MATERIALS AND METHODS

SAW Microchip fabrication

A single-phase uni-directional transducer (SPUDT) was fabricated using sputtering (Hummerr Tripletarget Magnetron Sputter System, Anatech, USA.) and standard UV photolithography with wet-etch techniques onto a 128° y-cut x-propagating lithium niobate (LiNbO_3) piezoelectric substrate surface. To achieve the most efficient atomization with limited power input, an enhanced SAW signal, which is located at the focus of the concentric transducers is also achievable by using curved, focusing electrodes. A focusing SPUDT layout is captured under microscope and presented in Fig 2 (inset). A high frequency electrical signal is supplied to the electrodes, generating mechanical oscillations on the substrate via the inverse piezoelectric effect, thereby inducing a SAW as the efficient atomization driving source (Qi et al., 2008; Qi et al., 2009; Qi et al., 2010).

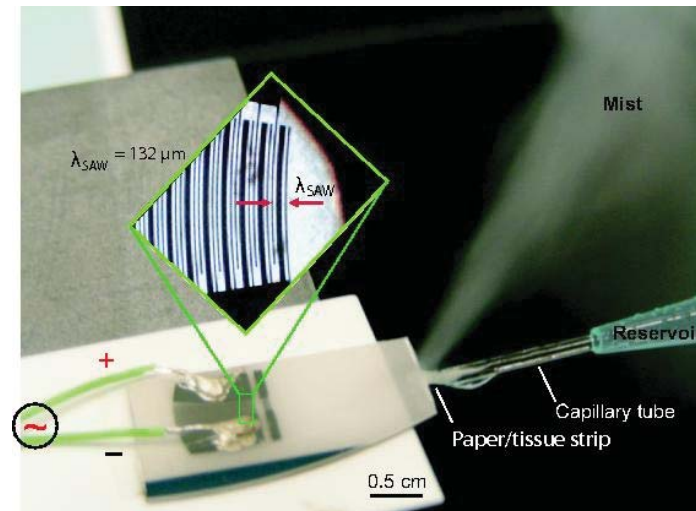


Fig. 2: Photo of a 30 MHz SPIDT SAW device and its electrode layout captured under microscope. A capillary tube was employed as a DNA and polymer supply scheme

Nanoparticle synthesis

A capillary tube with a tiny paper strip placed at one end was used to supply polymer solutions to the device substrate, as shown in Fig 2. As presented in our previous work (Qi et al., 2010), under SAW excitation, a paper can be used as a convenient media to automatically transport solutions from a reservoir to the device substrate for direct and efficient atomization without damaging the biomolecules. Since the paper strip employed in such setup is very small and the flow rate is also high within the paper such that the amount of molecules that could be left inside the paper is negligible.

In our experiment setup, a capillary tube filled with paper strip is mounted next to the SAW device, where the paper strip is in contact with substrate. A polymer solution is supplied from the other end of the capillary tube. A funnel was placed above the SAW device to collect the aerosols, which, following the air flow provided by a vacuum pump, subsequently passed through a long drying tube. The drying tube was fully embedded in a 300 ml hot water buffer and the temperature within the drying tube is kept between 40–50 degree. The aerosols are dried by evaporation inside the spiral tube, and shrank to small solid particles. These small particles are then deposited into another solution in a glass beaker. Dried particles will be able to bond to molecules with opposite charge instantaneously. Unbound polymers were removed by dialysis prior to sample characterization. As illustrated in Fig 3, if another layer is required, this suspension, can be collected and re-atomized into another polymer solution using the same experiment setup and atomization procedures described above.

Chitosan (Chi) (MW 50k-190k, Sigma), a positive charged natural polysaccharide with low cytotoxicity, (He et al., 1998; Boonsongrit et al., 2006) is employed as a model polymer in this study. Chi can efficiently condenses with plasmid DNA and can also increase permeability of macromolecules across gastrointestinal tract (Mayank & Bhavsar, 2007), thus making it an ideal vehicle for gene delivery and vaccines.

Carboxymethyl cellulose (CMC), is a negative charged polymer derived from cellulose. Polyelectrolyte complex can be formed by the electrostatic interaction between the -COOH group of CMC and the -NH₂ groups of chitosan (Anitha et al., 2009; Zhao et al.,

2009). In this study, we select CMC (Molecular weight 90k, Sigma) as the other model polymer. Chi was chosen to be the inner polymer layer, while CMC was selected to be the second layer of the multilayer polymeric nanoparticle to be synthesized by SAW atomization. We also employ Chi to form a third layer with CMC sandwiched between two layers of chitosan.

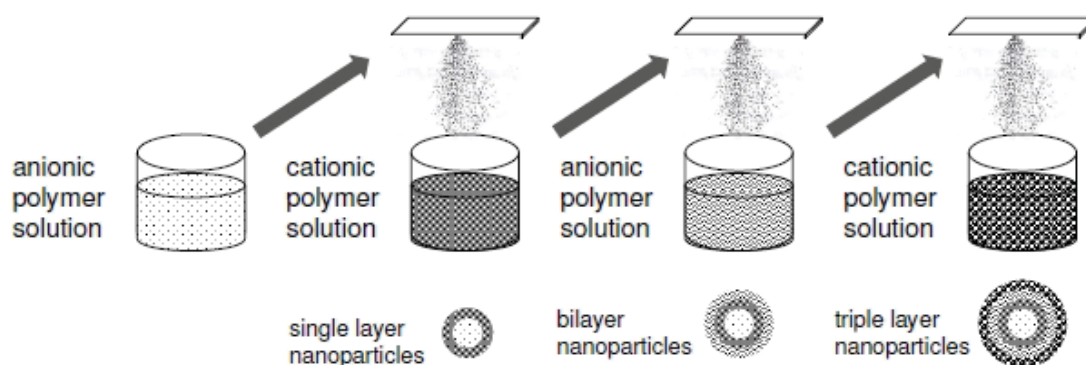


Fig. 3: Schematic diagram of multilayer nanoparticle preparation in layer-by-layer manner

Nano-aerosol atomization rate

In order to measure the amount of aerosol that our SAW microchip is capable of generating, we have set up a capillary flow meter apparatus as shown in Figure 4. The capillary flow meter consist of a glass tube that is marked at every 0.5cm with known inner diameter. We use a tissue paper embedded capillary tube as liquid delivery hose. One end of the wetted paper is placed upon the SAW microchip, while the other end is dipped in a fluid reservoir. A meniscus is formed between the paper and SAW microchip. The SAW wave draw liquid out from the paper as liquid on one end of the paper strip is consumed by atomization. The time for liquid to flow from one marker of the capillary tube to the consecutive marker was recorded, and the flow rate is calculated.

Particle characterization

In order to demonstrate the formation of bonding between polymeric layers, we characterize the properties of these LbL nanoparticles after each polymer atomization step using fourier transform spectroscopy (FTIR), size distribution and zeta-potential measurements. FTIR spectrum was employed to examine the chemical bonding between each polymer layer, thus providing evidence of polymer layers formation. Further evidence of the presence of polymer layering was obtained using zeta-potential measurements (Zetasizer Nano S, Malvern, UK). Particle size distribution was obtained using the Zetasizer Nano S (Malvern, UK). Particle size and morphology are further characterized using atomic force microscopy (AFM).

RESULTS AND DISCUSSION

The capacity the SAW microchip in terms of atomizing nano-size aerosol is measured as the flow rate of liquid being drawn by the SAW microchip during atomization. This

atomization rate is plot as a function of the input power for the SAW as shown in Fig 4. We observed that the atomization rate increases with increasing power, as expected given the larger energies delivered to the liquid to induce atomization by interfacial destabilization, this observation is in agreement with our earlier observations (Qi et al., 2009). The SAW microchip can generate aerosol up to $\sim 200 \mu\text{l}/\text{min}$ with a power supply as low as 4 W, despite the miniaturize size of the chip, indicating that SAW atomization is an efficient means to generate nano-size aerosol compare to conventional electro spraying (Tang & Gomez, 1995).

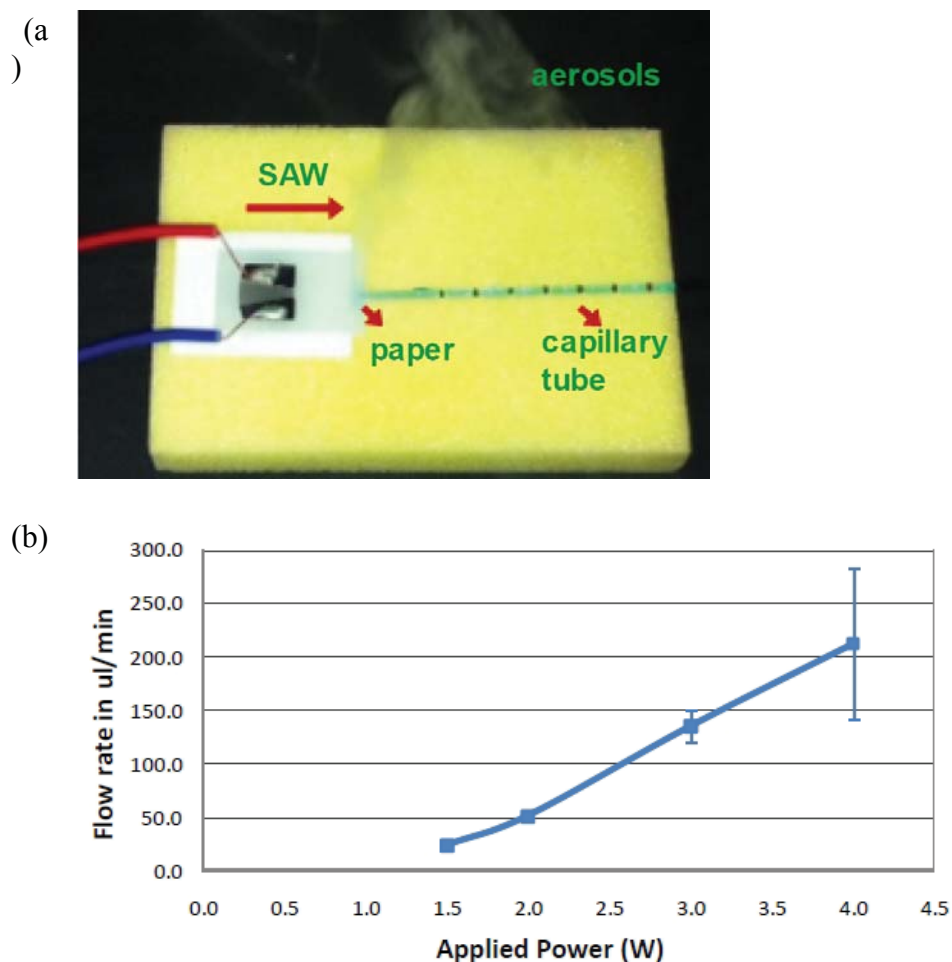


Fig. 4: (a) Photo of capillary flow meter set-up used to measure nano-aerosol atomization rate (b) Nano-aerosol atomization rate as a function of applied power. The trend line is included to aid visualization

Fourier transform spectroscopy (FTIR) was employed to examine the chemical bonding between each polymer layer, thus providing proof of the formation of the different polymer layers. Figure 5 shows the FTIR spectrum of polymeric particles. Curves 1 and 2 represent pure CMC and pure Chi molecules, respectively, while curves 3 and 4 show the varied spectrum of chitosan-CMC-chitosan triple-layer particle and chitosan-CMC double-layer particle, respectively. From curve 1, the bands at 1154 , 1058 , and 1026 cm^{-1} are corresponding to the polysaccharide skeletons of CMC. In Chi spectrum (curve

2), the characteristic bands at 1640 and 1558 cm^{-1} are assigned to the amide I and amide II, respectively. The bands at 1052 and 1020 cm^{-1} are the characteristic of the polysaccharide skeleton of Chi (Rosca et al., 2005). Clearly, curves 3 and 4 show characteristic spectrum different from those of Chi and CMC. The amide I band at 1640 cm^{-1} in the double layer and triple layer nanoparticles have shifted to 1660 and 1650 cm^{-1} , respectively, reflecting the interactions between the $-\text{COOH}$ groups of CMC and the $-\text{NH}_2$ groups of Chi. The shift in polysaccharide skeleton characteristic bands in the nanoparticles also suggested that ionic complexation between the Chi and CMC has successfully formed.

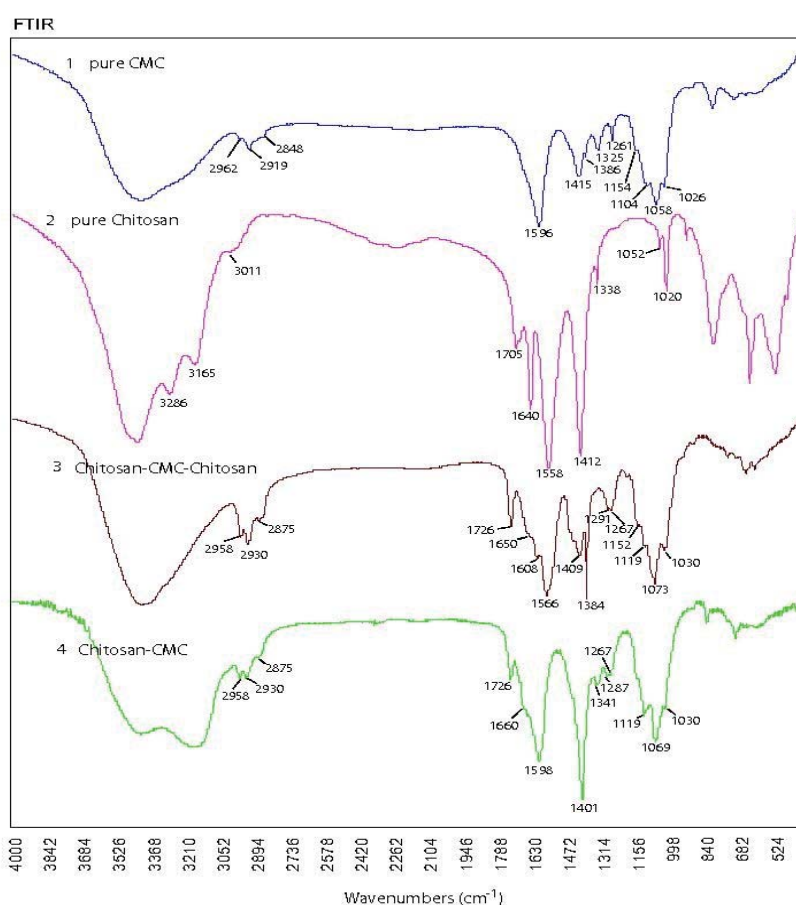


Fig. 5: FTIR spectrum of polymeric particles. Curves A and B are original CMC and chitosan samples, respectively. Curve C represents triple layer particles while curve D shows the spectrum of bilayer particles

Nano-sized particles are advantageous for a wide range of drug delivery administrations. We examined the size distribution of synthesized polymeric particles to see if the size obtained is in the required range, as shown in Fig. 6(a). Representative samples containing chitosan as the inner core and CMC as the outer layer exhibited a

hydrodynamic size of 198.2 ± 7.4 nm with narrow size distribution. As showed in Fig 6(b) AFM image, the nanoparticles exhibited oval shape, possibly due to the rigid and extended conformation of CMC. Particles with narrow size distribution offer various practical advantages compare to particle with similar average size but boarder size distribution such as better controlled drug release.

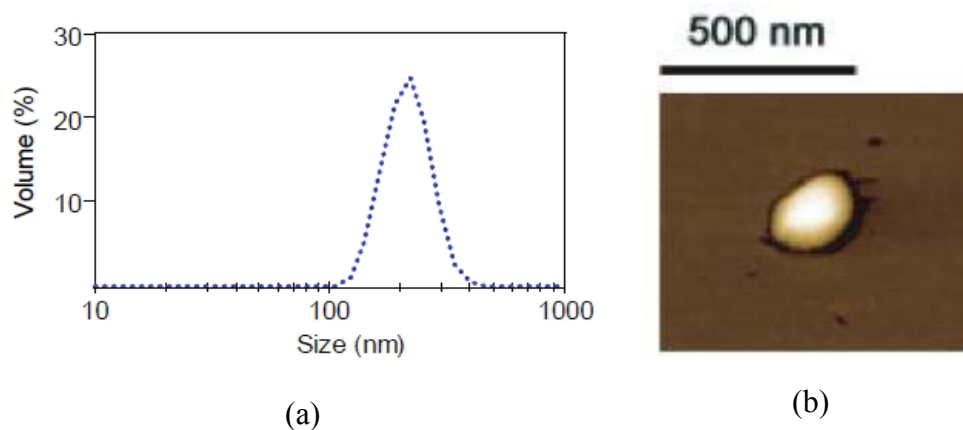


Fig. 6 (a) Particle size and size distribution, and (b) representative AFM image of nanoparticles generated by SAW microchip. The nanoparticles are composed of Chi core with CMC outer layer.

The variation of Zeta-potential of polymeric particle with different layers serves as another proof of bondings. Table 7 lists the change of zeta-potential after different polymeric layers was added on the nanoparticle by SAW atomization. Samples containing plasmid DNA exhibited negative charge due to the phosphate group present in each nucleotide. Nanoparticle containing DNA and Chi exhibited positive charge due to the present of positively charged Chi on the nanoparticle surface. Nanoparticle containing DNA/Chi core and CMC outer layer display negative charge due to the present of negatively charged CMC on the nanoparticle surface. The reversal of zeta potential is observed as the nanoparticle is further deposit into a complementary polymer solution, suggesting that a stepwise formation of layer on the nanoparticles.

Nanoparticle	Zeta potential (mV)
pDNA	-44.7 ± 3.2
pDNA/Chi	6.84 ± 4.0
pDNA/Chi/CMC	-18.2 ± 1.5
pDNA/Chi/CMC/Chi	38.5 ± 2.1

Tab.7: The zeta-potential of multilayer polymeric nanoparticles with Chi or CMC as outer layer

CONCLUSION

This study demonstrated using SAW atomization as a fast and efficient technique to synthesize multilayer polymeric nanoparticles for drug encapsulation usage. A serial of characterization have been conducted and shown the successful bonding between each polymeric layer. The size distribution obtained shows those synthesized multilayer

polymeric particles are in a narrow range (around 200 nm), which meets the requirement of many drug administrations (<1 μ m). Furthermore, unlike many conventional methods in producing polymeric particles, the usage of surfactant and templates are not required in SAW atomization. Compared to traditional spray drying methods, SAW atomization, driven at much higher frequency and lower power, has much less damage to drugs and vaccines, making it suitable for a wide range of drug deliveries and vaccines.

REFERENCES

- Alvarez, M., Friend, J., Yeo, L.Y., 2008, Rapid generation of protein aerosols and nanoparticles via surface acoustic wave atomization. *Nanotechnology* 19: 455103.
- Alvarez, M., Yeo, L. Y., Friend, J. R., and Jamriska, M., 2009. "Rapid production of protein-loaded biodegradable microparticles using surface acoustic waves". *Biomicrofluidics*, 3, p. 014102.
- Anitha, A., Rani, V. D., Krishna, R., Sreeja, V., Selvamurugan, N., Nair, S., Tamura, H., and Jayakumar, R., 2009. "Synthesis, characterization, cytotoxicity and antibacterial studies of chitosan, o-carboxymethyl and n,ocarboxymethyl chitosan nanoparticles". *Carbohydrate Polymers*, 78, pp. 672–677.
- Boonsongrit, Y., Mitrevej, A., and Mueller, B. W., 2006. "Chitosan drug binding by ionic interaction". *European Journal of Pharmaceutics and Biopharmaceutics*, 62, pp. 267–274.
- Cho, Y., Wang, X., Nie, Shuming, Chen, Z., Shin, D.M., "Therapeutic nanoparticles for drug delivery in cancer, *Clinical Cancer Research*, 14, pp 1310-1316.
- Fang, C., Shi, B., Pei, Y.-Y., Hong, M.-H., Wu, J., and Chen, H.-Z., 2006. "In vivo tumor targeting of tumor necrosis factor- α -loaded stealth nanoparticles: Effect of mepeg molecular weight and particle size". *European Journal of Pharmaceutical Sciences*, 27, pp. 27–36.
- Friend, J.R., Yeo, L.Y., Arifin, D.R., Mechler A., 2008, Evaporative self-assembly assisted synthesis of polymeric nanoparticles by surface acoustic wave atomization. *Nanotechnology*, 19, p145301.
- Gelperina, S., Kisich, K., Iseman, M.D., Heifets, L., The potential advantages of nanoparticles drug delivery systems in chemotherapy of tuberculosis, *American Journal of Respiratory and Critical Care Medicine*, 172, pp 1487-1490.
- He, P., Davis, S. S., and Illum, L., 1998. "Chitosan microspheres prepared by spray drying". *International journal of pharmaceutics*, 187, pp. 53–65.
- Hsieh, C., Balducci, A., and Doyle, P., 2007. "An experimental study of dna rotational relaxation time in nanoslits". *Macromolecules*, 40, pp. 5196–5205.
- Koziaraa, J. M., Lockmanb, P. R., Allenb, D. D., and Mumper, R. J., 2004. "Paclitaxel nanoparticles for the potential treatment of brain tumors". *Journal of controlled release*, 99, pp. 259–269.
- Kumar, M. N. V. R., ed., 2008. *Handbook of particular drug delivery*. American scientific publishers.
- Li, Y.-P., Pei, Y.-Y., Zhang, X.-Y., Gu, Z.-H., Zhou, Z.-H., Yuan, W.-F., Zhou, J.-J., Zhu, J.-H., and Gao, X.-J., 2001. "Pegylated plga nanoparticles as protein carriers: synthesis, preparation and biodistribution in rats". *Journal of controlled release*, 99, pp. 203–211.
- Mayank D Bhavsar, M. M. A., 2007. "Polymeric nanoand microparticle technologies for oral gene deliver". *Expert Opinion on Drug Delivery*, 4, pp. 197–213.
- Oxtoby, D., 1981. "Vibrational relaxation in liquids". *Annual Review of Physical Chemistry*, 32.
- Priest, C, Quinn, A., Postma, A., Zelikin, A. N., Ralston, J., and Caruso, F., 2008. "Microfluidic polymer multilayer adsorption on liquid crystal droplets for microcapsule synthesis". *Lab on a chip*, 8, pp. 2182–2187.
- Qi, A., Yeo, L., and Friend, J., 2008. "Interfacial destabilization and atomization driven by surface acoustic waves". *Physics of Fluids*, 20, p. 074103.
- Qi, A., Friend, J. R., and Yeo, L. Y., 2009. "Miniature inhalation therapy platform using surface acoustic wave microfluidic atomization". *Lab on a Chip*, 9, pp. 2184 –2193.
- Qi, A., Yeo, L., Friend, J., and Ho, J., 2010. "The extraction of liquid, protein molecules and yeast cells from paper through surface acoustic wave atomization". *Lab on a chip*, 10, pp. 470–476.
- Roney, C., Kulkarni, P., Arora, V., Antich, P., Bonte, F., Wu, A., Mallikarjuana, N., Manohar, S., Liang, H.-F., Kulkarni, A. R., Sung, H.-W., Sairam, M., and Aminabhavi, T. M., 2005. "Targeted nanoparticles for drug delivery through the bloodU" brain barrier for alzheimer's

- disease". *Journal of controlled release*, 108, pp. 193–214.
- Rosca, C., Popa, M. I., Lisa, G., and Chitanu, G. C., 2005. "Interaction of chitosan with natural or synthetic anionic polyelectrolytes. 1. the chitosanU" carboxymethylcellulose complex". *Carbohydrate Polymers*, 62, pp. 35–41.
- Tang, K., Gomez, A., 1995. "Generation of monodisperse water droplets from electrosprays in a corona-assisted cone-jet mode", *Journal of Colloid & Interface Science*, 175, pp326-332.
- Wong, E. H., 2009. "The development of a continuous encapsulation method in a microfluidic device". PhD thesis, The University of Queensland, Australia.
- Zhao, Q., Qian, J., An, Q., Gao, C., Gui, Z., and Jin, H., 2009. "Synthesis and characterization of soluble chitosan/sodium carboxymethyl cellulose polyelectrolyte complexes and the pervaporation dehydration of their homogeneous membranes". *Journal of Membrane Science*, 333, pp. 68–78.
- Zelikin, A. N., Li, Q., and Caruso, F., 2008. "Disulfidestabilized poly(methacrylic acid) capsules: Formation, cross-linking, and degradation behavior". *Chemistry of materials*, 20, pp. 2655–2661.

BRIEF BIOGRAPHY OF PRESENTER

Dr Peggy Chan received degree in bioprocess engineering, and Ph.D. in chemical engineering from University of New South Wales, Australia. Later she worked as a post-doctoral fellow in the drug & gene delivery group at Institute of Bioengineering & Nanotechnology, A-Star Singapore. She was actively participated in developing nano-biomaterials for gene, siRNA and drug delivery. Later she was promoted to research scientist. Her research activities include developing novel injectable hydrogels for therapeutic protein delivery and tissue engineering applications. Some of these researches have gained considerable attention for their novelties, which were reported in top journals and patent application. Dr Chan works as a Lecturer at Department of Chemical Engineering, Monash University since March 2009. Her recent research interests are in the microfluidic biomaterials area, particularly in the development of microengineered scaffold and microfluidic synthesized biomaterials for drug delivery.

Appendix E

A Portable Delivery System for Nano-Engineered Cargo Carrying Genetic Immuno-Therapeutics Driven by Surface Acoustic Wave Devices

Rajapaksa, A. E., Ho, J., Qi, A., Yeo, L.Y., Friend J.

Chemeca 2010


Adelaide, Australia

September 2010

A PORTABLE DELIVERY SYSTEM FOR NANO-ENGINEERED CARGO CARRYING GENETIC IMMUNO-THERAPEUTICS DRIVEN BY SURFACE ACOUSTIC WAVE DEVICES

Anushi Rajapaksa¹, Jenny Ho, Aisha Qi, Leslie Yeo, James Friend

¹ Department of Chemical Engineering
Monash University
Clayton, VIC 3800



ABSTRACT

Vaccination is regarded as the key intervention for emerging diseases such as influenza. Currently, the preventive bottleneck is primarily due to the lack of facilities to create and deliver suitable vaccines. Several features of DNA vaccines make them more attractive than conventional vaccines; thus, DNA vaccines have gained global interest for a variety of applications. However, several limitations such as ineffective cellular uptake and intracellular delivery, and degradation of DNA need to be overcome before clinical applications. In this study, a novel and scalable engineered technique has been developed to create a biodegradable polymer system, which enables controlled delivery of a well designed DNA vaccine as an immunotherapeutic. Surface Acoustic Wave (SAW) atomisation has been found as useful mechanism for atomising fluid samples for medical and industrial devices. Using surface acoustic waves at 8-150 MHz, post-atomisation bursting and sub-micron droplet formation were observed. A straightforward and rapid method for synthesis of un-agglomerated biodegradable nanoparticles (< 250 nm) in the absence of organic solvents would represent a major processing breakthrough for drug or biopharmaceutical encapsulation and delivery. Nanoscale polymer particles for DNA vaccines delivery were obtained through an evaporative process of the initial aerosol created by SAW, the final size of which could be controlled by modifying the initial polymer concentration and solid contents. In summary, SAW atomiser represent a promising alternative for the development of a low power device for producing nano-engineered cargo with a controlled and narrow size distribution as delivery system for genetic immuno-therapeutics.

Keywords: DNA vaccine, Influenza, Poly(D,L-lactide-*co*-glycolide) polymer, Surface Acoustic Wave Atomisation.

INTRODUCTION

The recent influenza A (H1N1) vaccine shortages have provided a timely reminder of the tenuous nature of the world's vaccine supply. The lack of vaccine to combat this virus, and the widespread of this virus throughout 74 countries and infected nearly 30000 people in less than two months time has rendered World Health Organization (WHO) to declare the first global flu pandemic in 41 years. The vaccines landscape is becoming much different now than it was compared to few years back. With increasing public awareness about preventive healthcare and increased spending by governments for the vaccination program, has put the spotlight on the vaccines. Moreover, the

success of a number of blockbuster products has changed dramatically the market place of vaccine; the worldwide vaccine market has registered revenue of US\$ 21 Billion in 2008(Renub Research, 2009).

Vaccination is the principal measure for preventing influenza and reducing the impact of pandemics; however, vaccines take up to 8–9 months to produce, and the global production capacity is woefully low. The application of new technologies such as gene-based vaccines and novel delivery systems represent promising approaches to creating safer and more potent vaccines. With production times as short as 2 weeks, improved safety and stability, and the ability to perform numerous therapeutic roles, DNA vaccines have the potential to meet the demands of emerging and existing diseases. As a consequence, more people will have faster access to more effective vaccines against a broader spectrum of infectious diseases especially the virus which can be deadly and mutate into a more frightening form easily. Thus DNA vaccine research has experienced a sharp growth in demand as indicated by its use in gene therapy trials and DNA vaccine related patents.

Nevertheless, the transfection efficiency of DNA vaccines is relatively low when compared to other vectors such as viruses, viral-like particles and cellular vectors. This is because, after administration, naked DNA molecules is susceptible to degradation by serum enzymes such as endonucleases, thereby reducing the amount of DNA that is available in hosts to express antigen gene. Thus, improved DNA delivery strategies are needed. At present, DNA-based vaccine deliveries in preclinical and clinical animal studies are achieved by using physical (e.g. injection, gene gun, electroporation or aerosol delivery), chemical (e.g. cationic lipid or polymer condensing agents) and biological (e.g. use of the cellular transport mechanism) approaches (Montgomery et al., 1997, Patil et al., 2005). The immune response associated with DNA vaccination is influenced by the site and mode of immunisation. Various routes of administration and different types of carriers such as liposomes, biodegradable polymeric particles, hydrogel, inorganic nanoparticles have been evaluated based on their ability to improve the efficiency of DNA vaccines (Nguyen et al., 2009). Advantages for using these delivery systems include increased safety, acceptability and treatment compliance; increased efficacy linked to a broader tissue distribution of the antigen; ease of use leading to self-administration; and administration of smaller doses of the antigen.

Polymeric nanoparticles are critical to a wide range of emerging applications, including *in-vivo* drug and gene delivery, and immunodiagnostics. A reliable, reproducible and efficient production method for synthesizing polymeric nanoparticles below 250 nm, however, has yet to be devised. The conventional techniques currently employed, which include solvent evaporation/extraction, spray drying, and nanoprecipitation typically require multi-step procedures, the use of a considerable amount of solvent, and often result in a wide distribution of particle sizes. The formulation of DNA in polymeric materials has proven to be a very effective strategy for passively targeting vaccines to pro-Antigen Presenting Cells (APC) and protects DNA from nuclease degradation. The polymeric system also provides a method of controlling release rates of DNA, which may be important for timing immune responses by coordinating dendritic cells migration to lymph nodes, maturation, and presentation of costimulatory molecules, peak gene expression, and antigen presentation. Significant efforts have been made to improve polymeric formulations for DNA vaccination by changing polymer physical

chemistry (molecular weight, hydrophilicity), methods of formulation, and addition of secondary materials such as cationic transfection agents.

In this work we demonstrate the use of surface acoustic wave (SAW) atomization together with a non-uniform evaporation and nucleation process to give monodisperse nanoparticles (Fig. 1). SAW atomization is a straightforward and energy efficient technique to generate relatively homogeneous particle size distributions that can be carried out on a chip-scale microdevice for portable drug delivery applications or scaled up for industrial production. It provides direct control over the size of the particles through adjustment of the operating frequency of the ultrasonic vibration and physical characteristics of fluid (viscosity and surface tension) (Qi et al., 2008). The droplet size can be estimated by using Equation (1) (Qi et al., 2008). We will use this technology to create biodegradable nanoparticles with narrow size distribution for DNA delivery.

$$D_{drop} \propto \lambda \approx \frac{\gamma R}{\mu} \quad (1) ,$$

where λ : capillary wave wavelength; μ : fluid viscosity; γ : surface tension; R: characteristic film or drop dimension

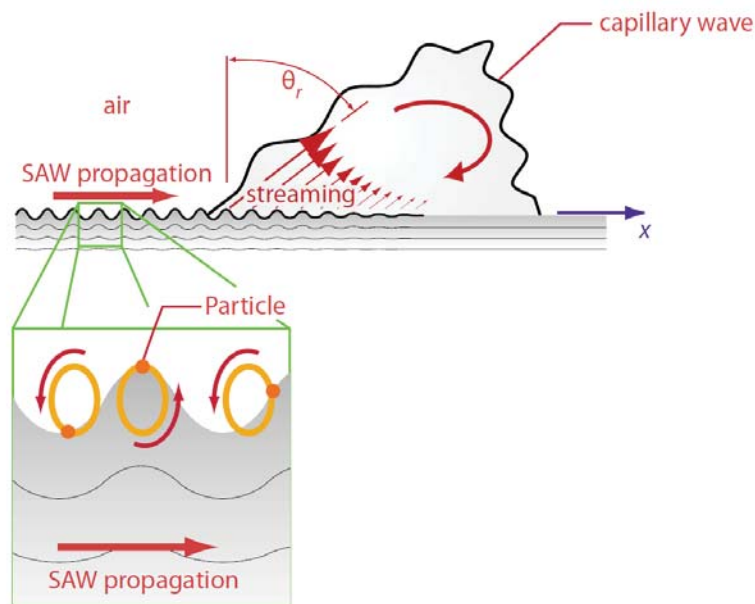


Fig. 1: Interaction of the SAW with a fluid drop causes the drop to deform into asymmetric conical shape leaning roughly at an angle corresponding to the Rayleigh angle θ_R ; and the elliptical trajectory of the particle elements on the surface as the SAW Rayleigh wave traverses the surface. Atomization of the liquid occurs from the free surface of the irradiated drop (Qi et al., 2008).

METHODOLOGY

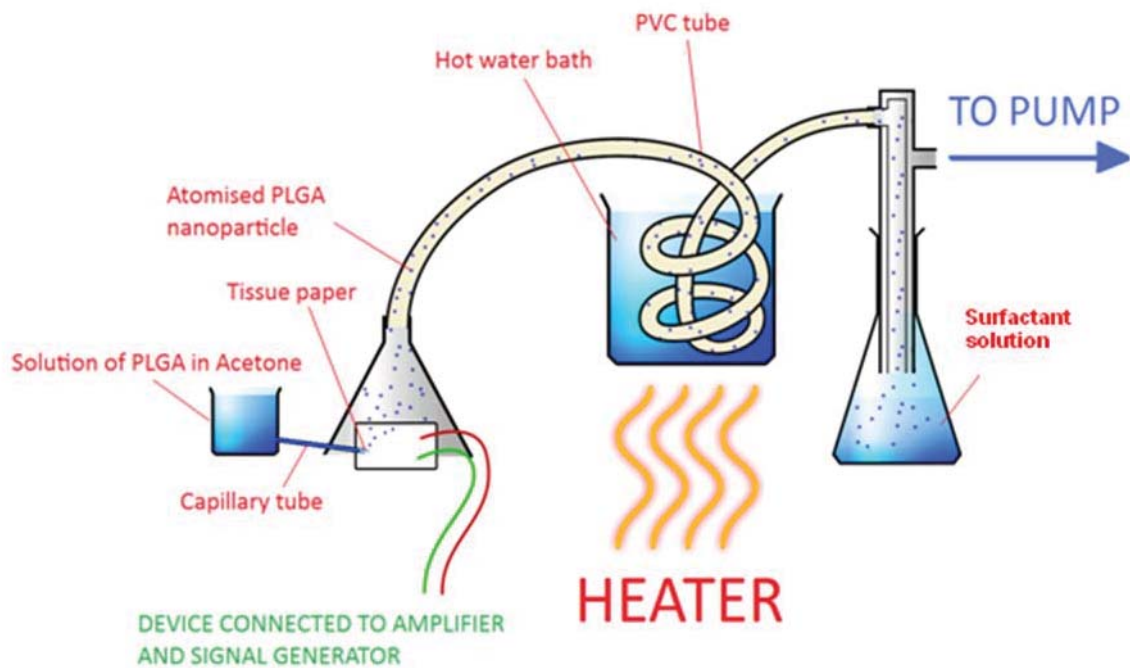


Fig. 2: Schematic representation of the nanoparticles generation system used in the study.

The polymeric solution was prepared by dissolving poly(D,L-lactide-*co*-glycolide) 50:50 (PLGA, Sigma-Aldrich), molecular weight (MW) 15000 Da in acetone (99.5%, LabScan) to create feedstock solution of PLGA at several % w/v (Tab. 1). The polymer solution feedstock was pumped onto the surface of low loss piezoelectric material lithium niobate (LiNbO₃ or LN). When a sinusoidal electrical signal is transmitted across the interdigital transducer (IDT), a SAW is generated perpendicular to the fingers' long axis and along the x axis of the substrate from both apertures (sides) of the IDT. The interaction of the SAW with the polymer solution causes acoustic streaming and sub-harmonic capillary wave to generate. When the acoustic stress exceeds the capillary stress, destabilization of the polymer solution surface causes atomisation which creates fine continuous droplets. The particles atomised via SAW are subsequently dried, drawn via a pump, through a 3m long PVC tube immersed in a hot water bath water held at temperatures of 40-50°C. Size distribution of the nanoparticles were determined using a Malvern Zetasizer Nano ZS series (ZEN 3600). The measurement values were analyzed by using the system software (Dispersion Technology Software, version 4.20, Malvern Instruments Ltd.) and their morphology studied using Scanning Electron Microscopy (SEM) using a JOEL 7001F field emission electron microscope (Monash Centre for Electron Microscopy) operated an accelerating voltage of 30KV.

RESULTS AND DISCUSSION

In this study, the polymer concentrations in the range of 0.25 – 1.0% (w/v) have been studied for their effect on the nanoparticles. The physical properties of PLGA in acetone are reported in Tab. 1. The increase in the solid content of polymer solution affected the

size distribution as seen in Fig. 3; the size distribution shifted to a larger size range when the polymer concentration was changed from 0.25% to 1%. Although viscosity of polymer solution increases with an increase in solid content, according to Equation (1) the droplet size should be smaller. However, the solid content was the determine factor when we collected the nanoparticles in collection fluid, where the acetone evaporated and polymer hardened. This is possibly due to the curling of the branches of the polymer around the core (Fig. 4) of the spherical particles (confirmed using SEM imaging also shown in Fig. 5) during the drying process. In addition to this observation, concentration of surfactant, poly(vinyl alcohol) (PVA, MW = 50000), was studied for its effect on the size distribution of hardened nanoparticles. As shown in Fig. 6, the 4% PVA give better and narrower size distribution as compared to 0.5% PVA since imparts better stability for nanoemulsions.

Tab. 1: Properties of poly(D,L-lactide-*co*-glycolide) in acetone

PLGA (% w/v) in acetone	Density (kg m ⁻³)	Surface tension, γ^a (N m ⁻¹)	Viscosity, η^b (Pa·s)
0.25	761.8	0.0238	3.31
0.5	780.9	0.0252	3.42
1.0	797.7	0.0260	3.53

^a Surface tension was measured via the capillary rise method at ambient conditions (T=23°C).

^b Viscosity was measured using a glass capillary viscometer at 20°C.

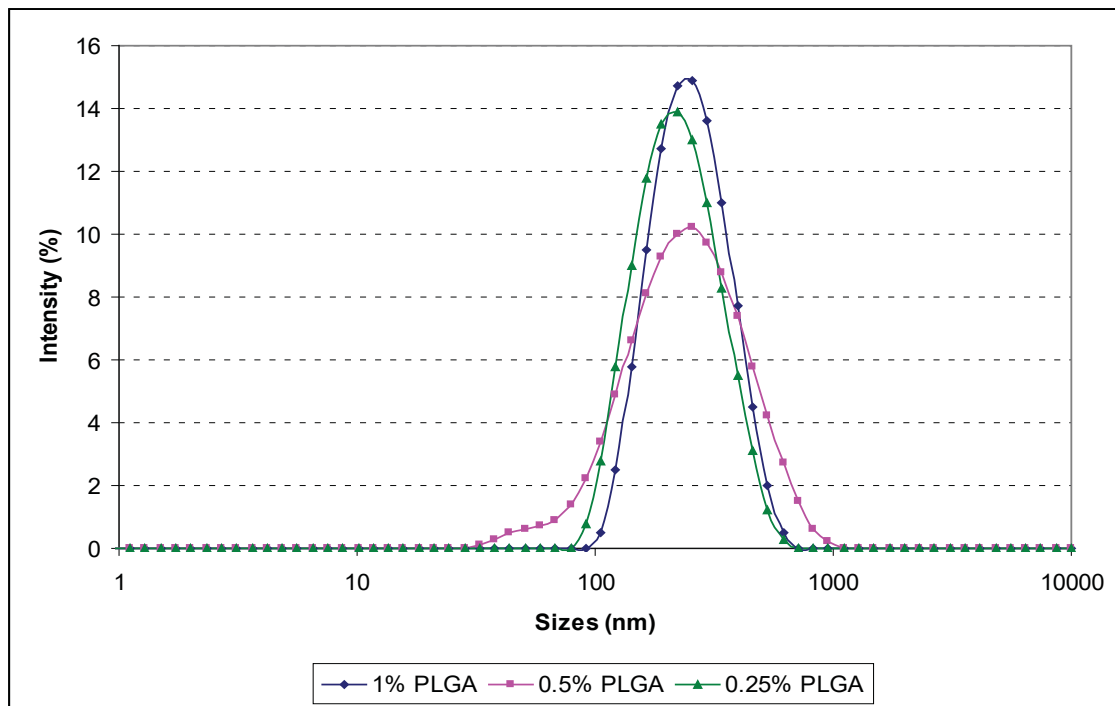


Fig. 3: Size distributions of PLGA nanoparticles produced with different %w/v and collected in collection fluid with 0.5% PVA as surfactant.

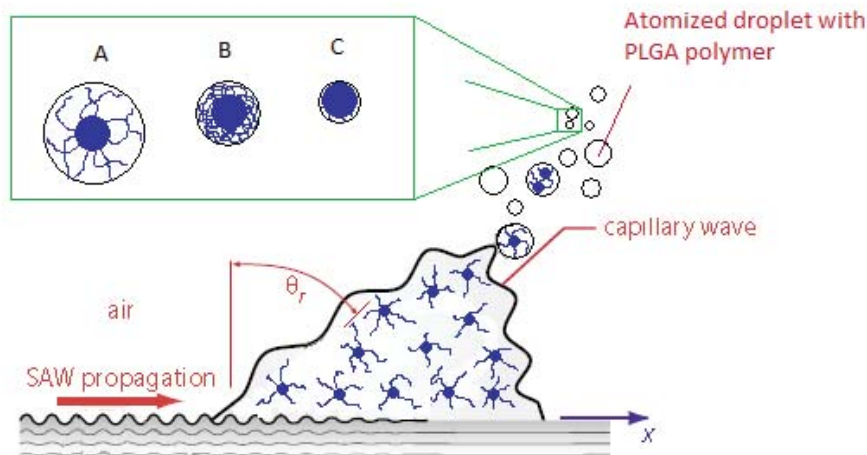


Fig. 4: A schematic representation of a solution containing PLGA (50/50) polymer being atomized by the surface acoustic waves. The schematic of droplet A showing an atomized particle containing a polymer of PLGA. As the droplet dries, the acetone evaporates and the branches of the polymer curl in around the core in B. The size of the resulting nanoparticle in C can be fine-tuned by varying the concentration of the original solution.

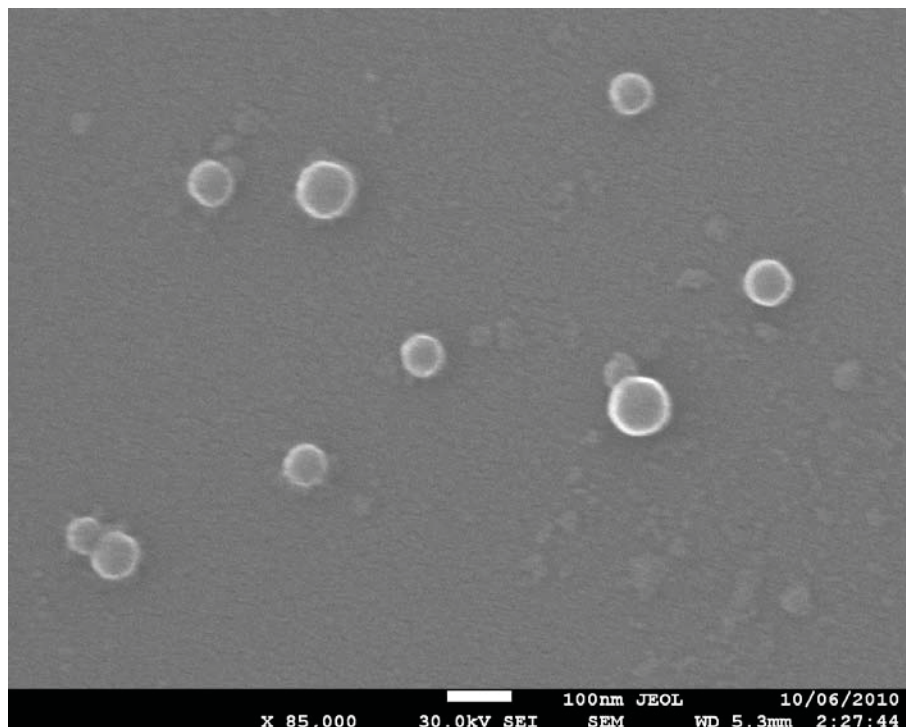


Fig.5: Scanning Electron Microscopic images showing spherical morphology of PLGA nanoparticles, collected in surfactant that were atomised via Surface Acoustic Waves.

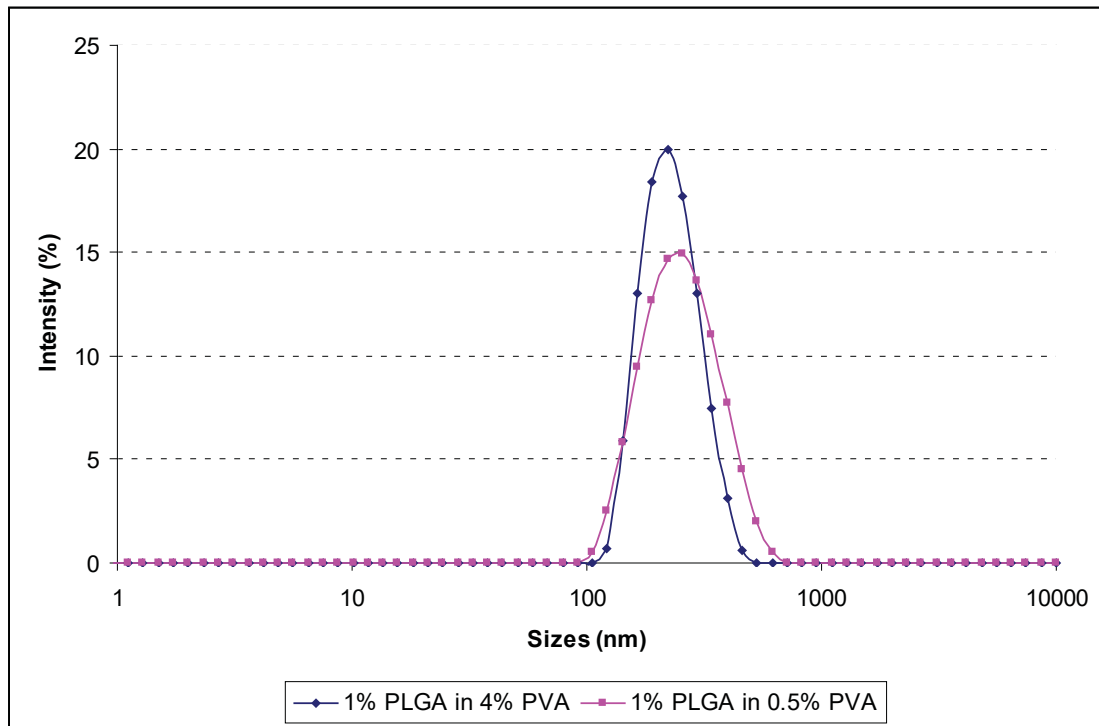


Fig. 6: Size distributions of PLGA nanoparticles in different concentrations of surfactant, poly(vinyl alcohol) (PVA, MW = 50000 Da) in collection fluid.

CONCLUSIONS

A reliable method to generate biodegradable polymer nanoparticles has been described, and relative to most other generation methods, this method is simple and straight forward. Suitable size ranges of nanoparticles have been obtained for usage in DNA delivery with further functionalization.

REFERENCES

- MONTGOMERY, D. L., ULMER, J. B., DONNELLY, J. J. & LIU, M. A. (1997) DNA vaccines. *Pharmacology & Therapeutics*, 74, 195-205.
- NGUYEN, D. N., GREEN, J. J., CHAN, J. M., LONGER, R. & ANDERSON, D. G. (2009) Polymeric Materials for Gene Delivery and DNA Vaccination. *Advanced Materials*, 21, 847-867.
- PATIL, S. D., RHODES, D. G. & BURGESS, D. J. (2005) DNA-based therapeutics and DNA delivery systems: A comprehensive review. *AAPS Journal*, 7, E61-E77.
- QI, A., YEO, L. Y. & FRIEND, J. R. (2008) Interfacial destabilization and atomization driven by surface acoustic waves. *Physics of Fluids*, 20.

RENUB RESEARCH (2009) World Vaccines Market 2008-2013: Future Forecast, Critical Trends and Developments. 1 ed., Renub Research Pvt. Ltd.

BRIEF BIOGRAPHY OF AUTHOR

Anushi Rajapaksa is a postgraduate student in the Department of Mechanical and Aerospace Engineering pursuing a PHD and is co-supervised by Prof. James Friend, Assoc. Prof. Leslie Yeo. She works at both the Micro/Nanophysics Research Laboratory (MNRL) and also at the Coppel Lab (Department of Microbiology) at Monash University, Australia. She completed her undergraduate studies in Electrical and Computer Systems Engineering from Monash University, Clayton in 2008, for which she was awarded first class honours and received acknowledgments from the Dean of Engineering of Monash University in 2006 & 2007 for outstanding academic achievements. Anushi was the recipient of the prestigious MGS (Monash Graduate Scholarship) and the MIPRS (Monash International Postgraduate Research Scholarship) to pursue her PHD studies and received student award for “Outstanding Research Contribution” at Monash Research Month in 2009.

Appendix F

Optimised Surface Acoustic Wave Atomisation via Amplitude Modulation

Rajapaksa, A. E., Qi, A., Chan, P., Yeo, L.Y., Friend, J.

Smart Nano-Micro Materials and Devices - SPIE 2011

Melbourne, Australia

December 2011

Optimised surface acoustic wave atomisation via amplitude modulation

Anushi Rajapaksa, Aisha Qi, Peggy Chan, James Friend, and Leslie Yeo
MicroNanophysics Research Laboratory, Monash University, Clayton, VIC 3800, Australia.

ABSTRACT

A miniaturized portable nebulizer platform has its distinct advantages in the current pulmonary drug delivery market for the treatments of both respiratory and non-respiratory conditions. An efficient hand-held nebulizer system also requires the optimization of the usage of available power systems in the simplest manner. Amplitude modulation (AM) is presented as a simple yet effective means for optimising the power requirement for a microfluidic nebulizer driven by surface acoustic waves (SAW). The effect of the AM on shear-sensitive biomolecules are shown to be minimal. Energy savings of around 40% can be obtained with more efficient atomisation achieved with AM less than 10 kHz. Together with these advantages, AM having little effect of the mean aerosol diameter, particularly important when therapies are to be targeted for the deep lung regions, holds great promise for its use in the SAW nebulizers for non-invasive inhalation therapy.

Keywords: Amplitude modulation, surface acoustic wave, atomisation

1. INTRODUCTION

Inhalation therapy represents a highly sort after means for the non-invasive treatment of lung diseases such as asthma, COPD, and cystic fibrosis and influenza due to reasons such large surface area offered by the lung that is lined by a thin epithelium being highly vascularised for the fast absorption of the drugs involved in the treatments^{1,2}

More recent developments in the miniature chip-based microfluidic nebulization platforms for inhalation therapy, offers several advantages compared to the conventional nebulizers.³ The microfabricated nebulizers can be designed such that the dimensions of the features are easily adjustable, whereas conventional nebulizers are mostly limited to the available tubing size.⁴ Additionally, the nebulizer chip can be mass produced allowing low cost of production. Most conventional nebulizers require time consuming and cumbersome assembly whereas nebulizer chips more convenient to use.⁵

A novel microfluidic based platform for the delivery of pulmonary drug therapies such as plasmid DNA based vaccines,⁶ proteins and other biomolecules^{3,7} has been recently developed using surface acoustic wave (SAW) nebulization. The SAW waves are an efficient method of transferring energy (1–3 W) into a fluid since they are MHz to GHz-order, transverse-axial polarized elliptical electroacoustic waves (displacement amplitudes of few nanometers) that are confined to a low-loss piezoelectric material (in this case single-crystal lithium niobate (LiNbO₃)) housing the fluid. The SAW waves generated by a sinusoidal electric field between the interlaced fingers of an interdigital transducer (IDT) electrode where the wave interaction with the fluid causes destabilization of the interface of the parent liquid volume containing the drug solution by overcoming the capillary stress to produce sub micron order aerosols within the optimum respirable size range (1–5 μ m) necessary for deep lung delivery.^{8–10}

Importantly, cavitation damage is largely absent during SAW nebulization when compared to conventional ultrasonic nebulizers that employ operational frequencies that range from 10 kHz–1 MHz. On the other hand, SAW devices operate at much high frequencies (of the 10–100 MHz order) the shear damage to the drug molecules is minimal since the period of the induced vibrations is much shorter than the molecular relaxation time scale associated with large molecules in liquids.^{11,12}

Moreover, the high lung delivery efficiencies attributed with SAW technology, demonstrated previously when a short-acting β 2-agonist salbutamol was nebulized, a successful respirable fraction greater than 70%, which far exceeds the typical 30–40% lung dose obtained through current nebulisation technology, thus proves the ability to precisely manipulate the droplet size and flow rate for deep lung delivery.³

Despite these attractive advantages, the bulky nature of power systems that drive the microfluidic devices including the SAW devices, largely attributed to the battery systems that occupy significant fractions of both mass and volume of the entire device somewhat retards their place in the current inhalation therapy market.¹³ Thus the resulting need for efficient power generation methods to enable portability has led to the investigation of optimization of the usage of available power systems.

Previously, modifications to the design such as adding a beam compressor, which consisted of a horn and a waveguide, was shown to be effective at reducing the required driving power by three times to achieve continuous wave atomisation with a comparable SAW nebulizer. However, the performance was dependent on the pump gap which is difficult to manage if the device was desirably made portable.

Modification of the input power signal represents an effective yet simple means of achieving improved power efficiencies. Pulse width modulation (PWM) at 1 kHz, where switching the signal on and off for a short period has been used to optimise the power delivered to a comparable SAW device.¹⁴ However, naturally PWM does not prove useful for optimization of sinusoidal signals.

In such a case, Amplitude modulation (AM) lends itself useful since the technique is already widely used in radio communication applications where the sinusoidal radio-frequency signal is modulated by an audio-frequency signal before transmission. The power of the transmitting signal is thus concentrated at the carrier frequency, and hence presents an useful means of power optimization. During the application of AM to SAW nebulization, it is important to appreciate that the aerosol generation mechanism in SAW atomisation is due to the capillary-viscous damping of the atomising fluid. As a result, the resonant frequency of the capillary wave will usually be in the order of 1–10 kHz.¹⁵ Therefore, if a carrier signal at the resonant capillary frequency level can be introduced into the driving signal of SAW, we expect to have the acoustic energy to be concentrated and subsequently cause more efficient SAW atomisation.

2. EXPERIMENTS AND MATERIALS

Here, we used the focused 30 MHz SAW device in our experiments. This device consists of a low-loss piezoelectric material, 127.86° *Y-X*-rotated single-crystal lithium niobate (LiNbO_3), sputtered with chromium-aluminum Single-Phase Uni-Directional Transducers (SPUDT) via standard UV photolithography processes.¹⁶ The curved shape of the transducers enhances the acoustic energy at the focal point at which point we place the liquid for optimal energy delivery. Images of a SAW atomizer and the SPUDT electrodes layout can be seen in Fig. 1(a) and (b).

Regarding the liquid supply, we employed a paper-wick embedded capillary tube as an automatic liquid delivery system.⁷ Specifically, when a wet paper is placed on the SAW device, a meniscus is formed between the paper and SAW device substrate. It is then the *Schlichting* streaming (or boundary layer streaming),^{17,18} that causes the SAW wave to pull the liquid out of the paper for continuous atomisation, as shown in Fig. 1(c). As at one end of the paper strip, the liquid is being consumed to cause atomisation, at the other end of the paper will be able to draw the liquid from the capillary tube that connects to the fluid reservoir. In such case, the flow rate in the capillary tube can be approximately considered as the atomisation rate.

Following experiments were performed in order to study the effect of amplitude modulation (AM) on SAW atomisation.

Effect of AM on the Rate of atomisation In this study, we used deionized water as the model fluid. The capillary tube was marked at every 0.5 cm and the time was recorded for the flow of water between two consecutive markers, as shown in Fig. 1(a). Experiments were repeated three times at each sample modulation frequencies, which were chosen as 500 Hz, 1 kHz, 5 kHz, 10 kHz, 20 kHz and 40 kHz sinusoidal signals, respectively. As the purpose of using AM is to achieve efficient atomisation while consuming less energy, therefore, with AM, the power input was kept at low levels (*eg.* 1.5 W and 2 W). In comparison with the experiments that were conducted for the observation the atomisation rate without the application of AM, applied power levels of 1.5 W, 2 W, 3 W and 4 W were investigated.

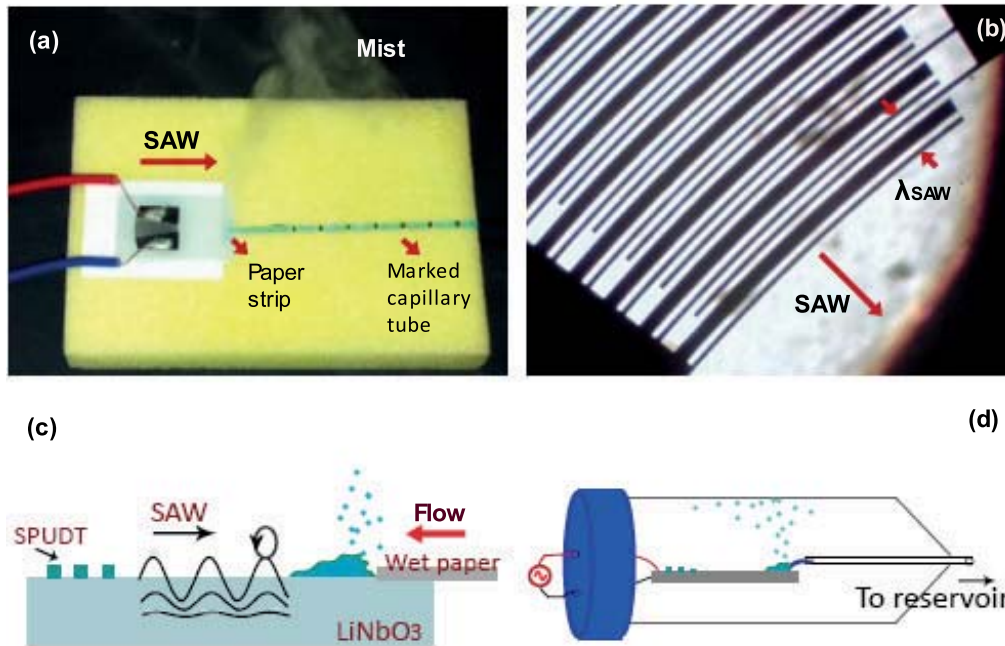


Figure 1. (a) Image of a working 30 MHz SPUDT SAW device with a paper strip embedded capillary tube as an automatic liquid delivery system. In order to record the flow rate, the capillary tube was marked at every 0.5 cm. (b) is the enlarged SPUDT electrodes layout captured under microscope. λ_{SAW} representing the SAW wavelength, for a 30 MHz device, $\lambda_{SAW}=132 \mu\text{m}$. (c) is the illustration of the SAW atomisation occurring on a liquid film which is formed at the tip of a wet paper strip. (d) shows the atomisation of pDNA and the antibody in a confined area. Aerosols condense on the wall and be collected subsequently.

Effect of AM modulation on Aerosol Size Distribution The aerosol size distributions of the DI water droplets were measured via the laser diffraction based Spraytec (Malvern Instruments, UK) for measurement covering the desired 1-10 μm range for pulmonary delivery. In order to characterise the aerosol size distribution, D_{v50} (volume median diameter, representing the 50th percentile of volume size distribution) was recorded during the measurements.

SAW atomisation, which operates at high frequency (>10 MHz), was previously demonstrated to be safe platform for delivering many biomolecules compared other atomisation methods,^{6,7} including shear-sensitive plasmid DNA molecules. As the modulation frequency is at a much lower range, 0.5–40 kHz, its effects when delivering biomolecules are therefore needed to be investigated. We choose the rabbit anti-YFP antiserum solution (diluted at 1:20) molecule as a model drug. Specifically, atomisation was performed in a confined area, a 50 ml conical Falcon tube (BD Bioscience, USA), as shown in Fig. 1(d). The antibody was then detected using dot blot analysed when $5\mu\text{l}$ of YFP protein solution was dotted onto PolyScreen PVDF transfer membrane for immunoblotting. The membranes were incubated in TBS/T (0.05M Tris-HCl pH 7.4, 0.15M NaCl, 0.05% Tween 20) containing 5% non-fat milk powder overnight at 4° . Subsequently, the membranes were probed with the atomised anti-YFP antiserum solutions for 1 h at room temperature, and washed three times in TBS/T for 10 min each time. Primary antibody reactivity to immunoblotted proteins was detected with anti-rabbit immunoglobulin conjugated to horse radish peroxidase (HRP) (Silenus Laboratories). The HRP was visualized by Renaissance Western Blot Chemiluminescence Reagent (NEN Life Science Products, PerkinElmer, Massachusetts, USA).

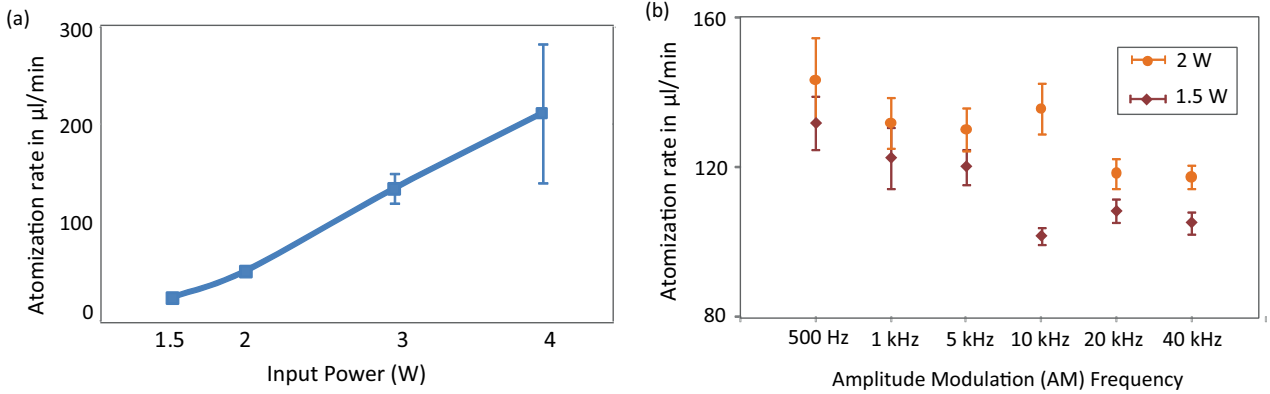


Figure 2. (a) atomisation without AM with input power of 1.5 W, 2 W, 3 W and 4 W. (b) atomisation at 1.5 W and 2 W, with AM at 500 Hz, 1 kHz, 5 kHz, 10 kHz, 20 kHz and 40 kHz, respectively.

3. RESULTS AND DISCUSSION

3.1 Comparison of atomisation rate

Figure 2 shows the SAW atomisation rate at each power level, with and without the application of AM. In order to maximise the atomisation efficiency whilst consuming less power, AM was only carried out at relatively low power levels (1.5 W and 2 W). As shown in Fig. 2(a), with limited power input (1.5 W and 2 W), the atomisation rates are only $23.4 \pm 2.1 \mu\text{l}/\text{min}$ $50.8 \pm 2.2 \mu\text{l}/\text{min}$, while as shown in Fig. 2(b), the atomisation rate was impressively optimised with the effect of AM. In general, with AM, the atomisation at 1.5 W and 2 W are approximately at the same level of atomisation with 2.5 W and 3 W power input, respectively, suggesting the energy is saved by nearly 40%. Specifically, more efficient atomisation was achieved with AM less than 10 kHz. We believe that this is due to the SAW atomisation mechanism. SAW atomisation, although operating at very high frequencies (10 MHz), is indeed the result of capillary-viscous damping. The capillary frequency of a thin water film, at which the capillary wave is destabilized, is in the order of 1–10 kHz.¹⁵ Hence, AM at lower frequencies clearly improves the atomisation effect by magnifying the capillary resonances.

3.2 Comparison of Aerosol size

The formation of aerosol occurs as a result of capillary-viscous damping^{19,20} and the aerosol size D is therefore governed by $D \sim \lambda \sim \frac{\gamma H^2}{\mu f_c L^2}$, where γ and μ are the surface tension and viscosity of the fluid being nebulized, f_c is the resonant capillary frequency which usually in the order of 1–10 kHz. H/L is the characteristic length scale of the drop/film on the SAW device substrate for atomisation.¹⁵ We do not expect that the capillary break-up mechanism will be changed through the introduction of an AM signal, whereas the only effect would be to concentrate the transmitting energy at the carrier frequency (*eg.* 1–10 kHz).

As shown in the above equation, for a certain type of fluids, *eg.* water in our case, the difference of aerosol size is a result of variant characteristic length scale of the water drop/film being nebulized. Generally, at relatively higher power level, the fluids can be moved to the edge of the device and form a conical shaped drop, resulting in a large H/L ratio and hence larger aerosol size; while at lower power levels, the fluid is more likely to spread out into a film with smaller H/L ratio and hence a smaller aerosol size would be obtained.^{3,15} This is consistent with the result in Tab. 1., with no AM, aerosol size distribution is obviously smaller at lower power level (1.5–2 W), compared to those obtained at the relatively higher power levels (> 3 W).

Since AM at low power magnifies the capillary resonances by concentrating the acoustic energy at, or near the resonant frequencies, the atomising fluid is expected to experience a more powerful excitation, similar to the effects observed when a higher power input is applied. Therefore, we expect the aerosol size to have a slight increase in size, as shown in Tab. 1. More specifically, when comparing these results to the observations in Fig. 2, AM at 500 Hz–10 kHz presents a higher flow rate, suggesting a stronger atomisation, which is interestingly consistent with relatively larger aerosol size distribution observed in Tab. 1. Moreover, effects of 40 kHz AM for either 1.5 W or 2 W are the least and the aerosol sizes are hence the smallest.

Input power (W)	Frequency of AM applied	D ₅₀ /μm
1.5	none	7.29 ± 0.90
2	none	8.53 ± 1.06
3	none	10.51 ± 1.09
4	none	10.18 ± 0.70
2	500 Hz	9.69 ± 1.38
	1 kHz	11.25 ± 0.61
	5 kHz	9.15 ± 0.53
	10 kHz	9.01 ± 1.36
	20 kHz	8.13 ± 0.10
	40 kHz	7.80 ± 0.34
1.5	500 Hz	9.75 ± 1.89
	1 kHz	8.55 ± 0.72
	5 kHz	7.94 ± 0.08
	10 kHz	8.63 ± 0.89
	20 kHz	8.32 ± 0.15
	40 kHz	7.76 ± 0.21

Table 1. Aerosol droplet diameter from the nebulization without AM with input power of 1.5 W, 2 W, 3 W and 4 W and nebulisation at 1.5 W and 2 W, with AM at 500 Hz, 1 kHz, 5 kHz, 10 kHz, 20 kHz and 40 kHz. Note that for every setting, atomisation was repeated 4 times and each atomisation was kept running for 20 seconds with 50 data were sampled at every second. Therefore 1000 data points were collected for each atomisation. The data presented at the right column is therefore the average of 4000 aerosol sizes.

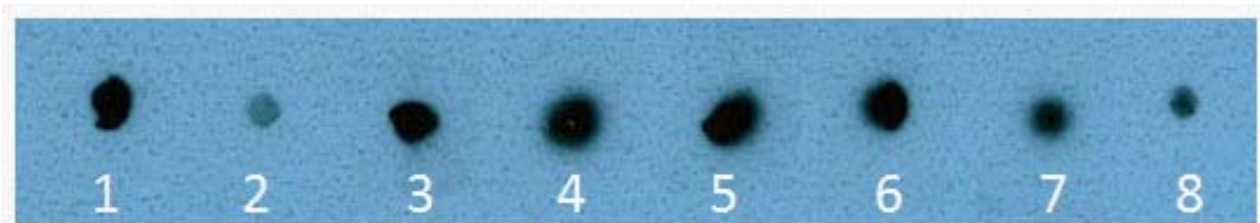


Figure 3. The post-atomised antibody samples nebulized with AM modulation at various frequencies were spotted on a dot blot showing the conservation of the bioactivity of the post-atomisation where lane 1: original sample , lane 2: atomisation without AM with power at 1.5W, lanes 3–8: atomisation with AM (1.5W) at 500 Hz, 1 kHz, 5 kHz, 10 kHz, 20 kHz and 40 kHz, respectively.

3.3 Physical stability of bio molecules post-atomisation

Antibodies constitute both sensitive and fragile proteins of which their bioactivity once tested post-atomisation will eliminate the safety concerns when using AM to deliver similar protein and peptide based drugs via inhalation. The dot blot in Fig. 3 confirms that there is no observed degradation of the active sites of the protein molecule during amplitude modulation at all investigated frequencies as YFP protein was spotted using the post-atomised rabbit anti-YFP antiserum solutions. These observations suggest AM causes no obvious damage to active site of protein molecules thus preserving its bioactivity, lending further confidence in the use of AM as an efficient mechanism for the power optimisation for the aerosol delivery of a wide range of drugs.

4. CONCLUSION

We have demonstrated the feasibility of using amplitude modulation for the effective SAW nebulization of future bio-therapeutics. The retained bioactivity of the atomisation of antibody molecules recovered after atomisation suggests that many protein based drugs can survive the AM optimized SAW nebulisation. Using the technique, the power consumption can be reduced by 40% with little effect on the mean aerosol aerosol diameters produced. This work therefore holds great promise for the development of a battery driven hand-held SAW nebulizer for pulmonary drug delivery purposes.

5. ACKNOWLEDGMENTS

The authors thank the Asthma Foundation Victoria (Australia) for the funding of "2011 Hon Walter Jona Paediatric Research Grant".

REFERENCES

- [1] S. Newman, J. Agnew, D. Pavia, and S. Clarke, "Inhaled aerosols: lung deposition and clinical applications," *Clin. Phys. Physiol. Meas.* **3**, pp. 1–12, 1982.
- [2] B. L. Laube, "The expanding role of aerosols in systemic drug delivery, gene therapy, and vaccination," *Respiratory Care* **50**, pp. 1161–1176, 2005.
- [3] A. Qi, J. R. Friend, and L. Y. Yeo, "Miniature inhalation therapy platform using surface acoustic wave microfluidic atomization," *Lab on a Chip* **9**, pp. 2184–2193, 2009.
- [4] A. K. Sen, J. Darabi, and D. R. Knapp, "Design, fabrication and test of a microfluidic nebulizer chip for desorption electrospray ionization mass spectrometry," *Sens Actuators B Chem.* **137**, p. 78979, 2009.
- [5] M. B. Dolovich, D. R. Hess, R. Dhand, and G. C. Smaldone, "Device selection and outcomes of aerosol therapy: Evidence-based guidelines," *Chest* **127**, pp. 335–371, 2005.
- [6] A. Rajapaksa, J. Ho, L. Yeo, J. Friend, M. P. McIntosh, D. Piedrafita, E. Meeusen, and D. A. V. Morton, "Pulmonary gene delivery platform via ultrafast microfluidics," in *Advances in Microfluidics and Nanofluidics and Asian-Pacific International Symposium on Lab on Chip*, 2011.
- [7] A. Qi, L. Yeo, J. Friend, and J. Ho, "The extraction of liquid, protein molecules and yeast cells from paper through surface acoustic wave atomization," *Lab on a Chip* **10**, pp. 470–476, 2010.
- [8] P. Barnes, "New treatments for chronic obstructive pulmonary disease," *Current Opinion in Pharmacology* **1**, pp. 217–222, 2001.
- [9] G. Scheuch, M. J. Kohlhäufel, P. Brand, and R. Siekmeier, "Clinical perspectives on pulmonary systemic and macromolecular delivery," *Advanced Drug Delivery Reviews* **58**, pp. 996–1008, 2006.
- [10] H. W. Frijlink and A. H. D. Boer, "Dry powder inhalers for pulmonary drug delivery," *Expert Opinion on Drug Delivery* **1**, pp. 67–86, 2004.
- [11] D. Oxtoby, "Vibrational relaxation in liquids," *Annual Review of Physical Chemistry* **32**, pp. 77–101, 1981.
- [12] C. C. Hsieh, A. Balducci, and P. S. Doyle, "An experimental study of dna rotational relaxation time in nanoslits," *Macromolecules* **40**, pp. 5196–5205, 2007.
- [13] L. Y. Yeo, J. R. Friend, M. P. McIntosh, E. Meeusen, and D. Morton, "Ultrasonic nebulization platforms for pulmonary drug delivery," *Expert Opinion on Drug Delivery* **7**, pp. 663–679, 2010.
- [14] K. Nagase, J. Friend, T. Ishii, K. Nakamura, and S. Ueha, "A study of new ultrasonic (sic) atomizing by two parallel saw devices," in *Proceedings of the 22nd Symposium on Ultrasonic Electronics*, **P3-49**, pp. 377–378 (in Japanese), (Ebina, Japan), 2001.
- [15] A. Qi, L. Yeo, and J. Friend, "Interfacial destabilization and atomization driven by surface acoustic waves," *Physics of Fluids* **20**, p. 074103, 2008.
- [16] L. Y. Yeo and J. R. Friend, "Ultrafast microfluidics using surface acoustic waves," *Biomicrofluidics* **3**, p. 012002, 2009.
- [17] S. Hardt and F. Schönfeld, *Microfluidic Technologies for Miniaturized Analysis Systems*, Springer, 2007.
- [18] W. P. Mason, ed., *Physical acoustics*, Academic Press, 1965.
- [19] L. Y. Yeo, D. Lastochkin, S.-C. Wang, and H.-C. Chang, "A new ac electrospray mechanism by maxwell-wagner polarization and capillary resonance," *Physical Review Letters* **92**, p. 133902, 2004.

- [20] Y.-J. Chen and P. H. Steen, “Dynamics of inviscid capillary breakup: collapse and pinchoff of a film bridge,” *Journal of Fluid Mechanics* **341**, pp. 245–267, 1997.

Appendix G

A Business Case for Respire[®]: A Novel Nebulizer for Pulmonary Drug Delivery

Rajapaksa, A. E.

Graduate Certificate in Research Commercialisation

Monash University, Australia

November 2011



Business Case

Respire®: A Novel Nebulizer for Pulmonary Drug Delivery

Table of Contents

1	EXECUTIVE SUMMARY.....	3
2	THE MARKET OPPORTUNITY.....	6
2.1	PULMONARY DRUG THERAPY.....	6
2.2	PULMONARY DRUG DELIVERY MARKET OVERVIEW	6
2.3	PORTABLE INHALER DEVICES OVERVIEW.....	9
2.4	CURRENT MARKET SEGMENTS FOR INHALATION TECHNOLOGIES.....	12
2.5	CHALLENGES IN PULMONARY DRUG THERAPY	13
2.6	RESPIRE®: A NOVEL NEBULIZER FOR PULMONARY DRUG DELIVERY	14
2.7	ADDRESSABLE PRIMARY MARKET FOR RESPIRE®	15
3	THE TEAM.....	18
3.1	THE RESEARCH INSTITUTIONS	18
3.2	THE INVENTORS/SCIENTISTS	18
3.3	COLLABORATIONS/ PARTNERSHIPS	21
4	THE PRODUCT/TECHNOLOGY	23
4.1	THE TECHNOLOGY	23
4.2	THE PRODUCTS	27
4.3	INTELLECTUAL PROPERTY HOLDINGS AND STRATEGIES.....	30
4.4	OTHER ADVANTAGES.....	32
4.5	FUTURE DIRECTION AND HURDLES	32
5	COMPETITION.....	35
5.1	KEY MARKET PLAYERS.....	35
5.2	COMPETITIVE ADVANTAGES OF RESPIRE®	36
6	DEVELOPMENT AND OBJECTIVES PLAN	38
6.1	PROJECT MILESTONES.....	38
6.2	PRODUCT/TECHNOLOGY LICENSING PIPELINE.....	40
6.3	PROJECT FUNDING	41
6.4	CLINICAL TESTING AND SMALL SCALE PRODUCT MANUFACTURE	42
7	THE BUSINESS MODEL AND MARKET ENGAGEMENT STRATEGY	44
7.1	SUCCESSFUL BUSINESS MODELS.....	44
7.2	MARKET ENTRY	45
7.3	POTENTIAL PURCHASERS: VERTICAL AND HORIZONTAL OPTIONS?.....	46
7.4	EXIT OPTIONS.....	47
8	THE FINANCE AND REVENUE MODEL.....	48

8.1	COSTING OF THE RESPIRE® NEBULIZER	50
9	PROJECT RISK ASSESSMENT	51
9.1	CURRENT ISSUES	51
9.2	PROPOSED MITIGATION STRATEGY	52
10	APPENDICES.....	54
	APPENDIX A: DISCOVERY	54
	APPENDIX B: AN INVESTIGATION INTO OBTAINING A SUCCESSFUL DESIGN REGISTRATION FOR A NOVEL PULMONARY DRUG DELIVERY DEVICE, RESPIRE®	
	APPENDIX C: PATENT ON THE MICROFLUIDIC APPARATUS FOR THE ATOMISATION OF ALIQUID	
	APPENDIX D: PATENT ON THE CONCENTRATION AND DISPERSION OF SMALL PARTICLES IN SMALL FLUID VOLUMES USING ACOUSTIC ENERGY	55
	APPENDIX C: PATENT ON THE MICROFLUIDIC APPARATUS FOR THE ATOMISATION OF ALIQUID	
	APPENDIX D: PATENT ON THE CONCENTRATION AND DISPERSION OF SMALL PARTICLES IN SMALL FLUID VOLUMES USING ACOUSTIC ENERGY	56
	APPENDIX D: PATENT ON THE CONCENTRATION AND DISPERSION OF SMALL PARTICLES IN SMALL FLUID VOLUMES USING ACOUSTIC ENERGY	57

Respire®: A Novel Nebulizer for Pulmonary Drug

Delivery

The proposal seeks funding to develop the Respire® nebuliser – a ‘first in class’ Surface Acoustic Wave (SAW) based nebuliser for the delivery of new liquid based formulations and drugs to the lungs. The use of SAW technology in a nebuliser is a paradigm shift for drug delivery to the lungs, enabling this as a route for the nebuliser based administration of a growing wave of biologic and nucleic acid medicaments.

The aim is to use the funding to address some clear technical milestones to de-risk the technology opportunity, create value and execute a short term licensing deal for a medium term capital return to investors at an IRR requisite of early stage seed investment.

The Respire® technology is a ‘first in class’ nebuliser based on Surface Acoustic Wave (SAW) technology for the delivery of atomised fluids containing novel medicament formulations to the lung. The competitive advantages of this technology are its ability to provide, orifice and mesh-free, uniformly-sized droplet mists during the inhalation cycle, with tunable size via changes to the liquid formulation to target specific sections of the lung, and the capacity to deliver both protein/peptide and nucleic acid based medicaments to the lungs. The last point, due to reduced shear in atomisation, provides a fundamental technical advance in drug delivery to the lung and opens a range of new drugs for tissue specific and/or systemic delivery to the lungs.

Respiratory drugs are the second largest therapeutic class and one of the fastest growing in the world. This is the result of the rising incidence of respiratory disorders together with innovations in pulmonary drug delivery technologies that are enabling new opportunities.

However, delivering therapeutics to the lung presents a number of technical challenges. From the current array of pulmonary formulation technologies and devices, generally only 15%-30% of the drug is delivered to the lung, the rest lost in the device and in the mouth and throat of the patient as a consequence of a broad particle size range and incorrect usage of inhalers by the patient. Of these administered drugs, only around 20% (or 3-6% of the total administered dose) reaches the deep lung, a waste of drug and a serious problem in estimating the actual dose delivered.

Driven by consumer demand, dry powder inhalation products are the fastest growing segment in this space. However, current drug options are essentially restricted to the delivery of small molecules for dry formulations, as larger molecules are degraded in the process of manufacture absent years of extraordinary effort (i.e., Relenza). The inability to straight forwardly formulate peptides and nucleic acids in dry particle form nor administer them in liquid formations with current technologies due to destructive shear during delivery inhibits the lungs being targeted with a burgeoning array of biologically based medications.

The Respire® technology offers a both clinical use and handheld nebuliser with the capacity to administer biologically based medications to the lungs with dose control through delivery timing upon inhalation and a broad ability to control droplet size through formulation to target specific regions of the lung most affected by disease. This technology opportunity offers a paradigm shift in drug delivery to the lungs.

The scientific team will be led by Professor James Friend and Associate Professor Leslie Yeo with commercial project management from respective Monash University nominated representatives.

Investments of \$365K would be required for the prototype development of the technology to enable successful launch of the technology into the market. The total cost per device was estimated to be

around \$15, with a small profit margin of 25%. A five year projected cash flows from the financial activities yielded a net present value of over \$14M, indicating a highly profitable project.

Monash University owns the IP. A license for rights to exploit the SAW technology, limited to the treatment of diabetes, has been executed with V-Patch Medical systems.

2 The Market Opportunity

2.1 Pulmonary Drug Therapy

Inhalation therapy is the most efficient method for the treatment of lung disease because of its assessability and large surface area for therapy; further, pulmonary delivery constitutes a pain-free non-invasive route that circumvents the challenges and risks associated with parenteral routes. The attractiveness of pulmonary delivery of drugs for the treatment of respiratory diseases stems from the fact that topical drug deposition to lung gives a fast therapeutic effect and reduces systemic side effects.¹ The most commonly used pulmonary delivery devices include metered dose inhalers (MDIs), dry powder inhalers (DPIs), Breath-Activated Metered Dose Inhalers (BAIs), jet or ultrasonic nebulizers and electrohydrodynamic (EHD) devices.

2.2 Pulmonary Drug Delivery Market Overview

The world market for pulmonary drugs is currently dominated by medications for asthma, chronic obstructive pulmonary and emphysema diseases (See *Figure 1*).

COPD is a lung disease caused by one or more health problems and includes chronic bronchitis and emphysema.² COPD is the fourth leading cause of death in the USA³ and is among the top 10 leading causes of death in Australian men and women.⁴ The illness causes serious long-term disability with little early warning signs. Currently there is no known cure, and as a result more than 12 million people are known to have COPD and up to 24 million undiagnosed cases. While COPD

¹ Birchall, J. Pulmonary delivery of nucleic acids. *Expert Opinion on Drug Delivery* 4, 575-578 (2007)

² The Australian Lung Foundation. COPD – emphysema and chronic bronchitis (fact sheet). Lutwyche, Queensland: ALF; 200

³ New Survey Suggests Growing Awareness of COPD, Nation's Fourth Leading Killer, Available at [online] <http://www.nih.gov/news/health/nov2008/nhlbi-13.htm> [10th November 2011], (2008).

⁴ Facts on COPD and Smoking Available at [online] Available at: <http://www.cancerwa.asn.au/resources/2009-12-22-Facts-on-COPD-and-smoking.pdf> [10th November 2011], (2011).

treatments are commonly administered via the lungs, there are a growing number of anti-fibrotic biologic medicaments (i.e. mAbs) that may benefit in efficacy through direct administration to the lung.

Asthma is a chronic lung disease that inflames and narrows the airways. Asthma causes recurring periods of wheezing, chest tightness, shortness of breath, and coughing. In the United States, more than 22 million people are known to have asthma with nearly 6 million of these people being children.⁵ In 2007, asthma burdened the USA with direct health care costs of \$14.7 billion; indirect costs (lost productivity) added another \$5 billion.⁶ Asthma can be life threatening if not properly managed. In 2005 there were 3,884 documented deaths due to asthma (as per National Vital Statistics Reports).

Lung Infections / Cystic Fibrosis (CF) constitutes hospital-Acquired, healthcare-associated and ventilator-associated pneumonias involving Gram-negative pneumonias are often the result of complications of other patient conditions or surgeries. Gram-negative pneumonia carries a mortality risk of over 50 percent in mechanically-ventilated patients and accounts for a substantial proportion of the pneumonias in intensive care units. In addition, there are 70,000 patients worldwide with CF.⁷ By the age of 18 years, more than 75% of CF patients are chronically infected with *Pseudomonas aeruginosa*. CF Foundation guidelines issued in 2007, call for chronic use of inhaled antibiotics in patients with moderate to severe lung disease and persistent infection with *Pseudomonas aeruginosa* in airways to prevent acute exacerbations and improve lung function. However, administration schedules with currently available options can be difficult for CF patients, leading to reduced adherence to therapy. Available data indicate that CF patients receive significantly less than the recommended number of courses of treatment per year. The pulmonary administration of antibiotics for CF patients chronically infected with Gram negative (i.e. *Pseudomonas aeruginosa*) or gram positive (i.e. MRSA) infections is a common area of commercial development and transaction in the pharmaceutical industry.

⁵ Asthma Statistics, Available at [online] <http://www.aafakc.org/statistics.html> [9th November 2011], (2011).

⁶ O'Day, By Ken et al., Asthma Disease Burden and Formulary Decision Making: MCO and Employer Perspectives, Available at [online] <http://dbt.consultantlive.com/respiratory-treatments/content/article/1145628/1469635> [10th November 2011], (2009)

⁷ Ranes, Justin L., Gordon, Steven, and Arroliga, Alejandro C., Hospital-Acquired, Health Care-Associated, and Ventilator-Associated Pneumonia, Available at [online] Available at: <http://www.clevelandclinicmeded.com/medicalpubs/diseasemanagement/infectious-disease/health-care-associated-pneumonia/> [10th November 2011], (2011).

Lung Cancer is the second-most commonly diagnosed cancer in both men and women.⁸ Although some progress has been made in the treatment of lung cancer, it is still the most common cause of deaths due to cancer in the western world. In 2010, more than 222,000 new cases were expected to be diagnosed and about 157,000 Americans were expected to die from lung cancer.⁸ Currently, there are no anti-lung tumour medications administered via the pulmonary route.

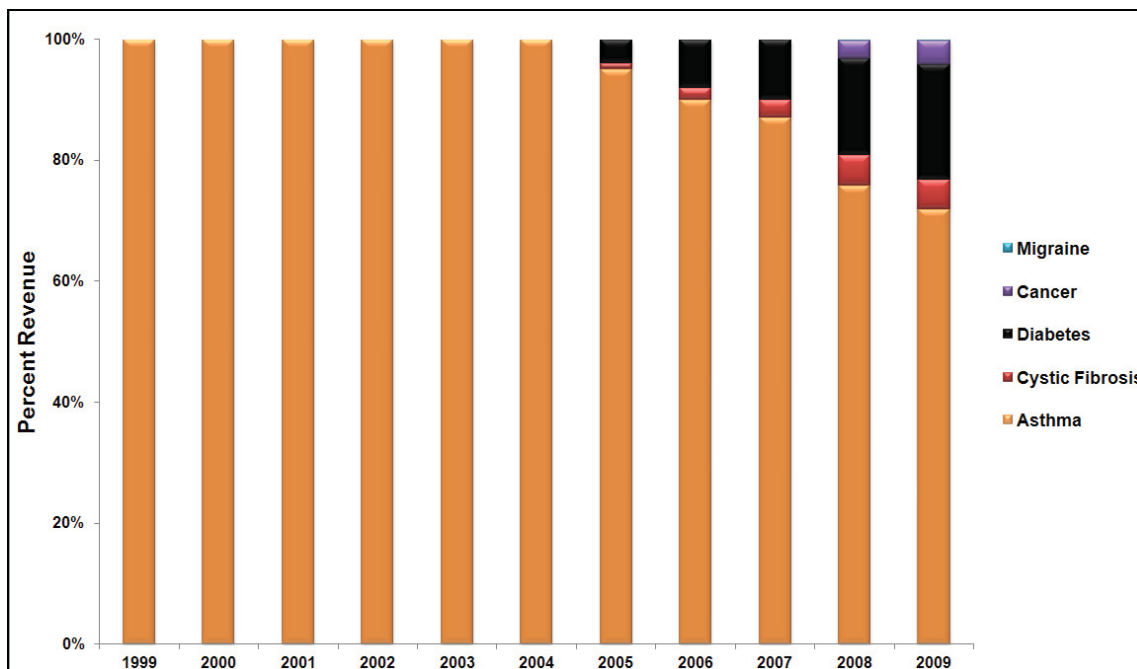
1.1.1 Pulmonary Drug Delivery Market Trends

The rising incidence of respiratory disorders, growing prevalence of asthma and COPD as chronic lifestyle induced disorders, innovations in pulmonary drug delivery technologies, and improved patient outcomes, will stimulate global pulmonary drug delivery technologies market to reach US\$37.7 billion by 2015.⁹ Primary drivers of growth, especially in the traditional pulmonary inhalables market, include rising incidence of respiratory disorders, growing prevalence of asthma and COPD as chronic lifestyle induced disorders, and increasing importance of drug self-administration for chronic conditions. Innovations in pharmaceutical formulations, the significant potential of protein-and peptide-based therapeutics, emergence of sophisticated inhaler device designs, consumer desire for alternatives to injections and growing obscurity between a drug and its delivery are few other factors, which currently guide growth patterns in the industry.

⁸ About Lung Cancer, Available at [online]<http://www.lungusa.org/lung-disease/lung-cancer/about-lung-cancer/> [10th November 2011], (2011).

⁹ Jose, San, Global Pulmonary Drug Delivery Technologies Market Is Projected to Reach US\$37.7 Billion by 2015, According to New Report by Global Industry Analysts, Available at [online] [www.prweb.com/prweb/3720994.htm](http://www.prweb.com/prweb.com/prweb/3720994.htm) [31st September 2011], (2010).

Figure 1: Pulmonary Drug delivery; Revenue by application (U.S.) 1999-2009¹⁰



2.3 Portable Inhaler Devices Overview

The respiratory disease market is becoming increasingly saturated for most drug classes, such as inhaled steroids and bronchodilators. Since this trend will continue in the near future, choice of device-rather than choice of drug-is set to become one of the driving forces behind pulmonary disease management. The development of novel devices with improved features is therefore become increasingly important for companies in order to differentiate their product offerings.¹¹

The principal behind pulmonary drug delivery is aerosolization of drug compounds to be delivered to bronchioles and alveoli. The available delivery systems include metered dose inhalers (MDIs), dry powder inhalers (DPIs), and nebulizers. MDIs were among the first to be introduced in the United States in the mid-1950s (See *Figure 2*). Since then, the technology continued to advance,

¹⁰ Ajmani, Dhiraj, Pulmonary Drug Delivery: From Dreams to Reality, Available at [online] Available at: <http://www.drugdeliverytech.com/ME2/dirmod.asp?sid=&nm=&type=Publishing&mod=Publications%3A%3Aarticle&mid=8F3A7027421841978F18BE895F87F791&tier=4&id=62F5FE3771B047AB9CE68A5D4B7769F8> [10th September 2011], (2008).

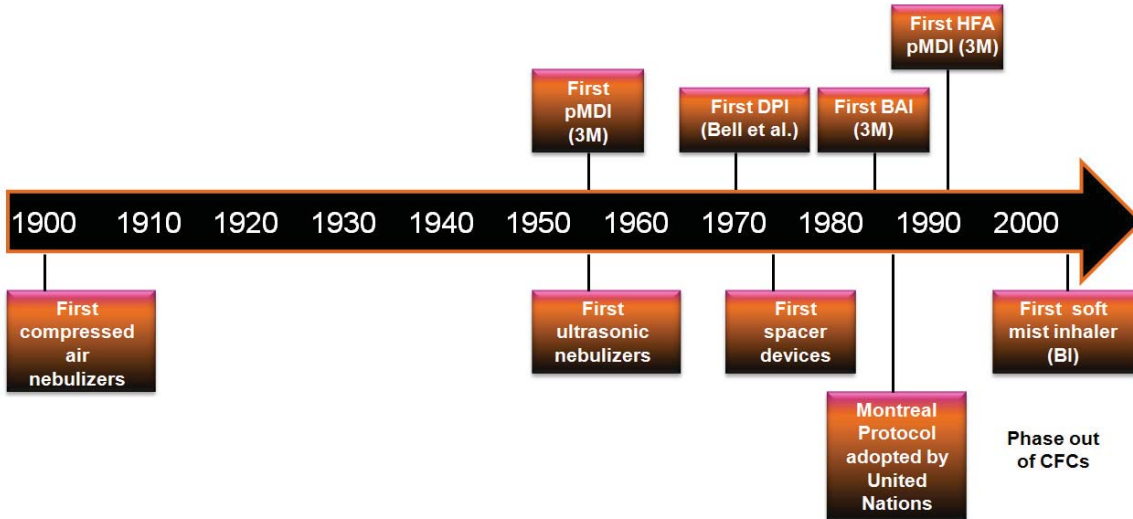
¹¹ Oversteegen, Lisette, Inhaled Medicines: Product Differentiation by Device. *Innovations in Pharmaceutical Technology* (2008).

improving drug delivery efficiency and patient convenience. Following the Montreal Protocol, chlorofluorocarbons (CFC)-based MDIs are being phased out to be replaced by hydrofluoroalkane (HFA)-based MDIs. The first HFA-based MDI was introduced in the United States in 1995. Although DPIs were introduced in the 1970s, their use has been limited due to the overwhelming dominance of MDIs. Also triggered by the 1987 Montreal Protocol, the use of DPIs has been increasing in the United States. Nebulizers are generally used within hospital settings and provide continuous aerosol spray with the help of an external energy source. Patients who are unable to use hand-held inhalers also use these nebulizers. Technological advances within the pulmonary drug delivery technologies markets are taking place in non-CFC-based MDIs, DPIs, and liquid-based inhalers (LBIs).¹²

Nebulizers traditionally fall into two broad categories depending on their operating principles. Table 1 outlines the key features and limitations of the different types of nebulizers currently available.




¹² Ajmani, Dhiraj, Pulmonary Drug Delivery: From Dreams to Reality, Available at [online] Available at: <http://www.drugdeliverytech.com/ME2/dirmod.asp?sid=&nm=&type=Publishing&mod=Publications%3A%3AArticle&mid=8F3A7027421841978F18BE895F87F791&tier=4&id=62F5FE3771B047AB9CE68A5D4B7769F8> [10th September 2011], (2008).

Figure 2: Timeline of the development of inhaler devices for pulmonary diseases






Source: Modified from Datamonitor, 2008 (Kayne, 2006; Dolovich et al., 2005)
 Acronyms used: pMDI: Pressurized Metered-Dose Inhalers , DPI: Dry Powder Inhaler, BAI: Breath-Actuated Inhaler

Table 1: Advantages and disadvantages of the three main types of portable inhaler devices

Advantages		Disadvantages
<ul style="list-style-type: none"> ▪ Portable and durable ▪ Accurate delivery, little respiratory effort ▪ Long shelf life ▪ Low cost of production 	<p>pMDIs</p> 	<ul style="list-style-type: none"> ▪ Time dependant dose variation ▪ Cold- Freon effect ▪ Large amount of depreciation in the mouth and throat ▪ Difficult to co-ordinate actuation and inspiration ▪ Phase-out of CFC TO HFA propellants
<ul style="list-style-type: none"> ▪ Stability of dry powder ▪ Easy co-ordination ▪ Low cost of Production 	<p>DPIs</p> 	<ul style="list-style-type: none"> ▪ Reservoir systems can be affected by environmental factors ▪ Reservoir systems have poor dose reproducibility ▪ Usually require a carrier or bulking agent – higher costs ▪ More complex manufacturing process ▪ Performance relies on strength process ▪ Performance relies on strength of inhalation
<ul style="list-style-type: none"> ▪ Easy co-ordination ▪ Preferred by patients and health care professionals ▪ Lower cost of overall treatment 	<p>BAIs</p> 	<ul style="list-style-type: none"> ▪ Lack of drugs available ▪ More complex manufacturing process ▪ Higher costs ▪ Performance relies on inspiratory volume ▪ Cold- Freon effect

Source: Modified from Datamonitor, 2008
 Acronyms used: pMDI: Pressurized Metered-Dose Inhalers , DPI: Dry Powder Inhaler, BAI: Breath-Actuated Inhaler

Table 2: Features and disadvantages of the three main types of portable inhaler devices

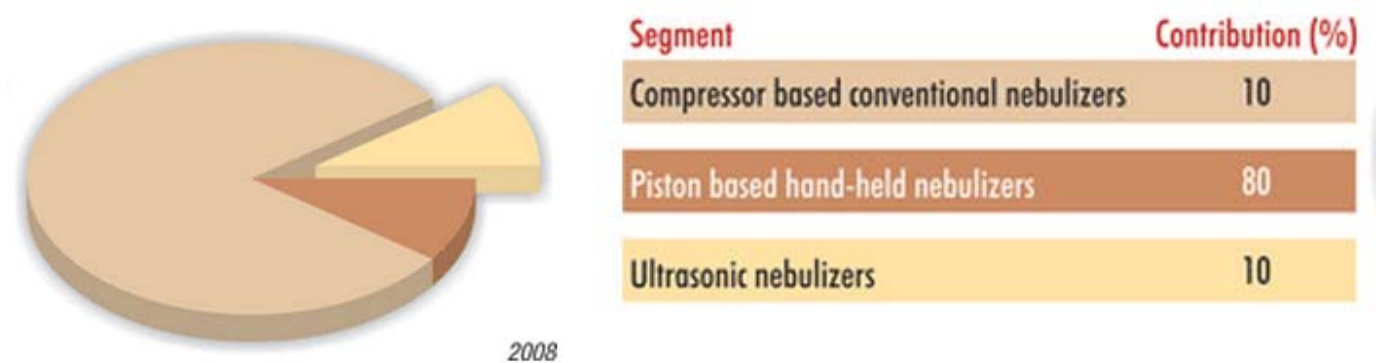
Features		Disadvantages
<ul style="list-style-type: none"> ▪ Uses a high-speed velocity air flow through a nozzle to draw liquid containing the drug from side feed tubes into the nozzle ▪ The liquid immediately breaks up into aerosol droplets as it emanates from the feed tubes 	<p>Jet nebulizer</p> 	<ul style="list-style-type: none"> ▪ The pressurized air jet is inadequate to supply sufficient air flow to comprise the full inhalation flow volume and so more air has to be inhaled by the patient ▪ Requires a heavy and/or bulky compressed gas cylinder, electrical compressor, hospital reticulated air system or bulky battery operated compressor. ▪ Only 12% of drug reaches the lung, the remaining drug is wasted
<ul style="list-style-type: none"> ▪ Relies on the use of an electronic oscillator to generate high frequency ultrasonic wave that causes the mechanical vibration of a piezoelectric element ▪ The vibrating element is in contact with a liquid reservoir and its high frequency vibration is sufficient to produce a vapor mist 	<p>Ultrasonic nebulizer (conventional)</p> 	<ul style="list-style-type: none"> ▪ Requires a large power source ▪ Heating involved that could lead to denaturation of drug molecules ▪ Less efficient for use with drug suspensions and viscous solutions
<ul style="list-style-type: none"> ▪ Relies on the use of a mesh/membrane with 1000-7000 laser drilled holes vibrating at the top of the liquid reservoir ▪ A mist of very fine droplets is pressures out through the holes ▪ Provides more uniform sized droplets defined by the orifice size 	<p>Vibrating Mesh nebulizer</p> 	<ul style="list-style-type: none"> ▪ The mesh requires careful cleaning to avoid clogging of the orifice ▪ The large surface area poses problems with bacterial contamination if not thoroughly cleaned ▪ The complex fabrication required for the laser-assisted drilling of the mesh orifices also adds significant costs to the device manufacturing

2.4 Current Market Segments for Inhalation Technologies

The DPIs (compressor based) are the highest-selling group of devices in the lung delivery market based on revenues, while the pMDIs are sold on the highest volumes (See *Figure 3*). BAIs overcome many of the compliance disadvantages associated with DPIs and pMDIs (i.e. coordination with inhalation), but they represent only a small share of the market due to their relatively high price per standard unit of drug delivered and limited availability. The markets well-served by inexpensive pMDIs and DPIs use small-molecule drugs like salbutamol that are effective at low doses yet are safe even at high doses, permitting the typically ineffective use of these delivery methods. Nebulisers form a small part of the market and are used to administer liquid formulations in the doctor's office that could often be administered via MDI but need to be administered over a longer period of time, often to patients with

poorer capacity to inhale drugs and for acute incidences of a particular lung disease. Further, nebulisers typically are always-on instruments, producing inhalable mists with a broad size range wasted as the patient exhales. For these reasons, nebulisers are more expensive per dose.

Figure 3: Nebulizer Market for a total 100,000 units as of 2008 ¹³



2.5 Challenges in Pulmonary Drug Therapy

Inhalers generally require either hand-inhalation coordination or passive breath-driven aerosolisation, rendering them ineffective for many patients unable to self-medicate, suffering from severe forms of chronic obstructive pulmonary disease (COPD).¹⁴ In addition, macromolecules such as pDNA are not soluble in propellants and have to be formulated as solid dispersed systems, resulting in instability of the formulations for practical use.¹⁵ A significant limitation in the use of nebulizers for pulmonary gene delivery to date arises due to the denaturing of non-complexed DNA as a consequence of the large hydrodynamic shear stresses or shock waves that arise during the jet or ultrasonic nebulization process.¹⁶ Although active aerosolisation methods such as nebulizers are more appropriate for these specific patient groups, these nebulizers lack efficiency, usability and the flexibility to accommodate patient breathing and lung variability, thus catering the “one-size-fits-all” strategy.

¹³ "Competitive yet Growing Market of Nebulizers," Medical Buyer: Medical Equipment and Devices 2009

¹⁴ "Inhaler technique in adults with asthma or COPD: Information paper for health professionals," 2008.

¹⁵ D. Lu and A. Hickey, "Pulmonary vaccine delivery," *Expert Review of Vaccines*, vol. 6, pp. 213-226, 2007.

¹⁶ Arulmuthu, Eugene R. et al., Studies on aerosol delivery of plasmid DNA using a mesh nebulizer. *Biotechnol. Bioeng.* **98** (5), 939 (2007)

Moreover, the delivery of sufficient drug into diseased lung remains challenging because it requires an inhaler which is able to generate drug particles in a narrow range of 1-5 μm to achieve optimal lung deposition (1-2 μm = Deep lung, 3-5 μm = upper lung).¹⁷ Current inhalers are simply unable to deliver, with published data showing over 50% of users with asthma cannot obtain the proper dose into their lungs due to improper use of the device.¹⁸ The incidence of misdosage in the treatment of COPD is far higher because of the broad variety of lung capacities and physiology among people with this disease. Furthermore, the formulation of particles of a drug suitable for pMDI, DPI, and BAI delivery can significantly add to its development cost (>20%)—for drugs that can be formulated into dry particles; a substantial fraction of candidate drugs cannot survive spray or freeze drying.¹⁹

Choosing a suitable device to administer a drug is therefore as crucial to effective treatment as the selection of the drug itself. Access to a well-designed device is essential to a company seeking to successfully differentiate their product. As such, there are opportunities in the respiratory market to gain market share by differentiation through matching an ideal inhaler device with an ideal drug.

An ideal device could therefore lead to improved disease control. However, none of the devices on the market have all the characteristics of an ideal device, meaning that physicians need to compromise in hoping the beneficial outcomes in selecting a match between a device, a drug and a patient population overcome the drawbacks of the delivery technology.

2.6 Respire®: A Novel Nebulizer for Pulmonary Drug Delivery

The Respire® technology is a 'first in class' nebuliser based on Surface Acoustic Wave (SAW) technology for the delivery of nebulised fluids containing biologically based medications to the lungs with dose control through delivery timing upon inhalation and a broad ability to control droplet size

¹⁷ P. J. Barnes, "New treatments for chronic obstructive pulmonary disease," *Current Opinion in Pharmacology*, vol. 1, pp. 217-222, 2001.

¹⁸ Melani AS, Zanchetta D, Barbato N et al. Inhalation technique and variables associated with misuse of conventional metered-dose inhalers and newer dry powder inhalers in experienced adults. *Ann Allergy Asthma Immunol* 2004; 93: 439-46

¹⁹ Oversteegen, Lisette, *Inhaled Medicines: Product Differentiation by Device. Innovations in Pharmaceutical Technology* (2008).

through formulation to target specific regions of the lung most affected by disease. This technology opportunity offers a paradigm shift in drug delivery to the lungs.

2.6.1 Our Aim

Our approach is to adopt a ubiquitous technology in another field but entirely new to drug delivery to eliminate these drawbacks. Surface acoustic wave technology has been used in mobile phones for years, multiplexing/demultiplexing voice and data in collision-free communication between many users' phones and the communications towers placed about a region to provide service to these phones. It also has been a key means to provide a controlled frequency and as a timer as the most common type of device anachronistically called a crystal. For decades, fluids—especially isopropyl alcohol—have been used to identify the vibration of these materials and confirm their operation. Surprisingly, the idea to manipulate fluids and nebulise them into a mist awaited someone that realised the potential applications for such technology.

In developing a miniaturized nebulizer using SAW technology we created a pulmonary drug delivery platform, termed Respire®. Our data suggests that through SAW nebulization and refined formulation technology development, we can solve the formulation and aerosol problems for drug delivery to the lung and create a discreet, handheld nebulizer that will accommodate unique drug classes and patient variability in inhalation profiles and dosage needs.

2.7 Addressable Primary Market for Respire®

The Respire® system has number of applications in wide range of lung disease therapy markets such as COPD (Chronic Obstructive Lung Disease), Asthma, Cystic Fibrosis (CF) and Lung cancer each of which presents great potential for exploitation. Within these markets, due to the unique characteristics of the Respire technology, three other major market segments can be identified.

Firstly, pulmonary delivery of small molecules (such as bronchodilators) for example in treatments for asthma would represent an already established market with standard unit-dose vials to be used

with the nebulizer system. Thus an initial market entry with such a product might provide the initial credibility in market place with some customers and access to local venture capital.

Secondly, the pulmonary delivery of large difficult bio-molecules protein or gene therapy for the treatment of influenza, for applications in vaccination, constitutes a younger market with immense potential predicted to reach \$484 million by 2015, with success yet to be achieved in developing completely curative therapeutic drugs.²⁰ To date, only one gene therapy drug Gendicine, developed by Shenzhen SiBiono Gene Technologies Co., has been approved, which is marketed in China. Market predictions for gene therapy highly depend on the regulatory approval of products currently in clinical trials. Most gene therapy products for cancer and cardiovascular diseases are in Phase III/ Phase II of clinical trials. Cost of the treatment and disease population are the other factors that affect the gene therapy market. Funding and research developments and acceptance of gene therapy products to use in medicine are also expected to impact the market in the near future. Hence large investments will be required for the validation of the biomolecules together with the device and the benefits from these investments could only be reaped once the nebulizer is able to gain initial market trust. Hence the Respire® system for the delivery of biomolecules such as plasmid DNA vaccines is seen as a “next generation” type device.

Thirdly, the stable drug creation using the novel layer-by layer technique driven by the Respire® technology for applications in both protein or gene therapy applications using biodegradable nanotechnology is also a young market with great potential. Currently, the healthcare nanotechnology market growth is largest in North America, at \$4.75bn in 2009, followed by Europe at \$3.65.²¹ The nanotechnology drug delivery market is expected to grow at 21.7% for the period 2009-14, to reach almost \$16bn by 2014.²² Candidate partners for co-development of the device would include pharmaceutical and biotech drug developers looking to administer peptides (e.g. monoclonal antibodies) and/or nucleic acids (i.e. pDNA/SiRNA) to treat lung diseases that are either difficult to deliver systemically (i.e. require injections) and/or are difficult to deliver in a tissue specific manner (siRNA). A more specific example could be a pre-clinical stage or a clinically

²⁰ World Gene Therapy Market To Reach \$484 Million By 2015, Available at [online]
http://www.strategyr.com/Gene_Therapy_Market_Report.asp [10th November 2011], (2011).

²¹ Biodegradable nanotechnology, Available at [online]
http://www.altprofits.com/ref/ct/nbo/mao/biodegradable_nanotechnology.html [7th November 2011], (2011).

approved drug that could be/is used to treat a lung disease via I.V. injection that could benefit from an increase in therapeutic window and efficacy through direct administration to the lung.

²² Biodegradable nanotechnology, Available at [online]
http://www.altprofits.com/ref/ct/nbo/mao/biodegradable_nanotechnology.html [7th November 2011], (2011).

3 The Team

3.1 The Research Institutions

Since the preliminary work conducted in Japan during 2000-2, the majority of the scientific discoveries that were both fundamental and applied research, in micro to nano fluidics and acoustics were carried out by the research team led by Professors James Friend and Leslie Yeo, at the Micro/Nanophysics Research Laboratory based at Monash University. The initial scientific work was funded by NanoVic during 2006-09, where the first working engineering prototype was made (See Appendix A for a list of historical events that led to the discovery of the technology). Following this work, a NHMRC Development grant was awarded during 2010-13 for the perusal of an animal trial for the further validation of the device. This work is currently underway at Monash University.

3.2 The inventors/scientists

Prof James Friend and A/Prof Leslie Yeo

Professor James Friend received his BS degree in aerospace engineering, and his MS and PhD degrees in mechanical engineering from the University of Missouri-Rolla in 1992, 1994, and 1998, respectively. James Friend joined Monash University in late 2004, and is currently a professor in the Department of Mechanical and Aerospace Engineering, with research interests in micro/nanodevices for biomedical applications.

Associate Prof. Leslie Yeo is currently an Australian Research Fellow and Associate Professor in the Department of Mechanical & Aerospace Engineering and Co-Director of the Micro/Nanophysics Research Laboratory at Monash University, Australia. Dr Yeo received his PhD from Imperial

College London in 2002, His work has been featured widely in the media, for example, on the Australian Broadcasting Corporation's science television program Catalyst and in various articles in Nature, Science, New Scientist, The Economist, The Washington Times, and The Sydney Morning Herald, amongst others.

Since arriving at Monash University in 2004/5, Prof Friend and A/Prof Yeo have together aggressively pursued the commercialisation of their research at the Mico/Nanophysics Research Laboratory (MNRL). As co-directors of MNRL, both Friend and Yeo have jointly filed three international PCT patent and seven provisional patent applications in that time have commercially-related research activity supported by Nanotechnology Victoria, CSIRO, MiniFAB and Varian. This continues from Friend's and Yeo's track record of patenting and commercial collaboration from their employment in USA and Japan, respectively. In the US, Yeo was involved with commercialisation of his research in AC electrokinetic devices for biomicrofluidic applications such as drug delivery, high throughput drug screening, miniaturised point-of-care medical diagnostics and biosensors at the Centre for Microfluidics and Medical Diagnostics (University of Notre Dame) through the Center's spin-out company Microfluidic Applications Ltd. Between 2003 and 2005, Yeo had applied for 2 full US Utility patents and 3 provisional patents on a novel AC electrospray and microelectrohydrodynamic mixing and bioparticle manipulation device he had discovered. While in Japan, Friend had collaborations with GE Panametrics in the US, Taiheiyo Cement, Kaijo Corporation, Kyocera, NTT/DoCoMo, NEC/Tokin, Hitachi, and Tokyo Electron, had previously consulted with Varian on ultrasonic atomiser technology for IPMC mass spectroscopy, and has applied for seven patents currently progressing through the Japanese system on microactuator, fabrication, and application methods and devices developed from Friend's research. Three of the patents have been licensed by Taiheiyo Cement Corporation, the largest advanced ceramics corporation in Japan, and two others by Kyocera and Tokyo Electron, respectively, reflecting their importance in microdevice fabrication and emerging microrobotics applications.

Dr. Aisha Qi

Dr Qi obtained her PhD from Mechanical Engineering Monash University. She is the post-doc expert currently working under Prof Friend and A/Prof Yeo, who also conducted the initial scientific

work underlying the discovery followed by the development of the first prototype of the SAW nebulizer, as part of her doctoral studies. Currently she is working with the group in the active completion of the animal trials.

Mrs. Anushi Rajapaksa

Lead PhD student, pursuing research under the supervision of Prof Friend and A/Prof Yeo at MNRL, on the pulmonary delivery of DNA vaccines via the “Respire” system. During her doctoral studies, she led the research findings on a novel method of DNA vaccination to the lung using the Respire system that was thus far impossible to achieve by other means of nebulisation. She is now leading animal trials to validate the device in a biological setting. Throughout her research, she has optimised the device performance, and was able to demonstrate that via using an amplitude modulation scheme, significant power savings could be achieved and importantly with little to no effects on bio molecules being nebulised. Several publications that encompass this work are under review and have obtained patent protection for her discoveries.

Dr. Peggy Chan

Dr Peggy Chan received degree in bioprocess engineering, and Ph.D. in chemical engineering from University of New South Wales, Australia. She has actively participated in developing nano-biomaterials for gene, siRNA and drug delivery. Her research interests are in the microfluidic biomaterials area, particularly in the development of microfluidic synthesized biomaterials for drug delivery with a strong research partnership with the MNRL team for the development of polymer nanoparticle generation for drug delivery and multilayer particles for targeted delivery via the SAW technology.

Professor Els Meeusen

Based at the Department of Physiology in Monash’s School of Biomedical Sciences, she is also Head of the Animal Biotechnology Research Laboratories (ABRL). In the treatment of asthma, Professor Meeusen’s group has developed a new sheep model of allergic asthma which displays similarities to human allergic asthma. Using the sheep model, asthma management systems such

as the Respire system is to be validated via a collaborative partnership between MNRL and ABRL that drives the animal work that is currently underway.

Professor Graham Jenkin

Based at the Monash Institute of Medical Research, Monash University) – is a world expert in cell therapies, neonatal well being. A recent collaboration with MNRL hopes to use the Respire system for the delivery of Human Amnion Derived Epithelial Stem Cells (hAECs) to premature babies' lungs that are underdeveloped, helping them to re-develop.

Dr. Jenny Ho

Dr. Ho received her PhD from Chemical Engineering at Monash University with expertise in plasmids, nucleic acid and protein based therapeutics production, analysis, formulation and delivery for anti-malarial and anti-measles vaccines and drugs. Her research background immensely supported the research findings on a novel method of DNA vaccination to the lung using the Respire® system.

Drs David Morton and Michelle McIntosh

Based at the Monash Institute of Pharmaceutical Sciences at Monash university) are experts in pharmacology and pharmacokinetics were involved in the initial characterisation of the first prototype in an in-vitro setting.

3.3 Collaborations/ Partnerships

Monash University has entered into a License and Pipeline agreement on the 3rd of February 2011 with V-Patch Medical Systems granting them the commercialisation rights and access to the future developments to the Respire® technology limited to the field of diabetes treatment.

V-Patch Medical Systems Limited develops medical systems for remote monitoring of patients vital signs in and out of the hospital environment. The company offers V-Patch Medical System (VMPS), an interactive system that collects, analyses, stores, and reports on human vital signs using

biosensors, R-F technology, cellular phone hardware, and the world wide Web. Its systems are used for long and short term monitoring in various fields, including cardiac diagnosis, clinical drug trials, cardiac rehabilitation, weight management, post-operative surveillance, sports medicine, and emergency medicine. The company is based in Victoria, Australia. According to the license agreement, V-Patch is obliged to pay 30% of all future costs relating to patent prosecution and maintenance fees. Potential future risks associated with this agreement is limited since the licence to V-Patch only allows the use of the technology only in a narrow field of diabetes treatment where Monash University has the rights for the exploitation of the Respire® technology for the in a wider range of applications due to its competitive advantages.

4 The Product/Technology

4.1 The Technology

The researchers have developed a promising alternative to ultrasonic nebulization based on surface acoustic wave (SAW) atomization. Surface acoustic waves are MHz to GHz-order, transverse-axial polarized elliptical electroacoustic waves with displacement amplitudes of just a few nanometers. In the present invention, they are generated on and traverse the surface along the x-axis of 127.86° y-rotated single-crystal lithium niobate (LiNbO₃), a low-cost piezoelectric material as a consequence of its ubiquitous usage in telecommunications for the past three decades. Unlike typical ultrasound, a bulk phenomenon, the SAW is confined close to the substrate surface, its amplitude decaying rapidly over a depth of four to five wavelengths (several hundred microns) into the substrate material, making mounting the device straightforward in contrast to standard ultrasonic atomisers. Further, compared to these same ultrasonic atomizers that consume power on the order of 10 W, SAW atomizers only consume between 0.5-3 W since most of the acoustic energy is isolated to a small region near the surface and efficiently transmitted into the fluid.

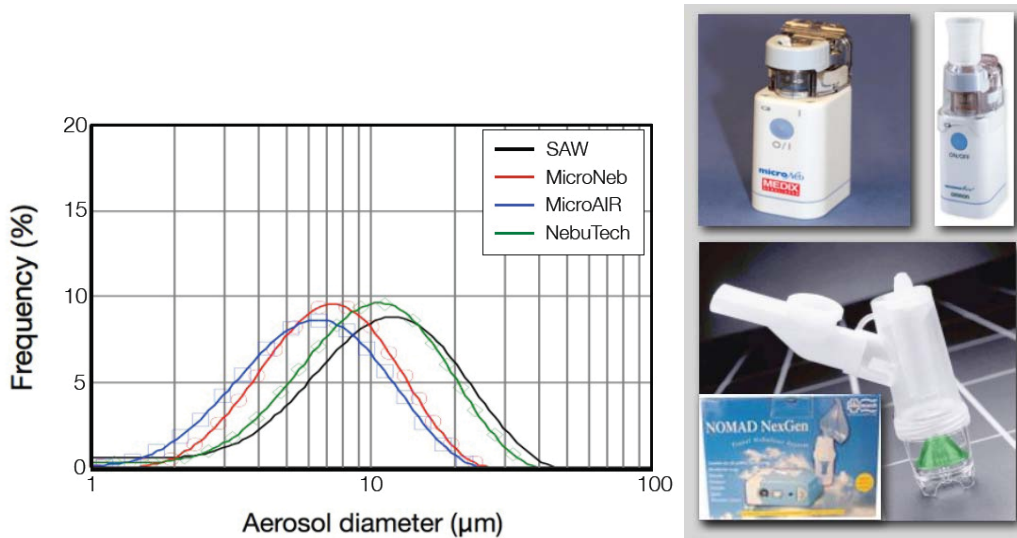
Moreover, the 10-100 MHz order frequency employed in SAW devices, significantly higher than the 10 kHz-1 MHz frequency range of typical ultrasonic devices, induces vibrations with a period much shorter than the molecular relaxation time scale associated with large molecules in liquids, and thus the risk of denaturing molecules or lysing cells is greatly reduced. Further, as the frequency is increased, the power required to induce cavitation increases far beyond what is needed for atomization, eliminating the effect of cavitation-induced lysis or shear in SAW atomizers.

The Respire® system generates monodisperse drug aerosols of controlled size, from 1 to 20 microns in diameter in a range definable by the characteristics of the atomizing fluid and atomizer design; over many runs of the device, the range of the droplet mist diameter falls within 100% of the target diameter. Most desktop nebulisers produce broadly polydisperse mists, from a few microns to hundreds of microns in diameter, wasting drug in the process. Only the latest mesh nebulisers avoid this problem by driving fluid through the orifices of a mesh. However, a mesh is easily clogged, difficult to clean and any alterations to a drugs formulation will not alter droplet size. The

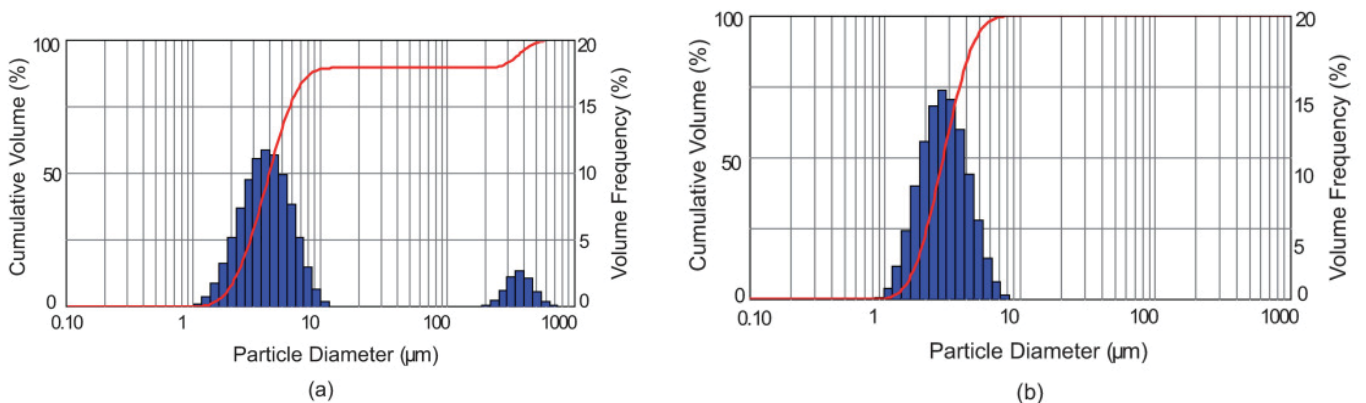
Respire® technology is a simple without need for multiple steps and skills to operate, is efficient enough to operate using battery power, and can deliver even large doses of drug in a few inhalations due to reduced waste, in notable contrast to the large nebulizers that are a fixture of doctors' offices. The design of the proposed device utilizes IC MEMS wafer-based manufacturing suitable for mass and therefore inexpensive production, making it practical for clinical translation.

In an in-vitro proof-of-concept study using a short acting β_2 -agonist, the Respire® technology generated a mean aerosol diameter of $2.84 \pm 0.14 \mu\text{m}$ (See Figure 4). This lies within the optimum size range, confirmed by a twin-stage impinger lung model, demonstrating that approximately 70 to 80% of the drug supplied to the atomizer is deposited within the lung as opposed to the typical 30%–40% lung dose obtained through current nebulisation technologies.

Figure 4: Performance of the Respire® system in comparison to some commercially available nebulizers with respect to aerosol size characteristics produced via the nebulizer

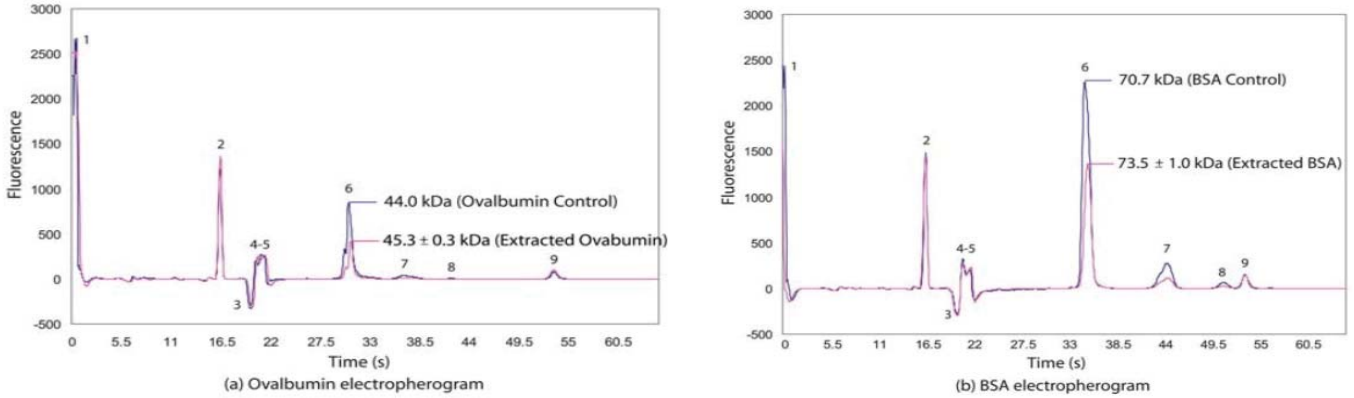


(a) Salbutamol solution nebulisation from as-supplied vial and without adjustment of fluid properties, showing a direct comparison of SAW atomisation versus other nebuliser technologies for delivery of a small molecule drug without formulation optimisation for the SAW Respire® system. All these devices will deliver such a drug to the lung based on these results. The SAW device allows such delivery with larger molecules (Figure 7), and by tailoring the fluid viscosity to the SAW technology the aerosol diameter can be substantially reduced (Figure 4 (b)).

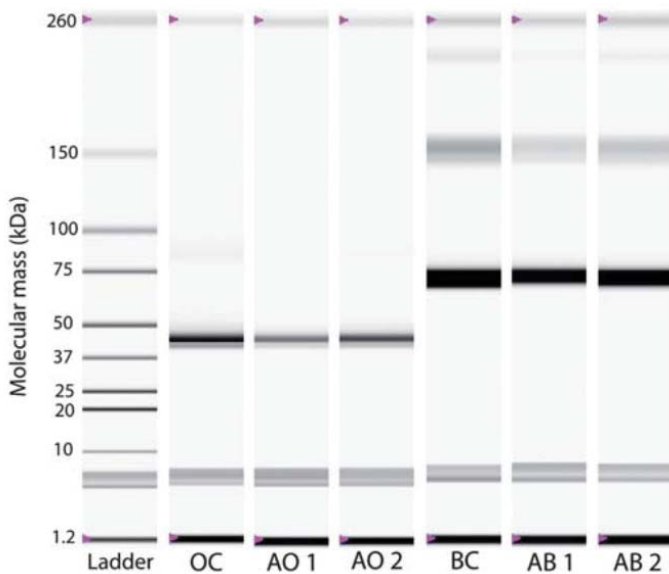


(b) Albuterol-Octanol atomization: aerosol size distribution acquired by using laser diffraction (a) size distribution based on aerosol number (b) size distribution based on aerosol volume. The column represents the number/volume of aerosols within different size bins with respect to the total number/volume of aerosols detected. The curve is the cumulative number/volume fraction.

Figure 5: Respire for the delivery of protein via inhalation showing little to no degradation once nebulized.



Protein electropherograms of (a) ovalbumin solution and (b) BSA solution. The blue curves represent the original ovalbumin/BSA solution before loading paper-the control-and the red curves represent the averaged fluorescence responses of four ovalbumin and BSA samples after atomization, respectively.



(c) The gel image of protein electropherograms. The first column on the left is the ladder associated with molecular masses from 19 kDa to 260 kDa. The ovalbumin control (OC) and BSA control (BC) columns stand for the original ovalbumin/BSA solutions before loading onto paper. Ovalbumin samples 1 and 2 (AO 1 and AO 2) and BSA samples 1 and 2 (AB 1 and AB 2) are examples of atomized protein molecules extracted from paper.

Table 3 : Data obtained through protein electrophoresis

	Molecular Mass (kDa)	Degradation (%)	Output (%)
Ovalbumin control	44.0	0	—
Atomized ovalbumin	45.3 ± 0.3	0.8 ± 0.4	55.75 ± 6.8
BSA control	70.7	0	—
Atomized BSA	75.3 ± 1	0.4 ± 0.3	67.2 ± 8.9

The Respire® technology can also be used to produce encapsulated peptide therapeutics using the novel “layer by layer” approach in contrast to the conventional technique, however, a sacrificial colloidal template over which the polyelectrolyte layers are deposited is not required. Instead, polymer nanoparticles are synthesized by nebulizing the solution containing a biodegradable polymer and suspended within a solution in which the complementary polymer of opposite charge is dissolved. Re-nebulizing this suspension then produces nanocapsules with a layer of the second polymer deposited over a core comprising the initial polymer. Successive nebulization–suspension layering steps can then be repeated again and again to produce as many additional layers as desired for controlled drug delivery applications. Using this technique, the encapsulation of drugs and therapeutic molecules within biocompatible and biodegradable polymeric excipients offers tremendous opportunities for controlling and targeting the release of drugs in vivo. Furthermore, using multiple layers of polyelectrolytes to encapsulate a drug enables the selection of a release profile in order to deliver the drug over a specific time and in a specific location within the body.

4.2 The products

Respire Clinical

An initial market entry with fixated nebulizer in a clinical setting might provide the initial credibility in market place due to the incomplete development of a hand held, battery powered prototype at present. The clinical setting could be outpatient, emergency department (ED), hospitalized inpatient, or intensive care setting or even the ambulance setting with active supervision by health

care professional. The fixated nebulizer would be inherently larger, where it would be powered by an external battery pack or the main power outlet where delivery upto 1000 hours would be possible for inhalation therapies such as protein vaccination (in a standard vial) could also be achieved through Respire Clinical. The power source (since this initial cost is high) would be leased to the customers and sales will be made from devices as they are consumed depending on the number of patients treated.

Compared to nebulizers that are already in the market in a clinical setting, that are recognized as potential nosocomial infection agents²³, the Respire Clinical system would address this issue by providing a “disposable device per patient” type system. The power source would remain attached to the main unit while a nebulizer chip with the drug cartridge could be replaced from patient to patient and disposed of once the inhalation therapy is complete

Additionally, obtaining regulatory approval would also be slightly straightforward, as the application supporting the approval of a new nebulizer would be reviewed by the Center for Devices and Radiologic Health (CDRH) under section 510(k) of the Food, Drug, and Cosmetics Act, under which a nebulizer would be a class II device, in the case of USA.²⁴ It can be demonstrated that the new device is substantially similar to a previously available product in its performance and other key attributes. Respire Clinical would be developed to deliver medication from standard plastic unit-dose vials (small molecules such as bronchodilators) and is intended to administer the drug in a manner consistent with instructions in the drug label and that there is no claim of unique clinical benefit from the drug administered via the new device. In Australia, the regulatory framework for the re-manufacture of medical devices labelled as single use (SUDs) applies to those persons who, in the process of re-manufacturing a SUD, also meet the definition of a manufacturer under section 41 BG Therapeutic Goods Act 1989. A TGA Conformity Assessment Certificate must be obtained through compliance with on site audit of the manufacturer’s quality management system to ISO 13485:2003 (relates to the essential principles for safety and performance).

²³ Tai, Chia-Hua, Lin, Nien-Tsung, Peng, Tai-Chu, and Lee, Ru-Ping, Cleaning Small-Volume Nebulizers: The Efficacy of Different Reagents and Application Methods. *Journal of Nursing Research* **19** (1), 61 (2011).

²⁴ Meyer, Robert J, Bringing New Nebulizer Technologies to Market: Regulatory Issues. (The Science Journal of the American Association for Respiratory Care, 2002).

Respire industrial

Respire industrial would be used to produce encapsulated peptide therapeutics using the novel “layer by layer” technology. Using this technique, the encapsulation of drugs and therapeutic molecules within biocompatible and biodegradable polymeric excipients offers tremendous opportunities for controlling and targeting the release of drugs *in vivo*.

For this application, the portability of the Respire® nebulizer not a requirement and so can be potentially licensed out to a pharmaceutical and biotech drug developers looking to administer peptides (e.g. monoclonal antibodies) and/or nucleic acids (i.e. pDNA/SiRNA) to treat lung diseases that are either difficult to deliver systemically (i.e. require injections) and/or are difficult to deliver in a tissue specific manner (siRNA). A more specific example could be a pre-clinical stage or a clinically approved drug that could be/is used to treat a lung disease via I.V. injection that could benefit from an increase in therapeutic window and efficacy through direct administration to the lung.

Mob Respire:

This would be the high volume generating product, where the hand-held SAW nebulizer would be used by a customer that is “on-the-go”, only realisable once the portable circuitry development is complete. The main unit would be battery powered with the nebulising compartment will be a “disposable chip (nebulizer chip with the drug cartridge) per treatment” type system. With such a system, hygiene is then not an issue when the intended use of the nebulizer is for the treatment of already ill patients. Similar regulatory approval would be required for the Mob Respire system as that for the Respire Clinical.

Gen Respire:

This would be the next generation nebulizer solely intended for the delivery of large bio-molecules such as proteins, intended as vaccines or even plasmid DNA vaccines, the latter only realisable once the DNA vaccines are successfully demonstrated for its safety and immunogenicity in human clinical trials.

4.3 Intellectual Property Holdings and Strategies

Currently, a patent that cover the technology underlying the operation of the device that is already at the PCT stage (See Table 4).²⁵ In addition to this, a recent invention disclosure regarding a power optimization strategy for the device to enable the device to be easily made portable and the novel “layer-by-layer” technology for the Respire® system was also filed at Monash University in order to protect these competitive advantages.^{26,27}

More recently, our team has been working on a device casing in order to build a working prototype for the commercialization of the technology for future clinical testing (See Figure 6). However, the team has not yet registered this design under the Designs Act 2003. Obtaining such a registration is pivotal and would give rise to a marketable asset allowing the use of the product for commercial purposes and will provide an effective restriction to infringers from adopting a similar or even an identical design. A comprehensive investigation was undertaken in order to whether such design registration could be obtained where the proposed design was tested against the requirements of being “new and distinctive”, together other important considerations (See Appendix B). In summary, it was safely concluded that the investigated design for the Respire® system is both new and distinctive from the prior art base and that a successful design registration could be obtained. Since the current design drawings are protected under copyright law, a design application could be filed closer to when small-scale manufacturing of around 50 devices is intended of a product including design, possibly even prior to device being used in clinical setting, during which there may be public display of the design. A design registration should also be requested from IP Australia to validate both new and distinctiveness of the design and also to protect the security of the design from infringement and unfair use.

²⁵ A. Rajapaksa et al, ' Microfluidic Apparatus for the Atomisation of a Liquid' [Patent at PCT stage] (WO/2010/129994)

²⁶ A. Rajapaksa et al, 'Amplitude Modulation Scheme as a Route Towards the Miniaturisation of Low Power Surface Acoustic Wave Microfluidic Drug Delivery Platforms' invention disclosure submitted in 2011

²⁷ Qi, A. et.al, “Synthesis of multilayer polymeric nanoparticles using surface acoustic wave atomization”, *Invention disclosure submitted in 2011*

Table 4: Patent protection currently obtained around the Respire® technology

Title	Filing Stage	Application Number	Priority Date	Inventors
Method and apparatus for mass spectrometry analysis using surface acoustic waves	Provisional	UND-2011-012 (filed in US by University of Notre Dame)	Jan 3, 11	Hsueh-Chia Change, David Go, Jenny Ho, James Friend, Leslie Yeo
Microfluidic apparatus for the atomization of a liquid	PCT	PCT/AU2010/000548	May 11, 09	James Friend, Leslie Yeo, Aisha Qi, Jenny Ho, Anushi Rajapaksa, David Morton, Michelle McIntosh
Concentration and dispersion of small particles in small fluid volumes using acoustic energy	National Phase	PCT/AU2007/000576	26-September-07	J. Friend; L. Yeo

Figure 6: The computer aided drawings showing several views of both the small and the large casings for Respire®



- (a) Front view including small and the large casings.
- (b) Cross section view of both casings where the red circle showing the drug dispenser.
- (c) A close up view of components in smaller casing, circled in red in image (b).

Monash University owns the IP rights to this technology. V-Patch systems have been licensed worldwide rights to the manufacture and use of the Respire® technology limited to the administration of medicaments for the treatment of diabetes. This agreement is the result of when commercialisation rights to the technology were held by NanoVentures. The agreement has since been novated to Monash University.

4.4 Other Advantages

The technology can also have potential applications in:

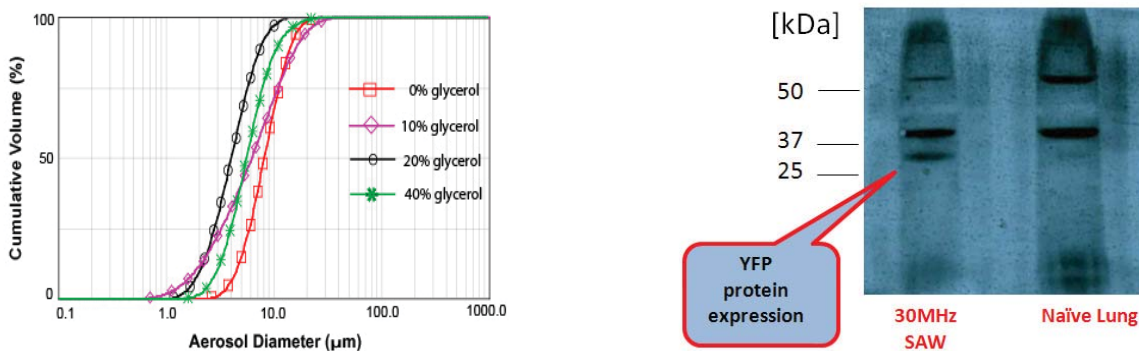
- Analytical chemistry
 - Mass spectroscopy for enhanced detection of heavy metals in drinking water and drugs in human blood for example.
 - Direct interface with microfluidics devices, for RT-LAMP PCR and ELISA on-a-chip to enable rapid detection of biologically relevant chemicals and processes.
- Industrial
 - Polymer nanoparticle generation for drug delivery, including solid crystalline forms of proteins and peptides for injection and skin microneedle patch delivery, multilayer particles for targeted delivery and delayed release of up to two months.
- Production of monodisperse, nonsedimenting aerosol mists of antibiotics for general disinfection in hospitals, fragrances and chemicals for air fresheners.

4.5 Future Direction and Hurdles

More recently, a study was conducted by the research team whereby monodispersed aerosol-laden plasmid DNA were produced using the Respire® system within a defined size range (0.5-5 µm) suitable for efficient pulmonary delivery to the lower respiratory airways for optimal dose efficacy (See Figure 7 (a)). Due to the extremely efficient transfer of acoustic radiation from the substrate into a drop comprising the DNA solution, the drop interface is rapidly destabilized and breaks up to form micron dimension aerosol droplets containing the DNA. A solution containing a plasmid DNA (pDNA) vector encoding a potential malaria vaccine candidate, 45 kDa merozoite surface protein 4/5 (MSP4/5), was nebulized using both 20 and 30 MHz SAW devices. High levels

of gene expression was observed in western blots from in vitro experiments conducted using COS-7 cells that were transfected with the condensed post-nebulized DNA. Further, in vivo gene expression of a condensed, un-protected plasmid DNA encoding a Yellow Florescent Protein (YFP) collected following SAW nebulization was observed in mouse lung epithelial cells, when delivered via intratracheal instillation (See Figure 7 (b)) . These, together with a low power requirement (typically 1 W) demonstrate the potential of the technology as a portable pulmonary delivery platform for gene therapy and DNA vaccination.

Figure 7: Respire for the delivery of pDNA (plasmid DNA) to the lung showing promising results for both aerosol size requirements and bioactivity



(a) Cumulative size distribution obtained from the nebulisation of 100 µg/ml pDNA with different glycerol weight ratios using a 30 MHz SAW device with SPUDTs under 3 W of applied RF power. The aerosol droplet diameters were measured by laser diffraction.

(b) Western blot YFP expression in the supernatant obtained from homogenized mice lungs harvested 24 hrs post-transfection with the condensed VR1020-YFP plasmid, previously nebulised using a 30 MHz SAW device (left lane) compared to that of an untreated mouse lung (right lane).

Despite, DNA vaccines being a third generation of new vaccines for humans, are either still in pre-clinical development or in early stage clinical trials, awaiting successful demonstration of its safety and immunogenicity in human clinical trials. In fact, the DNA vaccine market is so young that the global market for these vaccines is expected to increase from \$193.2 million this year to more than \$2.7 billion in 2014, for a five-year compound annual growth rate of 69.5%²⁸. So it is only in time

²⁸ DNA Vaccines: Technologies and Global Markets, Available at [online] <http://www.bccresearch.com/report/dna-vaccines-markets-bio067a.html> [28th September 2011], (2009).

that the successful nebulizer platform such as the SAW nebulizer could reap the benefits of being able to deliver highly sorted after vaccines of the future.

5 Competition

The use of SAW nebulisation will compete with existing nebulisers on the market that use a range of mechanisms to create a vapour, including jet nebulisation, ultrasonic wave nebulisation and ultrasonic vibrating mesh nebulisation.

5.1 Key Market Players

Key players operating in the marketplace in addition to those mentioned above include 3M Drug Delivery Systems Division, Akela Pharma Inc, Alkermes Inc, Aradigm Corporation, Inc, Chiesi Farmaceutici SpA, Consort Medical Plc, Dey Pharma L.P., Graceway Pharmaceuticals LLC, Oriel Therapeutics Inc, Sepracor Inc, SkyePharma Plc, Valois S.A.S., and Vectura Group Plc, among others.

The major competitors for Respire® are nebulisers on the market and produced by developers such as:

- Pari Pharma GmbH
- Aerogen
- Omron

Omron is a large medical device company, while Aerogen and Pari Pharma are specialty pharma/biotech companies focused on developing drugs and delivery devices for treating lung disorders.

5.2 Competitive Advantages of Respire®

The use of SAW technology has several distinct competitive advantages over these technologies that may align these devices with suitable drugs for inhalation. The competitive advantages of the SAW nebuliser are summarised below:

- Delivery of a broad variety of peptides and nucleic acids (NA) without the risk of shear damage
- Mean droplet size (250 nm-10 µm) adjustable through formulation optimization (viscosity/surface tension)
- Tailorable delivery time during inhalation cycle with atomization on demand (on/off in 30 ms)
- No mesh or orifices to clog with product: a *solid-state* nebulizer

None of the companies above produce devices that have the competitive advantages of the SAW Respire® technology for the delivery of peptides and NAs. As such, these companies are potential natural acquirers as well as competitors.

The researchers have developed a predictive comparator table based on Respire® data and disclosed data from various publications regarding competitor devices as outlined in Table 5 below.

Table 5: Comparative Overview of inhaler devices

	Mechanism	MMAD ¹	Aerosol output rate	Lung Deposition Efficiency	Aerosol deposition rate	Residual volume	Power Consumption	Approximate Price
GSK Advair Diskus®	Dry powder inhaler	NA	NA	8-30%	NA	NA	Mechanical: breath actuated	~US\$80-150
Pari LC® & Proneb® Ultra Compressor	Jet nebuliser	3-5 µm	0.2-0.3 ml/min	~23%	9 mg/min	>1.2 ml	Proneb: 98 W, mains	LC: ~US\$20 Proneb: ~US\$90
Omron MicroAir® NE-U22V	Ultrasonic (180 kHz); Static mesh	4-7 µm	0.2-0.3 ml/min	~35%	6.6 mg/min	0.3 ml	1.5 W, battery	~US\$260
Aerogen Aeroneb® Go	Vibrating mesh (128 kHz)	3-5 µm	0.3-0.5 ml/min	~24%	37.1 mg/min	0.3-0.9 ml	< 2 W, battery	~US\$400
Pari eFlow® Rapid	Vibrating mesh (117 kHz)	3-5 µm	0.3-0.7 ml/min	~25%	5 mg/min	>1.2 ml	2 W, battery	~US\$1000
Respire®	SAW (10-100 MHz)	~2-5 µm	0.1-0.15 ml/min	~70-80%²	~10-50 mg/min³	NA	1-2 W, battery	NA

¹ Mass median aerodynamic diameter

² Twin-stage impinger data

³ Estimated from lung deposition efficiency (twin-stage)

Other potential additional advantages associated with the Respire technology could also be noted,

- Inexpensive materials that rely on scalable IC production techniques
- Instantaneous atomization, from zero to full-power atomization in 20 microsec.
- Ability to work with small fluid samples (down to 1 µl)
- Hand-held battery powered technology
- Clog-free atomization from an inert surface
- Adjustable nebulisation rates from 0.001-1 ml/min
- No heat associated degradation of drugs.

These competitive advantages are significant and align this delivery system technology with potential partners looking to deliver protein/peptide or NA drugs from liquid formulations into patients using novel formulations.

6 Development and Objectives Plan

Monash would envisage that through addressing some minor technical milestones, the technology will be essentially ready for a partnering deal with a pharma/biotech or medical device partner that seeks to treat lung specific diseases for a licensing exit. SAW forms drug aerosols via SAW atomization combined with a paper-based microfluidic drug supply scheme in a handheld unit. The Respire® device will accommodate patient variability in inhalation profiles and dosage needs. It can be developed into a platform for the delivery of drugs suitable for discreet use by a patient with COPD and other lung disorders or for systemic delivery of select drugs via the lungs. The technology has additional potential competitive advantages that are likely to arise as the device is developed into a clinically useful product.

6.1 Project Milestones

Preliminary milestones for the first tranche of the project are outlined below. These comparative studies are likely to be a minimal requirement for attracting a partner and seek to test the competitive advantages of the SAW technology directly against competitor devices to exemplify its claims. These studies are then likely to be repeated by the partner using its proprietary formulations prior to *in vivo* animal model testing.

Comparative study of SAW nebulisation against the Pari LC Plus and AeronexGo using glycerol formulation for atomisation of pDNA and protein (BSA) per ISO 27427:2010, swapping albuterol for the target drug.

Proposed schedule

1. Emitted dose, dose uniformity, and emitted fraction analysis

- *Fine particle dose and fraction below 5.0 μm (FPF5.0), for Next Generation Impactor (NGI), Anderson Cascade Impactor (ACI) and Malvern Spray Diffraction System.*
- *Fine particle dose and fraction below 3.0 μm (FPF3.0), for NGI only*

2. Aerodynamic particle size: median mass aerodynamic diameter (MMAD) analysis

3. Mass balance for NGI runs

4. DNA/protein ex-vivo degradation assessment

5. Optimisation of Formulation(s) based on results

Milestone: SAW nebulisation produces equivalent/improved performance in aerosol formation when compared with incumbent nebulisers in absence of degradation of peptide/NA in formulations.

Development of a battery-powered portable, handheld circuit suitable for controlling the Respire® SAW nebuliser

Proposed schedule

1. Circuit designed to accommodate small rechargeable Li battery for several hour operation of the nebulizer, 3 x 3cm format, incorporating space for mounting SAW device and according to ISO 27427 standards regarding electrically driven nebulisers.

2. Documentation appropriate for mass production of circuit, including bills of materials, PCB layouts, schematics, etc.

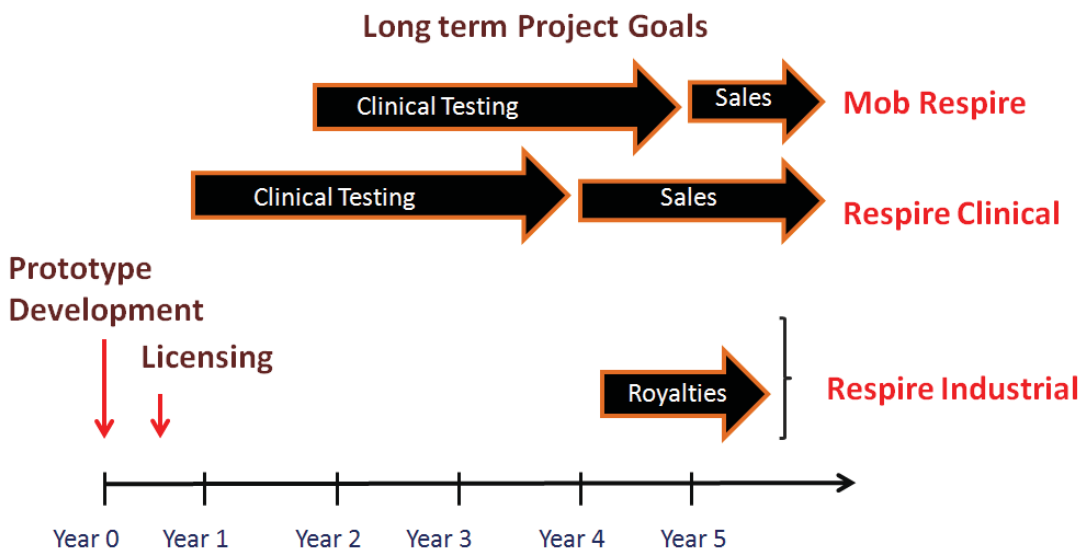
3. Twenty-four functioning prototype circuits.

Milestone: Operating handheld nebuliser devices, unenclosed.

Subsequent tranches of funding will need to be directed towards development of the commercial prototype with enclosures and user interfaces per regulatory standards, all towards a clinically useful device. However, this is likely to be best done in collaboration with a partner organisation at a later stage.

6.2 Product/Technology Licensing Pipeline

Figure 8: Product/Technology licensing pipeline



The four main products that encompass the Respire® technology proposed were Respire Clinical, Respire Industrial, Mob Respire and Gen Respire. Except for the Respire Clinical, Respire Industrial, the completion of the portable circuit development is mandatory for the Mob Respire and Gen Respire. Hence the prototype development together with full characterisation of performance *in-vitro* of the Respire® system is to be conducted by the end of year 1 (See Figure 8).

Pharmacokinetics and pharmacodynamics data that dictates the underlying operation of the Mob Respire and the Respire Clinical would be established before the clinical testing would commence to establish the efficacy and safety data. Performance in clinical studies, including testing of devices

returned for failure and testing of a portion of devices at end of trial for *in vitro* performance would also be conducted.

The Respire Clinical system for the treatment of Asthma in clinical setting could be implemented in the market by year 4. Starting with low volume sales, growth in sales could be expected until the end of year 5, if “penetration pricing strategies” are adopted, where a strategically low price could be set initially in order to gain access to the market. In year 2, we will also commence clinical testing of the Mob Respire with (Ventolin®) system in preparation for launch into the market in year 5.

In year 1, co-partners for the industrial application of the “Respire Industrial” system would be sorted after and a licensing deal to be made with an initial cash injection followed by 20% royalty rate at progressive years if drugs successfully enters \$16bn market using the proprietary technology.

The product, Gen Respire is not considered in this five year product pipe line due to the relatively young market share currently available coupled with the high risks. Significant amounts of cash investments would be necessary for the completion of clinical trials associated with the validation of the Gen Respire together with a DNA vaccine with potential risks associated with the successful demonstration of safety and immunogenicity. However, minor Research and development activities with existing collaborations could be conducted during the five year period.

6.3 Project Funding

Portable Circuit Development

Portable circuit development: six months to produce 12 handheld prototype driver circuits for the nebuliser and all required documents for subsequent mass production (bills of materials, PCB layouts, schematics, etc.): \$62K.

Dave Blau Consulting, Campbell, CA USA (<http://www.blauproductdevelopment.com/>)

- Hardware: custom circuit boards, components, batteries: \$30K
- Consultant time for circuit design and engineering team’s fabrication of devices

- Dave Blau 8.5 weeks at 35h/week, \$200/h: \$60K
- Engineering team for assembly/limited run of 24 drivers: \$12K

Pharmacokinetics and Pharmacodynamics Evaluation

Comparative study of SAW nebulization using pDNA and protein (BSA) against potential competitors using US FDA and EU: \$99K.

- Post-doc expert, Dr Aisha Qi, to conduct work, 6 months at 100%FTE including 35.86% on-costs: \$55K
- Consumables for project, including SAW device fabrication and custom mounting for impactors, assay costs: \$20K
- Access to impactors and droplet sizing equipment for nebulization device comparison. The Malvern laser diffraction system provides precision data on droplet size distribution and number at exit of device. The Anderson and next-generation impactors are classical and modern sizing systems generally accepted by regulatory authorities (USP and the Ph.Eur.) to assess droplet size for inhalation. Note the impactors will be operated per ISO 27427:2010.
 - School of Pharmacy, Monash University: Anderson Impactor and [Malvern Spray Laser Diffraction](#) system. Proposed cost for access: \$50/h x 280h total = \$14K
 - [Paul Young](#), Pharmaceuticals, University of Sydney: [Next-Generation Impactor](#). Proposed cost for access: \$75/h x 100h total + room and board for Aisha for 2wk (\$250/day x 10 days) = \$10K

6.4 Clinical Testing and Small scale Product Manufacture

Clinical testing could be conducted by establishing collaborations with the medical researchers in a hospital setting. An ARC linkage grant or some local venture capital funding could be used to support the costs of such a randomized controlled trial.

Small scale product manufacturing could be implemented via contracting a company such as MiniFAB (<http://www.minifab.com.au/>) based in Melbourne with extensive experience in the development of lab-on-a-chip microfluidic systems, disposable cartridges for point of care diagnostics, micro and nano engineered medical devices and systems such as the Respire®

system. Once, the products, Respire Clinical and Mob Respire is launched into the market, a small warehouse could be rented in order to store and power sources (bought elsewhere) required for the operation of the device.

7 The Business Model and Market Engagement strategy

7.1 Successful Business Models

A review of successful business models in the drug delivery to the lung market segment suggests that there is a need to develop a lung drug delivery device in close association with a specific drug technology. This drug is then used to exemplify the efficacy of the device. The device is then used by additional companies that seek to match their drugs with devices already in clinical use.

Successful companies that specifically make Nebulisers combine their delivery technologies with drugs from biotech and large pharmaceutical companies such as:

- **Pari Pharma GmbH** (Proprietary devices and formulations – partnered devices and formulation services with Genzyme/Sanofi Aventis, Genentech, AstraZeneca, Novartis and Gilead)
- **Vectura Group plc** (proprietary formulations and devices – partnered devices and formulations with Boehringer Ingelheim, Merck, Novartis, Sandoz, GSK, Baxter and others)
- **Aerogen** (Proprietary devices – partnered nebulization device with Dance Pharma)
- **MAP Pharma** (proprietary formulation and pMDI)
- **Nektar** (proprietary Liquid Inhalation technology and a DPI)

Successful biotech companies that have licensed devices to deliver their new formulations include:

- **MPEX Pharmaceuticals** (Proprietary formulation and Pari E-Flow Nebuliser – recently acquired by Axcan)

A review of transactions in this space has revealed that deals involving proprietary drugs and devices attract high exit values that acquisition/in-licensing of devices alone (See *Table 6*).

Table 6: Pulmonary Administered Drug/Nebuliser Deals

Company/Partner Device Year	Upfront Payment	Milestones	Stage of Development	Rights Transected (Regions)
Mpex / Axcan PARI eFlow Nebulizer System 2011	6 million	1.5 million + 10 million and up to 195 million	phase III clinical	Aeroquin an aerosol formulation of levofloxacin (cystic fibrosis-associated lung infection) (World)
Elevation/PARI GmbH PARI eFLOW Nebulizer System 2010	Undisclosed	Undisclosed		EP-101--is a long-acting bronchodilator targeted at patients with chronic obstructive pulmonary disease. Elevation partnered with PARI Pharma for development of EP-101 in combination with an investigational eFlow nebulizer customized to deliver Elevation's drug candidates. (N/D)
Sepracor/ Arrow International Ltd Ultrasonic Nebulizer 2008	\$250,000	up to \$22.5 million milestone and further royalties		IP rights for stable sterile steroid suspension formulations and other nebule technology for the use in developing ciclesonide, a corticosteroid for asthma and COPD (World http://www.fiercebiotech.com/press-releases/sepracor-and-arrow-sign-global-license-and-development-agreement)
Nektar/Aerogen Jet Nebuliser 2005	32 million (\$8 million in cash, \$24 million in stock)	Undisclosed		buys advanced inhaleable liquid drug technologies from Aerogen. (N/D)
Aerogen/Biota Aeroneb Go nebulizer 2005				The company has an agreement with Biota Holdings, Ltd. for the development of CS-8958, a long-acting neuraminidase inhibitor for use with Aerogen's proprietary Aeroneb Go. The development work will be funded under a US\$5.6 million grant to Biota from the US National Institutes of Health (NIH). (N/D)

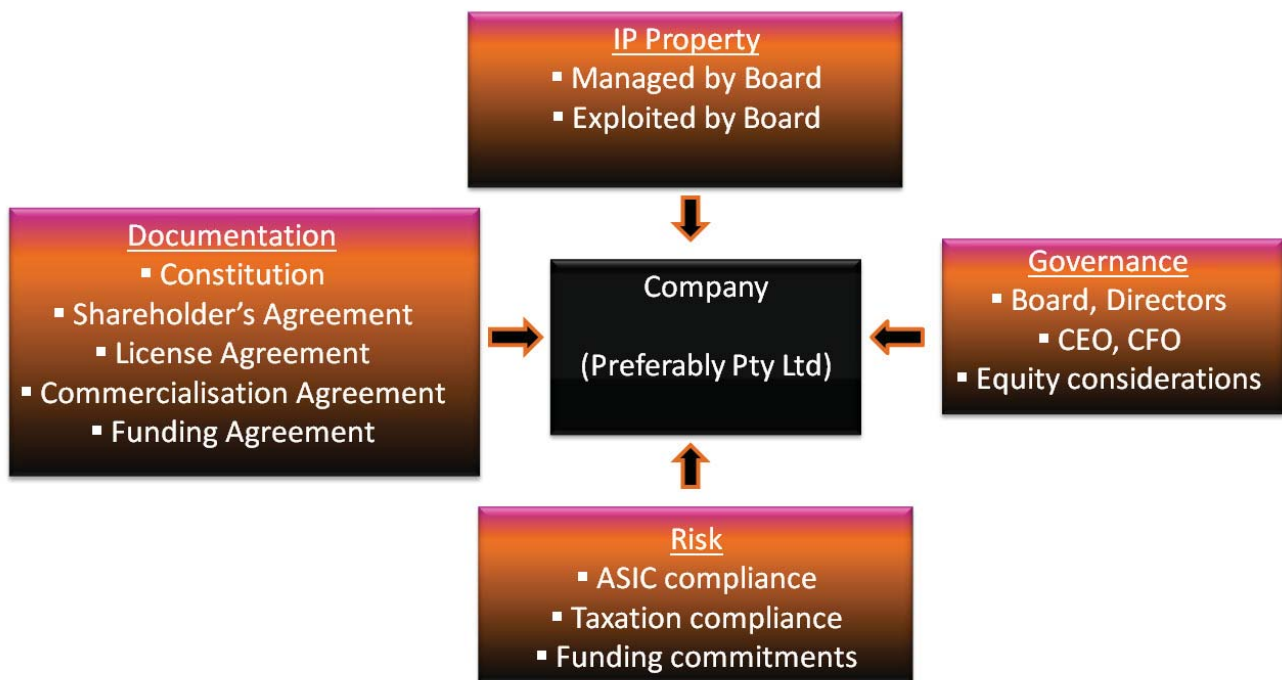
7.2 Market Entry

As such, three paths to market can be considered:

1. License the SAW to the current nebulisation device developers; or
2. Partner with a pharma/biotech company that requires the competitive advantages of the SAW devices in order to develop a key drug in its pipeline.
3. Formation of an independent spin-out company- a number of factors such as IP property management, Governance, Risk Management and Documentation need to be considered (See *Figure 9*)

To achieve either of these exit/partnership options, Monash must develop this technology to a proximal value inflection point through the achievement of technical milestones that will allow a partnership deal with a suitable partner to be executed.

Figure 9: Factors for consideration during the formation of a spin-out company



7.3 Potential purchasers: vertical and horizontal options?

The potential partners or natural acquirers depend on the path to market.

A 'low hanging fruit' approach would be to execute an exclusive license deal with Pari Pharma GmbH, Aerogen or Omron, or potentially other medical device manufacturers that distribute Omron devices such as GE Healthcare or Philips (Respronic). This is likely to be a lower risk/low reward approach.

An alternate approach is to partner the SAW technology with a biotech/pharma company developing a drug(s) that require the competitive advantages of the SAW technology around

delivery of NA's /peptides and the ability to control/generate novel formulations. Under this scenario, initial capital funding could be used to fund the development of the SAW technology within a small venture backed entity with outstanding management and compatible technology. In this latter case, the potential purchaser is likely to be an acquirer of the venture backed company.

7.4 Exit Options

The strategy for the Respire® opportunity is to achieve some preliminary technical milestones and partner with either a pulmonary device developer or a suitable biotech or pharmaceutical company that is able to match a drug in development in its pipeline against a pulmonary indication, with the competitive advantages of Respire®.

The nature of the final exit for the opportunity and its investors will be dependent on the balance sheet of the partner at the time of the partnership deal and the nature of the partnership arrangement. If a device developer or a small biotech acquires the rights to the technology, any exit for investors will be linked to the success of the program and a trade sale/partnering of that company/asset to a large pharmaceutical company.

8 The Finance and Revenue Model

All estimates for the financials are conservative and are based on available industry averages and the assumption that the cash investment of 365k will be acquired and a licensing deal is made with a co-partnering drug developing pharmaceutical company.

There is a negative cash position in both years 2 and 3 due to estimated costs incurred for the clinical trials for Mob Respire and Respire Clinical (See *Figure 10 and Table 7*). Recovery is soon observed for years 4 and 5 with estimated sales revenue with increasing cash inflows. Importantly, the development of the Respire technology projected a net present value of over \$14M, with a payback period of around 4 years. Hence the investment can be seen to bring immense future benefit for the inventors and licensee.

Figure 10 : Cash Flows for the product development of Respire®

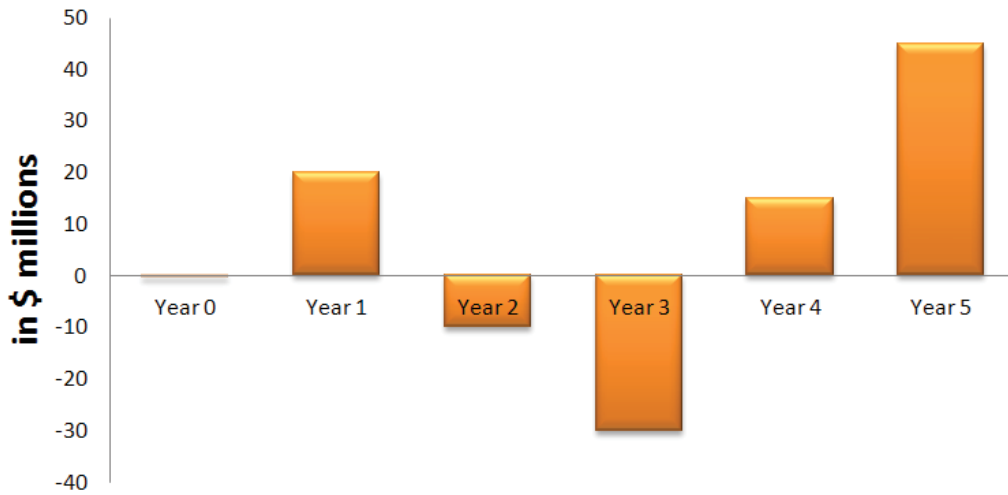


Table 7: Table showing the future projections of Cash Flows for the Respire® project

in \$ millions	Year 0	Year 1	Year 2	Year 3	Year 4	Year 5
Revenue						
Licensing (Respire Industrial)		30				
Royalty payments (Respire Industrial)					10	30
Sales (Mob Respire)						10
Sales (Respire Clinical)					10	20
Expenses						
Prototype development	-0.365					
Clinical testing costs for (RespireClinical + Mob Respire)		-10	-10	-25		
Product manufacture (Mob Respire + RespireClinical)					-5	-15
Regulatory approval costs				-5		
Administrative expenses		-0.01	-0.01	-0.01	-0.01	-0.01
Cash at beginning		-0.365	20	-10	-30	15
Cash at end	-0.365	20	-10	-30	15	45
Gross Profit	-0.365	19.99	-10.01	-30.01	14.99	44.99
Investments Required	0.365					
NPV(@ r=20%)	\$14.43					

8.1 Costing of the Respire® Nebulizer

Once the fixed costs such as clean room usage for device fabrication (access, mask aligner use, metal sputtering and dicing of the wafers) and variable costs such as costs of the casing and cost of an example drug (in this case Ventolin®) is taken into account the total cost per device was estimated to be around \$15, with a small profit margin of 25% (See Table 8).

Table 8: Cost of manufacture per device and the proposed selling price

Item	Cost
Fixed Costs (for 500 devices)	
Clean room wafers (SSP, 4 inch, LN wafers, 128YX saw grade 25 (10 wafers)	\$750
Chemical and other Materials (10 wafers = 500 devices)	\$100
Clean room access costs (@ \$50 ph for 10 hours)	\$500
Mask Aligner (\$100 ph for 2 hours)	\$200
Sputtering (\$100 ph for 2 hours)	\$200
Dicing (\$75 ph for 1 hour)	\$75
Technicians wage (2 days @ \$50 ph)	\$800
Reusable Power Pack (50 to be leased @ \$50)	\$2500.00
Variable Costs	
Casings (\$2 per case)	\$400
Cost of Drug (Ventolin® Ampoules 2.5mg-2.5ml - 100 Amps)	\$400
Total manufacturing costs	\$5,925
Cost per device (500 devices in total)	\$11.85
Profit margin (below industry average)	25%
Selling price (per disposable device)	\$14.81

9 Project Risk Assessment

Inhaled drugs are increasingly being developed for systemic use in non-pulmonary diseases such as chemotherapy-driven fatigue, diabetes, Parkinson's disease, and pain. Reasons behind this include improved patient acceptance and compliance, especially when offering an alternative to injectable drugs and a faster onset of action. However, the market failure of Pfizer's inhaled dry powder insulin, Exubera, illustrates the difficulties in choosing the appropriate drug for pulmonary delivery. Disadvantages such as low reproducibility, high costs and unknown long-term safety can be major barriers to successfully launching such products. As such, while Monash has an agreement with V-Patch, it does not see companies developing pulmonary delivered drugs for systemic delivery as an ideal partner.

9.1 Current Issues

The major current issues are:

- Lack of a partner pharma/biotech drug development partner to exemplify the utility of the device.
- Early stage of technology development with respect to commercial milestones.
- Incomplete development of a hand held, battery powered prototype that would be suitable for a clinical trial and likely to be required for a partnership deal.

Due to these issues, the following key risks to delivering milestones are identifiable in the short term are identifiable along with key long-term issues that could potentially affect the progress are also summarised (See *Table 9*).

Table 9: Keys short term and long term risks associated with Respire®

Issue	Probability of Risk	Impact on Progress
Short-term		
Particle size data does not directly compete with competitors to allow efficient deep lung delivery	Low	High
High viscosity formulations do not support the administration of potential protein/NA based medicaments	Medium	High
Technical aspects of the device do not support a hand held portable nebulizer	High	High
Management/Personnel	High	High
Partnering/Financing Risk	High	High
Long-term		
Demographic Shifts (effects of an ageing population)	High	High
Distribution Channels (internet dealer market space)	High	High
Health Care Cost Containment (Governments and other regulatory authorities)	High	High
Increased Demand for Home Care Products	High	High

9.2 Proposed Mitigation Strategy

The following mitigation strategies can be implemented,

1. The technical milestones will mitigate this risk.
2. Identify a partner with a specific drug formulation to then test this formulation *in vitro* (repeat of the technical milestones stated above) and in an animal model.
3. This technical risk may need to be assessed and mitigated by a suitably qualified external advisor.
4. The identification of a potential partner will be mitigated through achievement of the technical milestones and business development skills of the management.

Since Monash University does not have in house skills to drive commercial development/project management of inhalation drug devices. There are skilled people that are or could be involved in the project as advisors (including Dr. David Morton – co-founder of Vectura).

Appendix A: Discovery

An outline of the historical events that led to the discovery of the Respire® system are shown below.

Figure 11: Brief Historical list of events that led to the discovery of Respire®

Date	Milestone
2001-3	Initial studies on SAW atomisation phenomena, high risk low commitment effort.
2005	Discovery of means to form polymer nanoparticles 10-100 nm in diameter using MHz-order atomisation and evaporation.
2007-8	First papers on SAW atomisation to form protein aerosols and nanoparticles via SAW atomisation (these reporting the results of work in our group). (Generation 1 device)
2008	Explanation of mechanism of SAW atomisation using novel measurement and analysis techniques.
2009	First publication on Respire platform system and its ability to deliver nebulised mists of salbutamol. (Generation 2 device)
2010	First publication on Respire platform showing ability to deliver mists of proteins (ovalbumin and bovine serum albumin) and cells (yeast) (nebulised)

Bibliography

- [1] J. A. Mikszta, J. B. Alarcon, J. M. Brittingham, D. E. Sutter, R. J. Pettis, and N. G. Harvey, “Improved genetic immunization via micromechanical disruption of skin-barrier function and targeted epidermal delivery,” *Nature Medicine*, vol. 8, no. 4, pp. 415–419, 2002.
- [2] A. Qi, L. Yeo, and J. Friend, “Interfacial destabilization and atomization driven by surface acoustic waves,” *Physics of Fluids*, vol. 20, p. 074103, 2008.
- [3] J. Birchall, “Pulmonary delivery of nucleic acids,” *Expert Opinion on Drug Delivery*, vol. 4, no. 6, pp. 575–578, 2007.
- [4] B. Ferraro, M. P. Morrow, N. A. Hutnick, T. H. Shin, C. E. Lucke, and D. B. Weiner, “Clinical applications of DNA vaccines: Current progress,” *Clinical Infectious Diseases*, vol. 53, no. 3, pp. 296–302, 2011.
- [5] S. Jose, “Pulmonary drug delivery technologies - global strategic business report,” tech. rep., Global Industry Analysts, Inc., 2010.
- [6] L. Oversteegen, “Inhaled medicines: Product differentiation by device,” *Innovations in Pharmaceutical Technology*, 2008.
- [7] “Inhaler technique in adults with asthma or COPD: Information paper for health professionals,” tech. rep., 2008.

- [8] D. Lu and A. Hickey, "Pulmonary vaccine delivery," *Expert Review of Vaccines*, vol. 6, no. 2, pp. 213–226, 2007.
- [9] E. Arulmuthu, D. Williams, H. Baldascini, H. Versteeg, and M. Hoare, "Studies on aerosol delivery of plasmid DNA using a mesh nebulizer," *Biotechnology and Bioengineering*, vol. 98, no. 5, pp. 939–955, 2007.
- [10] P. Barnes, "New treatments for chronic obstructive pulmonary disease," *Current Opinion in Pharmacology*, vol. 1, pp. 217–222, 2001.
- [11] A. Melani, D. Zanchetta, N. Barbato, P. Sestini, C. Cinti, P. Canessa, S. Aiolfi, and M. Neri, "Inhalation technique and variables associated with misuse of conventional metered-dose inhalers and newer dry powder inhalers in experienced adults," *Annals of Allergy, Asthma & Immunology*, vol. 93, no. 5, pp. 439–46, 2004.
- [12] N. A. Doria-Rose and N. L. Haigwood, "DNA vaccine strategies: candidates for immune modulation and immunization regimens," *Methods*, vol. 31, no. 3, pp. 207–216, 2003.
- [13] S. Shiokawa, Y. Matsui, and T. Ueda, "Liquid streaming and droplet formation caused by leaky rayleigh waves," in *Ultrasonics Symposium, 1989. Proceedings., IEEE 1989*, vol. 1, pp. 643–646, 1989.
- [14] A. Qi, J. Friend, L. Yeo, D. Morton, M. McIntosh, and L. Spiccia, "Miniature inhalation therapy platform using surface acoustic wave microfluidic atomization," *Lab on a Chip*, vol. 9, no. 15, pp. 2184–2193, 2009.
- [15] C. Colin, *Surface Acoustic Wave Devices for Mobil and Wireless Communications*. Academic Press, Inc., 1998.
- [16] J. West and D. M. Rodman, "Gene therapy for pulmonary diseases," *Chest*, vol. 119, no. 2, pp. 613–617, 2001.

- [17] M. Bivas-Benita, T. Ottenhoff, H. Junginger, and G. Borchard, "Pulmonary DNA vaccination: concepts, possibilities and perspectives," *Journal of Controlled Release*, vol. 107, no. 1, pp. 1–29, 2005.
- [18] S. H. E. Kaufmann, "Front matter," in *Novel Vaccination Strategies* (S. H. E. Kaufmann, ed.), 2004.
- [19] A. K. Abbas and A. H. Lichtman, *Basic Immunology: Functions and Disorders of the Immune System*. Philadelphia: Saunders, 3 ed., 2009.
- [20] "Landscape analysis: Trends in vaccine availability and novel vaccine delivery technologies: 2008-2025," tech. rep., World Health Organisation, 2009.
- [21] E. L. Giudice and J. D. Campbell, "Needle-free vaccine delivery," *Advanced Drug Delivery Reviews*, vol. 58, no. 1, pp. 68 – 89, 2006.
- [22] Y. Lentz, T. Anchordoquy, and C. Lengsfeld, "Rationale for the selection of an aerosol delivery system for gene delivery," *Journal of Aerosol Medicine*, vol. 19, no. 3, pp. 372–384, 2006.
- [23] E. Arulmuthu, D. Williams, and H. Versteeg, "The arrival of genetic engineering the arrival of genetic engineering strategies for delivery of nonviral plasmid DNA-based gene therapy," *Engineering in Medicine and Biology Magazine, IEEE*, vol. 28, no. 1, pp. 40–54, 2009.
- [24] J. Holmgren and C. Czerkinsky, "Mucosal immunity and vaccines," *Nature Medicine*, 2005.
- [25] S. D. Xiang, A. Scholzen, G. Minigo, C. David, V. Apostolopoulos, P. L. Mottram, and M. Plebanski, "Pathogen recognition and development of particulate vaccines: Does size matter?," *Methods*, vol. 40, no. 1, pp. 1–9, 2006.

- [26] T. Ebensen, C. Link, and C. A. Guzman, “Classical and novel vaccination strategies: A comparison,” in *Novel Vaccination Strategies* (S. Kaufmann, ed.), Weinheim: Wiley VCH GmbH and Co. KGaA, 2004.
- [27] “Hundreds of gene therapy experiments failed,” tech. rep., BBC News Sci/Tech, 2000.
- [28] R. D. Blake and S. G. Delcourt, “Thermal stability of DNA,” *Nucleic Acids Research*, vol. 26, no. 14, pp. 3323–3332, 1998.
- [29] M. A. Liu, B. Wahren, and G. B. K. Hedestam., “DNA vaccines: Recent developments and future possibilities,” *Human Gene Therapy*, vol. 11, pp. 1051–1061, 2006.
- [30] M. A. Liu, “DNA vaccines: a review,” *Journal Of Internal Medicine*, vol. 253, no. 4, pp. 402–410, 2003.
- [31] P. Wilson, “Giving developing countries the best shot: An overview of vaccine access and r&d,” tech. rep., Global Alliance for Vaccines and Immunization (GAVI), 2010.
- [32] WHO, “Injection safety,” tech. rep., World Health Organisation Media centre, 2006.
- [33] “Priority technologies and operational strategies to increase access to immunization,” tech. rep., Global Alliance on Vaccines and Immunization (GAVI), 2002.
- [34] E. Maggio, “Noninvasive delivery offers opportunities for large and small pharma,” tech. rep., Life Science Leader, 2012.
- [35] R. M. Jacobson, A. Swan, A. Adegbenro, S. L. Ludington, P. C. Wollan, and

- G. A. Poland, "Making vaccines more acceptable—methods to prevent and minimize pain and other common adverse events associated with vaccines," *Vaccine*, vol. 19, no. 17-19, pp. 2418–2427, 2001.
- [36] "Prescribing information for influenza A (H1N1) 2009 monovalent vaccine live, intranasal," tech. rep., Food and Drug Administration:Center for Biologics Evaluation and Research, 2009.
- [37] S. van Drunen and L. V. den Hurk, "Novel methods for the non-invasive administration of DNA therapeutics and vaccines," *Current Drug Delivery*, vol. 3, no. 1, pp. 3–15, 2006.
- [38] H. Fan, Q. Lin, G. R. Morrissey, and P. A. Khavari, "Immunization via hair follicles by topical application of naked DNA to normal skin," *Nature Biotechnology*, vol. 17, no. 9, pp. 870–872, 1999.
- [39] A. Udvardi, I. Kufferath, H. Grutsch, K. Zatloukal, and B. Volc-Platzer, "Uptake of exogenous DNA via the skin," *Journal of Molecular Medicine*, vol. 77, no. 10, pp. 744–750, 1999.
- [40] W. H. Yu, M. Kashani-Sabet, D. Liggitt, D. Moore, T. D. Heath, and R. J. Debs, "Topical gene delivery to murine skin," *Journal of Investigative Dermatology*, vol. 112, no. 3, pp. 370–375, 1999.
- [41] M.-J. Kang, C.-K. Kim, M. Y. Kim, T. S. Hwang, S. Y. Kang, W.-K. Kim, J. J. Ko, and Y.-K. Oh, "Skin permeation, biodistribution, and expression of topically applied plasmid DNA," *The Journal of Gene Medicine*, vol. 6, no. 11, pp. 1238–1246, 2004.
- [42] A. Domashenko, S. Gupta, and G. Cotsarelis, "Efficient delivery of transgenes to human hair follicle progenitor cells using topical lipoplex," *Nature Biotechnology*, vol. 18, no. 4, pp. 420–423, 2000.

- [43] R. Langer, "Transdermal drug delivery: past progress, current status, and future prospects," *Advanced Drug Delivery Reviews*, vol. 56, no. 5, pp. 557–558, 2004.
- [44] A. G. Doukas and N. Kollias, "Transdermal drug delivery with a pressure wave," *Advanced Drug Delivery Reviews*, vol. 56, no. 5, pp. 559–579, 2004.
- [45] S. Mitragotri and J. Kost, "Low-frequency sonophoresis: A review," *Advanced Drug Delivery Reviews*, vol. 56, no. 5, pp. 589–601, 2004.
- [46] M. R. Prausnitz, "Microneedles for transdermal drug delivery," *Advanced Drug Delivery Reviews*, vol. 56, no. 5, pp. 581–587, 2004.
- [47] J.-M. Song, Y.-C. Kim, E. O. R. W. Compans, M. R. Prausnitz, and S.-M. Kang, "DNA vaccination in the skin using microneedles improves protection against influenza," *Molecular Therapy*, vol. 20, no. 7, pp. 1472–1480, 2012.
- [48] X. Chen, T. W. Prow, M. L. Crichton, D. W. K. Jenkins, M. S. Roberts, I. H. Frazer, G. J. P. Fernando, and M. A. F. Kendall, "Dry-coated microprojection array patches for targeted delivery of immunotherapeutics to the skin," *Journal of Controlled Release*, vol. 139, no. 3, pp. 212–220, 2009.
- [49] H. S. Gill, "Cutaneous vaccination using microneedles coated with hepatitis C DNA vaccine," *Gene Therapy*, vol. 17, no. 6, pp. 811–814, 2010.
- [50] H. Gill and M. Prausnitz, "Coating formulations for microneedles," *Pharmaceutical Research*, vol. 24, no. 7, pp. 1369–1380, 2007.
- [51] Y. N. Kalia, A. Naik, J. Garrison, and R. H. Guy, "Iontophoretic drug delivery," *Advanced Drug Delivery Reviews*, vol. 56, no. 5, pp. 619–658, 2004.
- [52] A.-R. Denet, R. Vanbever, and V. Prat, "Skin electroporation for transdermal and topical delivery," *Advanced Drug Delivery Reviews*, vol. 56, no. 5, pp. 659–674, 2004.

- [53] I. Lavon and J. Kost, "Ultrasound and transdermal drug delivery," *Drug Discovery Today*, vol. 9, no. 15, pp. 670–676, 2004.
- [54] J. Hartikka, L. Sukhu, C. Buchner, D. Hazard, V. Bozoukova, M. Margalith, W. K. Nishioka, C. J. Wheeler, M. Manthorp, and M. Sawdey, "Electroporation-facilitated delivery of plasmid DNA in skeletal muscle: Plasmid dependence of muscle damage and effect of poloxamer 188," *Molecular Therapy*, vol. 4, no. 5, pp. 407–415, 2001.
- [55] G. J. Prud'homme, R. Draghia-Akli, and Q. Wang, "Plasmid-based gene therapy of diabetes mellitus," *Gene Therapy*, vol. 14, no. 7, pp. 553–564, 2007.
- [56] L. Zhang, E. Nolan, S. Kreitschitz, and D. P. Rabussay, "Enhanced delivery of naked DNA to the skin by non-invasive in vivo electroporation," *Biochimica et Biophysica Acta (BBA) - General Subjects*, vol. 1572, no. 1, pp. 1–9, 2002.
- [57] A. D. Cristillo, D. Weiss, L. Hudacik, S. Restrepo, L. Galmin, J. Suschak, R. Draghia-Akli, P. Markham, and R. Pal, "Persistent antibody and t cell responses induced by HIV-1 DNA vaccine delivered by electroporation," *Biochemical and Biophysical Research Communications*, vol. 366, no. 1, pp. 29–35, 2008.
- [58] L. A. Hirao, L. Wu, A. S. Khan, A. Satishchandran, R. Draghia-Akli, and D. B. Weiner, "Intradermal/subcutaneous immunization by electroporation improves plasmid vaccine delivery and potency in pigs and rhesus macaques," *Vaccine*, vol. 26, no. 3, pp. 440–448, 2008.
- [59] J. W. Hooper, J. W. Golden, A. M. Ferro, and A. D. King, "Smallpox DNA vaccine delivered by novel skin electroporation device protects mice against intranasal poxvirus challenge," *Vaccine*, vol. 25, no. 10, pp. 1814–1823, 2007.
- [60] Z. Dincer, S. Jones, and R. Haworth, "Preclinical safety assessment of a DNA vaccine using particle-mediated epidermal delivery in domestic pig, minipig and

- mouse,” *Experimental and Toxicologic Pathology*, vol. 57, no. 5-6, pp. 351–357, 2006.
- [61] R. J. Drape, M. D. Macklin, L. J. Barr, S. Jones, J. R. Haynes, and H. J. Dean, “Epidermal DNA vaccine for influenza is immunogenic in humans,” *Vaccine*, vol. 24, no. 21, pp. 4475–4481, 2006.
- [62] S. Jones, K. Evans, H. McElwaine-Johnn, M. Sharpe, J. Oxford, R. Lambkin-Williams, T. Mant, A. Nolan, M. Zambon, J. Ellis, J. Beadle, and P. T. Loudon, “DNA vaccination protects against an influenza challenge in a double-blind randomised placebo-controlled phase 1b clinical trial,” *Vaccine*, vol. 27, no. 18, pp. 2506–2512, 2009.
- [63] L. K. Roberts, L. J. Barr, D. H. Fuller, C. W. McMahon, P. T. Leese, and S. Jones, “Clinical safety and efficacy of a powdered hepatitis B nucleic acid vaccine delivered to the epidermis by a commercial prototype device,” *Vaccine*, vol. 23, no. 40, pp. 4867–4878, 2005.
- [64] R. Wang, J. Epstein, F. M. Baraceros, E. J. Gorak, Y. Charoenvit, D. J. Carucci, R. C. Hedstrom, N. Rahardjo, T. Gay, P. Hobart, R. Stout, T. R. Jones, T. L. Richie, S. E. Parker, D. L. Doolan, J. Norman, and S. L. Hoffman, “Induction of CD4+ T cell-dependent CD8+ type 1 responses in humans by a malaria DNA vaccine,” *Proceedings of the National Academy of Sciences*, vol. 98, no. 19, pp. 10817–10822, 2001.
- [65] J. E. Epstein, E. J. Gorak, Y. Charoenvit, R. Wang, N. Freyberg, O. Osinowo, T. L. Richie, E. L. Stoltz, F. Trespalacios, J. Nerges, J. Ng, V. Fallarme-Majam, E. Abot, L. Goh, S. Parker, S. Kumar, R. C. Hedstrom, J. Norman, R. Stout, and S. L. Hoffman, “Safety, tolerability, and lack of antibody responses after administration of a

- PfCSP DNA malaria vaccine via needle or needle-free jet injection, and comparison of intramuscular and combination intramuscular/intradermal routes,” *Human Gene Therapy*, vol. 13, no. 13, pp. 1551–1560, 2002.
- [66] S. Aboud, “Strong HIV-specific CD4+ and CD8+ T-lymphocyte proliferative responses in healthy individuals immunized with an HIV-1 DNA vaccine and boosted with recombinant modified vaccinia virus ankara expressing HIV-1 genes,” *Clinical and Vaccine Immunology*, vol. 17, no. 7, pp. 1124–1131, 2010.
- [67] A. H. C. Choi, K. Smiley, M. Basu, M. M. McNeal, M. Shao, J. A. Bean, J. D. Clements, R. R. Stout, and R. L. Ward, “Protection of mice against rotavirus challenge following intradermal DNA immunization by biojector needle-free injection,” *Vaccine*, vol. 25, no. 16 SPEC. ISS., pp. 3215–3218, 2007.
- [68] K. Raviprakash, D. Ewing, M. Simmons, K. R. Porter, T. R. Jones, C. G. Hayes, R. Stout, and G. S. Murphy, “Needle-free biojector injection of a dengue virus type 1 DNA vaccine with human immunostimulatory sequences and the GM-CSF gene increases immunogenicity and protection from virus challenge in aotus monkeys,” *Virology*, vol. 315, no. 2, pp. 345–352, 2003.
- [69] M. Foldvari, S. Babiuk, and I. Badea, “DNA delivery for vaccination and therapeutics through the skin,” *Current Drug Delivery*, vol. 3, no. 1, pp. 17–28, 2006.
- [70] D. T. Page and S. Cudmore, “Innovations in oral gene delivery: challenges and potentials,” *Drug Discovery Today*, vol. 6, no. 2, pp. 92–101, 2001.
- [71] E. Sheu, S. Rothman, M. German, X. Wang, M. Finer, and B. M. McMahon, “The gene pill and its therapeutic applications,” *Current Opinion in Molecular Therapeutics*, vol. 5, no. 4, pp. 420–427, 2003.
- [72] D. R. Sizemore, A. A. Branstrom, and J. C. Sadoff, “Attenuated shigella as a DNA

- delivery vehicle for DNA-mediated immunization,” *Science*, vol. 270, no. 5234, pp. 299–302, 1995.
- [73] A. Darji, S. zur Lage, A. I. Garbe, T. Chakraborty, and S. Weiss, “Oral delivery of DNA vaccines using attenuated salmonella typhimurium as carrier,” *FEMS Immunology and Medical Microbiology*, vol. 27, no. 4, pp. 341–349, 2000.
- [74] Y. Yang, Z. Zhang, J. Yang, X. Chen, S. Cui, and X. Zhu, “Oral vaccination with Ts87 DNA vaccine delivered by attenuated salmonella typhimurium elicits a protective immune response against trichinella spiralis larval challenge,” *Vaccine*, vol. 28, no. 15, pp. 2735–2742, 2010.
- [75] S. D. Jazayeri, A. Ideris, Z. Zakaria, S. K. Yeap, and A. R. Omar, “Improved immune responses against avian influenza virus following oral vaccination of chickens with HA DNA vaccine using attenuated salmonella typhimurium as carrier,” *Comparative Immunology, Microbiology and Infectious Diseases*, vol. 35, no. 5, pp. 417–427, 2012.
- [76] P. Paglia, E. Medina, I. Arioli, C. A. Guzman, and M. P. Colombo, “Gene transfer in dendritic cells, induced by oral DNA vaccination with salmonella typhimurium, results in protective immunity against a murine fibrosarcoma,” *Blood*, vol. 92, no. 9, pp. 3172–3176, 1998.
- [77] S. Somavarapu, V. W. Bramwell, and H. O. Alpar, “Oral plasmid DNA delivery systems for genetic immunisation,” *Journal of Drug Targeting*, vol. 11, no. 8-10, pp. 547–553, 2003.
- [78] D. H. Jones, S. Corris, S. McDonald, J. C. S. Clegg, and G. H. Farrar, “Poly(dl-lactide-co-glycolide)-encapsulated plasmid DNA elicits systemic and mucosal antibody responses to encoded protein after oral administration,” *Vaccine*, vol. 15, no. 8, pp. 814–817, 1997.

- [79] K. A. Howard, X. W. Li, S. Somavarapu, J. Singh, N. Green, K. N. Atuah, Y. Ozsoy, L. W. Seymour, and H. O. Alpar, "Formulation of a microparticle carrier for oral polyplex-based DNA vaccines," *Biochimica et Biophysica Acta (BBA) - General Subjects*, vol. 1674, no. 2, pp. 149–157, 2004.
- [80] S. C. Chen, D. H. Jones, E. F. Fynan, G. H. Farrar, J. C. S. Clegg, H. B. Greenberg, and J. E. Herrmann, "Protective immunity induced by oral immunization with a rotavirus DNA vaccine encapsulated in microparticles," *Journal of Virology*, vol. 72, no. 7, pp. 5757–5761, 1998.
- [81] J. E. Herrmann, S. C. Chen, D. H. Jones, A. Tinsley-Bown, E. F. Fynan, H. B. Greenberg, and G. H. Farrar, "Immune responses and protection obtained by oral immunization with rotavirus VP4 and VP7 DNA vaccines encapsulated in microparticles," *Virology*, vol. 259, no. 1, pp. 148–153, 1999.
- [82] K. Roy, H.-Q. Mao, S. K. Huang, and K. W. Leong, "Oral gene delivery with chitosan-DNA nanoparticles generates immunologic protection in a murine model of peanut allergy," *Nature Medicine*, vol. 5, no. 4, pp. 387–391, 1999.
- [83] J.-P. Amorij, G. F. A. Kersten, V. Saluja, W. F. Tonnis, W. L. J. Hinrichs, B. Sltter, S. M. Bal, J. A. Bouwstra, A. Huckriede, and W. Jiskoot, "Towards tailored vaccine delivery: Needs, challenges and perspectives," *Journal of Controlled Release*, vol. 161, no. 2, pp. 363–376, 2012.
- [84] T. Borrs, "Recent developments in ocular gene therapy," *Experimental Eye Research*, vol. 76, no. 6, pp. 643–652, 2003.
- [85] C. Andrieu-Soler, R. A. Bejjani, T. de Bizemont, N. Normand, D. BenEzra, and F. Behar-Cohen, "Ocular gene therapy: A review of non-viral strategies," *American Journal of Ophthalmology*, vol. 143, no. 4, p. 732, 2007.

- [86] S. U. Stechschulte, A. M. Jousseaume, H. A. von Recum, V. Poulaki, Y. Moromizato, J. Yuan, R. J. D'Amato, C. Kuo, and A. P. Adamis, "Rapid ocular angiogenic control via naked DNA delivery to cornea," *Investigative Ophthalmology & Visual Science*, vol. 42, no. 9, pp. 1975–1979, 2001.
- [87] P. C. Issa and R. E. MacLaren, "Non-viral retinal gene therapy: a review," *Clinical and Experimental Ophthalmology*, vol. 40, no. 1, pp. 39–47, 2011.
- [88] R. E. MacLaren, "An analysis of retinal gene therapy clinical trials," *Current Opinion in Molecular Therapeutics*, vol. 11, no. 5, pp. 540–546, 2009.
- [89] J. W. B. Bainbridge, A. J. Smith, S. S. Barker, S. Robbie, R. Henderson, K. Balagagan, A. Viswanathan, G. E. Holder, A. Stockman, N. Tyler, S. Petersen-Jones, S. S. Bhattacharya, A. J. Thrasher, F. W. Fitzke, B. J. Carter, G. S. Rubin, A. T. Moore, and R. R. Ali, "Effect of gene therapy on visual function in leber's congenital amaurosis," *New England Journal of Medicine*, vol. 358, no. 21, pp. 2231–2239, 2008.
- [90] R. Farjo, J. Skaggs, A. B. Quiambao, M. J. Cooper, and M. I. Naash, "Efficient non-viral ocular gene transfer with compacted DNA nanoparticles," *PLoS ONE*, vol. 1, no. 1, p. e38, 2006.
- [91] Y. Osorio, J. Cohen, and H. Ghiasi, "Improved protection from primary ocular HSV-1 infection and establishment of latency using multigenic DNA vaccines," *Investigative Ophthalmology & Visual Science*, vol. 45, no. 2, pp. 506–514, 2004.
- [92] T. D. Frye, H. C. Chiou, B. E. Hull, and N. J. Bigley, "The efficacy of a DNA vaccine encoding herpes simplex virus type 1 (hsv-1) glycoprotein D in decreasing ocular disease severity following corneal HSV-1 challenge," *Archives of Virology*, vol. 147, no. 9, pp. 1747–1759, 2002.

- [93] K. Hu, J. Dou, F. Yu, X. He, X. Yuan, Y. Wang, C. Liu, and N. Gu, "An ocular mucosal administration of nanoparticles containing DNA vaccine pRSC-gD-IL-21 confers protection against mucosal challenge with herpes simplex virus type 1 in mice," *Vaccine*, vol. 29, no. 7, pp. 1455–1462, 2011.
- [94] J.-P. Kraehenbuhl, "Mucosa-targeted DNA vaccination," *Trends in Immunology*, vol. 22, no. 12, pp. 646–648, 2001.
- [95] L. Illum and S. S. Davis, "Nasal vaccination: a non-invasive vaccine delivery method that holds great promise for the future," *Advanced Drug Delivery Reviews*, vol. 51, no. 1-3, pp. 1–3, 2001.
- [96] S. Sharma, T. K. S. Mukkur, H. A. E. Benson, and Y. Chen, "Pharmaceutical aspects of intranasal delivery of vaccines using particulate systems," *Journal of Pharmaceutical Sciences*, vol. 98, no. 3, pp. 812–843, 2009.
- [97] A. Kichler, M. Chillon, C. Leborgne, O. Danos, and B. Frisch, "Intranasal gene delivery with a polyethylenimine-PEG conjugate," *Journal of Controlled Release*, vol. 81, no. 3, pp. 379–388, 2002.
- [98] S. I. Tanaka, T. Yamakawa, M. Kimura, I. Aoki, J. Kamei, K. Okuda, and C. Mobbs, "Daily nasal inoculation with the insulin gene ameliorates diabetes in mice," *Diabetes Research and Clinical Practice*, vol. 63, no. 1, pp. 1–9, 2004.
- [99] J. P. Wong, M. A. Zabielski, F. L. Schmaltz, G. G. Brownlee, L. A. Bussey, K. Marshall, T. Borralho, and L. P. Nagata, "DNA vaccination against respiratory influenza virus infection," *Vaccine*, vol. 19, no. 17-19, pp. 2461–2467, 2001.
- [100] K. Khatri, A. K. Goyal, P. N. Gupta, N. Mishra, A. Mehta, and S. P. Vyas, "Surface modified liposomes for nasal delivery of DNA vaccine," *Vaccine*, vol. 26, no. 18, pp. 2225–2233, 2008.

- [101] T. W. Kim, H. Chung, I. C. Kwon, H. C. Sung, T. H. Kang, H. D. Han, and S. Y. Jeong, "Induction of immunity against hepatitis B virus surface antigen by intranasal DNA vaccination using a cationic emulsion as a mucosal gene carrier," *Molecules and Cells*, vol. 22, no. 2, pp. 175–181, 2006.
- [102] A. Musacchio, D. Quintana, A. M. Herrera, B. Sandez, J. C. Alvarez, V. Falcon, M. C. la Rosa, F. Alvarez, and D. Pichardo, "Plasmid DNA-recombinant opc protein complexes for nasal DNA immunization," *Vaccine*, vol. 19, no. 27, pp. 3692–3699, 2001.
- [103] S. Kodama, T. Hirano, K. Noda, S. Umemoto, and M. Suzuki, "Nasal immunization with plasmid DNA encoding P6 protein and immunostimulatory complexes elicits nontypeable haemophilus influenzae-specific long-term mucosal immune responses in the nasopharynx," *Vaccine*, vol. 29, no. 10, pp. 1881–1890, 2011.
- [104] P. G. Djupesland, A. Skretting, M. Winderen, and T. Holand, "Bi-directional nasal delivery of aerosols can prevent lung deposition," *Journal of Aerosol Medicine and Pulmonary Drug Delivery*, vol. 17, no. 3, pp. 249–259, 2004.
- [105] H. Bakke, H. H. Samdal, J. Holst, F. Oftung, I. L. Haugen, A. C. Kristoffersen, A. Haugan, L. Janakova, G. E. Korsvold, G. Krogh, E. A. S. Andersen, P. Djupesland, T. Holand, R. Rappuoli, and B. Haneberg, "Oral spray immunization may be an alternative to intranasal vaccine delivery to induce systemic antibodies but not nasal mucosal or cellular immunity," *Scandinavian Journal of Immunology*, vol. 63, no. 3, pp. 223–231, 2006.
- [106] P. G. Djupesland, A. Skretting, M. Winderen, and T. Holand, "Breath actuated device improves delivery to target sites beyond the nasal valve," *The Laryngoscope*, vol. 116, no. 3, pp. 466–472, 2006.

- [107] W. D. Bennett, J. S. Brown, K. L. Zeman, S. C. Hu, G. Scheuch, and K. Sommerer, "Targeting delivery of aerosols to different lung regions," *Journal of Aerosol Medicine and Pulmonary Drug Delivery*, vol. 15, no. 2, pp. 179–188, 2002.
- [108] A. Hanninen, A. Braakhuis, W. R. Heath, and L. C. Harrison, "Mucosal antigen primes diabetogenic cytotoxic t-lymphocytes regardless of dose or delivery route," *Diabetes*, vol. 50, no. 4, pp. 771–775, 2001.
- [109] F. Administration and Drug, "Flumist: Highlights of prescribing information," tech. rep., Food and Drug Administration, 2012.
- [110] S. J. Eastman, "Optimization of formulations and conditions for the aerosol delivery of functional cationic lipid: DNA complexes," *Human Gene Therapy*, vol. 8, no. 3, p. 313, 1997.
- [111] S. Eastman, J. Tousignant, M. Lukason, Q. Chu, S. Cheng, and R. Scheule, "Aerosolization of cationic lipid: pDNA complexes-in vitro optimization of nebulizer parameters for human clinical studies," *Human Gene Therapy*, vol. 9, no. 1, pp. 43–52, 1998.
- [112] C. L. Densmore, "Aerosol delivery of robust polyethyleneimineDNA complexes for gene therapy and genetic immunization," *Molecular Therapy*, vol. 1, no. 2, p. 180, 2000.
- [113] L. Davies, G. McLachlan, S. Sumner-Jones, D. Ferguson, A. Baker, P. Tennant, C. Gordon, C. Vrettou, E. Baker, J. Zhu, *et al.*, "Enhanced lung gene expression after aerosol delivery of concentrated pDNA/PEI complexes," *Molecular Therapy*, vol. 16, no. 7, pp. 1283–1290, 2008.
- [114] S. Eastman, M. Lukason, J. Tousignant, H. Murray, M. Lane, J. George, G. Akita,

- M. Cherry, S. Cheng, and R. Scheule, "A concentrated and stable aerosol formulation of cationic lipid: DNA complexes giving high-level gene expression in mouse lung," *Human Gene Therapy*, vol. 8, no. 6, pp. 765–773, 1997.
- [115] A. Canonico, J. Conary, B. Meyrick, K. Brigham, *et al.*, "Aerosol and intravenous transfection of human alpha 1-antitrypsin gene to lungs of rabbits," *American Journal of Respiratory Cell and Molecular Biology*, vol. 10, no. 1, p. 24, 1994.
- [116] G. McLachlan, A. Baker, P. Tennant, C. Gordon, C. Vrettou, L. Renwick, R. Blundell, S. Cheng, R. Scheule, L. Davies, *et al.*, "Optimizing aerosol gene delivery and expression in the ovine lung," *Molecular Therapy*, vol. 15, no. 2, pp. 348–354, 2007.
- [117] C. L. Densmore, T. H. Giddings, J. C. Waldrep, B. M. Kinsey, and V. Knight, "Gene transfer by guanidinium-cholesterol: dioleoylphosphatidyl-ethanolamine liposome-DNA complexes in aerosol," *The Journal of Gene Medicine*, vol. 1, no. 4, pp. 251–264, 1999.
- [118] C. Rudolph, A. Ortiz, U. Schillinger, J. Jauernig, C. Plank, and J. Rosenecker, "Methodological optimization of polyethylenimine (PEI)-based gene delivery to the lungs of mice via aerosol application," *The Journal of Gene Medicine*, vol. 7, no. 1, pp. 59–66, 2005.
- [119] E. W. Alton, M. Stern, R. Farley, A. Jaffe, S. L. Chadwick, J. Phillips, J. Davies, S. N. Smith, J. Browning, M. G. Davies, M. E. Hodson, S. R. Durham, D. Li, P. K. Jeffery, M. Scallan, R. Balfour, S. J. Eastman, S. H. Cheng, A. E. Smith, D. Meeker, and D. M. Geddes, "Cationic lipid-mediated CFTR gene transfer to the lungs and nose of patients with cystic fibrosis: a double-blind placebo-controlled trial," *The Lancet*, vol. 353, no. 9157, pp. 947–54, 1999.

- [120] F. E. Ruiz, "A clinical inflammatory syndrome attributable to aerosolized lipid-DNA administration in cystic fibrosis," *Human Gene Therapy*, vol. 12, no. 7, p. 751, 2001.
- [121] H. D. C. Smyth, "The influence of formulation variables on the performance of alternative propellant-driven metered-dose inhalers," *Advanced Drug Delivery Reviews*, vol. 55, no. 7, pp. 807–828, 2003.
- [122] H. Milgrom, B. Bender, L. Ackerson, P. Bowrya, B. Smith, and C. Rand, "Non-compliance and treatment failure in children with asthma," *The Journal of Allergy and Clinical Immunology*, vol. 98, no. 6, pp. 1051–1057, 1996.
- [123] D. E. Geller, "Comparing clinical features of the nebulizer, metered-dose inhaler, and dry powder inhaler," *Respiratory Care*, vol. 50, no. 10, pp. 1313–1322, 2005.
- [124] P. W. Barry and C. O'Callaghan, "The influence of inhaler selection on efficacy of asthma therapies," *Advanced Drug Delivery Reviews*, vol. 55, no. 7, pp. 879–923, 2003.
- [125] G. Taylor and M. Gumbleton, "Aerosols for macromolecule delivery: Design challenges and solutions," *American Journal of Drug Delivery*, vol. 2, no. 3, pp. 143–155, 2004.
- [126] R. O. Williams Iii, M. K. Barron, M. Jos Alonso, and C. Remun-Lpez, "Investigation of a pMDI system containing chitosan microspheres and P134a," *International Journal of Pharmaceutics*, vol. 174, no. 1-2, pp. 209–222, 1998.
- [127] B. K. Bains, J. C. Birchall, R. Toon, and G. Taylor, "In vitro reporter gene transfection via plasmid DNA delivered by metered-dose inhaler," *Journal of Pharmaceutical Sciences*, vol. 99, no. 7, pp. 3089–3099, 2011.
- [128] H. Y. Li, P. C. Seville, I. J. Williamson, and J. C. Birchall, "The use of absorption

- enhancers to enhance the dispersibility of spray-dried powders for pulmonary gene therapy,” *The Journal of Gene Medicine*, vol. 7, no. 8, pp. 1035–1043, 2005.
- [129] H. Y. Li, P. C. Seville, I. J. Williamson, and J. C. Birchall, “The use of amino acids to enhance the aerosolisation of spray-dried powders for pulmonary gene therapy,” *The Journal of Gene Medicine*, vol. 7, no. 3, pp. 343–353, 2005.
- [130] K. Mohri, T. Okuda, A. Mori, K. Danjo, and H. Okamoto, “Optimized pulmonary gene transfection in mice by spray-freeze dried powder inhalation,” *Journal of Controlled Release*, vol. 144, no. 2, pp. 221–226, 2010.
- [131] H. Okamoto and K. Danjo, “Local and systemic delivery of high-molecular weight drugs by powder inhalation,” *Yakugaku Zasshi*, vol. 127, no. 4, pp. 643–653, 2007.
- [132] H. Okamoto, K. Shiraki, R. Yasuda, K. Danjo, and Y. Watanabe, “Chitosan-interferon- β gene complex powder for inhalation treatment of lung metastasis in mice,” *Journal of Controlled Release*, vol. 150, no. 2, pp. 187–195, 2011.
- [133] “Inhaler technique in adults with asthma or COPD: Information paper for health professionals,” tech. rep., 2008.
- [134] R. Dalby and J. Suman, “Inhalation therapy: technological milestones in asthma treatment,” *Advanced Drug Delivery Reviews*, vol. 55, no. 7, pp. 779–791, 2003.
- [135] E. Kleemann, L. Dailey, H. Abdelhady, T. Gessler, T. Schmehl, C. Roberts, M. Davies, W. Seeger, and T. Kissel, “Modified polyethylenimines as non-viral gene delivery systems for aerosol gene therapy: investigations of the complex structure and stability during air-jet and ultrasonic nebulization,” *Journal of Controlled Release*, vol. 100, no. 3, pp. 437–450, 2004.
- [136] Y. Lentz, L. Worden, T. Anchoadoquy, and C. Lengsfeld, “Effect of jet nebulization on DNA: Identifying the dominant degradation mechanism and mitigation methods,” *Journal of Aerosol Science*, vol. 36, no. 8, pp. 973–990, 2005.

- [137] L. A. Schwarz, J. L. Johnson, M. Black, S. H. Cheng, M. E. Hogan, and J. C. Waldrep, "Delivery of DNA-cationic liposome complexes by small-particle aerosol," *Human Gene Therapy*, vol. 7, no. 6, pp. 731–741, 1996.
- [138] D. Deshpande, P. Blezinger, R. Pillai, J. Duguid, B. Freimark, and A. Rolland, "Target specific optimization of cationic lipid-based systems for pulmonary gene therapy," *Pharmaceutical Research*, vol. 15, no. 9, pp. 1340–1347, 1998.
- [139] M. Stern, F. Sorgi, C. Hughes, N. J. Caplen, J. E. Browning, P. G. Middleton, D. C. Gruenert, S. J. Farr, L. Huang, D. M. Geddes, and E. W. Alton, "The effects of jet nebulisation on cationic liposome-mediated gene transfer in vitro," *Gene Therapy*, vol. 5, no. 5, pp. 583–593, 1998.
- [140] A. A. Gautam, C. L. C. Densmore, B. B. Xu, and J. C. J. Waldrep, "Enhanced gene expression in mouse lung after PEI-DNA aerosol delivery," *Molecular Therapy*, vol. 2, no. 1, pp. 63–70, 2000.
- [141] C. Rudolph, R. H. Miller, and J. Rosenecker, "Jet nebulization of PEI/DNA polyplexes: physical stability and in vitro gene delivery efficiency," *The Journal of Gene Medicine*, vol. 4, no. 1, pp. 66–74, 2002.
- [142] J. Birchall, I. Kellaway, and M. Gumbleton, "Physical stability and in-vitro gene expression efficiency of nebulised lipid-peptide-DNA complexes," *International Journal of Pharmaceutics*, vol. 197, no. 1-2, pp. 221–231, 2000.
- [143] Z. Mohammadi, F. A. Dorkoosh, S. Hosseinkhani, K. Gilani, T. Amini, A. R. Najafabadi, and M. R. Tehrani, "In vivo transfection study of chitosan-DNA-FAP-B nanoparticles as a new non viral vector for gene delivery to the lung," *International Journal of Pharmaceutics*, vol. 421, no. 1, pp. 183–188, 2011.
- [144] Y. Lentz, T. Anchordoquy, and C. Lengsfeld, "DNA acts as a nucleation site for

- transient cavitation in the ultrasonic nebulizer,” *Journal of Pharmaceutical Sciences*, vol. 95, no. 3, pp. 607–619, 2006.
- [145] R. Pillai, K. Petrak, P. Blezinger, D. Deshpande, V. Florack, B. Freimark, G. Padmabandu, and A. Rolland, “Ultrasonic nebulization of cationic lipid-based gene delivery systems for airway administration,” *Pharmaceutical Research*, vol. 15, no. 11, pp. 1743–1747, 1998.
- [146] C. Guillaume, P. Delpine, C. Droal, T. Montier, G. Tymen, and F. Claude, “Aerosolization of cationic lipid-DNA complexes: Lipoplex characterization and optimization of aerosol delivery conditions,” *Biochemical and Biophysical Research Communications*, vol. 286, no. 3, pp. 464–471, 2001.
- [147] L. A. Dailey, E. Kleemann, T. Merdan, H. Petersen, T. Schmehl, T. Gessler, J. Hnze, W. Seeger, and T. Kissel, “Modified polyethylenimines as non viral gene delivery systems for aerosol therapy: effects of nebulization on cellular uptake and transfection efficiency,” *Journal of Controlled Release*, vol. 100, no. 3, pp. 425–436, 2004.
- [148] S. Moghimi, P. Symonds, J. Murray, A. Hunter, G. Debska, and A. Szewczyk, “A two-stage poly (ethylenimine)-mediated cytotoxicity: implications for gene transfer/therapy,” *Molecular Therapy*, vol. 11, no. 6, pp. 990–995, 2005.
- [149] J. E. Baatz, Y. Zou, and T. R. Korfhagen, “Inhibitory effects of tumor necrosis factor- α on cationic lipid-mediated gene delivery to airway cells in vitro,” *Biochimica et Biophysica Acta (BBA) - Molecular Basis of Disease*, vol. 1535, no. 2, pp. 100–109, 2001.
- [150] J. Waldrep, A. Berlinski, and R. Dhand, “Comparative analysis of methods to measure aerosols generated by a vibrating mesh nebulizer,” *Journal of Aerosol Medicine*, vol. 20, no. 3, pp. 310–319, 2007.

- [151] L. Davies, K. Hannavy, N. Davies, A. Pirrie, R. Coffee, S. Hyde, and D. Gill, “Electrohydrodynamic comminution: a novel technique for the aerosolisation of plasmid DNA,” *Pharmaceutical Research*, vol. 22, no. 8, pp. 1294–1304, 2005.
- [152] M. Köping-Höggård, M. Issa, T. Köhler, A. Tronde, K. Vårum, and P. Artursson, “A miniaturized nebulization catheter for improved gene delivery to the mouse lung,” *The Journal of Gene Medicine*, vol. 7, no. 9, pp. 1215–1222, 2005.
- [153] L. Rayleigh, “On waves propagated along the plane surface of an elastic solid,” *Proceedings of the London Mathematical Society*, vol. 17, no. 4, 1885.
- [154] F. Voltmer and R. White, “Direct piezoelectric coupling to surface elastic waves,” *Applied Physics Letters*, vol. 7, no. 12, p. 314, 1965.
- [155] D. R. Morgan, “Surface acoustic wave devices and applications: 1. introductory review,” *Ultrasonics*, vol. 11, no. 3, pp. 121–131, 1973.
- [156] J. Friend and L. Yeo, “Microscale acoustofluidics: Microfluidics driven via acoustics and ultrasonics,” *Reviews of Modern Physics*, vol. 83, no. 2, p. 647, 2011.
- [157] Z. Wang and J. Zhe, “Recent advances in particle and droplet manipulation for lab-on-a-chip devices based on surface acoustic waves,” *Lab on a Chip*, vol. 11, pp. 1280–1285, 2011.
- [158] A. Wixforth, C. Strobl, C. G. A. Toegl, J. Scriba, and Z. Guttenberg, “Acoustic manipulation of small droplets,” *Analytical and Bioanalytical Chemistry*, vol. 379, pp. 982–991, 2004.
- [159] M. K. Tan, J. R. Friend, and L. Y. Yeo, “Exploitation of surface acoustic waves to drive size-dependent microparticle concentration within a droplet,” *Lab on a Chip*, vol. 7, pp. 618–625, 2007.

- [160] S. Girardo, M. Cecchini, F. Beltram, R. Cingolani, and D. Pisignano, “Polydimethylsiloxane–LiNbO₃ surface acoustic wave micropump devices for fluid control into microchannels,” *Lab on a Chip*, vol. 8, pp. 1557–1563, 2008.
- [161] M. Tan, L. Yeo, and J. Friend, “Rapid fluid flow and mixing induced in microchannels using surface acoustic waves,” *Europhysics Letters*, vol. 87, p. 47003, 2009.
- [162] L. Masini, M. Cecchini, S. Girardo, R. Cingolani, D. Pisignano, and F. Beltram, “Surface-acoustic-wave counterflow micropumps for on-chip liquid motion control in two-dimensional microchannel arrays,” *Lab on a Chip*, vol. 10, pp. 1997–2000, 2010.
- [163] K. Sritharan, C. Strobl, M. Schneider, A. Wixforth, and Z. Guttenberg, “Acoustic mixing at low Reynold’s numbers,” *Applied Physics Letters*, vol. 88, p. 054102, 2006.
- [164] R. Shilton, M. K. Tan, L. Y. Yeo, and J. R. Friend, “Particle concentration and mixing in microdrops driven by focused surface acoustic waves,” *Journal of Applied Physics*, vol. 104, p. 014910, 2008.
- [165] M. Tan, J. Friend, and L. Yeo, “Interfacial jetting phenomena induced by focused surface vibrations,” *Physical Review Letters*, vol. 103, no. 2, p. 24501, 2009.
- [166] H. Li, J. Friend, and L. Yeo, “Surface acoustic wave concentration of particle and bioparticle suspensions,” *Biomedical Microdevices*, vol. 28, pp. 4098–4104, 2007.
- [167] J. Shi, H. Huang, Z. Stratton, Y. Huang, and T. J. Huang, “Continuous particle separation in a microfluidic channel via standing surface acoustic waves (SSAW),” *Lab on a Chip*, vol. 9, pp. 3354–3359, 2009.
- [168] K. Kulkarni, J. Friend, L. Yeo, and P. Perlmutter, “Surface acoustic waves as an energy source for drop scale synthetic chemistry,” *Lab on a Chip*, vol. 9, pp. 754–755, 2009.

- [169] K. P. Kulkarni, S. H. Ramarathinam, J. Friend, L. Yeo, A. W. Purcell, and P. Perlmutter, "Rapid microscale in-gel processing and digestion of proteins using surface acoustic waves," *Lab on a Chip*, vol. 10, pp. 1518–1520, 2010.
- [170] A. Renaudin, V. Chabot, E. Grondin, V. Aimez, and P. G. Charette, "Integrated active mixing and biosensing using surface acoustic waves (SAW) and surface plasmon resonance (SPR) on a common substrate," *Lab on a Chip*, vol. 10, pp. 111–115, 2010.
- [171] S. Heron, R. Wilson, S. Shaffer, D. Goodlett, and J. Cooper, "Surface acoustic wave nebulization of peptides as a microfluidic interface for mass spectrometry," *Analytical Chemistry*, vol. 82, pp. 3985–3989, 2010.
- [172] J. Ho, M. K. Tan, D. B. Go, L. Y. Yeo, J. R. Friend, and H.-C. Chang, "Paper-based microfluidic surface acoustic wave sample delivery and ionization source for rapid and sensitive ambient mass spectrometry," *Analytical Chemistry*, vol. 83, pp. 3260–3266, 2011.
- [173] R. P. Hodgson, M. Tan, L. Yeo, and J. Friend, "Transmitting high power rf acoustic radiation via fluid couplants into superstrates for microfluidics," *Applied Physics Letters*, vol. 94, p. 024102, 2009.
- [174] R. Wilson, J. Reboud, Y. Bourquin, S. L. Neale, Y. Zhang, and J. M. Cooper, "Phononic crystal structures for acoustically driven microfluidic manipulations," *Lab on a Chip*, vol. 11, pp. 323–328, 2011.
- [175] J. Friend, L. Yeo, D. Arifin, and A. Mechler, "Evaporative self-assembly assisted synthesis of polymeric nanoparticles by surface acoustic wave atomization," *Nanotechnology*, vol. 19, p. 145301, 2008.
- [176] M. Kurosawa, A. Futami, and T. Higuchi, "Characteristics of liquids atomization using surface acoustic wave," p. 801, 1997.

- [177] M. Kurosawa, T. Watanabe, A. Futami, and T. Higuchi, "Surface acoustic wave atomizer with pumping effect," *Sensors and Actuators*, vol. 50, no. 1, p. 69, 1995.
- [178] L. Yeo and J. Friend, "Ultrafast microfluidics using surface acoustic waves," *Biomechanics*, vol. 3, p. 012002, 2009.
- [179] L. Yeo, J. Friend, M. McIntosh, E. Meeusen, and D. Morton, "Ultrasonic nebulization platforms for pulmonary drug delivery," *Expert Opinion on Drug Delivery*, vol. 7, no. 6, pp. 663–679, 2010.
- [180] O. Boussif, F. Lezoualc'h, M. Zanta, M. Mergny, D. Scherman, B. Demeneix, and J. Behr, "A versatile vector for gene and oligonucleotide transfer into cells in culture and in vivo: polyethylenimine," *Proceedings of the National Academy of Sciences*, vol. 92, no. 16, p. 7297, 1995.
- [181] A. Phillips, "The challenge of gene therapy and DNA delivery," *Journal of Pharmacy and Pharmacology*, vol. 53, no. 9, pp. 1169–1174, 2001.
- [182] G. Banks, R. Roselli, R. Chen, and T. Giorgio, "A model for the analysis of nonviral gene therapy," *Gene Therapy*, vol. 10, no. 20, pp. 1766–1775, 2003.
- [183] N. Bessis, F. GarciaCozar, and M. Boissier, "Immune responses to gene therapy vectors: influence on vector function and effector mechanisms," *Gene Therapy*, vol. 11, pp. S10–S17, 2004.
- [184] D. Ganderton, "Workshop on targeting drugs to the lung," (Bagshot, England), pp. 13–16, W B Saunders Co Ltd, 1997.
- [185] S. Wieshammer and J. Dreyhaupt, "Dry powder inhalers: which factors determine the frequency of handling errors?," *Respiration*, vol. 75, no. 1, pp. 18–25, 2008.
- [186] S. Fineberg, T. Kawabata, D. Finco-Kent, C. Liu, and A. Krasner, "Antibody response to inhaled insulin in patients with type 1 or type 2 diabetes. an analysis of

- initial phase II and III inhaled insulin (Exubera) trials and a two-year extension trial,” *Journal of Clinical Endocrinology & Metabolism*, vol. 90, no. 6, p. 3287, 2005.
- [187] L. Mastrandrea and T. Quattrin, “Clinical evaluation of inhaled insulin,” *Advanced Drug Delivery Reviews*, vol. 58, no. 9-10, pp. 1061–1075, 2006.
- [188] E. Alton *et al.*, “Use of nonviral vectors for cystic fibrosis gene therapy,” in *Proceedings of the American Thoracic Society*, vol. 1, p. 296, American Thoracic Society, 2004.
- [189] “Points to consider in the manufacture and testing of monoclonal antibody products for human use,” tech. rep., US Food and Drug Administration, Drug Administration Center for Biologics Evaluation and Research, 1997.
- [190] D. Fischer, Y. Li, B. Ahlemeyer, J. Krieglstein, and T. Kissel, “In vitro cytotoxicity testing of polycations: influence of polymer structure on cell viability and hemolysis,” *Biomaterials*, vol. 24, no. 7, pp. 1121–1131, 2003.
- [191] E. Moreau, M. Domurado, P. Chapon, M. Vert, and D. Domurado, “Biocompatibility of polycations: in vitro agglutination and lysis of red blood cells and in vivo toxicity,” *Journal of Drug Targeting*, vol. 10, no. 2, pp. 161–173, 2002.
- [192] D. Oxtoby, “Vibrational relaxation in liquids,” *Annual Review of Physical Chemistry*, vol. 32, no. 1, pp. 77–101, 1981.
- [193] C. Hsieh, A. Balducci, and P. Doyle, “An experimental study of DNA rotational relaxation time in nanoslits,” *Macromolecules*, vol. 40, no. 14, pp. 5196–5205, 2007.
- [194] H. Li, J. Friend, L. Yeo, A. Dasvarma, and K. Traianedes, “Effect of surface acoustic waves on the viability, proliferation and differentiation of primary osteoblast-like cells,” *Biomicrofluidics*, vol. 3, p. 034102, 2009.

- [195] T. Richie, A. Saul, *et al.*, “Progress and challenges for malaria vaccines,” *Nature*, vol. 415, no. 6872, pp. 694–701, 2002.
- [196] A. Coll-Seck, “Who controls malaria control?,” *Nature*, vol. 466, no. 7303, pp. 186–187, 2010.
- [197] L. Wang, L. Kedzierski, L. Schofield, and R. Coppel, “Influence of glycosylphosphatidylinositol anchorage on the efficacy of DNA vaccines encoding *Plasmodium yoelii* merozoite surface protein 4/5,” *Vaccine*, vol. 23, no. 32, pp. 4120–4127, 2005.
- [198] S. Projan, S. Carleton, and R. Novick, “Determination of plasmid copy number by fluorescence densitometry,” *Plasmid*, vol. 9, no. 2, pp. 182–190, 1983.
- [199] L. Wang, C. Black, V. Marshall, and R. Coppel, “Structural and antigenic properties of merozoite surface protein 4 of *Plasmodium falciparum*,” *Infection and Immunity*, vol. 67, no. 5, p. 2193, 1999.
- [200] V. Marshall, W. Tieqiao, and R. Coppel, “Close linkage of three merozoite surface protein genes on chromosome 2 of *Plasmodium falciparum*,” *Molecular and Biochemical Parasitology*, vol. 94, no. 1, pp. 13–25, 1998.
- [201] H. Frijlink and A. De Boer, “Dry powder inhalers for pulmonary drug delivery,” *Expert Opinion on Drug Delivery*, vol. 1, no. 1, pp. 67–86, 2004.
- [202] G. Scheuch, M. Kohlhaeuff, P. Brand, and R. Siekmeier, “Clinical perspectives on pulmonary systemic and macromolecular delivery,” *Advanced Drug Delivery Reviews*, vol. 58, no. 9-10, pp. 996–1008, 2006.
- [203] R. Renne, A. Wehner, B. Greenspan, H. DeFord, H. Ragan, R. Westerberg, R. Buschbom, G. Burger, A. Hayes, R. Suber, *et al.*, “2-week and 13-week inhalation studies of aerosolized glycerol in rats,” *Inhalation Toxicology*, vol. 4, no. 2, pp. 95–111, 1992.

- [204] S. Kong, N. Titchener-Hooker, and M. Levy, "Plasmid DNA processing for gene therapy and vaccination: Studies on the membrane sterilisation filtration step," *Journal of Membrane Science*, vol. 280, no. 1-2, pp. 824–831, 2006.
- [205] J. Robertson, J. Ackland, and A. Holm, "Guidelines for assuring the quality and nonclinical safety evaluation of DNA vaccines," tech. rep., World Health Organization, 2007.
- [206] C. Lengsfeld and T. Anchordoquy, "Shear-induced degradation of plasmid DNA," *Journal of Pharmaceutical Sciences*, vol. 91, no. 7, pp. 1581–1589, 2002.
- [207] C. Levinthal and P. Davison, "Degradation of deoxyribonucleic acid under hydrodynamic shearing forces," *Journal of Molecular Biology*, vol. 3, no. 5, pp. 674–683, 1961.
- [208] R. Bowman and N. Davidson, "Hydrodynamic shear breakage of DNA," *Biopolymers*, vol. 11, no. 12, pp. 2601–2624, 1972.
- [209] R. Adam and B. Zimm, "Shear degradation of DNA," *Nucleic Acids Research*, vol. 4, no. 5, pp. 1513–1538, 1977.
- [210] M. Levy, I. Collins, S. Yim, J. Ward, N. Titchener-Hooker, P. Ayazi Shamlou, and P. Dunnill, "Effect of shear on plasmid DNA in solution," *Bioprocess and Biosystems Engineering*, vol. 20, no. 1, pp. 7–13, 1999.
- [211] S. Schultz-Cherry and J. C. Jones, "Influenza vaccines: the good, the bad, and the eggs," *Advanced Virus Research*, vol. 77, pp. 63–84, 2010.
- [212] S. Rockman, P. Schoofs, and M. Greenberg, "Development and testing of the Australian pandemic influenza vaccine - a timely response," *Microbiology Australia*, vol. 32, no. 1, pp. 10–14, 2011.

- [213] Y. Cai, S. Rodriguez, and H. Hebel, "DNA vaccine manufacture: scale and quality," *Expert Review of Vaccines*, vol. 8, no. 9, pp. 1277–91, 2009.
- [214] N. M. Ferguson, D. A. Cummings, C. Fraser, J. C. Cajka, P. C. Cooley, and D. S. Burke, "Strategies for mitigating an influenza pandemic," *Nature*, vol. 442, no. 7101, pp. 448–52, 2006.
- [215] G. Forde, "Rapid-response vaccines-does DNA offer a solution?," *Nature Biotechnology*, vol. 23, no. 9, pp. 1059–1062, 2005.
- [216] B. Kinsey, C. Densmore, and F. Orson, "Non-viral gene delivery to the lungs," *Current Gene Therapy*, vol. 5, no. 2, pp. 181–194, 2005.
- [217] E. Bos, A. Van der Doelen, N. Van Rooy, and A. Schuurs, "3, 3', 5, 5'-tetramethylbenzidine as an Ames test negative chromogen for horseradish peroxidase in enzyme-immunoassay," *Journal of Immunoassay and Immunochemistry*, vol. 2, no. 3-4, pp. 187–204, 1981.
- [218] K. Meyer, M. Thompson, M. Levy, L. Barron, F. Szoka Jr, *et al.*, "Intratracheal gene delivery to the mouse airway: characterization of plasmid DNA expression and pharmacokinetics," *Gene Therapy*, vol. 2, no. 7, p. 450, 1995.
- [219] J. Zhang, A. Wilson, S. Alber, Z. Ma, Z. Tang, E. Satoh, O. Mazda, S. Watkins, L. Huang, B. Pitt, *et al.*, "Prolonged gene expression in mouse lung endothelial cells following transfection with epstein–barr virus-based episomal plasmid," *Gene Therapy*, vol. 10, no. 9, pp. 822–826, 2003.
- [220] L. Torrieri-Dramard, B. Lambrecht, H. Ferreira, T. Van den Berg, D. Klatzmann, and B. Bellier, "Intranasal DNA vaccination induces potent mucosal and systemic immune responses and cross-protective immunity against influenza viruses," *Molecular Therapy*, vol. 19, no. 3, pp. 602–611, 2010.

- [221] J. Wee, J. Scheerlinck, K. Snibson, S. Edwards, M. Pearse, C. Quinn, and P. Sutton, "Pulmonary delivery of ISCOMATRIX influenza vaccine induces both systemic and mucosal immunity with antigen dose sparing," *Mucosal Immunology*, vol. 1, no. 6, pp. 489–496, 2008.
- [222] L. Babihk, R. Pontarollo, S. Babiuk, B. Loehr, and S. van Drunen Littel-van den Hurk, "Induction of immune responses by DNA vaccines in large animals," *Vaccine*, vol. 21, no. 1, pp. 649–658, 2003.
- [223] E. Meeusen, K. Snibson, S. Hirst, and R. Bischof, "Sheep as a model species for the study and treatment of human asthma and other respiratory diseases," *Drug Discovery Today: Disease Models*, vol. 6, no. 4, pp. 101–106, 2009.
- [224] A. Qi, L. Yeo, J. Friend, and J. Ho, "The extraction of liquid, protein molecules and yeast cells from paper through surface acoustic wave atomization," *Lab on a Chip*, vol. 10, no. 4, pp. 470–476, 2010.
- [225] J. Denyer, K. Nikander, and N. Smith, "Adaptive aerosol delivery (AAD)," *Expert Opinion on Drug Delivery*, vol. 1, pp. 1656–1676, 2004.
- [226] B. L. Laube, "The expanding role of aerosols in systemic drug delivery, gene therapy, and vaccination," *Respiratory Care*, vol. 50, pp. 1161–1176, 2005.
- [227] W. Soluch and T. Wrobel, "Low driving power SAW atomiser," *Electronics Letters*, vol. 42, p. 1432, 2006.
- [228] K. Nagase, J. Friend, T. Ishii, K. Nakamura, and S. Ueha, "A study of new ultrasonic (sic) atomizing by two parallel saw devices," in *Proceedings of the 22nd Symposium on Ultrasonic Electronics*, vol. P3-49, (Ebina, Japan), pp. 377–378 (in Japanese), 2001.
- [229] M. Filipovic, *Radio Receivers*. mikroElektronika, 2007.

- [230] B. Michael, B. Philippe, M. Olivier Bou, and H. Etienne, “Low power sessile droplets actuation via modulated surface acoustic waves,” *Applied Physics Letters*, vol. 100, no. 15, p. 154102, 2012.
- [231] J. Friend and L. Yeo, “Using laser doppler vibrometry to measure capillary surface waves on fluid–fluid interfaces,” *Biomicrofluidics*, vol. 4, no. 2, p. 026501, 2009.
- [232] M. Alvarez, J. Friend, and L. Yeo, “Rapid generation of protein aerosols and nanoparticles via surface acoustic wave atomization,” *Nanotechnology*, vol. 19, p. 455103, 2008.
- [233] M. K. Tan, J. R. Friend, O. K. Matar, and L. Y. Yeo, “Capillary wave motion excited by high frequency surface acoustic waves,” *Physics of Fluids*, vol. 22, p. 112112, 2010.
- [234] D. Klinman, S. Klaschik, D. Tross, H. Shirota, and F. Steinhagen, “FDA guidance on prophylactic DNA vaccines: Analysis and recommendations,” *Vaccine*, vol. 28, no. 16, pp. 2801–2805, 2010.
- [235] T. C. Pereira and I. Lopes-Cendes, “Emerging RNA-based drugs: siRNAs, microRNAs and derivatives,” *Central Nervous System Agents in Medicinal Chemistry*, vol. 12, no. 3, pp. 217–232, 2012.
- [236] J. Burnett and J. Rossi, “Rna-based therapeutics: Current progress and future prospects,” *Chemistry and biology*, vol. 19, no. 1, pp. 60–71, 2012.